UNIVERSIDAD DE CÓRDOBA

Aportaciones de la histopatología y de la histología molecular al diagnóstico e inmunopatogenia de la tuberculosis animal

---

Contributions of histopathology and molecular histology to the diagnosis and immunopathogenesis of animal tuberculosis

Memoria presentada para optar al grado de doctor por la Universidad de Córdoba con mención internacional

Fernanda Isabel Larenas Muñoz

Directores
Jaime Gómez Laguna
Irene Magdalena Rodríguez Gómez

Departamento anatomía y anatomía patológica comparadas y toxicología
Programa de doctorado de biociencias y ciencias agroalimentarias
Córdoba, septiembre 2023

TITULO: *Aportaciones de la histopatología y de la histología molecular al diagnóstico e inmunopatogenia de la tuberculosis animal*

AUTOR: *Fernanda Isabel Larenas Muñoz*

© Edita: UCOPress. 2023
Campus de Rabanales
Ctra. Nacional IV, Km. 396 A
14071 Córdoba

https://www.uco.es/ucopress/index.php/es/
ucopress@uco.es

INFORME RAZONADO DE LAS/LOS DIRECTORAS/ES DE LA TESIS

Este documento se presentará junto con el depósito de la tesis en https://moodle.uco.es/ctp3/

DOCTORANDA/O

Fernanda Isabel Larenas Muñoz

TÍTULO DE LA TESIS:

Aportaciones de la histopatología y de la histología molecular al diagnóstico e inmunopatogenia de la tuberculosis animal

INFORME RAZONADO DE LAS/LOS DIRECTORAS/ES DE LA TESIS
(se hará mención a la evolución y desarrollo de la tesis, así como a trabajos y publicaciones derivados de la misma)

El trabajo de esta tesis doctoral surge para dar respuesta a dos aspectos fundamentales en el control de la tuberculosis animal, enfermedad de gran trascedencia tanto en salud pública como en sanidad animal, y que son, en primer lugar, trabajar sobre la mejora en el diagnóstico de la enfermedad y, en segundo lugar, avanzar en el conocimiento de los mecanismos patogénicos involucrados en el desarrollo de la misma.

La tesis está estructurada en tres bloques, en el primero se evaluó la incorporación de la histopatología como herramienta de diagnóstico. Los resultados mostraron que el uso conjunto de esta técnica junto las técnicas de referencia para esta enfermedad, permite tanto confirmar de manera rápida los animales positivos a las técnicas anteriores así como identificar animales falsos negativos a dichas técnicas, posicionándola como una herramienta complementaria de gran valor. Fruto de este trabajo se ha publicado el artículo "The role of histopathology as a complementary tool in the monitoring of bovine tuberculosis" en la revista Frontiers in Veterinary Science (factor de impacto de 3,2; D1). En el segundo bloque se profundizó en el estudio de la polarización de los macrófagos de los granulomas tuberculosos en los nódulos linfáticos de bovinos y porcinos. Fruto de este trabajo se ha visto que en la polarización de macrófagos en el ganado bovino, inicialmente predomina un ambiente proinflamatorio, evolucionando hacia una polarización antiinflamatoria en granulomas de estadios más avanzados. Sin embargo, en el porcino, es esta última polarización macrofágica la que predomina. Este trabajo, con título "Macrophage polarization in lymph node granulomas from cattle and pigs naturally infected with Mycobacterium tuberculosis complex" ha sido enviado a la revista Veterinary Pathology y está siendo actualmente revisado. Finalmente, en el último estudio, se empleó la técnica de histología molecular MALDI-MSI para identificar nuevas moléculas diana de la patogenía de la tuberculosis, observándose que ambas especies comparten, pero también difieren, en sus rutas de señalización. El estudio derivado de este trabajo "Proteomic analysis of granulomas from cattle and pigs naturally infected with Mycobacterium tuberculosis complex by MALDI-imaging" se encuentra también evaluándose en la revista Molecular & Celular Proteomics.

La doctoranda, ha podido ampliar sus conocimientos en esta enfermedad gracias a una estancia de tres meses en el Departamento de Patología del "UK Health Security Agency (UKHSA)" en Reino Unido, donde trabajó en la evaluación histopatológica de granulomas tuberculosos en cobayas, fruto del cual ha publicado el trabajo "Characterisation and development of histopathological lesions in a guinea pig model of Mycobacterium tuberculosis infection" en la revista Frontiers in Veterinary Science.

Además, la doctoranda ha mostrado una gran capacidad de trabajo y dedicación, adaptándose y colaborando con todas las actividades desarrolladas en el grupo de investigación y que, sin duda, le ayudarán en su desarrollo profesional y personal.

Esta tesis doctoral ha sida posible gracias al proyecto "Nuevas medidas y técnicas de control de la tuberculosis bovina en Andalucía" (GOP2i-CO-16-0010) de la Junta de Andalucía y a la beca del gobierno de Chile "2019/72200324" de la Agencia Nacional de Investigación y Desarrollo (ANID) que ha financiado los estudios de doctorado de Dña. Fernanda Isabel Larenas Muñoz.

Por todo ello, se autoriza la presentación de la tesis doctoral.

Córdoba, a 28 de septiembre de 2023

Las/los directoras/es

RODRIGUEZ GOMEZ IRENE MAGDALENA - 71222354W

Firmado digitalmente por RODRIGUEZ GOMEZ IRENE MAGDALENA - 71222354W
Fecha: 2023.09.29 00:20:18 +02'00'

GOMEZ LAGUNA JAIME - 30835532F

Firmado digitalmente por GOMEZ LAGUNA JAIME - 30835532F
Fecha: 2023.09.28 06:04:11 +02'00'

Fdo.:IRENE M. RODRÍGUEZ GÓMEZ
JAIME GÓMEZ LAGUNA

A mi famila, en especial a mi abuelo

Success is the ability to go from one failure to another with no loss of enthusiasm.

Winston Churchill

Este trabajo fue llevado a cabo por el proyecto de investigación “Nuevas medidas y técnicas de control de la tuberculosis bovina en Andalucía” (apoyo financiero a los grupos operativos de la asociación europea de innovación para la productividad y la sostenibilidad agrícola (EIP-AGRI) (GOP2i-CO-16-0010).
Fernanda Isabel Larenas Muñoz fue apoyada por una beca de doctorado de ANID (Beca de doctorado chile/2019/72200324).

This work was supported by the research project” New measures and techniques to control bovine tuberculosis in Andalusia” (financial support for operational groups of the European innovation partnership for agricultural productivity and sustainability (EIP-AGRI) (GOP2i-CO-16-0010).
Fernanda Isabel Larenas Muñoz was supported by a doctoral grant from ANID (Chilean national doctoral grant chile/2019/72200324).

GLOSARIO DE TÉRMINOS

GLOSARY OF TERMS

Arg1 : Arginasa 1; Arginase 1
ACMR : Ancestro común más reciente
AFB : Acid fast bacilli
BAAR : Bacilo ácido alcohol resistente
BALT : Tejido linfoide asociado a bronquios; Bronchus-Associated Lymphoid Tissue
BSA : Suero de albúmina bovino; Bovine serum albumin
CE : Célula epitelioide; Epithelioid cell
CD4⁺ : Linfocito T colaboradores CD4⁺
CD8⁺ : Linfocito T colaboradores CD8⁺
CMI : Inmunidad mediada por células; cell-mediated immunity
CMT : Complejo *Mycobacterium tuberculosis; Mycobacterium tuberculosis* complex
CMH : Complejo mayor de histocompatibilidad; Major histocompatibility **c**omplex
dPCR : PCR digital; digital PCR
ddPCR : PCR digital a gotas; droplet digital PCR
ELISA : Ensayo por Inmunoabsorción Ligado a Enzimas; Enzyme-Linked Immunosorbent Assay
GO : Ontología de Genes; Gene Ontology
H&E. : Hematoxilina Eosina; Haematoxylin eosin
iNOS : Óxido nítrico sintasa inducible; Inducible Nitric Oxide Sintetasa
IC95 : Intervalo de confianza al 95%; Confidence intervals at 95 %
IFN-γ : Interferon gamma;
IL : Interleuquina; Interleukin
M1 : Macrófago tipo 1; Macrophage type 1
M2 : Macrófago tipo 2; Macrophage type 2
MAP : Macrófago alveolar pulmonar; pulmonary alveolar macrophage
M. bovis : *Mycobacterium bovis*
MNGC : Células gigantes multinucleadas tipo Langhas; Langhans-type multinucleated giant cells
MALDI-MSI : Matrix-assisted laser desorption/ionization mass spectrometry imaging
OMSA : Organización mundial de la salud animal
NK : Células naturales asesinas; Natural killers cell
NL*s* : Nódulos linfáticos; Lymph nodes
NGS : Suero normal caprino; Normal Goat Serum
PAS : Ácido peryódico Schiff.
pb : Pares de bases
PCR : Reacción en cadena de la polimerasa; Polimerasa chain reaction

PPD : Derivado proteico purificado; Purified protein derivate
PIO : Piogranuloma.
IDTB : Intradermotuberculinización
IDTBS : Intradermotuberculinización simple;
IDTBC : Intradermotuberculinización comparada
NO : Oxído nítrico; Nixic oxygen
SIT : Prueba de tuberculina simple; single intradermal tuberculin test
TLR : Receptores tipo toll; Toll like receptors
TB : Tuberculosis
TBb : Tuberculosis bovina; bovine tuberculosis
TBL : Lesiones compatibles con tuberculosis;Tuberculosis like lesions
TLR : Receptores tipo Toll, toll like receptor
Th1 : Linfocito T helper 1
Th2 : Linfocito T helper 2
TNF-α : Factor de necrosis tumoral alfa;Tumour necrosis factor alpha
UFC : Unidad formadora de colonia
ZN : Ziehl Neelsen.

ÍNDICE GENERAL - GENERAL INDEX

ÍNDICE DE FIGURAS - FIGURES – INDEX

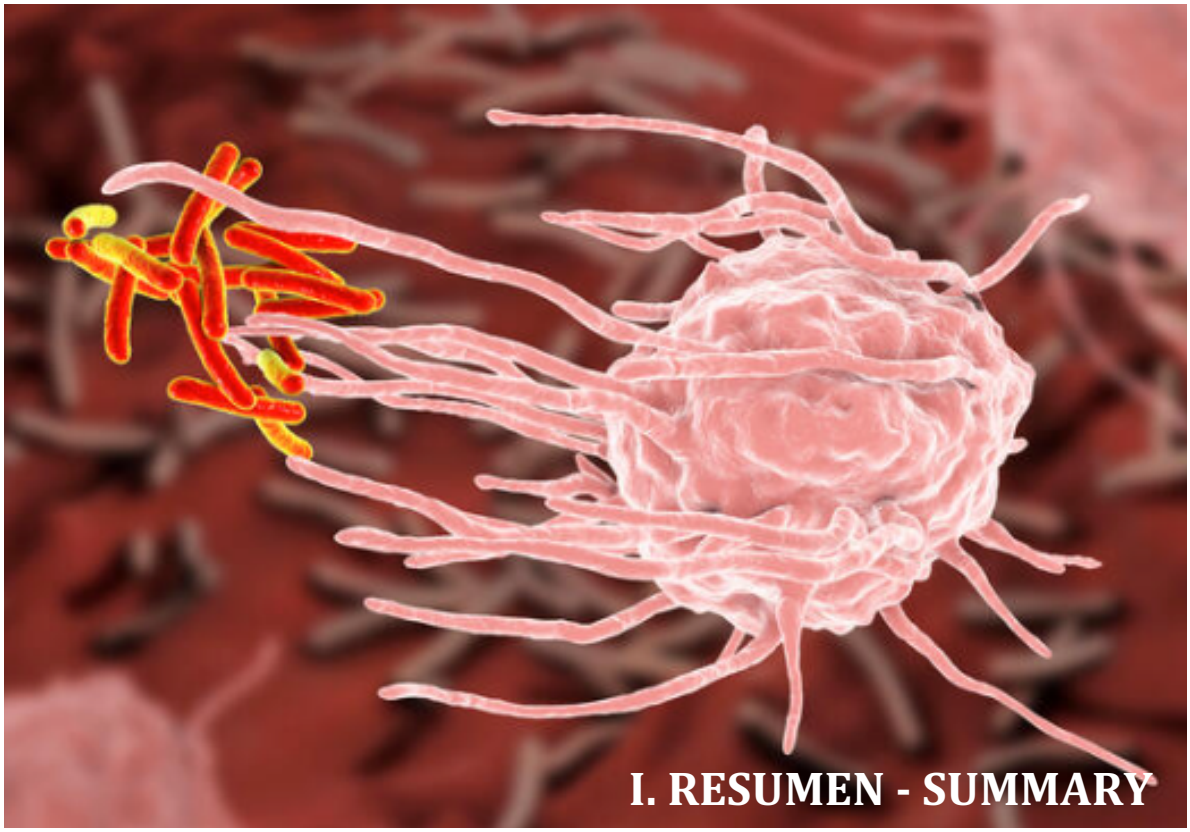

I. RESUMEN - SUMMARY

Resumen

La tuberculosis (TB) es una enfermedad infecciosa causada por el complejo *Mycobacterium tuberculosis* (CMT) que afecta tanto al humano como a una amplia gama de especies animales, incluidos animales domésticos y silvestres. En salud pública es una de las principales causas de muerte por enfermedades infecciosas en el mundo. En los animales, es una de las enfermedades más importantes para el sector ganadero a nivel mundial, ya que produce decaimiento, anorexia y pérdida de peso lo que conlleva a grandes pérdidas económicas por el sacrificio de animales enfermos. Posee además un potencial zoonósico, ya que algunas cepas del CMT pueden transmitirse al humano lo que representa un riesgo para salud pública.

El control de la TB animal es esencial para prevenir la transmisión a humanos y reducir la carga de la enfermedad en ambas poblaciones. Esto implica la aplicación de medidas de bioseguridad, detección temprana de animales infectados, sacrificio de animales enfermos y prácticas de higiene adecuadas en la producción y manipulación de productos de origen animal.

Es importante señalar que los detalles y enfoques específicos de la gestión de la TB en los animales pueden variar según el país o la región y la especie animal de que se trate. Deben consultarse las autoridades y las directrices veterinarias locales para obtener información precisa y actualizada sobre la TB en los animales.

Considerando lo anteriormente descrito, la presente tesis doctoral se centra en la puesta en valor de la histopatología como herramienta complementaria al diagnóstico de la TB y la expresión de diferentes marcadores de interés en nódulos linfáticos (NLs), así como la aproximación a la histología molecular en busca de profundizar en la inmunopatogenia de la TB en bovinos y porcinos infectados naturalmente con el CMT.

El primer estudio de esta tesis evalúa el uso de la histopatología como herramienta complementaria para el diagnóstico de la tuberculosis bovina (TBb): así, de un total de 230 bovinos sometidos al programa de control y erradicación de TBb en España se cogieron muestras de sangre (212) y NLs (681) para análisis serológicos, bacteriológicos e histopatológicos. Setenta y un NLs y 59 bovinos resultaron positivos

para bacteriología, y 59 NLs y 48 bovinos resultaron positivos en la PCR a tiempo real a partir de tejido fresco. Aproximadamente el 19 % (40/212) de las muestras de suero fueron positivos a ELISA. Se observaron lesiones tipo tuberculosas en el 11,9 % (81/681) de los NLs y el 30,9 % (71/230) de los bovinos. Sin embargo, en 18 de 83 animales SIT/PCR/cultivo negativo, de los cuales 11/18 fueron positivos a la técnica de Ziehl-Neelsen y dos de ellos positivos a la PCR digital (dPCR) IS6110. Seis de estos 11 ZN^+ correspondían a NLs mesentéricos y se confirmaron positivos a paratuberculosis. La histopatología proporcionó una sensibilidad del 91,3 % (IC95: 83,2 - 99,4 %) y una especificidad del 84,4 % (IC95: 78,6 - 89,3 %) con una buena concordancia (k = 0,626) en comparación con la PCR en tiempo real. Nuestros resultados señalan el importante papel que desempeña la histopatología en el diagnóstico y control de la TBb, y destaca la necesidad de considerar esta técnica junto al uso de otras herramientas de diagnóstico para un mejor control de la enfermedad.

El segundo estudio consiste en analizar la polarización de los macrófagos en granulomas de NLs de ganado vacuno y porcino procedentes de animales infectados naturalmente por el CMT. Los granulomas tuberculosos se clasificaron microscópicamente en 4 estadios y se analizaron mediante inmunohistoquímica utilizando un panel de marcadores de células mieloides (CD172a/MAC387), polarización de macrófagos M1 (iNOS/CD68/CD107a) y polarización de macrófagos M2 (Arg1/CD163). Los resultados mostraron que CD172a y MAC387 siguieron una misma cinética, siendo la expresión de este último mayor en los granulomas de fase tardía en cerdos. Del panel M1, la expresión de iNOS y CD68 prevaleció en bovino comparado con el porcino, siendo la expresión mayor en granulomas de estadio temprano. El marcaje frente a CD107a sólo se observó en los granulomas porcinos, con una mayor expresión en los granulomas de estadio I. Para el panel M2, la expresión de células $Arg1^+$ fue significativamente mayor en porcino que en bovino, particularmente en granulomas de estadio tardío. El análisis cuantitativo de las células $CD163^+$ mostró una cinética similar en ambas especies con una frecuencia consistente de células inmunomarcadas a lo largo de los diferentes estadios del granuloma. Nuestros resultados indican que la polarización de macrófagos M1 predomina en el ganado

vacuno durante los granulomas en estadios iniciales (I y II), mientras que también se observa un fenotipo M2 en estadios posteriores. Por el contrario, y debido principalmente a la expresión de Arg1, la polarización de macrófagos M2 es predominante en todos los estadios de granuloma del cerdo.

El tercer estudio se centra en comparar la firma proteica de granulomas en NLs pertenecientes a bovinos y cerdos infectados naturalmente por el CMT mediante MALDI-MSI, identificando la potencial participación de estas proteínas en vías biológicas e inmunológicas activadas a lo largo de la enfermedad, así como aquellas expresadas diferencialmente entre bovinos y cerdos. Para esto, se utilizaron muestras de 4 NLs de bovinos y porcinos con presencia de granuloma tuberculoso y, positivos al CMT por cultivo bacteriológico y/o PCR a tiempo real. Las imágenes de MALDI-MSI se realizaron utilizando un espectrómetro de masas AB-Sciex 5800 MALDI TOF/TOF (AB Sciex, Alemania). Los resultados mostraron una clara separación entre las masas de bovino y porcino, evidenciado un proteoma diferente en los granulomas de ambas especies. Sorprendentemente, algunos términos Gene Ontology (GO) coincidieron en ambas especies, presentando algunas proteínas en común. Es así como algunos de los términos GO que se encontraron fueron: “Complement activation” se observó en ambas especies, mientras que GO "Natural killer cell degranulation" se observó en bovinos y "Negative regulation of natural killer cell-mediated immunity" en porcinos. Estos resultados aportan nuevos conocimientos sobre la respuesta inmunitaria del huésped en la TB de bovinos y porcinos, destacando la importancia de la vía de activación del complemento y la regulación de la inmunidad mediada por células NK en la lucha contra la infección tuberculosa.

Summary

Tuberculosis (TB) is an infectious disease caused by the *Mycobacterium tuberculosis* complex (MTC), which affects both humans and a wide range of animal species, including domestic and wild animals. In the field of public health, it stands as one of the primary causes of death due to infectious diseases worldwide. Among animals, it holds immense significance for the global livestock sector, as it induces wasting, anorexia, and weight loss, ultimately resulting in substantial economic losses due to the culling of sick animals. Furthermore, it carries a zoonotic potential, as certain strains of MTC can be transmitted to humans, thereby posing a public health risk.

The control of animal TB is essential to prevent its transmission to humans and to reduce the disease burden in both populations. This entails implementing biosecurity measures, early detection of infected animals, culling of diseased animals, and adhering to proper hygienic practices in the production and handling of animal products.

It is important to note that the specific details and approaches to TB management in animals may vary depending on the country or region and the animal species involved. Local veterinary authorities and guidelines should be consulted for accurate and up-to-date information on TB in animals.

Taking into account the aforementioned, this PhD thesis concentrates on the valorisation of histopathology as a complementary tool for TB diagnosis, the assessment of various markers of interest in lymph nodes (LNs), and the exploration of molecular histology to provide insights into the immunopathogenesis of TB in cattle and pigs naturally infected with MTC.

The first study in this thesis assesses the utility of histopathology as a supplementary tool for diagnosing bovine tuberculosis (bTB). A total of 230 cattle enrolled in the bTB control and eradication programme in Spain contributed blood samples (212) and LNs (681) for serological, bacteriological, and histopathological analysis. Among these, 71 LNs and 59 cattle tested positive through bacteriological examination, while real-time PCR detected positivity in 59 lymph nodes and 48 cattle from fresh tissue. Approximately 19 % (40 out of 212) of the serum samples showed

positivity in ELISA tests. Tuberculous-like lesions were identified in 11.9 % (81 out of 681) of the LNs and 30.9 % (71 out of 230) of the cattle. Notably, 18 out of 83 animals tested negative in SIT/PCR/culture, of which 11 out of 18 exhibited Ziehl-Neelsen positivity, with two of them testing positive for IS*6110* digital PCR (dPCR). Six of these 11 ZN+ cases were associated with mesenteric lymph nodes and were confirmed to be positive for paratuberculosis. Histopathology demonstrated a sensitivity of 91.3 % (95 % CI: 83.2 - 99.4 %) and a specificity of 84.4 % (95 % CI: 78.6 - 89.3 %) with substantial concordance (k = 0.626) when compared to real-time PCR. Our findings underscore the significant role of histopathology in bTB diagnosis and monitoring, emphasizing the importance of incorporating this technique alongside other diagnostic tools to enhance disease control.

The second study aims to analyse macrophage polarisation within granulomas in the LNs of cattle and pigs naturally infected with MTC. The tuberculous granulomas were microscopically categorized into four stages and examined through immunohistochemistry, utilizing a panel of myeloid cell markers (CD172a/MAC387), markers for M1 macrophage polarisation (iNOS/CD68/CD107a), and markers for M2 macrophage polarisation (Arg1/CD163). The results revealed that CD172a and MAC387 exhibited similar patterns, with the latter displaying higher expression in late-phase granulomas in pigs. Within the M1 panel, iNOS and CD68 expression predominated in cattle compared to pigs, particularly showing higher expression in early-stage granulomas. CD107a labelling was observed exclusively in porcine granulomas, with greater expression in stage I granulomas. Concerning the M2 panel, the expression of $Arg1^+$ cells was significantly higher in pigs than in cattle, particularly in late-stage granulomas. Quantitative analysis of $CD163^+$ cells demonstrated consistent kinetics in both species, with a consistent frequency of immunolabelled cells across different granuloma stages. Our findings indicate that M1 macrophage polarisation prevails in cattle during the early stages of granulomas (I and II), while an M2 phenotype is also observed in later stages. In contrast, primarily due to Arg1 expression, M2 macrophage polarisation predominates in all granuloma stages in pigs.

The third study focuses on comparing the protein signature of granulomas in NLs belonging to cattle and pigs naturally infected by MTC by MALDI-MSI, identifying the potential involvement of these proteins in biological and immunological pathways activated throughout the disease, as well as those differentially expressed between cattle and pigs. For this, samples from 4 NLs from cattle and pigs with presence of tuberculous granuloma and, positive for MTC by bacteriological culture and/or real-time PCR, were used. MALDI-MSI was performed using an AB-Sciex 5800 MALDI TOF/TOF mass spectrometer (AB Sciex, Germany). The results showed a clear separation between bovine and porcine masses, evidencing a different proteome in the granulomas of both species. Surprisingly, some Gene Ontology (GO) terms coincided in both species, presenting some proteins in common. Among the GO terms observed, "Complement activation" was found in both cattle and pigs, while "Natural killer cell degranulation" was evident in cattle and "Negative regulation of natural killer cell-mediated immunity" in pigs. These findings offer fresh insights into the host immune response in bovine and porcine TB, underscoring the significance of the complement activation pathway and the regulation of NK cell-mediated immunity in combating tuberculosis infection.

II. INTRODUCCIÓN – INTRODUCTION

Introducción - Introduction

La tuberculosis (TB) es una enfermedad infecciosa, crónica, causada por micobacterias pertenecientes al complejo *Mycobacterium tuberculosis* (CMT). Esta enfermedad presenta una amplia variabilidad de hospedadores y un complejo modelo epidemiológico que involucra la interacción entre animales domésticos, de vida libre y seres humanos, lo que representa un problema significativo de salud pública. Además, la TB tiene una importancia económica considerable en la producción ganadera, debido a su capacidad para mermar el crecimiento y producción de los animales enfermos, así como la necesidad de implementar mejores medidas de vigilancia y control como la mejora de la higiene en las instalaciones de alojamiento de los animales, incluyendo la identificación temprana y sacrificio de animales infectados.

Las micobacterias que forman parte del CMT están estrechamente relacionadas entre sí y, a pesar de que existen diferencias, principalmente en virulencia, las similitudes entre ellas permiten extrapolar los datos obtenidos de una especie a otra. Estos factores han suscitado un creciente interés en el estudio de la TB en el ganado bovino y porcino, ya que estas especies son importantes reservorios de la enfermedad y, por lo tanto, su estudio y comprensión son cruciales para establecer medidas de prevención y control efectivas.

En el ámbito del diagnóstico, la histopatología desempeña un papel crucial como herramienta complementaria en la monitorización y diagnóstico de la TB, ya que permite la detección temprana de lesiones compatibles con TB, como son los granulomas. Además, resulta fundamental en la confirmación de diagnósticos en casos ambiguos y en el seguimiento de la progresión de la enfermedad. Se sabe que el desarrollo del granuloma tuberculoso es un proceso clave en la respuesta inmunitaria ante la infección, lo que lo ha convertido en objeto de estudio en el campo de la inmunopatogenia de esta enfermedad.

La inmunohistoquímica ha sido ampliamente utilizada para evaluar la expresión de marcadores específicos en TB y para comprender mejor los mecanismos que tienen lugar en el desarrollo de la enfermedad. En esta línea, se ha evaluado la expresión de

marcadores relacionados con la polarización de macrófagos M1 (proinflamatoria) y M2 (antiinflamatoria), donde se han observado diferencias en la expresión de marcadores específicos entre bovinos y porcinos, lo que evidencia la plasticidad de los macrófagos en el desarrollo del granuloma tuberculoso.

Asimismo, el auge de nuevas técnicas moleculares que permiten detectar la enfermedad en menor tiempo y con mayor precisión y eficacia ha dado lugar a la aparición de otras herramientas de interés, entre las que cabe destacar el uso de la PCR a tiempo real, así como nuevas herramientas de histología molecular como la imagenología por espectrometría de masas (MALDI-MSI, del inglés *Matrix-Assisted Laser Desorption/Ionization Mass Spectrometry Imaging*). Mediante esta técnica se pretende mejorar la comprensión de la distribución y localización espacial de moléculas relacionadas con procesos concretos en muestras de tejido para entender mejor la patogénesis de la enfermedad, identificando potenciales biomarcadores para el diagnóstico y tratamiento, así como desarrollar una mejor comprensión de los mecanismos de resistencia a los fármacos.

En general, en el sector ganadero, la investigación sobre la TB ha experimentado un notable avance en los últimos años, más marcado en el ganado bovino comparado con el porcino, cuyo enfoque principal ha sido la mejora del diagnóstico, desarrollo de vacunas eficaces y en las que los animales vacunados puedan ser diferenciados de los infectados y, aplicación de medidas de vigilancia y control más eficientes para prevenir la propagación de la enfermedad tanto entre los animales domésticos y silvestres como hacia las personas. El objetivo final de estos esfuerzos es lograr la erradicación de esta costosa enfermedad en aquellos países que aún no son libres de ella como es el caso de España.

1. LA TUBERCULOSIS Y SUS ANTECEDENTES HISTÓRICOS

1.1. Origen y evolución de la tuberculosis

El origen de la tuberculosis (TB) se remonta a tiempos ancestrales, siendo una enfermedad que ha estado presente en la naturaleza durante milenios y que ha existido tanto en animales como en seres humanos a lo largo de la historia . Si bien en la literatura existe controversia sobre el origen de la TB, algunos autores apoyan la idea de que el ganado bovino transmitió esta enfermedad al humano (Stead, 1997; Wolfe et al., 2007), mientras que otros postulan que los humanos fueron el origen de la TB para el ganado, debido a que las variantes del complejo *Mycobacterium tuberculosis* (CMT) aparecieron antes de la domesticación de animales (Gibbons, 2008). Las pruebas actuales sugieren que el CMT está formado por una serie de grupos de bacterias estrechamente relacionados, y que cada uno de estos grupos desciende de una única célula de un "*ancestro común más reciente*" (ACMR) que existió en un momento y lugar determinado del pasado. Así, la filogenia del CMT sugiere que el único linaje de cepas que dio lugar a todas las del CMT, adaptadas a los animales, descendía del ACMR (N. H. Smith et al., 2009). Por otro lado, se cree que a medida que los seres humanos empezaron a domesticar y criar animales, la TB se transmitió de los animales salvajes a los animales domésticos. Posteriormente, la interacción entre los animales domésticos y los seres humanos facilitó la propagación de la enfermedad (Wolfe et al., 2007). Se ha observado en estudios que la bacteria responsable de la TB puede persistir y sobrevivir incluso después de la muerte del hospedador (Weed & Baggenstoss, 1951) por períodos que oscilan durante semanas o varios meses, lo cual dependerá de las condiciones ambientales, siempre que estén protegidas de la luz solar, ya que las temperaturas elevadas y la luz UV inactiva las micobacterias (Dorronsoro & Torroba, 2007).

Por otro lado, estudios de análisis de ADN en muestras fósiles de bisonte de 17.000 años de antigüedad han confirmado el diagnóstico e infección por el CTM (Rothschild et al., 2001). Otros estudios sugieren que la especie progenitora de *M. tuberculosis,* especie que forma parte del complejo, se originó hace unos 15.000 a 20.000 años atrás

(Sreevatsan et al., 1997), e incluso que puede tener una antigüedad de hasta 3 millones de años (Gutiérrez et al., 2005).

En el siglo V a.C., en la antigua Grecia, Hipócrates fue el primero en designar a la TB como phthisis, concretamente a la forma pulmonar, definiéndola como "*la enfermedad más grave de todas, la de curación más difícil y la más fatal*" (Daniel, 2006; Ledermann, 2003). En la edad media, la escrófula (actual TB linfática cervical), se describió como una nueva forma clínica de la TB, en la que se afectaban los nódulos linfáticos (NLs) cervicales. En Inglaterra y Francia, la enfermedad se conocía como "el mal del rey", y se creía que las personas afectadas podían curarse tras un toque real (Murray et al., 2016).

En el año 1865 se hicieron algunos de los primeros hallazgos de la TB, en el que Jean-Antoine Villemin demostró mediante experimentos animales, que la TB podía inocularse desde el bovino hacia el conejo y cobayas, observándose que el esputo de un animal enfermo podía infectar a un conejo (Sakula, 1982). Pero no fue hasta el 24 de marzo de 1882 cuando Robert Koch anunció públicamente en la reunión de la sociedad de Fisiología de Berlín el descubrimiento del bacilo tuberculoso, el cual por primera vez había sido aislado de animales con presencia de "tubérculos grises" en los pulmones y que habían muerto 4 semanas tras la infección. Es así, como más tarde se acuñó el término y se dio a conocer como el "bacilo de Koch" (Sakula, 1982, 1983).

Años después, Koch siguió investigando en búsqueda de la cura de la enfermedad. Fue así como en 1890 en un intento fallido por la cura, descubrió una sustancia a la que llamó tuberculina, una solución purificada de antígenos del bacilo tuberculoso presentes en el sobrenadante de un medio de cultivo tras su inactivación por calor, la cual podría utilizarse para el diagnóstico (Barberis et al., 2017; Daniel, 2006).

Posteriormente, en 1908, se desarrollaron las pruebas de la tuberculina por Clemens Freiherr Von Pirquet y Charles Mantoux, mientras que Florence Seibert desarrolló el derivado proteico purificado (PPD, del inglés *purified protein derivative*) (Barbier & Wirth, 2016; Daniel, 2006), avances que posteriormente han derivado en la actual práctica de la prueba de intradermotuberculinización (IDTB) con aplicación de

PPD. Más tarde, Albert Calmette y Camille Guérin desarrollaron la única vacuna registrada a fecha actual, basada en bacilos de *Mycobacterium bovis* vivos atenuados y la cual lleva el nombre de sus investigadores (BCG, bacilo de Calmette-Guérin) (Barbier & Wirth, 2016), disponible desde 1927 (Cardona, 2017) y que actualmente se sigue utilizando en distintos estudios de inmunoprofilaxis para determinar correlatos de protección e inmunidad (Aspatwar et al., 2022; Martins, 2021).

1.2. Importancia de la tuberculosis en salud pública

A lo largo de la historia, la TB se ha considerado como una de las plagas más antiguas de la humanidad, sugiriendo que *Mycobacterium tuberculosis* puede haber matado a más personas que cualquier otro patógeno microbiano (Daniel, 2006), y describiéndose como un patógeno humano de gran éxito, matando a casi 3 millones de personas cada año (Gutiérrez et al., 2005). Sin embargo, a pesar de que *M. tuberculosis* es el principal agente de la TB en humanos, no es posible diferenciar la sintomatología clínica de infecciones causadas por *M. bovis* (Cosivi et al., 1998), así como por otros miembros pertenecientes al CMT, y que son los principales responsables de su transmisión de los animales al hombre (zoonosis). *M. bovis*, se estima que es el responsable de la TB zoonósica, alcanzando hasta un 10 % de casos de TB en humanos (Organización Mundial de la Sanidad Animal, OMSA, 2022). Antiguamente estaba descrito que la transmisión de TB bovina (TBb) a los seres humanos se producía por la vía digestiva, principalmente por el consumo de productos lácteos contaminados, no pasteurizados (LoBue et al., 2003), pero hoy en día con la práctica de la pasteurización, la vía digestiva ha perdido importancia. Sin embargo, en la industria de la carne, la infección por vía aérea sigue siendo frecuente entre los trabajadores de los mataderos (Thoen et al., 2006). A pesar de esto, en países poco desarrollados como África, la población de riesgo que convive estrechamente en la interfaz ganado – humano tienen un mayor riesgo de contraer la enfermedad por *M. bovis*, debido al consumo de leche no pasteurizada y productos lácteos derivados de rebaños con TBb no controlada (Ayele et al., 2004). Al mismo tiempo, los pacientes inmunocomprometidos por

infección con el virus de la inmunodeficiencia humana (VIH) presentan una mayor susceptibilidad asociada a la coinfección con *M. tuberculosis*, la principal causa de TB en humanos (Michel et al., 2010; Valerga et al., 2005).

Según datos de la Organización Mundial de la Salud (OMS, 2023) en el año 2021, se diagnosticaron 10,6 millones de nuevos casos a nivel mundial y se recogieron 1,6 millones de muertes a causa de la TB. En la actualidad, según el reporte global de tuberculosis en 2022, hasta la pandemia de la COVID-19, la TB era la principal causa de muerte por un único agente infeccioso, por encima del VIH (OMS, 2022). Por lo tanto, la TB continúa siendo una de las enfermedades más importantes en salud pública a nivel mundial, cuyo nivel de prevalencia presenta marcadas diferencias dependiendo del área geográfica.

1.3. Clasificación y especies incluidas en el complejo *Mycobacterium tuberculosis*

El CMT está formado por un grupo de micobacterias pertenecientes al género *Mycobacterium* y a la familia *Mycobacteriaceae*, en la cual se han descrito más de 190 micobacterias, las que se caracterizan por ser bacterias Gram positivas y ácido alcohol resistentes (Dorronsoro & Torroba, 2007). Las micobacterias son bacilos relativamente cortos y delgados de 0,2 - 0,3 µm de ancho y 1,0 - 4,0 µm de largo, que poseen metabolismo oxidativo (aerobio) y crecimiento lento (16 – 20 horas) (Beste et al., 2009). Se caracterizan por tener una elevada proporción de lípidos (ácido micótico, fosfolípidos) y su pared celular consta de peptidoglicanos con ácido diaminopimélico, arabinosa y galactosa, lo que explica la resistencia a la decoloración con ácidos, después de ser teñidos con fucsina (Poole, 1997). Su ADN contiene una elevada proporción de guanina y citosina, lo que aumenta la estabilidad del ADN, siendo capaces de resistir la desecación y congelación, y de sobrevivir durante semanas o meses sobre objetos inanimados, siempre que estén protegidos de la luz solar, puesto que la luz ultravioleta y el calor (>65 ºC durante 30 minutos) las inactiva (Dorronsoro & Torroba, 2007; Poole, 1997).

Las micobacterias que conforman el CMT comparten genéticamente una secuencia idéntica del ARNr 16S y una identidad en nucléotidos superior al 99,9 % (Dorronsoro & Torroba, 2007; Mostowy & Behr, 2005). Hasta la fecha se han aislado un total de 12 micobacterias pertenecientes al CMT, las cuales reciben su nombre de acuerdo a la especie en la que se han aislado inicialmente, a tal forma que las 4 especies que tradicionalmente forman parte del CMT incluyen a *M. tuberculosis* conocido como el patógeno principal que afecta al humano (Barbier & Wirth, 2016), *M. africanum* que ha sido aislado de pacientes africanos (Castets et al., 1968), *M. microti* aislado de topillos (Mostowy & Behr, 2005) y *M. bovis* aislado del bovino (Karlson & Lessel, 1970). Dentro de estas especies, se considera que *M. tuberculosis* y *M. bovis,* son las especies más importantes del CMT, como agentes causantes de la TB humana y animal (Mohamed, 2020), pero también forman parte del mismo *M. caprae,* aislado de cabras (Aranaz et al., 2003), *M. bovis* BCG que como se ha comentado anteriormente corresponde a la cepa atenuada de *M. bovis* y que dio origen a la vacuna conocida como BCG (Daniel, 2006), *M. pinnipedi* aislado de pinnípedos (focas) (Cousins et al., 2003)*, M. canettii* aislado en pacientes en Francia, inicialmente, y en pacientes africanos posteriormente (Van Soolingen et al., 1997) , *M. suricattae* aislado de suricatas de vida libre y notificado por primera vez en el año 2002 (Parsons et al., 2013)*, M. orygis* (bacilo del oryx) el cual ha sido aislado de miembros de la familia bovidae, género oryx como gacelas, ciervos, antílopes y antílopes acuáticos, aunque podrían ser más las especies a las que afecta, además de a humanos de África y sur de Asia (Van Ingen et al., 2012), el bacilo del dassie descrito por primera vez en 1954 en damanes de El Cabo (*Provocatia capensis*) (N. Smith, 1965; Wagner et al., 1958) y *M. mungi* aislado de mangosta rayada (*Mungos mungo*) entre los año 2000 - 2010 (Alexander et al., 2010).

1.4. La tuberculosis animal y sus hospedadores

Como hemos puesto de relieve previamente, la TB es una enfermedad que afecta a una amplia gama de animales domésticos y salvajes, incluido el humano (Rodríguez-Campos et al., 2014), lo que la hace una enfermedad multihospedador.

El bovino es considerado el principal hospedador de *M. bovis*. Cousins, 2001; Palmer et al., 2007; Schiller et al., 2010). Sin embargo, dentro de los animales hospedadores se ha visto que afecta a otros animales domésticos como ovejas, cabras, equinos, camellos, perros, gatos, cerdos (Cardoso-Toset et al., 2015; Cousins, 2001; de Lisle et al., 1990; Pesciaroli et al., 2014) y alpacas (García-Bocanegra et al., 2010), entre otros.

Por otro lado, en la fauna silvestre también se ha notificado la infección en un abanico variado de especies, como el tejón (Corner et al., 2011, 2014), venado de cola blanca (Fitzgerald et al., 2000), jabalí (García-Jiménez et al., 2012), gamo (García-Jiménez et al., 2012), búfalo, bisonte, antílope, zorro, visón, hurón, rata, primate, tapir, elefante, sitatunga, rinoceronte, ardilla de tierra, nutria, topo, mapache, coyote y varios felinos depredadores como leones, tigres, leopardos y linces (Cousins, 2001; Fitzgerald & Kaneene, 2013; Mostowy & Behr, 2005).

En relación a los animales domésticos, y desde el punto de vista de la ganadería, la infección por *M. bovis* genera grandes pérdidas económicas debido a la disminución en la producción de los animales enfermos y el sacrificio de éstos, debido a las campañas de control y erradicación de la enfermedad (González Llamazares et al., 1999; Good et al., 2018; Michel et al., 2010; Mohamed, 2020; Rodriguez-Campos et al., 2014) Gracias a las mismas, la infección en los rebaños ha sido controlada en la mayoría de los países; sin embargo, la eliminación completa de la enfermedad es compleja, debido, entre otros factores, a que existe una infección persistente en los animales de vida silvestre, como por ejemplo el jabalí europeo y el ciervo rojo en España (Naranjo et al., 2008), los tejones europeos en el Reino Unido, los ciervos de cola blanca en diversas localizaciones de los Estados Unidos de América y zarigüeyas de cola de cepillo en Nueva Zelanda (OMSA, 2020).

Asimismo, se ha visto que tanto en España como en diferentes países europeos, la prevalencia de la enfermedad en el ganado bovino está directamente relacionada con la interacción de la fauna silvestre, principalmente el jabalí y el ciervo (Gortázar et al., 2005; Naranjo et al., 2008), especialmente en sistemas extensivos, en la cual no sólo se

ve afectado el ganado bovino, sino también otras especies de interés como el porcino e incluso también el ganado ovino o el caprino, lo cual es un factor de riesgo de la infección de TB (Corner, 2006). Las campañas de control y erradicación sobre el ganado bovino (y caprino), así como, la implantación de medidas de bioseguridad con respecto a la fauna silvestre, han conseguido que la prevalencia de la TB haya disminuido en las especies domésticas, tanto en el ganado bovino como en el porcino (Pesciaroli et al., 2014). En este sentido, cabe destacar que el ganado porcino se afecta principalmente por *M. bovis* (Parra et al., 2003; Pesciaroli et al., 2014) pero también es susceptible a la infección por *M. caprae* (Lipiec et al., 2019) e incluso otras especies del CMT.

En la cabra y ovejas se ha visto que la enfermedad puede estar causada por *M. bovis* y *M. caprae* (Álvarez et al., 2008a; Crawshaw et al., 2008; Marianelli et al., 2010; Muñoz Mendoza et al., 2012; Sharpe et al., 2010). Además, en cabras en régimen extensivo también se ha visto que pueden verse afectadas por *M. tuberculosis* (Kassa et al., 2012), lo que podría jugar un papel importante en los animales de vida libre (de Lisle et al., 2002; Fitzgerald & Kaneene, 2013), mientras que en las ovejas, aunque se ha visto que la incidencia de TB es baja (Jiménez-Martín et al., 2023) se pueden considerar como una fuente potencial de TB para los bovinos (Muñoz-Mendoza et al., 2015).

1.5. Situación de la tuberculosis animal en España

En España, la TBb continúa siendo una amenaza para la sanidad animal y la salud humana, además del importante impacto económico que supone en la producción de carne y leche. Según lo establecido en el Reglamento Delegado (UE) 2020/689 de la comisión de 17 de marzo de 2019, la TB animal es causada principalmente por *M. bovis*, *M. caprae* y *M. tuberculosis*, destacando entre ellas *M. bovis*, cuyo hospedador principal es el ganado bovino.

Para el control y erradicación de la TBb, el Ministerio de Agricultura, Pesca y Alimentación (MAPA) es el responsable de coordinar y gestionar los programas a nivel nacional(MAPA, 2023a). Las pruebas oficialmente establecidas para el control de la

enfermedad incluyen la prueba de la IDTB simple (IDTBS) y comparada (IDTBC), así como la prueba del interferon-gamma (IFN-γ), las cuales se describen en el Real Decreto 2611/1996, de 20 de diciembre, por el que establece la regulación de los programas nacionales de erradicación de enfermedades de los animales. En base a esto, y de acuerdo al resultado de la prueba de la IDTB, se establece una clasificación de las explotaciones en las diferentes comarcas a nivel nacional, las que se clasifican de la siguiente manera:

a) **Explotaciones bovinas del tipo T1**: las explotaciones en las que se desconocen los antecedentes clínicos y la situación en cuanto a la reacción de la prueba de tuberculina, en los dos últimos años.

b) **Explotaciones bovinas del tipo T2:** las explotaciones en las que se conocen los antecedentes clínicos, la situación en cuanto a la reacción de la tuberculina y en las que se efectúan pruebas de control de rutina para hacer pasar a dichas explotaciones al tipo T3. Éstas además se pueden subclasificar en:

- **Explotación bovina del tipo T2 negativa** (o no calificada a TB): aquella que, sin haber alcanzado aún la calificación de oficialmente indemne de TBb, todo el censo de la explotación, susceptible por su edad de ser examinado, haya superado, con resultado favorable, al menos una de las pruebas de diagnóstico previstas en él.
- **Explotación bovina del tipo T2 positiva:** aquella que, sin haber alcanzado aún la calificación de oficialmente indemne de TBb, al menos un animal, susceptible por su edad de ser examinado, no haya sido sometido a la totalidad de las pruebas de diagnóstico previstas en el (Real Decreto 1716/2000, 2000), o no las haya superado con resultado favorable.

c) **Explotaciones bovinas del tipo T3**: las explotaciones oficialmente indemnes de TB, según lo establecido en el (Real Decreto 1716/2000, 2000). Aquella que ha obtenido resultados negativos en 2 pruebas de IDTB separadas 6 meses como mínimo, habiéndose realizado la primera prueba al menos 6 meses después del sacrificio de los animales positivos. Se considerará como explotación

T3H como aquella que al menos en los 3 últimos años haya mantenido el estatus T3 sin ser retirado, de forma ininterrumpida.

d) **Explotaciones bovinas del tipo TS**: las explotaciones de tipo T3 a las que se les ha suspendido la calificación sanitaria, de conformidad con lo dispuesto en el Real Decreto 1716/2000, ya sea porque se hayan introducido animales con un estatus sanitario inferior, haya animales sospechosos de padecer alguna de las enfermedades objeto de campañas de saneamiento ganadero o hayan incurrido en acciones contrarias a la legislación vigente.

e) **Explotaciones bovinas del tipo TR:** las explotaciones de tipo T3 a las que se les ha retirado la calificación sanitaria, de conformidad con lo dispuesto en el Real Decreto 1716/2000 que, habiendo tenido asignada la calificación de oficialmente indemne o indemne, hayan realizado una última prueba con resultados positivos.

En cuanto a la prevalencia de la TBb en España, recientemente en junio del presente año, se ha publicado oficialmente el informe técnico sobre los resultados anuales de los programas de control y erradicación de la TBb en el año 2022 (MAPA, 2023b), donde del total de 101.501 rebaños investigados (99,1 % de cobertura), se observó positividad en 1.422 rebaños (1.424 en 2021), obteniendo así una prevalencia del rebaño de 1,40 %, muy cercano a lo obtenido en 2021 (1,48 %).

En relación al conjunto de rebaños positivos, se identificaron 815 nuevos casos positivos, lo que representa una incidencia de rebaño del 0,8 %. Esta cifra es ligeramente mayor en comparación con la prevalencia de animales positivos o el número de animales infectados en el año 2022 (Figura 1), que fue de 13.714 con una incidencia del 0,3 %.

El programa nacional de control y erradicación ha contribuido a un descenso moderado de la enfermedad en los últimos 15 años, notable hasta el año 2013. Aunque hubo un incremento en el indicador entre 2015 y 2016, a partir de 2017 se han registrado descensos anuales significativos, con la excepción del año 2022. Estos

avances demuestran los esfuerzos continuos y efectivos del programa para combatir la enfermedad.

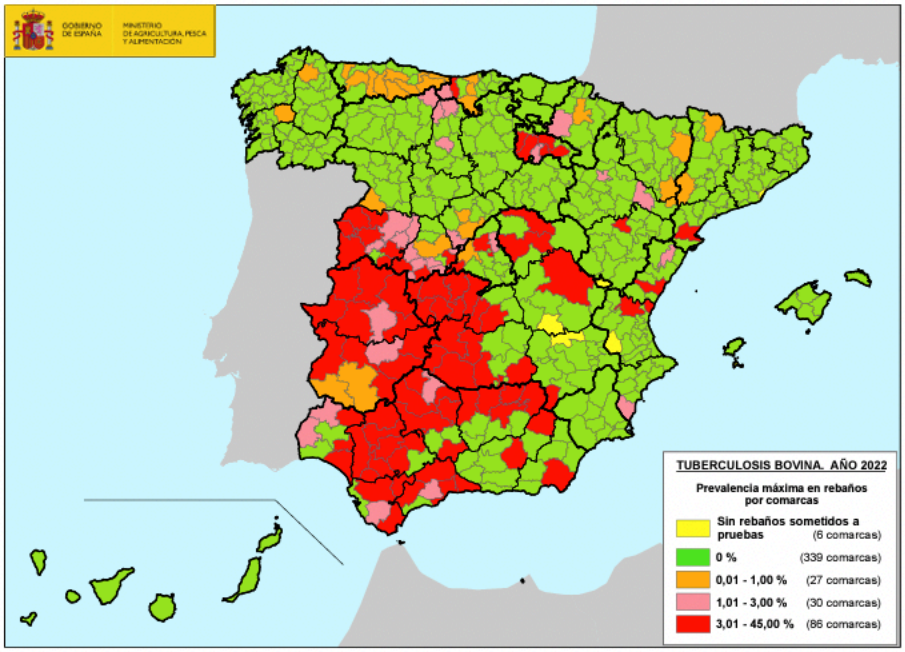

Figura 1. Mapa de prevalencia de TBb por comarcas en España en rebaños para el año 2022 *(MAPA, 2023a).*

En la figura 2 se pueden observar las comunidades autónomas que desde años anteriores se encuentran libres de TBb y que corresponden a Asturias, Canarias, Galicia y País Vasco. Además, recientemente la Comisión Europea ha publicado y declarado de estatuto libre de TBb a las comunidades autónomas de Baleares, Cataluña y Murcia, según se recoge en el Reglamento de ejecución 2023/150 publicado en el Diario Oficial de la Unión Europea (DOUE), por lo que se espera que, en un futuro, los programas de control y erradicación sigan avanzando y se puedan añadir nuevas regiones o provincias con el objetivo de declarar al país libre de TBb.

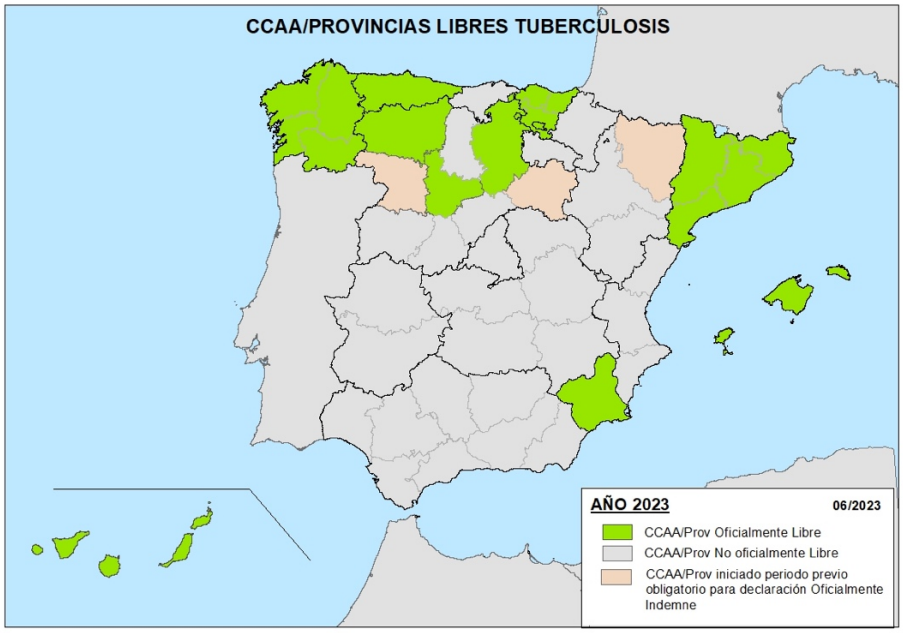

Figura 2. Mapa actualizado a junio de 2023 que indica las provincias oficialmente libres de TBb *(MAPA, 2023b).*

2. INMUNOPATOGENIA DE LA TUBERCULOSIS

2.1. Patogénesis de la tuberculosis en ganado bovino y porcino

La principal vía de entrada de la micobacteria en el organismo es la vía aerógena (Bermejo et al., 2007; Bezos et al., 2014; Parra et al., 2003; Pesciaroli et al., 2014), permitiendo mediante la inhalación de pequeñas gotas que contienen micobacterias, la llegada de éstas al tracto respiratorio y pulmones, produciendo la infección (Bermejo et al., 2007; Caswell & Williams, 2016; Neill et al., 1994). Aunque menos frecuente, la vía digestiva también puede ser una fuente de contagio a tener en cuenta en el ganado bovino, donde se han descrito infecciones transmitidas por el consumo de leche y/o pastos contaminados (Neill et al., 1994). En el caso del ganado porcino, tanto la vía aerógena como digestiva juegan un papel importante en la enfermedad (Cardoso-Toset et al., 2015), observándose una transmisión indirecta asociada al carácter omnívoro y al comportamiento natural de hozar de esta especie, produciéndose la infección tanto

al respirar en estrecho contacto con alimentos contaminados, como por vía digestiva por el consumo directo de estos alimentos o de cadáveres de animales infectados con TB (Parra et al., 2003). Otras vías menos frecuentes de transmisión de la enfermedad son la vía congénita (madre-feto) y la vía percutánea, teniendo en cuenta que las micobacterias se pueden eliminar también a través de la orina, secreciones vaginales, semen y heces (Bermejo et al., 2007; Cousins, 2001; Pritchard DG, 1988).

Una vez que se produce la inhalación de los aerosoles con bacterias del CMT, estas llegan al alvéolo pulmonar donde entran en contacto con los macrófagos alveolares pulmonares (MAPs) que intentarán fagocitar el bacilo con el objetivo de destruirlo (García et al., 2009). Sin embargo, en esta etapa, la supervivencia o destrucción del bacilo por parte del macrófago dependerá de varios factores, dentro de los que se encuentran: la capacidad infectiva del bacilo en sí, la calidad del aerosol y la carga bacteriana. Esto se debe a que no todos los animales enfermos serán capaces de generar gotitas con la capacidad de penetrar en el alvéolo de otro animal susceptible y generar la infección (Cardona, 2018). Por otro lado, los factores de virulencia de cada micobacteria que forma parte del CMT difieren entre sí (Corner et al., 2011), encontrándose micobacterias más virulentas que otras, lo que dependerá además de la especie hospedadora, ya que en las especies susceptibles se cree que la dosis necesaria para establecer la infección es menor. Además, una mayor carga bacteriana se asocia, normalmente, a una patología más grave y un curso más rápido de la enfermedad (Palmer, 2013). Por otro lado, al igual que en humanos, los animales inmunocomprometidos, sometidos a factores estresantes o que cursan con otras enfermedades debilitantes, tendrán una mayor dificultad para contener la micobacteria y serán más susceptibles a la enfermedad, mientras que los animales inmunocompetentes lograrán contener la infección y generar una respuesta inmunitaria protectora durante el resto de su vida (Bermejo et al., 2007; Risco et al., 2013, 2014; Rook & Hernandez-Pando, 1996).

Al llegar al alvéolo pulmonar, la micobacteria es internalizada en el interior del MAP a través de un proceso de endocitosis mediada por receptores de manosa

presentes en el macrófago (Kumar et al., 2015b) que se unen al lipoarabinomanano, un glucolípido presente en la superficie de las micobacterias y, a los receptores del complemento c3b que fijan las micobacterias opsonizadas (Bezos, 2009; McAdam et al., 2015; Schlesinger, 1993). Por otro lado, además de encontrarse con el MAP, los aerosoles que contienen las micobacterias entran en contacto con la sustancia tensioactiva (o también llamada surfactante pulmonar) producida por los neumocitos tipo II, la cual aporta protección frente a agentes patógenos como virus y bacterias (Arcos et al., 2011; Cardona, 2016). En base a esto, previamente se ha descrito que la calidad de la sustancia surfactante puede modular la interacción inicial de *M. tuberculosis* con el MAP (Arcos et al., 2011; Ferguson & Schlesinger, 2000); de este modo, la sustancia surfactante, podría destruir la pared lipofílica de la micobacteria dejándola vulnerable para ser destruida por el MAP una vez que es fagocitada (Cardona, 2018).

Para internalizar la micobacteria, el macrófago emite pseudópodos dando lugar a la formación de un fagosoma, proceso que es dependiente de la polimerización de los filamentos de actina, por lo que no es de extrañar que las señales que desencadenan este proceso sean similares a las implicadas en la quimiotaxis (Kumar et al., 2015b). En la infección con *M. tuberculosis*, se ha visto que esto impulsa la actividad patógena del bacilo, secretando ESAT-6 (del inglés *early secretory antigenic target-6*) y CFP-10 (del inglés *culture filtrate protein 10-kDa*), péptido esencial que impide la unión fagosoma-lisosoma y apoptosis, favoreciendo la supervivencia del bacilo en el citoplasma del macrófago (Mitchell et al., 2016), por lo que el bacilo se multiplicaría libremente dentro de fagosoma aproximadamente cada 24 horas (Cardona, 2018), bloqueando la fusión fagolisosoma mediante la inhibición de las señales de Ca^{2+} y la captación y ensamblaje de las proteínas que participan en la fusión entre el fagosoma y el lisosoma (McAdam et al., 2015), como el reclutamiento de enzimas hidrolíticas lisosomales, producción de especies reactivas de oxígeno y nitrosas, apoptosis y evasión de la presentación de antígeno (Echeverria-Valencia et al., 2018). Esto generará la ruptura del macrófago, lo que dará lugar a una serie de eventos que atraerán por quimiotaxis a monocitos y células inflamatorias al sitio de infección (García et al., 2009). A continuación, los

monocitos se diferenciarán a macrófagos para fagocitar nuevamente las micobacterias con el objetivo de destruirlas (García et al., 2009). Si estos nuevos macrófagos no son capaces de eliminar la micobacteria, el resultado será la formación de un granuloma tuberculoso o "lesión primaria" en el pulmón, en la cual se producirán una serie de interacciones complejas entre las células inmunitarias del hospedador y las micobacterias, con el objetivo de intentar controlar la infección (Caswell & Williams, 2016) (Figura 3).

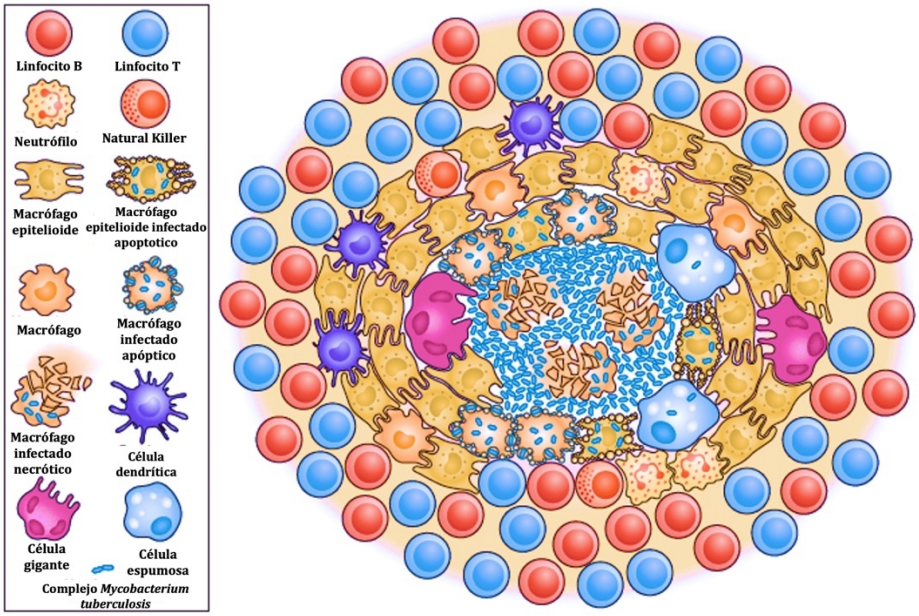

Figura 3. Ilustración de las células presentes en el desarrollo del granuloma tuberculoso *(Modificado de Ramakrishnan, 2012).*

Si la enfermedad progresa, los bacilos que logran escapar del MAP, llegarán al intersticio, donde serán transportados por capilares vasculares y/o linfáticos hasta alcanzar el tejido linfoide asociado a bronquios y los NLs (Orme & Cooper, 1999), infectándose los macrófagos y células dendríticas de los NLs, lo que dará lugar a una respuesta inflamatoria en el NL generando una ~~(~~linfadenitis~~)~~ (Cardona, 2018; Caswell & Williams, 2016). Cuando la enfermedad se desarrolla, produce lesiones en el pulmón y el NL, dando lugar a lo que se conoce como "complejo primario completo" (Ghon)

(Caswell & Williams, 2016; López & Martinson, 2021; Neill et al., 1994; Thoen & Barletta, 2006), mientras que si sólo se observa lesión en NL regional se habla de "complejo primario incompleto" (Balseiro et al., 2020). Por otro lado, en animales enfermos, y especialmente en aquellos que están inmunocomprometidos, los bacilos pueden alcanzar la circulación sistémica y distribuirse en el parénquima de órganos tales como pulmón, hígado, bazo, riñón, testículo, glándula mamaria, médula ósea y meninges, dando lugar a la denominada "tuberculosis miliar" (por su similitud con las semillas de mijo) (Caswell & Williams, 2016; Karlson, 1980; López & Martinson, 2021; Neill et al., 2001; Scanlan, 1991). Cuando la diseminación de la micobacteria se produce por vía linfohemática, aparecen nódulos aislados o en racimos que afectan las serosas del pericardio, pleuras y peritoneo, dando origen al cuadro conocido como *tisis* perlada (Balseiro et al., 2020; Karlson, 1980; López & Martinson, 2021).

En cuanto a la distribución de las lesiones, numerosos trabajos coinciden que los tejidos que se afectan con mayor frecuencia en el caso del bovino corresponden a los NLs retrofaríngeos, traqueobronquiales y mediastínicos y, menos frecuentemente en las tonsilas y los NLs mandibulares, parotídeos y mesentéricos (Caswell & Williams, 2016; Comer, 1994; Palmer et al., 2007; Sánchez-Carvajal et al., 2021), mientras que en el porcino se ha visto asociado con frecuencia a los NLs mandibulares y retrofaríngeos, afectando ocasionalmente al hígado, bazo y pulmones (Di Marco et al., 2012; Parra et al., 2003). Sin embargo, se debe tener en cuenta, que el ganado bovino al estar inmerso en los programas de control y erradicación de la TBb (Real Decreto 2611/1996, 1996) está sometido a sacrificios temprano, por lo que es más común observar lesiones localizadas, además en infecciones experimentales con CMT, se ha visto que es más factible encontrar lesiones generalizadas afectando a otros órganos (López & Martinson, 2021; Palmer et al., 2007, 2019).

2.2. Respuesta inmunitaria y desarrollo del granuloma tuberculoso

La respuesta inmunitaria y el desarrollo del granuloma tuberculoso juegan un papel importante en la comprensión de la infección por el CMT. En especies domésticas

y específicamente en el bovino, se han llevado a cabo diferentes estudios (Buddle et al., 2009; Cassidy, 2008; Palmer et al., 2007; Pollock & Neill, 2002; Schiller et al., 2010; Waters et al., 2011) para comprender mejor la respuesta inmunitaria de los animales frente a la TB, así como diferentes pruebas diagnósticas (Bezos, 2011). Dentro de estos aspectos, la respuesta inmunitaria de base celular (CMI, del inglés *Cell-mediated immune responses*) ha sido una de las más estudiadas en TB, puesto que es la primera respuesta en establecerse (de la Rua-Domenech et al., 2006; Palmer & Waters, 2006; Pollock & Neill, 2002; Schiller et al., 2010).

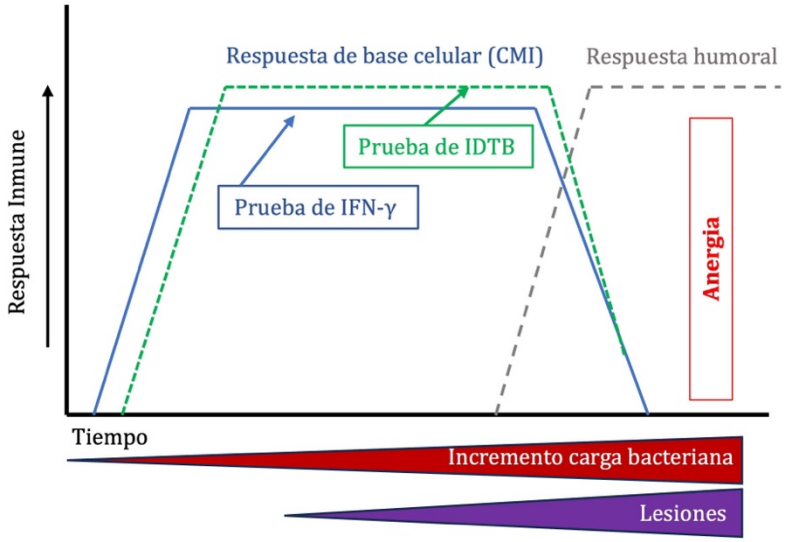

Figura 4. Representación del espectro de respuestas inmunitarias en el bovino tras la infección por M. bovis y respuestas a las pruebas de IDTB e IFN-γ *(Modificado de de la Rua et al., 2006).*

Tal y como se muestra en la figura 4, inicialmente se establece una respuesta CMI, mientras que la respuesta humoral de anticuerpos se desarrolla a medida que aumenta la carga bacilar. En la enfermedad avanzada, se puede producir un estado de "anergia", en el que no se detecta CMI. Los cambios patológicos iniciales se asocian a la aparición de respuestas CMI y la patología aumenta a medida que la enfermedad progresa.

En esta enfermedad, tiene que considerarse que existe una compleja interacción entre la respuesta inmunitaria innata y adaptativa, estableciendo un sistema

interactivo y cooperativo (Figura 5). Así, la respuesta inmunitaria innata activa al sistema inmunitario adquirido en respuesta a la infección, y además, actúa para eliminar a las micobacterias (Jagatia & Tsolaki, 2021; Pollock et al., 2005; Toche, 2012). La primera es una respuesta más rápida en la cual se ven involucradas barreras físicas y químicas (epitelios y enzimas), células fagocíticas (neutrófilos y macrófagos), células asesinas naturales (NK, del inglés *Natural Killer*), sistema del complemento, citoquinas y receptores tipo Toll (TLR, del inglés *Toll-like receptors*) (Dranoff, 2004; Pollock et al., 2005; Snyder, 2021; Toche, 2012), mientras que en la respuesta adaptativa existe una mayor implicación de los linfocitos T, los cuales desempeñan un papel fundamental en la producción de anticuerpos, manifestando una hipersensibilidad de tipo retarda (DTH, del inglés *delayed-type hypersensitivity*) (Cassidy et al., 1998; de la Rua-Domenech et al., 2006; Jagatia & Tsolaki, 2021; Neill et al., 2001; Pollock et al., 2005; Pollock & Neill, 2002; Warren et al., 2017).

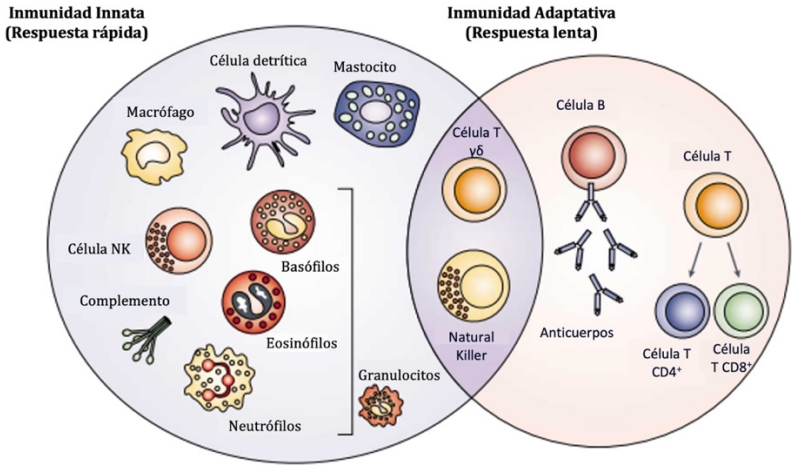

Figura 5. Células presentes en la respuesta inmunitaria innata y adaptativa *(Modificado de Dranoff, 2004).*

2.2.1. Respuesta inmunitaria innata

La respuesta inmunitaria innata es la primera línea de defensa contra la infección, incluye respuestas rápidas y generales que no dependen del reconocimiento específico

del patógeno (Figura 6). Sin embargo, juegan un papel crucial en las etapas iniciales de la defesa del organismo (Snyder, 2021). En la TB, las células fagocíticas, como los macrófagos, juegan un papel fundamental, puesto que establecen el primer contacto entre el sistema inmunitario innato del animal y la micobacteria (Bezos, 2011). En el caso de una infección por vía aerógena, una vez que la micobacteria supera las barreras físicas de protección del animal (epitelios, pH), ingresa al alvéolo pulmonar, donde es fagocitada por los MAPs para destruirlas a través de la formación de fagolisosomas (García et al., 2009), lo que es posible gracias al reconocimiento antigénico y la fagocitosis de la micobaceria a través de los diferentes receptores de las células presentadoras de antígenos (APCs, del inglés *antigen presenting cells*) (Bezos, 2009).

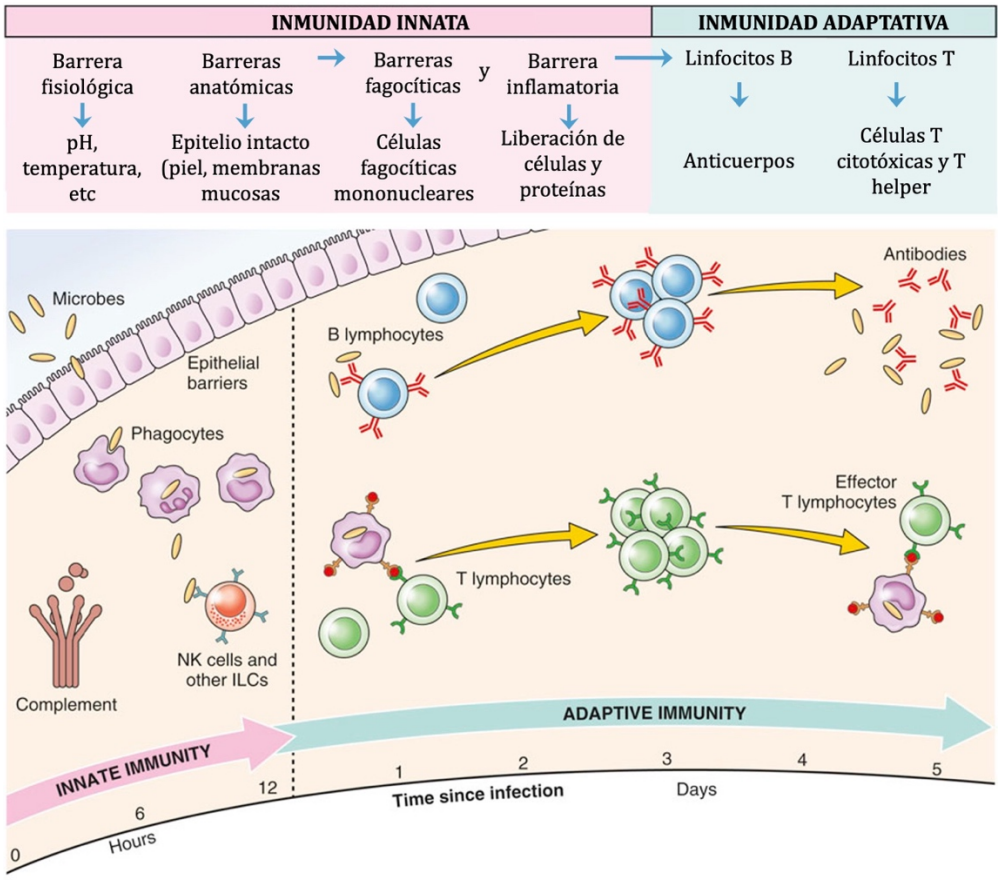

Figura 6. Mecanismos involucrados en la respuesta inmunitaria innata (inespecífica) y adaptativa (específica) *(Modificado de Snyder 2021).*

La figura 7 representa un esquema de los receptores de las APCs implicados en el reconocimiento de patógenos, propuesto por Bezos et al. (2009), en el que se detalla como la micobacteria, cuando está opsonizada, puede unirse a las APC a través de receptores del complemento. En el caso de que la micobacteria no esté opsonizada, como ocurre en el primer encuentro con el patógeno, el proceso se lleva a cabo mediante receptores de manosa, que reconocen la manosa y la fructosa en la superficie de la micobacteria, o a través de los receptores scavenger, que tienen la función de reconocer lipoproteínas de baja densidad.

Como se indica en la figura 7, la destrucción de la micobacteria en los fagolisosomas, activa una quinasa asociada al receptor de la interleuquina-1 (IL-1R-associated kinase-IRAK), la cual, a su vez, activa el factor de transcripción nuclear kappa B (NF-kB) y desencadena la liberación de diversas citoquinas.

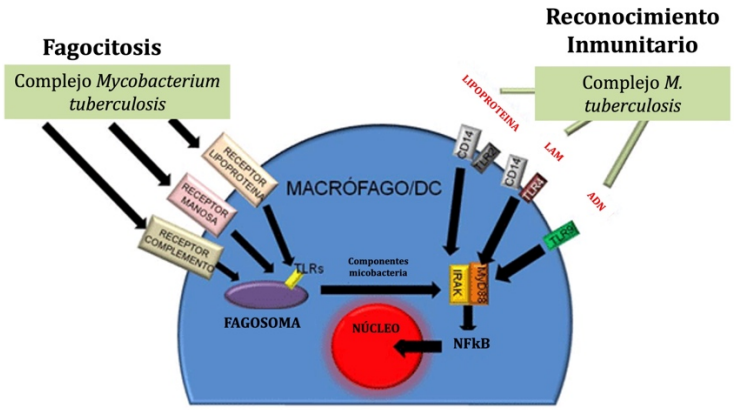

Figura 7. Esquema de los receptores de las células presentadoras de antígeno implicados en el reconocimiento inmunitario y la fagocitosis de las micobacterias del CMT *(Modificado de Bezos, 2009).*

De manera simultánea, los TLRs presentes en la membrana de las APC se activan, involucrando a la proteína MyD88 (del inglés *myeloid differentiation protein 88*) como intermediaria entre los TLR e IRAK, y esto es esencial para la activación de las APC inducida por micobacterias. La participación de los TLR funcionales en la membrana

de las APC y la formación de fagolisosomas son tan cruciales que la activación de las APC no ocurriría sin ellos, incluso cuando se produce la fagocitosis.

2.2.2. Respuesta inmunitaria adaptativa

La respuesta inmunitaria adaptativa o respuesta inmunitaria específica, se desarrolla después de la respuesta innata y es específica para el patógeno. En la TB, los linfocitos T y B desempeñan un papel crucial. Los linfocitos T colaboradores ($CD4^+$) coordinan la respuesta inmunitaria al interactuar con los macrófagos y liberar citoquinas que amplifican la respuesta. Los linfocitos T citotóxicos ($CD8^+$) pueden atacar directamente las células infectadas por *M. tuberculosis*, mientras que los linfocitos B producen anticuerpos que pueden ayudar en la opsonización y eliminación de bacterias (McAdam et al., 2015; North & Jung, 2004; Ramakrishnan, 2012).

2.2.2.1. Respuesta inmunitaria de base celular (CMI)

La CMI es inducida por macrófagos activados y es detectada por primera vez a los 14-28 días después de la infección (Caswell & Williams, 2016; García et al., 2009). Los linfocitos T son los protagonistas clave de esta respuesta, especialmente los linfocitos T $CD4^+$. Estas células reconocen fragmentos de proteínas bacterianas presentadas por las APCs, como los macrófagos. La activación de los linfocitos T $CD4^+$ y T $CD8^+$ conducen a la liberación de citoquinas como el IFN-γ, que estimula la actividad de los macrófagos y refuerza la respuesta inmunitaria (Figura 8) (Gordon & Martinez, 2010; Liu et al., 2017; Sica et al., 2015).

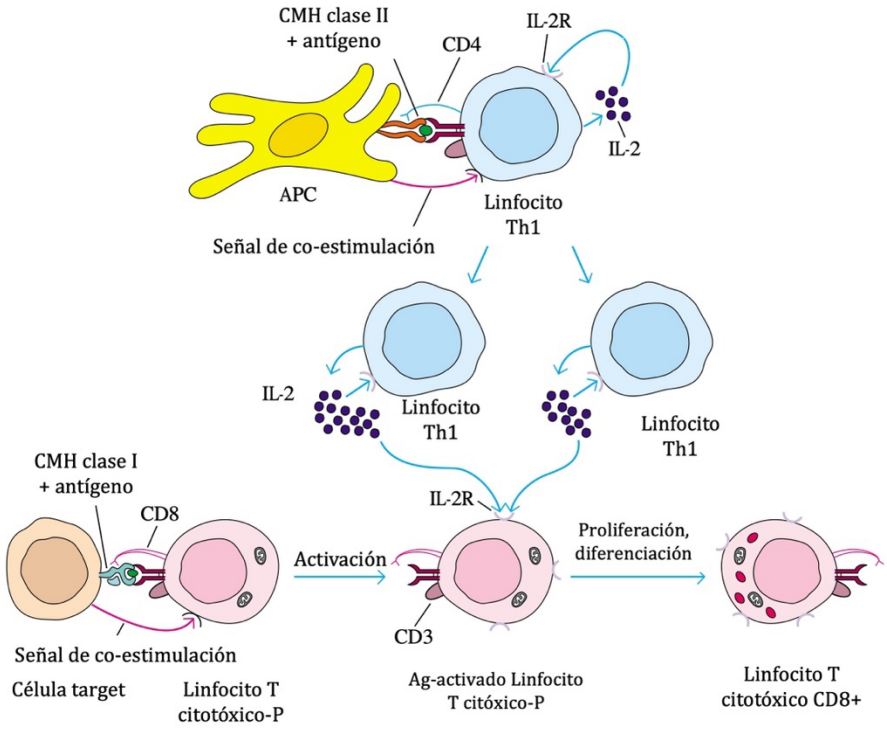

Figura 8. Linfocitos T CD4⁺ y CD8⁺ en la respuesta inmunitaria T colaboradora tipo 1 (Th1) (Modificado de Osborne et al., 2007).

Los linfocitos T CD8⁺, están restringidos al complejo mayor de histocompatibilidad de clase I (CMH-I), mientras que los linfocitos T CD4⁺ al CMH de clase II (CMH-II). La respuesta inmunitaria mediada por linfocitos T CD8⁺ puede dividirse en dos fases, que reflejan diferentes aspectos de la respuesta. En la primera fase, los linfocitos T CD4⁺ secretan citoquinas específicas (IFN-γ y TNF-α [del inglés tumour necrosis factor α]), que estimulan la respuesta T colaboradora de tipo 1 (Th1), lo que activa y diferencia los linfocitos T en linfocitos T efectores funcionales. En la segunda fase, los linfocitos T CD8⁺ son activados por las señales proporcionadas por los linfocitos T CD4⁺ y las células dendríticas. Una vez activados, los linfocitos T CD8⁺ se dividen y se diferencian en células T citotóxicas efectoras, lo que les lleva a destruir las células infectadas por patógenos intracelulares como el CMT (Osborne et al., 2007).

2.2.2.2. Hipersensibilidad de tipo retardada (DTH)

La DTH (Figura 9) es una reacción inmuninaria exagerada que ocurre en el sitio de la infección debido a la exposición repetida a antígenos. Fue descrita en 1890 por Robert Koch, el cual observó que al inyectar por vía intradérmica un infiltrado derivado de cultivo de micobacterias a individuos infectados con *M. tuberculosis,* desarrollaban una reacción inflamatoria localizada a la cual llamó "reacción a la tuberculina" (Kindt et al., 2007). Se basa en la respuesta de linfocitos T sensibilizados y es un indicador de la inmunidad previa o la infección latente (de la Rua-Domenech et al., 2006; Pollock & Neill, 2002).

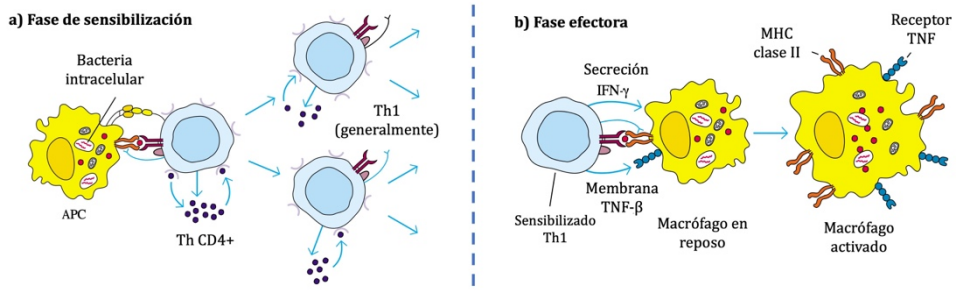

Figura 9. Hipersensibilidad de tipo retartada (DTH) o tipo IV. *(a) En la fase de sensibilización tras el contacto inicial con el antígeno (péptidos derivados de bacterias intracelulares, como CMT), los linfocitos T proliferan y se diferencian en linfocitos Th1. Las citoquinas secretadas por los linfocitos T se muestran con puntos azul oscuro. (b) En la fase efectora tras la exposición de los linfocitos Th1 sensibilizados al antígeno, secretan una variedad de citoquinas y quimioquinas. Estos factores atraen y activan macrófagos y otras células inflamatorias inespecíficas. Los macrófagos activados son más eficaces en la presentación del antígeno, perpetuando así la respuesta DTH, y funcionan como células efectoras primarias en esta reacción (Modificado de Osborne et al., 2007).*

La DTH se inicia con una primera fase de sensibilización que se produce una a dos semanas después del contacto inicial con el antígeno, durante la cual las APCs participan en la activación de la reacción de DTH, entre ellas macrófagos y células de Langerhans presentes en la epidermis, que captan el antígeno que entra por la piel y lo transportan hasta los NLs regionales, en los que este antígeno activa a los linfocitos T.

En esta fase de sensibilización se activan principalmente linfocitos T $CD4^+$ (Th1), pero en algunos casos también se activan linfocitos T $CD8^+$ (Figura 9a). La exposición repetida al antígeno induce la fase efectora (Figura 9b) la cual se evidencia a partir de las 24 horas después del segundo contacto con el antígeno; alcanzando el máximo 48 a 72 horas después del segundo contacto. Durante esta fase los linfocitos Th1 secretan diversas citoquinas que reclutan y activan macrófagos y otras células inflamatorias inespecífcas (Kindt et al. 2007).

En una segunda etapa, alrededor de las 3 a 12 semanas desde la infección, se produce la fase crónica de la enfermedad, denominada infección latente, que implica la supervivencia de los bacilos en los macrófagos y una respuesta Th1 (García et al., 2009; Jagatia & Tsolaki, 2021). En primer lugar, los linfocitos T $CD4^+$ colaboradores secretan citoquinas como la IL-2, que es un factor de crecimiento que actúa sobre los linfocitos T estimulando su proliferación, lo que lleva a un aumento del número de linfocitos específicos frente al antígeno. A su vez inducen la secreción de IFN-ɣ para activar a los macrófagos iniciando así una respuesta Th1 (Kumar et al., 2015a; Maison, 2022). En ratones se ha visto que la velocidad de esta respuesta por parte de los linfocitos T es más rápida cuando existe una carga bacteriana alta (Vilaplana et al., 2014). Esto permitirá la maduración del fagolisosoma en los macrófagos, con lo que las bacterias son expuestas a un medio ácido y oxidante letal. Seguidamente el macrófago estimula la expresión de la enzima óxido nítrico sintetasa por la cual producirá óxido nítrico, el cual se combina con otros agentes oxidantes y da lugar a compuestos reactivos nitrogenados para la destrucción de las micobacterias (Kumar et al., 2021; McClean & Tobin, 2016). Finalmente, el IFN-γ estimula la autofagia, un proceso que consiste en la captación y posterior destrucción de orgánulos dañados y de bacterias intracelulares como las micobacterias del CMT (McClean & Tobin, 2016).

Además, los macrófagos activados liberarán TNF-α, el cual induce la diferenciación de los macrófagos en células epitelioides y continúa reclutando más monocitos, los que además por alguna causa que aún es desconocida podrán fusionarse para formar células gigantes multinucleadas (MNGCs, del inglés *multinucleated giant cells*) (Kumar

et al., 2021; Palmer et al., 2022). Es así como se sigue desarrollando el granuloma tuberculoso para tratar de contener la micobacteria (Palmer et al., 2022; Ramakrishnan, 2012). Las células involucradas en la formación del granuloma (Figura 10) incluyen linfocitos Th1, linfocitos T reguladores (Tregs), células NK, linfocitos B, MNGCs, células dendríticas, neutrófilos, macrófagos, macrófagos espumosos y macrófagos epitelioides (Flynn et al., 2011; García-Jiménez, Salguero, et al., 2013; Maison, 2022; Palmer et al., 2016; Ramakrishnan, 2012; Wangoo et al., 2005).

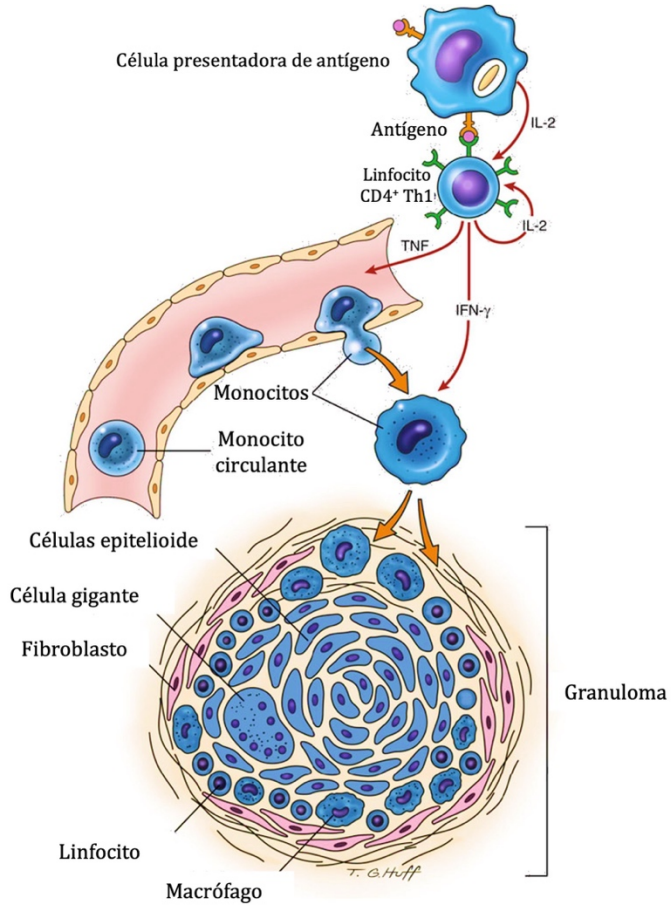

Figura 10. Formación del granuloma tuberculoso en una reacción de hipersensibilidad retardada o tipo IV *(Modificado de Ackermann 2021).*

En el desarrollo del granuloma, a medida que avanza la enfermedad y se cronifica, se destruyen tanto micobacterias como tejido, lo que genera una necrosis caseosa

(Maison, 2022), que suele observarse alrededor de las 6 semanas después de la infección en bovinos (Palmer et al., 2007). Se ha visto que el ambiente hipóxico dentro del granuloma restringe temporalmente el crecimiento de la micobacteria (Maison, 2022; Ramakrishnan, 2012) y que la necrosis caseosa inhibe el crecimiento extracelular, lo que conlleva a que la infección se convierta en estacionaria o latente (García et al., 2009). Sin embargo, también se ha descrito que esta hipoxia sirve como fuente de nutrientes y barrera protectora para este patógeno a través del aumento de la angiogénesis en el granuloma (Maison, 2022), ya que la infección de los macrófagos desencadena la inducción de factor de crecimiento endotelial, lo que se traduce en el desarrollo de nuevos vasos aberrantes alrededor del granuloma, lo que sería beneficioso para la proliferación del patógeno dentro de los granulomas (Polena et al., 2016; Uusi-Mäkelä & Rämet, 2018).

A medida que las células inmunitarias se acumulan en el sitio de la infección, se desarrolla el granuloma tuberculoso o "hallmark lesion" (Figura 10), la lesión característica de la TB (Kemal et al., 2019; Ramakrishnan, 2012), en respuesta a una estimulación antigénica crónica (Palmer et al., 2022).

Histopatológicamente, el granuloma ha sido previamente descrito y categorizado en cuatro estadios diferentes (I - IV), de acuerdo-con su composición celular, tamaño, y la presencia de fibrosis y necrosis (Wangoo et al., 2005), en el cual diferentes estudios han seguido esta clasificación con pequeñas modificaciones de acuerdo con la especie evaluada (Cardoso-Toset, et al., 2015; García-Jiménez, et al., 2013; Larenas-Muñoz et al., 2022; Turner et al., 2003). A modo general, dentro de la clasificación de los 4 estadios del granuloma se establece lo siguiente: estadio I (inicial), se caracterizan por la presencia de abundantes macrófagos epitelioides con presencia de linfocitos en la periferia, neutrófilos y, en ocasiones pueden observarse MNGCs tipo Langhans, las que se caracterizan por tener varios núcleos dispuestos en forma de herradura en la periferia. No presentan necrosis ni tejido conectivo; estadio II (sólido), se caracterizan por macrófagos epitelioides rodeados por una fina cápsula de tejido conjuntivo, en donde puede haber infiltrado de neutrófilos y linfocitos junto con MNGCs. En este

estadio, se observan los primeros indicios de necrosis, aunque no siempre ocurre; estadio III (necróticos), se caracterizan por tener un centro necrótico caseoso que puede tener pequeños focos de mineralización, rodeado por una zona de macrófagos epitelioides interpuesto con linfocitos y algunas MNGCs, las cuales pueden estar presentes o no. Externamente, están capsulados con una capa más gruesa de tejido conectivo fibroso; estadio IV (necrosis y mineralización), se caracterizan por granulomas coalescentes con una encapsulación fibrosa completa y necrosis central extensa con mineralización, rodeada de una delgada capa de macrófagos epitelioides y/o MNGCs, aunque éstas últimas suelen ser menos habituales (Caswell & Williams, 2016; Hughes & Tobin, 2022; Johnson et al., 2006; Palmer et al., 2022; Ramakrishnan, 2012; Wangoo et al., 2005) (Figura 11).

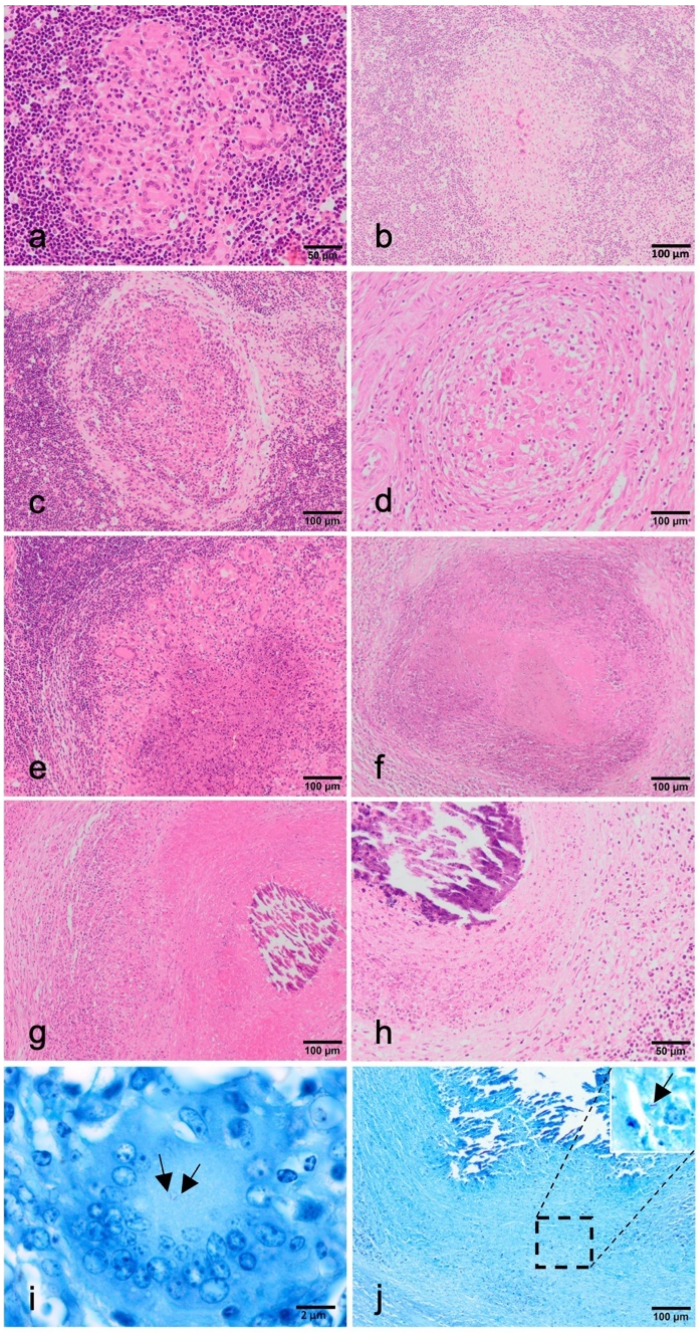

Figura 11. Estadios de granulomas tuberculosos en NLs de bovino (columna izquierda y porcino (columna derecha) infectados con el CMT (*a y b) Estadio I (Inicial). H&E 50 y 100 µm respectivamente. (c y d) Estadio II (sólido). H&E 100 µm. (e y f) Estadio III (necrosis mínima). H&E 100 µm. (g y h) Estadio IV (necrosis y*

mineralización). H&E 50 y 100 µm. (j) Célula gigante con presencia de BAAR (flecha) ZN 2 µm. (j) Centro necrótico con presencia de BAAR, inset: BAAR, ZN 2 µm.

2.2.3. El macrófago: polarización y respuesta de citoquinas

El macrófago es una célula fagocítica mononuclear del sistema inmunitario que se encarga principalmente de la fagocitosis y destrucción de microorganismos patógenos y desechos celulares (Ackermann, 2021; Cardona, 2016). Derivan de los monocitos de la médula ósea, algunos circulan por la sangre mientras que otros se localizan en el tejido de forma fisiológica. En el pulmón se localizan en los septos alveolares y alvéolos, como MAPs, y en algunas especies como el ganado bovino y porcino también hay una población de macrófagos intravasculares pulmonares (MIPs). En los NLs, estos se encuentran como macrófagos libres y fijos (Ackermann, 2021), principalmente a nivel de los senos subcapsulares y medulares, lo que facilita su exposición a antígenos (Snyder, 2021). En una respuesta inflamatoria, rápidamente en 12 a 48 horas, se produce una migración de los monocitos desde el torrente sanguíneo a los tejidos, diferenciándose hacia diferentes tipos de macrófagos: activados, epitelioides, espumosos o MNGCs, dependiendo de las características biológicas del agente desencadenante y del tipo de respuesta inflamatoria que induzca (Ackermann, 2021).

En la infección frente al CMT, el macrófago desempeña un papel fundamental, puesto que es la célula diana donde sobrevive y se replica la micobacteria (Caswell & Williams, 2016). El macrófago se encarga de fagocitarla, lo que desencadena una cascada de eventos que incluyen procesado y presentación de antígeno, producción de citoquinas y formación del granuloma tuberculoso (Dannenberg, 1994; Fernández et al., 2017; J. L. Flynn et al., 2011; Palmer et al., 2022). El macrófago es la célula principal en todos los estadios del granuloma (I-IV), estando presente en diferentes cantidades (Wangoo et al., 2005), ya que se ha visto que su porcentaje disminuye a medida que avanza el estadio del granuloma (Aranday-Cortes et al., 2013).

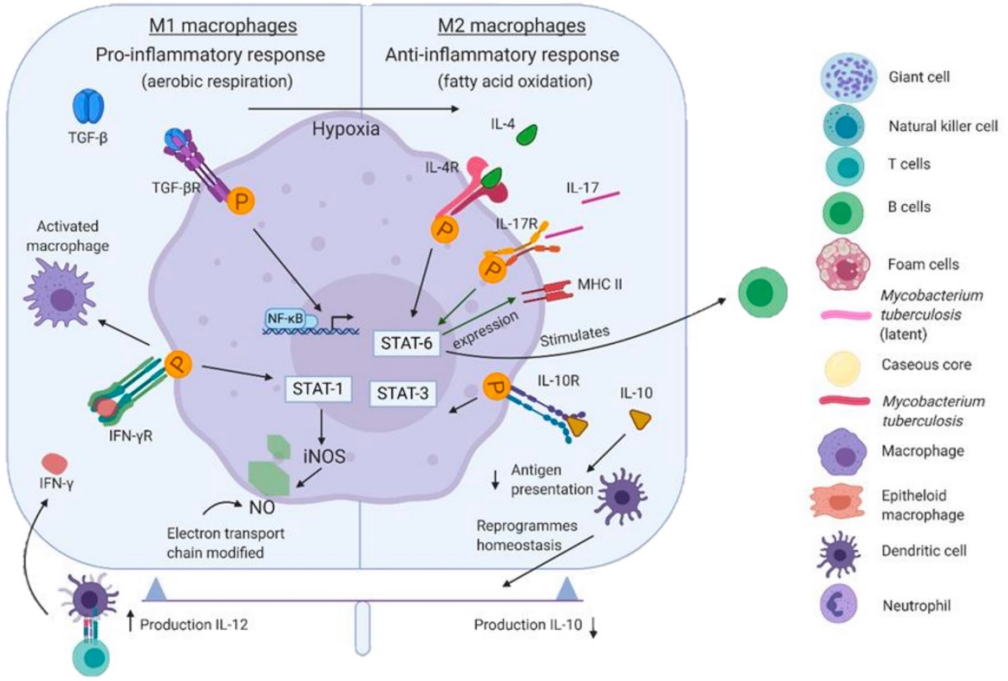

Figura 12. Polarización de macrófagos M1 y M2 *(Modificado de Jagatia & Tsolaki, 2022). La polarización de macrófagos en M1 y M2 es equilibrada por el huésped para gestionar la infección crónica. Estos grupos de macrófagos son distintos; los macrófagos M1 promueven una respuesta proinflamatoria mediante la respiración glucolítica, mientras que los macrófagos M2 promueven una respuesta antiinflamatoria.*

El macrófago es una célula versátil que poseen una gran plasticidad, con capacidad de adoptar diferentes estados funcionales y características fenotípicas en respuesta a señales procedentes del microambiente en el que se encuentre (Gordon & Martinez, 2010; Shapouri-Moghaddam et al., 2018). Los macrófagos activados clásicamente o macrófagos M1 (pro-inflamatorios) son efectores clave de la respuesta del hospedador frente a las bacterias intracelulares y producen una respuesta Th1 y Th17 (Figura 12). La activación de estos macrófagos está inducida por la expresión de citoquinas como el TNF-α, IFN-γ o por estímulos microbianos como los lipopolisacáridos de la membrana (Gordon & Martinez, 2010; Liu et al., 2017; Sica et al., 2015). Una vez activados, los macrófagos M1 puede dar lugar a la secreción de interleuquina-1β (IL-

1β), IL-6, factor estimulante de colonias de granulocitos y monocitos (GM-CSF, del inglés *Granulocyte macrophage-colony stimulating factor*) y la producción de NO (Gordon & Martinez, 2010; Liu et al., 2014). En contraste, los macrófagos M2 (anti-inflamatorios) activados alternativamente, son células con escasa capacidad de presentación antigénica y supresoras de la respuesta Th1, son inducidos por IL-4 e IL-13, así como por IL-10 y TGF-β (Gordon & Martinez, 2010; Liu et al., 2014; Shapouri-Moghaddam et al., 2018). En función de diferentes estímulos y cambios transcripcionales, los macrófagos M2 pueden subdividirse en diferentes subconjuntos (M2a, M2b, M2c, M2d) que son activados por diferentes estímulos (Ge et al., 2021; Klopfleisch, 2016; Ma et al., 2022). Se ha demostrado que estas poblaciones adicionales de macrófagos desempeñan funciones importantes en el mantenimiento del estrecho equilibrio entre la patología exacerbada y el control del crecimiento de las micobacterias (Liu et al., 2017). Aunque los macrófagos de tipo M1 y M2 aún no se han caracterizado completamente en el ganado bovino (Palmer et al., 2022), se sabe que existen poblaciones de macrófagos con fenotipos pro- y anti-inflamatorios, que se distribuyen espacialmente dentro del granuloma, en donde se ha observado que los macrófagos cercanos al centro necrótico son pro-inflamatorios y los situados más periféricamente son anti-inflamatorios (Marakalala et al., 2016). En este contexto, en bovinos se ha visto que la expresión de iNOS, marcador M1, disminuye a medida que progresa la enfermedad (Palmer et al., 2007), mientras que en ratones infectados con *M. tuberculosis* se ha visto que macrófagos deficientes en arginasa-1 (Arg1), enzima distintiva de los macrófagos M2, demuestran una mejor protección frente a la micobacteria (Kasmi et al., 2009).

2.2.4. Células epitelioides y células gigantes multinucleadas tipo Langhans (MNGCs)

Como se ha visto en la sección anterior, las células epitelioides y las MNGCs corresponden a un subtipo de macrófago, presentes en el granuloma tuberculoso (Ackermann, 2021). Las células o macrófagos epitelioides son una de las primeras

células del granuloma en formación y son su sello distintivo (Palmer et al., 2022); estas tienen una forma poligonal de gran tamaño con un núcleo vesiculoso eucromático y alargado. Su citoplasma es pálido y poco definido, contiene numerosos lisosomas, abundantes mitocondrias y un complejo de Golgi prominente (Adams, 1974; Biberstein, 1994). Poseen membranas celulares estrechamente interdigitadas similares a cremalleras que unen las células adyacentes entre sí (Ramakrishnan, 2012). En pez cebra se han identificado proteínas desmosómicas (desmoplaquina, desmogleína y desmocolina), proteínas de unión adherente (E-cadherina, plakoglobina, cateniana α, β, δ) y moléculas de unión ocluyente (ZO-1 y ZO-2) presentes entre macrófagos epitelioides (Cronan et al., 2016). Desde el punto de vista funcional, las células epitelioides se consideran células activas, ya que presentan una ultraestructura compleja, con vacuolas de pinocitosis, fagocitosis y formación de pseudópodos (Adams, 1974) y con una alta capacidad fagocítica, aunque en algunos casos pueden no contener bacterias (Ramakrishnan, 2012). Sin embargo, se cree que las células epitelioides son menos fagocíticas y más secretoras que los macrófagos activados (Turk & Narayanan, 1982).

Las MNGCs son el resultado de la fusión de múltiples células epitelioides (Ramakrishnan, 2012). Son células que poseen un citoplasma teñido con menor intensidad y que se caracterizan por tener varios núcleos dispuestos periféricamente siguiendo un patrón circular, lo que asemeja la forma de una herradura (Biberstein, 1994). El papel de las MNGCs en la formación del granuloma no se conoce del todo (Palmer et al., 2016, 2022; Ramakrishnan, 2012). Sin embargo, se ha visto que las cepas de micobacterias virulentas son más eficaces para inducir la formación de MNGCs (Peterson et al., 1996), aunque estas MNGCs solo contienen unos pocos bacilos ácido alcohol resistentes (BAAR) (Ramakrishnan, 2012). Más desconocido aún es el mecanismo que promueve la fusión de célula a célula. Así, se cree que la formación de MNGCs en el interior de un granuloma es inducida por el microambiente local mediado por citoquinas y señales derivadas de bacterias, parásitos u otros materiales extraños en el que pueden estar implicadas varias moléculas y que puede conducir a la acción de múltiples glicoproteínas que median en la unión y fusión de membranas (Helming

& Gordon, 2008). Estudios *in vitro* han demostrado que el cambio en el perfil de citoquinas influye en la formación de MNGCs, por lo que el cambio hacia un perfil de citoquinas anti-inflamatorias puede contribuir a la resolución de los granulomas y al control de la infección tuberculosa (Shrivastava & Bagchi, 2016). En la infección con *M. tuberculosis* se ha visto que, a diferencia de las células epitelioides, las MNGCs pueden desempeñar un control en la replicación y propagación de las micobacterias al expresar más citoquinas anti-inflamatorias, presentando una mayor carga de antígeno, pero una menor capacidad micobactericida (Mustafa et al., 2008). En MNGCs de granulomas de bovinos se ha demostrado la expresión de IL-10, TGF-β, TNF-α, IFN-γ e IL-17A (Palmer et al., 2016).

2.2.5. Linfocitos en el granuloma tuberculoso

Los linfocitos desempeñan un papel fundamental en el desarrollo de la respuesta inmunitaria adaptativa que incluye tanto la inmunidad humoral como la inmunidad celular (Kumar et al., 2015a). Según su receptor, los linfocitos T se clasifican en: linfocitos T γδ y linfocitos T αβ. Estos últimos, dependiendo de la función que realizan, se subdividen a modo general en: linfocitos T $CD4^+$, linfocitos T citotóxicos ($CD8^+$) y Tregs ($CD4^+CD25^+Foxp3^+$) mientras que los linfocitos B se clasifican en dos tipos: B-1 que producen anticuerpos IgM y los B-2 (convencionales) (González-Fernández et al., 2005).

La clasificación más básica de la respuesta inmunitaria desencadenada por los linfocitos T los divide en Th1, Th2 y Th17 (Pollock et al., 1996). Los linfocitos Th1 son responsables de una hipersensibilidad de tipo retardada, que producen IFN-γ, TNF-α e IL-2 con el objetivo de destruir patógenos intracelulares como las micobacterias. En cambio, los linfocitos Th2, cooperan con los linfocitos B en las respuestas humorales frente a patógenos extracelulares como bacterias y helmintos secretando IL-4, IL-5, IL-10 e IL-13 (Abebe, 2019; González-Fernández et al., 2005). La respuesta Th17 contribuye a la defensa inmune del huésped mediante la inducción de quimioquinas y citoquinas responsables del reclutamiento temprano de neutrófilos y la formación de

granulomas (Okamoto Yoshida et al., 2010; Steinbach et al., 2016; Umemura et al., 2007), además la producción temprana de IL-17A es necesaria para impulsar una respuesta inmune Th1 eficaz y una producción adecuada de IFN-γ (Khader et al., 2007).

En el granuloma tuberculoso, la interacción entre macrófagos y linfocitos T puede dar lugar a una inmunidad protectora (McGill et al., 2014). En el bovino se ha visto que determinadas subpoblaciones de linfocitos T (linfocitos T γδ, linfocitos T $CD4^+$ y linfocitos T $CD8^+$) participan en la respuesta inmunitaria antimicobacteriana (Pollock et al., 2005). El estudio de las subpoblaciones de linfocitos en el ganado bovino infectado experimentalmente con *M. bovis* ha puesto de manifiesto una mayor frecuencia de linfocitos T γδ, seguidos por linfocitos T $CD4^+$ (Pollock et al., 1996) en los estadios iniciales de granulomas (Plattner et al., 2009), dando paso a una mayor implicación de linfocitos T $CD8^+$ a medida que la infección progresa (Pollock et al., 1996). Es de destacar que los linfocitos T $CD8^+$ en ganado bovino son capaces de liberar IFN-γ en respuesta a antígenos micobacterianos vivos y solubles (Liebana et al., 2007), lo que pone de manifiesto un papel crucial de esta subpoblación de linfocitos en la inmunopatogenia de la enfermedad.

2.2.6. Participación de los neutrófilos en la tuberculosis

Los neutrófilos, que pertenecen al grupo de leucocitos conocidos como polimorfonucleares (PMNs) o granulocitos, son los leucocitos más abundantes en el organismo y forman parte de la respuesta inmunitaria innata considerándose por excelencia la primera línea de defensa frente a los patógenos invasores (Kobayashi & DeLeo, 2009; Malech et al., 2020; Palmer et al., 2022). Los neutrófilos son células efectoras de vida corta (6 a 8 horas) con tres funciones antimicrobianas principales: fagocitosis, degranulación y liberación de material en forma de NET (del inglés *neutrophil extracellular traps*) con el objetivo de enredar y destruir los patógenos invasores (Borkute et al., 2021; Hilda et al., 2020; Palmer et al., 2022), para posteriormente desarrollar una compleja organización basada en eventos de transducción de señales (Kobayashi & DeLeo, 2009) que pueden incluir la liberación

de moléculas señalizadoras, como citoquinas y quimioquinas, que reclutan y activan células inmunitarias específicas en el sitio de la infección (Figura 13). Además, pueden involucrar la interacción directa entre neutrófilos, y otras células como los macrófagos para coordinar respuestas efectivas contra la micobacteria (Borkute et al., 2021)

Entre los mecanismos desarrollados por los neutrófilos para desarrollar su acción de destrucción microbiana, además de los NET, también comprende las especies de oxígeno reactivo (EOR o ROS del inglés *reactive oxygen species)* y péptidos antimicrobianos, así como, diversas hidrolasas y enzimas (Borkute et al., 2021; Hilda et al., 2020). Las enzimas antimicrobianas de los neutrófilos se almacenan en gránulos (Faurschou & Borregaard, 2003), los cuales se clasifican en gránulos primarios (azurófilos), que contienen enzimas lisosómicas, como la mieloperoxidasa, la elastasa y catepsina G; gránulos secundarios (específicos), que contienen proteínas antimicrobianas, como la lactoferrina, la lipocalina unida a la gelatinasa y la defensina; gránulos terciarios (gelatinasa o secretorios), que son menos abundantes y contienen enzimas gelatinasas, como la gelatinasa neutrofílica y la colagenasa, que tienen un papel en la degradación de la matriz extracelular y la remodelación tisular (Borkute et al., 2021; Faurschou & Borregaard, 2003).

En humanos se ha demostrado que los neutrófilos que se encuentran en apoptosis, como resultado del ingreso de *M. tuberculosis*, producen la liberación de NET y Hsp72 (del inglés *heat shock protein 72*), lo que inicia la secreción de TNF-α por parte de los macrófagos, reflejando una respuesta proinflamatoria (Braian et al., 2013; Persson et al., 2008). Además, se ha demostrado que los neutrófilos apoptóticos modulan la respuesta de citoquinas de los macrófagos infectados por *M. tuberculosis* a través de un proceso dependiente de la caspasa-1 y de la IL-1β (Andersson et al., 2014). Por otro lado, en bovinos se ha observado que existe una mayor producción de NET frente a micobacterias muertas en comparación con las vivas (Ladero-Auñon et al., 2021). También se ha observado que los neutrófilos inducen la activación antiinflamatoria mediante la liberación de IL-10 por parte de los macrófagos reguladores (Andersson et al., 2014).

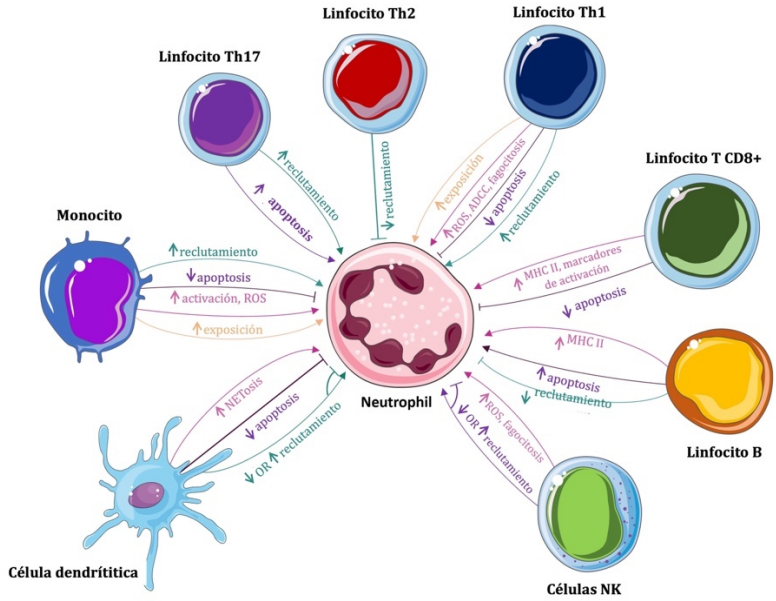

Figura 13. Modulación de las células inmunitarias sobre los neutrófilos. *Estas células afectan el reclutamiento, la exposición, supervivencia, activación y las funciones efectoras de los neutrófilos, como la producción de ROS, NETosis, fagocitosis y ADCC. ADCC, citotoxicidad celular dependiente de anticuerpos; NETosis, liberación de trampas celulares (Modificado de (Gaffney et al., 2022).*

Aunque la presencia de neutrófilos en el caso de la especie humana se ha asociado principalmente a lesiones cavitarias avanzadas, así como en granulomas de estadios más avanzados (Eum et al., 2010), en el caso de especies de animales domésticos, como el ganado bovino o el ganado porcino, se ha descrito la presencia de neutrófilos en los distintos estadios identificados a lo largo de la enfermedad (Cardoso-Toset, Gómez-Laguna, et al., 2015; Wangoo et al., 2005), siendo más abundantes en la especie porcina. En estos casos los neutrófilos son más abundantes en los granulomas de estadios más avanzados y se identifican cerca del centro necrótico, apareciendo en su mayoría como neutrófilos degenerados (Bolin et al., 1997; Cassidy et al., 1998). También se ha destacado la presencia de neutrófilos en los granulomas asociados a la TB en otras especies (Corner et al., 2011; García-Jiménez et al., 2012; García-Jiménez, et al., 2013; Johnson et al., 2008), destacando una mayor cantidad de neutrófilos en granulomas de

macacos (Rayner et al., 2013). En bovinos infectados de forma natural, se ha visto que las cargas bacterianas más elevadas producen un reclutamiento persistente de neutrófilos, sobre todo en granulomas más avanzados (Menin et al., 2013). En cuanto a la distribución dentro del granuloma, en general se ha visto grupos de neutrófilos en el centro de la lesión rodeados por macrófagos (Palmer et al., 2019), aunque existen algunas diferencias a nivel de especie, ya que en el caso del ganado porcino se observan tanto a nivel del centro de necrosis como intercalados en la cápsula de tejido conectivo que rodea al granuloma.

Aunque los neutrófilos son importantes en la TB, los estudios existentes no permiten establecer un papel claro de esta población a lo largo de la inmunopatogenia de la enfermedad con respecto a otros componentes del sistema inmunitario (Hilda et al., 2020; Malech et al., 2020). Así, mientras que algunos estudios sugieren que los neutrófilos pueden desempeñar un doble papel en los granulomas tuberculosos, ya que por un lado, pueden participar en la respuesta inmunitaria inicial contra la infección, contribuyendo a la formación del granuloma y limitando la propagación bacteriana, otros indican que los neutrófilos podrían estar involucrados en respuestas inflamatorias excesivas que pueden contribuir al daño tisular y la cronicidad de la enfermedad (Hilda et al., 2020; Lowe et al., 2012).

3. DIAGNÓSTICO DE LA TUBERCULOSIS ANIMAL

El diagnóstico de la TB animal se basa en una combinación de métodos clínicos, pruebas de laboratorio y evaluación epidemiológica (Álvarez et al., 2015; Bermejo et al., 2007; Bezos et al., 2014; Buddle et al., 2009; Comer, 1994; Gormley, 2007; Guta et al., 2014; Ramos et al., 2015; J. Thomas et al., 2021). En este contexto, la OMSA establece diferentes enfoques para el diagnóstico en función del estado de la enfermedad en una región determinada y la especie animal afectada (OMSA, 2022). Un diagnóstico adecuado de la TB animal, siguiendo las pautas de la OMSA es esencial para garantizar la salud y bienestar de los animales, proteger la seguridad alimentaria y mantener la integridad del comercio internacional de productos animales. Asimismo, contribuye a reducir el riesgo de transmisión de la enfermedad a los seres humanos, fortaleciendo así la salud pública y la cooperación global en la lucha contra esta enfermedad milenaria.

3.1 Pruebas de diagnóstico *antemortem*

Actualmente, de acuerdo al RD (UE)1047/2003 las técnicas y medios utilizados, su normalización y la interpretación de los resultados deben ajustarse a los que se precisan en el capítulo 2.3.3 (TBb) de la cuarta edición (2000) del Manual de normas para las pruebas de diagnóstico y las vacunas de la OMSA, el diagnóstico *antemortem* de la TB, puede realizarse por detección directa del microorganismo o por pruebas basadas en la respuesta inmunitaria celular, con la prueba de IDTB, la prueba de liberación del IFN-γ o pruebas de detección de anticuerpos (OMSA, 2022).

3.2 Prueba de Intradermorreacción (IDTB)

La prueba de la IDTB es el método convencional utilizado para detectar la TB en diversos mamíferos, como el ganado bovino, ovino, caprino y ciervos (OMSA, 2022). El fundamento de la IDTB se basa en la inmunidad mediada por células y tiene como base inmunológica la reacción de hipersensibilidad retardada (Figura 14) o hipersensibilidad tipo IV (Neill et al., 1994; Pollock & Neill, 2002; Schiller et al., 2010).

La prueba consiste en la administración intradérmica de un derivado proteico purificado de la tuberculina bovina (PPD bovina, derivado proteico purificado de cultivo de *M. bovis*, cepa AN-5) en la cual, si el animal ha tenido contacto previo con la micobacteria, se induce una reacción inflamatoria local en el punto de aplicación a las 72 horas (OMSA, 2022).

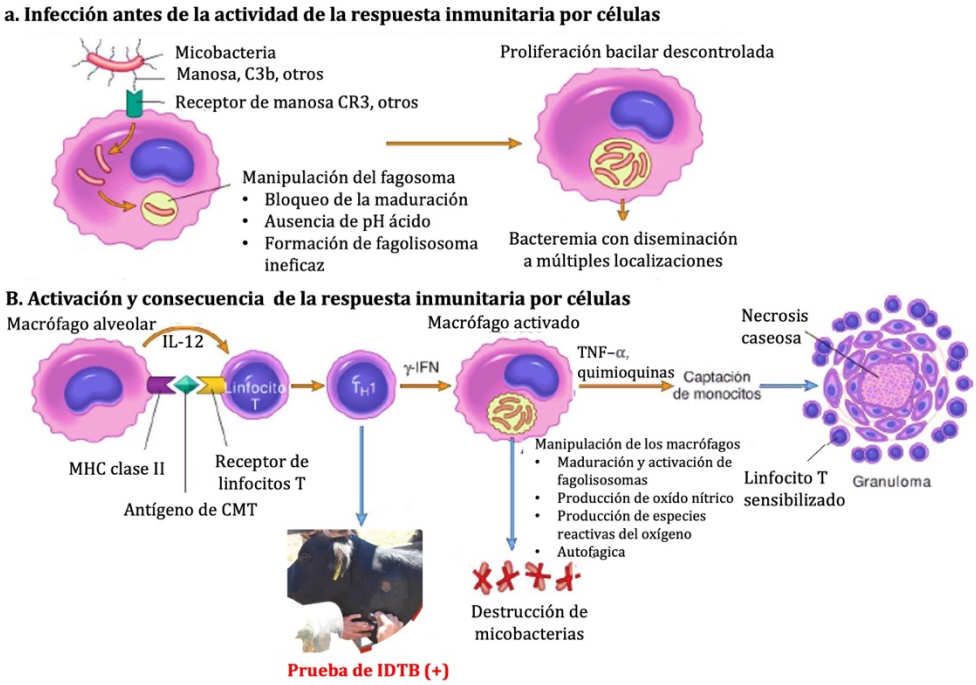

Figura 14. Respuesta inmunitaria celular de tipo retardado (DTH) con respuesta a la prueba de intradermotuberculinización (IDTB). *(a) Acontecimientos que ocurren durante las primeras fases de la infección, antes de que se activen los mecanismos inmunitarios mediados por linfocitos T. (b). Activación y consecuencias de la respuesta inmunitaria mediada por linfocitos T. El desarrollo de resistencia al organismo viene acompañado de la aparición de una respuesta positiva a la IDTB (Modificado de McAdam et al., 2015).*

La interpretación estándar de la IDTB tiene una sensibilidad (Se) del 68-96,8 % y una especificidad (Sp) del 75,5-98,8 % (Núñez-García et al., 2018; Schiller et al., 2010). Según lo dispuesto en el Reglamento (CE) nº 1226/2002 de la Comisión, de 8 de julio,

por el que se modifica el anexo B de la Directiva 64/432/CEE del Consejo, se establece que la prueba de IDTB puede ser realizada de forma simple (IDTBS) (Figura 15a), utilizando solo PPD bovina, o bien de manera comparativa (IDTBC) (Figura 15b), al aplicar simultáneamente dos tipos de PPD (PPD bovina y aviar, siendo esta última un derivado proteico *M. avium* subespecie *avium* cepa D4 ER) en distintos puntos de aplicación.

La principal ventaja de la IDTBC radica en su mayor Sp, a costa de una disminución en la Se, sus valores oscilan entre 52 - 100 % de Se y 78,8 - 100 % de Sp (de la Rua-Domenech et al., 2006; Schiller et al., 2010), por lo que se recomienda especialmente en regiones con baja prevalencia de TB y en situaciones epidemiológicas donde existe sospecha de infección por micobacterias distintas a las incluidas en el CMT (de la Rua-Domenech et al., 2006; Santos et al., 2010). Respecto a la metodología, según lo indicado en el Reglamento (CE) nº 1226/2002 de la Comisión y, de acuerdo a lo que se describe en el manual de procedimiento sanitario (Bezos et al., 2019), la aplicación de la IDTBS se aplica a bovinos mayores de 45 días y generalmente se realiza en la tabla del cuello, puesto que es la zona de dermis con mayor sensibilidad.

La interpretación de las reacciones se basará en las observaciones clínicas, así como los signos propios de la inflamación en los puntos de inyección, que incluyen eritema de la zona, tumefacción, dolor a la palpación o linfadenopatías regionales. De esta forma, la interpretación de la prueba dará lugar a tres posibilidades diferentes que se consideran estándar, severa o estricta.

- En el caso de la IDTBS:
  - Interpretación estándar, considera un animal negativo si la diferencia entre las mediciones (0- 72 horas) es:
    - Negativa: Menor o igual a 2 mm.
    - Dudosa: Mayor a 2 mm o menor a 4 mm.
    - Positiva: Igual o mayor 4 mm.

- Interpretación severa, considera los resultados dudosos como positivos cuando al menos se ha identificado un animal positivo en el rebaño.
- Interpretación estricta, considera los resultados dudosos como positivos independientemente de que se haya detectado o no un animal positivo en el rebaño.

- En el caso de la IDTBC:
  - Para la interpretación de los resultados se tienen en cuenta las mediciones correspondientes a la aplicación de la PPD bovina y la PPD aviar interpretadas de la siguiente forma.
    - Negativo: reacción frente a la PPD bovina es negativa o es positiva o dudosa pero ≤ a la reacción positiva o dudosa frente a la PPD aviar.
    - Dudosa: reacción frente a la PPD bovina sea positiva o dudosa y > en 1 a 4 mm frente a la PPD aviar.
    - Positiva: reacción frente a la PPD bovina sea positiva y > a 4 mm en comparación con la PPD aviar.

La prueba de la IDTBS (Figura 14a)se aplica de forma rutinaria en el marco de los programas de control y erradicación de la TBb, ya que es una técnica oficial y validada en esta especie (Bezos et al., 2019). Sin embargo, a excepción de los cérvidos, a pesar de que esta prueba no se encuentra validada en otras especies, se han obtenido buenos resultados en caprino (Bezos et al., 2018). Por otro lado, de acuerdo con lo descrito en el Manual terrestre de los animales de la OMSA (2022), esta prueba puede realizarse e interpretarse en algunas especies como las siguientes:

- **Interpretación de los resultados en los cerdos:**

En los cerdos, las reacciones pueden ser muy intensas y concentraciones más altas de PPD pueden ocasionar necrosis en la piel. El lugar preferido para la aplicación es la piel suelta en la superficie dorsal de la oreja, en el surco entre la cabeza y la oreja. Se inyecta PPD aviar en la base de la oreja izquierda y PPD bovina en la base de la oreja derecha. La reacción puede ser evaluada después

de 48 o 72 horas. La interpretación sigue el mismo esquema que la IDTBC del bovino de acuerdo a la legislación local aplicable.

Figura 15. Esquema de aplicación y lectura de la prueba de intradermotuberculinización (a) simple (IDTBS) y (b) comparada (IDTBC) en bovino *(Modificado de VISAVET, 2017).*

- **Interpretación de los resultados en ovejas y cabras:**

La prueba de IDTB puede realizarse en ambas especies en la zona cervical media o en la zona escapular utilizando la IDTBS o la IDTC o en el pliegue caudal de la cola (Kassa et al., 2012). Pueden utilizarse otras zonas libres de lana, como por ejemplo, las zonas internas superiores a la altura del muslo de las patas traseras, lo que evita la pérdida de calidad de la lana.

Algunas desventajas de la prueba de IDTB es la falta de detección temprana, ya que la IDTB no es efectiva para detectar animales recién infectados, así como su falta de eficacia en la detección de animales en estado de anergia en etapas avanzadas de la enfermedad (Álvarez et al., 2012; Bezos et al., 2012; Bezos, Casal, et al., 2014; de la Rua-Domenech et al., 2006). Por otro lado, los cuadros de inmunosupresión (Bezos, Casal, et al., 2014), así como la infección con otras micobacterias, como la infección por *M. avium* subspecie *paratuberculosis* (Álvarez, 2008), causante de la paratuberculosis en el caso del bovino (Álvarez et al., 2009; Bezos, Casal, et al., 2014) y del caprino (Álvarez et al., 2008b), porcino (Aranaz et al., 2006; Cardoso-Toset, Gómez-Laguna, et al., 2015). puede presentar resultados positivos debido a la interferencia con estas micobacterias (Álvarez et al., 2008b).

Después de la administración intradérmica de tuberculina en el ganado infectado, se observa una disminución temporal en la reactividad cutánea ante una segunda inyección. Este fenómeno, denominado desensibilización, puede resultar en la falta de identificación de animales infectados tanto en estudios experimentales como en situaciones naturales como reactores positivos (Buddle et al., 2009; de la Rua-Domenech et al., 2006). Con el propósito de contrarrestar el efecto de pérdida de sensibilidad frente a la tuberculina, los protocolos internacionales para las pruebas cutáneas establecen un intervalo mínimo de 42 días entre dos pruebas consecutivas (de la Rua-Domenech et al., 2006). Por lo tanto, se recomienda un período de espera de 45 a 60 días entre pruebas sucesivas de la IDTB. Esta ventana temporal permite que el sistema inmunológico del animal y los tejidos se recuperen adecuadamente, evitando posibles alteraciones en los resultados de la prueba.

3.1.2. Ensayos serológicos

Los ensayos serológicos para el diagnóstico de la TB en animales han aumentado en los últimos tiempos, demostrando ser una herramienta de gran utilidad como diagnóstico auxiliar y complementario a pruebas como la IDTB, lo que ha permitido mejorar la Se y tener un mayor control de la Tb en animales domésticos y salvajes (Casal et al., 2017; R. Thomas & Chambers, 2021).

3.1.2.1. Ensayos del IFN- γ

El ensayo del IFN-γ es una técnica *in vitro* ampliamente empleada en el diagnóstico de la TBb, y que se usa en paralelo junto con la prueba de IDTB con objeto de incrementar la Se, y maximizar la detección de animales infectados en una explotación o región (Bezos et al., 2019; Buddle et al., 2009; Wood & Jones, 2001). En el caso de España, esto se encuentra estipulado en el Reglamento (CE) nº 1226/2002 de la Comisión, de 08 de julio, donde se indica que los Estados miembros de la UE tienen la opción de autorizar el uso de la prueba de IFN-γ junto con la prueba de IDTB de acuerdo a lo que se indica en el manual de normas para las pruebas de diagnóstico y las vacunas de la OMSA (Bezos et al., 2019). Adicional a esto, en caso de utilizar la prueba del IFN-γ en paralelo con la IDTB, siempre deberá cogerse primero la muestra de sangre para el ensayo de IFN-γ, seguido de la aplicación de la IDTB (Buddle et al., 2009; Wood & Jones, 2001). En aquellos animales que cuenten previamente con una prueba de IDTB, se debe esperar un tiempo mínimo de 60 días desde su última aplicación (Bezos et al., 2019).

Con respecto a la Se y Sp, esta prueba ha demostrado tener ambos parámetros más elevados (Se: 73,0 – 100 %; Sp: 85,0 – 99,6 %) en comparación con la prueba de la IDTB (Aranaz et al., 2006; Núñez-García et al., 2018; Schiller et al., 2010). El ganado bovino y la especie humana es donde más se ha utilizado esta prueba (de la Rua-Domenech et al., 2006), estando indicada su aplicación, en el caso de los bovinos, desde los 6 meses de edad en adelante (Bezos et al., 2019). Existe evidencia de que el uso del ensayo de IFN-γ es una herramienta que puede ser utilizada para la vigilancia y el manejo de la infección por *M. bovis* en poblaciones porcinas, incluso en animales en ausencia de lesiones visibles (Pesciaroli et al., 2012). También se ha descrito su uso en cabras (Bezos et al., 2018, 2019) y en primates no humanos (Primagam®) (Garcia et al., 2004), aunque el uso en primates se recomienda en paralelo con la IDTB (Vervenne et al., 2004). Dentro de la fauna silvestre destacan estudios en cérvidos (Risalde et al., 2017; Waters et al., 2008), alpacas (Rhodes et al., 2012), tejones (Dalley et al., 2008), elefantes (Angkawanish et al., 2013), y diversos felinos (Rhodes et al., 2011), incluyendo los leones (Maas et al., 2012).

El fundamento de este ensayo consiste en medir la liberación de IFN-γ en un cultivo de sangre completa. Para esto, los linfocitos T sensibilizados previamente durante 16-24 a 37 ºC por la exposición a PPD bovina y aviar, liberarán IFN-γ (OMSA, 2022), lo que en condiciones de infección natural o controlada provocará la activación de los macrófagos, permitiendo a estas células ser más eficaces a la hora de eliminar patógenos intracelulares como las micobacterias (Buddle et al., 2009).

La interpretación de los resultados se debe realizar en laboratorios autorizados y siguiendo las instrucciones del fabricante y acorde al programa de control y erradicación de la TBb (Bezos et al., 2012a).

Con el propósito de incrementar la especificidad de la técnica de diagnóstico, se han llevado a cabo ensayos utilizando distintos antígenos en el ganado bovino, especialmente con el objetivo de reemplazar a las PPDs, ya que esto representa una de las principales limitaciones. Entre los antígenos evaluados, destacan las proteínas ESAT-6 y CFP-10, las cuales se encuentran presentes en las bacterias *M. tuberculosis*, *M. bovis* y *M. caprae*, y han demostrado ser opciones prometedoras para abordar esta cuestión (Buddle et al., 2009; Pollock & Andersen, 1996; Van Pinxteren et al., 2000; Vordermeier et al., 2001). Una de las principales ventajas de estas proteínas es su especificidad, ya que están ausentes en la mayoría de las especies de micobacterianas ambientales, por lo que su uso se ha evaluado también como una alternativa para implementarlas tanto en la IDTB como en el ELISA para el desarrollo de pruebas diagnósticas más específicas (Flores-Villalva et al., 2012).

Dentro de las ventajas de esta técnica, es que ofrece una mejor Se comparada con la prueba de IDTB, y que los animales deben ser manipulados solo una vez, lo que es de gran utilidad sobre todo en animales peligrosos o de difícil manejo (Gormley, 2007; OMSA, 2022; Schiller et al., 2010).

Algunos inconvenientes del ensayo del IFN-γ son su coste y la necesidad de procesar rápidamente la sangre después de su extracción, puesto que es imprescindible la presencia de células vivas, por lo que la muestra se debe transportar al laboratorio en tubos de sangre con anticoagulante de heparina de litio y a Tª ambiente en un plazo

de entre 24 – 30 horas como máximo desde su recogida (Buddle et al., 2009; OMSA, 2022). Así, se recomienda que las muestras de sangre sean procesadas en el laboratorio antes de las 8 horas desde que se extrajeron, ya que tiempos superiores podrían afectar a la sensibilidad de la técnica. Además, también se ha descrito que la utilización de cualquier otro anticoagulante, así como la refrigeración, reducen drásticamente la viabilidad de los linfocitos (Balseiro et al., 2020; Bezos et al., 2019).

3.1.2.2. Ensayo de ELISA

La técnica de ELISA (del inglés *Enzyme-Linked Immunosorbent Assay*) es una prueba validada por la OMSA (2022) para el diagnóstico de TBb, y permite detectar anticuerpos específicos frente a *M. bovis* (Daftary et al., 1994; Plackett et al., 1989). Esta técnica se ha utilizado ampliamente para evaluar la respuesta inmunitaria humoral frente a *M. bovis* en diferentes especies animales (Bezos et al., 2014; Cardoso-Toset et al., 2017; Lilenbaum et al., 1999; Sun et al., 2021). Además, ha demostrado utilidad para detectar infecciones con *M. bovis* en animales silvestres (OMSA, 2022). Su reacción se basa en la interacción de los anticuerpos presentes en el suero de animales infectados con CMT, con un antígeno que está adherido a las paredes de un pocillo de una placa de microtitulación (IDEXX, *Mycobacterium bovis* Antibody Test kit, Westbrook, Maine, USA). Se considera una técnica con una Se muy variable, oscilando entre un 45,0 a un 98,6 %, al igual que su Sp, que varía desde un 52,5 % llegando en algunos casos incluso al 100 % (Bezos et al., 2014).

Esta técnica ha demostrado ser útil en la detección de TB en-porcinos (Cardoso-Toset et al., 2017) demostrando ser una herramienta de cribado fiable para detectar explotaciones infectadas con mejores valores de Se con un promedio de 78,2 % (Cardoso-Toset et al., 2016; Thomas et al., 2019), e incluso con valores de Se de 84,1 % y Sp de 98,4 % (Thomas et al., 2019), lo que ofrece una alternativa rápida, económica y fácil de realizar en relación a otros métodos tradicionales de diagnóstico (Ramos et al., 2015), permitiendo el análisis de una gran cantidad de muestras a la vez (Garbaccio et al., 2019). Además, en el ganado bovino se ha descrito que puede ser de utilidad en la detección de vacas "anérgicas" que no han logrado ser detectadas por las pruebas de la

IDTB e IFN-γ (Bezos et al., 2012; Bezos et al., 2014; Plackett et al., 1989; Ramos et al., 2015), aunque su Se es cuestionada (Larenas-Muñoz et al., 2022), ya que a pesar de que la Se aumenta con la gravedad de la enfermedad, en infecciones tempranas se puede observar una Se reducida (Waters et al., 2011), lo que ofrece una limitación para detectar animales que se encuentran en las primeras fases de infección, lo que puede dar lugar a falsos negativos (Garbaccio et al., 2019) y, por lo que esta prueba se recomienda realizarla junto a otras técnicas, y no como prueba única (Lilenbaum et al., 1999; Lilenbaum & Fonseca, 2006; Waters et al., 2011) (Figura 4).

Adicionalmente, posibles falsos positivos pueden ocurrir debido a la presencia de interferencias o variabilidad en la respuesta inmunitaria de los animales a causa del uso de fármacos inmunosupresores (Buddle et al., 2009; de la Rua-Domenech et al., 2006; Garbaccio et al., 2019; Plackett et al., 1989).

3.1.2.3 Ensayo de flujo lateral

El ensayo de flujo lateral es una técnica serológica que se basa en el principio de cromatografía para detectar la presencia de anticuerpos específicos contra CMT en una muestra de sangre. Su uso está indicado principalmente en animales de vida libre (OMSA, 2022), en los que la prueba se indica como primera opción en estas especies (Thomas & Chambers, 2021). En un estudio realizado con dromedarios se observó una alta Se (90 %) y Sp (99 %) (Ranjan et al., 2018). Sin embargo, la Se y Sp de esta técnica pueden variar dependiendo de la población y la región geográfica en la que se utilice (Lyashchenko et al., 2008; Ranjan et al., 2018; Stewart et al., 2017).

La OMSA (2022) describe su uso para demostrar la ausencia de infección en la población y en animales antes de efectuar un desplazamiento, por lo que puede contribuir en las políticas de los planes de erradicación.

En el estudio de Lyashchenko et al. (2008) se realizó un ensayo de detección de anticuerpos simple en animales de vida libre, dentro de los que se incluyeron tejones, ciervos, zarigüeyas y jabalíes, para lo cual se utilizó un cóctel de antígenos seleccionados de *M. bovis* , incluidos ESAT-6, CFP-10 y MPB83 (Greenwald et al., 2003; Waters et al., 2006). Lo resultados mostraron valores de Se y Sp diferentes para cada

especie, obteniendo mejores resultados y similares en el ciervo (Se 75,0 % - Sp 98,9 %) y jabalí (76,6 % - Sp 97,3 %), por lo que los autores sugieren que el ensayo de flujo lateral es una prueba rápida de diagnóstico de TB y que puede proporcionar una herramienta de detección útil para ciertas especies de vida silvestre, las cuales podrían jugar un papel fundamental en el mantenimiento y la transmisión de *M. bovis.* Sin embargo, es importante tener en cuenta que el ensayo de flujo lateral no es una prueba definitiva para el diagnóstico de la TB (OMSA, 2022). La presencia de anticuerpos no siempre indica una infección activa, ya que estos pueden persistir en el cuerpo incluso después de que la infección haya sido controlada (Casal et al., 2017; Stewart et al., 2017). Por lo tanto, los resultados positivos deben ser confirmados mediante pruebas adicionales, como cultivos bacterianos o pruebas moleculares, para asegurar un diagnóstico preciso. Además, es importante señalar que el ensayo de flujo lateral tiene algunas limitaciones como los resultados falsos positivos y negativos.

3.2 Pruebas de diagnóstico *postmortem*

El diagnóstico *postmortem* durante la inspección en matadero o en la necropsia es la forma más habitual de identificar lesiones macroscópicas compatibles con TB. Sin embargo, en el caso de animales procedentes de saneamiento (animales que han sido positivos a la prueba de IDTB y/o IFN-γ, los cuales deben sacrificarse en un plazo de máximo de 15 días desde su diagnóstico) y que han resultado positivos a la prueba de IDTB, pueden presentar lesiones no visibles macroscópicamente, por lo cual, de rutina se toman muestras que incluyen NLs retrofaríngeos, traqueobronquiales, y mediastínicos (Balseiro et al., 2020; OMSA, 2022), ya que se ha descrito que estos son los NL en lo que con mayor frecuencia se encuentran lesiones tuberculosas o similares a TB en el caso del bovino (Palmer et al., 2007), aunque según el manual de toma y envío de muestras para el estudio microbiológico de VISAVET (2017), en el caso de ausencia de lesiones compatibles a normativa, incluye un muestreo más amplio de al menos un NL de cada uno de los siguientes linfocentros:

1. Cabeza: NL retrofaríngeo y mandibular
2. Cavidad torácica: NLs mediastínico y traqueobronquiales

3. Miembro torácico: NL cervical superficial
4. Cavidad abdominal: NL mesentérico y hepático
5. Glándula mamaria: NL mamario

3.2.1. Cultivo bacteriológico

Según las pautas establecidas por la OMSA (2022), el cultivo bacteriológico se considera la técnica "*gold standard*" o de referencia para alcanzar un diagnóstico definitivo de TB (Gormley et al., 2014), lo cual está descrito dentro en el Real Decreto 2611/1996, que establece la normativa para el control y erradicación de la TB en animales en España, y especificado en el "Manual de procedimiento de toma y envío de muestras para diagnóstico mediante PCR directa y cultivo microbiológico en infecciones por miembros del CMT" (Romero et al., 2021).

Uno de los principales factores que influyen en el diagnóstico de la TB a través del cultivo microbiológico, es el tiempo que tarda en crecer la micobacteria, siendo este de entre 8 y 12 semanas (Courcoul et al., 2014; Lorente-Leal et al., 2021), aunque lo habitual es que este tiempo sea mayor a 12 semanas, puesto que se recomienda un período de incubación mayor con el objetivo de mejorar la Se (Corner et al., 2012), ya que en el caso de sospechar de *M. microti*, se recomienda hasta un máximo de 16 semanas (OMSA, 2022).

Con respecto a los valores de Se y Sp, el cultivo bacteriológico presenta unos valores de Se que oscilan entre el 30 - 95 % (Corner et al., 2012; Hines et al., 2006) y Sp del 78,1 - 99,1 % (Courcoul et al., 2014). La marcada diferencia que hay en los valores de Se, puede explicarse porque para el desarrollo de la técnica existen varios factores que pueden influir en la precisión y fiabilidad de este diagnóstico. Así, de acuerdo a lo descrito previamente en el manual de toma y envío de muestras por Romero (2021), la forma en que se recolecta la muestra, la elección de la misma y las condiciones de almacenamiento pueden afectar la Se y el diagnóstico. Idealmente las muestras que se seleccionan para el cultivo siempre incluyen tejidos con presencia de lesiones macroscópicas compatibles con TB en NLs (principalmente NLs mandibulares,

retrofaríngeos, traqueobronquiales, mediastínicos y mesentéricos) y órganos parenquimatosos, como pulmón, hígado o bazo (Gormley et al., 2014; Real Decreto 2611/1996). Sin embargo, con el objetivo de mejorar la Se, igualmente se seleccionan muestras de tejidos con lesiones no visibles macroscópicamente (Gormley et al., 2014), ya que existe la posibilidad de que los animales con TB se encuentren en etapas iniciales de la infección, en donde los granulomas aún no se hayan formado o sean muy pequeños para detectarlos en la inspección macroscópica (Balseiro et al., 2020), por lo que probablemente tendrán una escasa carga bacteriana (Palmer et al., 2007). Las muestras deben recogerse utilizando recipientes estériles (Romero et al., 2021) y almacenarse refrigeradas a 4 ºC durante el transporte, sin exceder las 36 horas de llegada al laboratorio, recomendándose la congelación de las mismas por debajo de -20 ºC si el transporte excede este tiempo, ya que estas condiciones mejoran la viabilidad celular e impide el crecimiento de otros microorganismos (Gormley et al., 2014) que pueden contaminar la muestra y enmascarar la presencia de bacterias del CMT (Balseiro et al., 2020; Romero et al., 2021). Además, el transporte, deberá seguir la normativa del Real Decreto 664/1997, sobre la exposición a Agentes Biológicos, ya que las especies del CMT están clasificadas en el grupo de riesgo 3 debido a su capacidad infecciosa. Por lo tanto, el cultivo requiere de un laboratorio con un nivel de bioseguridad equivalente (nivel de bioseguridad 3) para proteger al personal especializado y al medio ambiente (OMSA, 2022).

Para procesar las muestras, se selecciona una sección del tejido y se procede a realizar una homogenización mediante disrupción mecánica con el objetivo de liberar las micobacterias que se encuentran en el tejido (Balseiro et al., 2020), seguido de una descontaminación del homogeneizado con un ácido o álcali, ya sea 5 % de ácido oxálico o 2-4 % de hidróxido sódico (NaOH) (Gormley et al., 2014; OMSA, 2022). Este paso es necesario, ya que las micobacterias son de crecimiento lento y muy exigentes, por lo que requieren del uso de medios de cultivo nutritivos, lo que podría provocar el crecimiento de bacterias oportunistas de crecimiento más rápido y con menor requerimientos que el CMT, provocando así una competición por nutrientes y enmascarar el crecimiento de CMT (Balseiro et al., 2020). Sin embargo, en este punto

se debe tener precaución, ya que algunos descontaminantes como 2 % p/v de NaOH, 0,75 % p/v y 0,075 % p/v de cloruro de cetilpiridinio y 0,5 % p/v de cloruro de benzalconio han demostrado cierto grado de toxicidad, ya que se ha observado un menor desarrollo de colonias en comparación con solución salina (Gormley et al., 2014). No obstante, las condiciones óptimas de los laboratorios de hoy en día garantizan la eliminación del mayor número de microorganismos contaminantes sin afectar a la viabilidad de las micobacterias (Balseiro et al., 2020).

De acuerdo con las pautas de la OMSA (2022) para llevar a cabo el aislamiento inicial, el sedimento se introduce habitualmente en diferentes medios sólidos que contienen huevo, como el de Lowestein-Jensen, el medio base de Coletsos o el medio de Stonebrinks. Estos medios deben contener piruvato o glicerol, o ambas sustancias. Asimismo, se recomienda emplear un medio de agar, como el de Middlebrook 7H10 u 7H11. En *M. bovis* se ha observado que tiene un mejor crecimiento en medios enriquecidos, pero su crecimiento es lento y las colonias no aparecen hasta pasados más de 7 días, por lo que el crecimiento se ve favorecido con la adición de piruvato al medio, mientras que el glicerol lo inhibe (Gormley et al., 2014). Estas bacterias son aeróbicas o microaerófilas, y se desarrollan a una temperatura de 37 ºC, mostrando un patrón de cordonamiento cuando se cultivan en medios líquidos (Gormley et al., 2014) como el MIGIT, los cuales permiten un crecimiento en menor tiempo y una detección más rápida de las mismas (OMSA, 2022; Rageade et al., 2014). No obstante, los inconvenientes son una tasa de contaminación mayor y la imposibilidad de establecer un diagnóstico inicial en base a las características morfológicas de las colonias (OMSA, 2022).

Se puede obtener un diagnóstico preliminar de CMT basándose en el patrón de crecimiento y la morfología de las colonias bacterianas. Sin embargo, esto debe confirmase mediante la técnica molecular de PCR, ya que para garantizar la Sp hay que confirmar que las bacterias corresponden al CMT y no a otro microorganismo (Balseiro et al., 2020; Gormley et al., 2014; OMSA, 2022). Además, para la interpretación de los resultados se requiere de un personal de laboratorio capacitado que pueda realizar una interpretación precisa de los resultados y minimizar los errores en el diagnóstico

(Dorronsoro & Torroba, 2007). En base a esto y según Balseiro et al. (2020), los resultados de un informe microbiológico se pueden interpretar de la siguiente manera:

1. Cultivo positivo (presencia de crecimiento) – PCR C positiva: se detecta crecimiento microbiano en los medios de cultivo y mediante PCR se identifica el crecimiento de bacterias del CMT o a nivel de especie (ejemplo, *M. bovis*). El resultado final es POSITIVO a CMT o *M. bovis*.

2. Cultivo negativo (ausencia de crecimiento): no se detecta crecimiento microbiano en los medios de cultivo y, por lo tanto, no se realiza ninguna PCR de identificación. El resultado final es NEGATIVO a CMT.

3. Cultivo positivo (presencia de crecimiento) – PCR CMT negativa: se detecta crecimiento microbiano en los medios de cultivo y mediante PCR no se identifica el crecimiento de bacterias del CMT o a nivel de especie (ejemplo, *M. bovis*). El resultado final es NEGATIVO a CMT o *M. bovis*.

3.2.2 Herramientas de biología molecular: PCR a tiempo real y PCR digital

Existe una creciente necesidad e interés en el avance de técnicas de diagnóstico rápido para la detección de micobacterias motivado por la baja Se y el tiempo requerido para obtener un diagnóstico cuando se usa el cultivo microbiológico como técnica de referencia. Por esta razón, en los últimos años se han introducido diversos métodos de diagnóstico que emplean técnicas moleculares como la PCR.

3.2.2.1. PCR en tiempo real

La PCR en tiempo real es una técnica ampliamente utilizada en el diagnóstico de la TB (Lim et al., 2019; Sevilla et al., 2015) tanto en humanos (Machado et al., 2019) como en animales (Lorente-Leal et al., 2019; Sánchez-Carvajal et al., 2021). De hecho, la PCR se utiliza de rutina para la confirmación del CMT desde colonias que han crecido en el cultivo microbiológico (Romero et al., 2021), ya que ha demostrado una mayor Se, permitiendo incluso identificar la micobacteria dentro de las pertenecientes al CMT. Esto resulta útil a la hora de hacer trazados epidemiológicos (Lim et al., 2019). No obstante, recientemente la PCR directa desde tejido ha avanzado en el campo del

diagnóstico de CMT en animales. En humanos, por otro lado, se utiliza rutinariamente desde hace algún tiempo en el diagnóstico del CMT, principalmente en muestras de esputo (OMSA, 2022).

Diferentes estudios han demostrado que la PCR a tiempo real directa desde tejido es una herramienta valiosa para la detección rápida y precisa del CMT, lo que acelera el proceso diagnóstico (Cardoso et al., 2009; Gholoobi et al., 2014; Lorente-Leal et al., 2019, 2021; OMSA, 2022; Sánchez-Carvajal et al., 2021; Thacker et al., 2011). En España, en el manual para la realización de estudios de PCR directa desde tejido (MAPA, 2023c) se indica el protocolo a utilizar para la detección de CMT basado en la *"PCR EURLAB: PE/013/MYC PROCEDURE FOR DETECTION of Mycobacterium tuberculosis COMPLEX MICROORGANISMS THROUGH REAL TIME PCR"* utilizando cebadores específicos (IS*6110*-forward: 5′-GGT AGC AGA CCT CAC CTA TGT GT-3′; IS*6110*-reverse: 5′-AGG CGT CGG TGA CAA AGG-3′) y sonda (IS*6110*- probe: 5′-FAM-CAC GTA GGC GAA CCC-MGBNFQ-3′).

El gen *MPB70* se ha utilizado en el diagnóstico de PCR a tiempo real ya que codifica una proteína antigénica expresada mayoritariamente en *M. bovis,* pero conservada en todos los miembros del CMT en donde han obtenido unos diferentes valores de Se (88,41 %) y Sp (92,37 %) (Lorente-Leal et al., 2019). Sin embargo, se han identificado otras dianas de interés específicas para MTC como la IS*1081*, la que se ha utilizado ampliamente en pruebas de diagnóstico para TBb (Collins & Stephens, 1991; Van Soolingen et al., 1992) y recientemente en muestras de leche (Zeineldin et al., 2023). Otros cebadores como el *IS4*, basado en la secuencia de inserción *6110*, se ha usado en muestras clínicas con buenos resultados, lo que la convierte en una buena alternativa de diagnóstico (Wang et al., 2019).

Actualmente, la PCR directa desde tejido es considerada como una alternativa al cultivo microbiológico para confirmar aquellos casos sospechosos (Romero et al., 2021). Sin embargo, en los rebaños o establecimientos T3H, aquellos en los que al menos en los 3 últimos años mantuvo el estatuto de T3 sin ser retirado de forma

ininterrumpida (MAPA, 2023c), se debe seguir utilizando el cultivo microbiológico para confirmar los casos sospechosos (Romero et al., 2021).

Las principales ventajas que ofrece la PCR en tiempo real desde tejido son una alta Se y Sp, muy cercanos al cultivo microbiológico y con una rapidez notablemente mayor, ya que en cuestión de horas permite tener un diagnóstico (Courcoul et al., 2014; Lorente-Leal et al., 2019). Lorente et al. (2019) obtuvo valores de Se 94,59 % y Sp 96,03 % frente los resultados de Courcoul et al. (2014) con valores similares de Se y Sp de 87,7 % y 97.0 % respetivamente y a los de Sánchez-Carvajal et al. (2021) con valores de Se del 77,0 % y una Sp del 99,4 %.–Sin embargo, también hay algunas consideraciones a tener en cuenta y es que la técnica puede ser más costosa con respecto a otras pruebas de diagnóstico menos sofisticadas, lo que puede limitar su uso en países con bajos recursos donde se obstaculizada la implementación por desafíos relacionado con la infraestructura, los costos, la capacitación del personal y el almacenamiento de datos en áreas con limitaciones de informática–(Courcoul et al., 2014).

Para el desarrollo de la técnica, las muestras se obtienen de tejidos de animales sospechosos de TB, de acuerdo al manual de toma de muestras (Romero et al., 2021), destacando la importancia de incluir parte de la lesión (granuloma) y tejido sano adyacente a ésta, ya que estos granulomas se caracterizan por tener pocas micobacterias, lo que puede ser una limitante a la hora de extraer ADN micobacteriano. Además, la estructura propia del granuloma por la presencia de fibrosis y calcificación dificultan el proceso de aislamiento y purificación del ADN (Liébana et al., 1995). Para mejorar esto, los protocolos de extracción de ADN de la muestra incluyen un homogeneizado previo del tejido, ya que mejora la Se, aunque se ha visto que la Se es aún mejor cuando el ADN se ha aislado sólo desde lesiones (Taylor et al., 2007).

El protocolo de la técnica consiste en una primera etapa en realizar la extracción de ADN a partir de tejidos, de los cuales se efectuará un homogeneizado de cada muestra por separado, utilizando un sistema de lisis con bolas de cristal (Extraction Beads-*VK)* para favorecer la obtención de ADN. Y, en una segunda etapa se lleva a cabo la técnica

de PCR a tiempo real utilizando el segmento IS6110 para el diagnóstico de CMT de acuerdo al protocolo establecido (MAPA, 2023c).

Para el desarrollo de la técnica, es importante tener en consideración la rigurosidad del procesamiento de las muestras y la técnica de PCR empleada, ya que la selección de la diana de interés es clave para la técnica (Balseiro et al., 2020). Para la extracción de ADN es recomendable el uso de kits de extracción de alta calidad para eliminar potenciales inhibidores como la parafina, en caso de trabajar con muestras fijadas en formol e incluidas en parafina (FFPE, del inglés *formalin-fixed paraffin embedded*) (Gómez-Laguna et al., 2010; Kim, 2003), el etanol o restos de heparina en caso de trabajar con muestras de sangre completa. Además ante la sospecha de la presencia de inhibidores, considerando la cuantificación inicial del ADN, se puede diluir la concentración de la muestra hasta en 10 veces, para reducir el ADN genómico (Lorenz, 2012). De acuerdo a las indicaciones de los fabricantes en general, para la PCR es importante considerar siempre un control heterólogo de inhibición exógena (control de amplificación interna), además de controles internos positivos y negativos en cada placa de PCR (Lorenz, 2012), ya que los controles negativos ayudarán a identificar la contaminación cruzada, mientras que los controles positivos permitirán verificar la eficacia de la reacción. Por otro lado, en cada laboratorio es necesario ajustar las condiciones de la PCR, como la temperatura de ensamblaje y el tiempo de extensión, para optimizar la Sp y eficiencia de la amplificación (Lorenz, 2012; Rychlik et al., 1990).

3.2.2.2. PCR digital en gotas (ddPCR)

La ddPCR (del inglés *droplet digital PCR*) es una técnica avanzada de tercera generación de la PCR y que se utiliza para la detección y cuantificación precisa de material genético, como el ADN o el ARN, presente en una muestra, basándose en la tecnología de generación de gotas (aproximadamente 20.000) en una emulsión de agua y aceite (Baker, 2012; Devonshire et al., 2016; Nyaruaba et al., 2019, 2020) (Figura 16). Para esto, se han descrito diferentes plataformas de dPCR, las cuales difieren principalmente en la estrategia que utilizan para compartimentar la muestra y generar

particiones o gotas, así como en el número de particiones que producen (Baker, 2012). Entre los primeros instrumentos disponibles, Fluidigm Corporation (San Francisco, CA) y Life Technologies (Carlsbad, CA) ofrecen una compartimentación basada en chips microfluídicos que da lugar a cientos o miles de particiones, mientras que Bio-Rad (Hercules, CA) y RainDance (Lexington, MA) se centran en una compartimentación basada en emulsiones que puede generar desde decenas de miles (sistemas QX100 y 200, Bio-Rad) hasta millones de gotas (RainDrop® System, RainDance) (Gutiérrez-Aguirre et al., 2015) en la que cada gotita puede contener una o más copias de la secuencia diana o ninguna (Baker, 2012; Devonshire et al., 2016; Nyaruaba et al., 2019, 2020) (Figura 16).

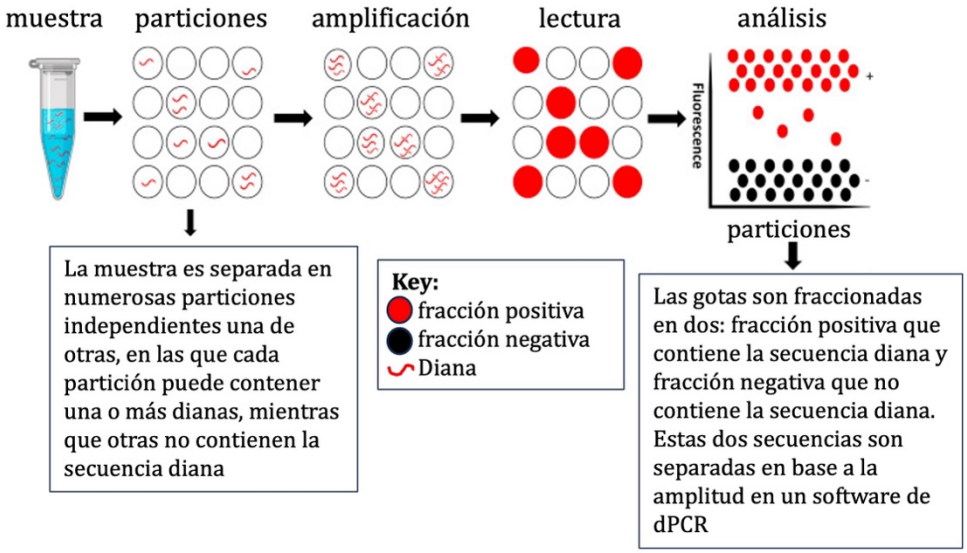

Figura 16. Principio de ddPCR. División y amplificación de una sola muestra para detectar múltiples copias *(Modificado de Nyaruaba et al., 2019).*

La ddPCR presenta muchas ventajas sobre la PCR convencional o a tiempo real, como es una Se superior al ser capaz de detectar un bajo número de copias de ADN o ARN en muestras con baja concentración, cuantificación más precisa, detección de mutaciones y variantes genéticas (Cao et al., 2020; Chen et al., 2021; Nyaruaba et al., 2019). Desde hace algunos años, se ha utilizado para distinguir la expresión diferencial de alelos (Chen et al., 2012), detectar y cuantificar virus asociados a bacterias

ambientales (Tadmor et al., 2011), cuantificar genes cancerosos (Wang et al., 2010) y detectar aneuploidías en ADN fetal en sangre circulante (Dennis Lo et al., 2007). En el campo de la TB, ha demostrado ser útil en el diagnóstico para detectar ADN en muestras de sangre (Yang et al., 2017), plasma (Lyu et al., 2020) y recientemente en la resistencia a antibióticos (Aung et al., 2023; Zhang et al., 2023).

Para la realización de la ddPCR, las muestras se colocan en un generador de microgotas que contienen una mezcla con la muestra y los reactivos necesarios de la PCR (enzimas, nucleótidos, cebadores y sondas específicas) junto con una fase oleosa, la cual se dispersa en pequeñas gotas (Figura 16). Cada microgota actúa como una microrreacción independiente que contiene solo unas pocas moléculas de material genético, lo que permite una detección más precisa (Baker, 2012).

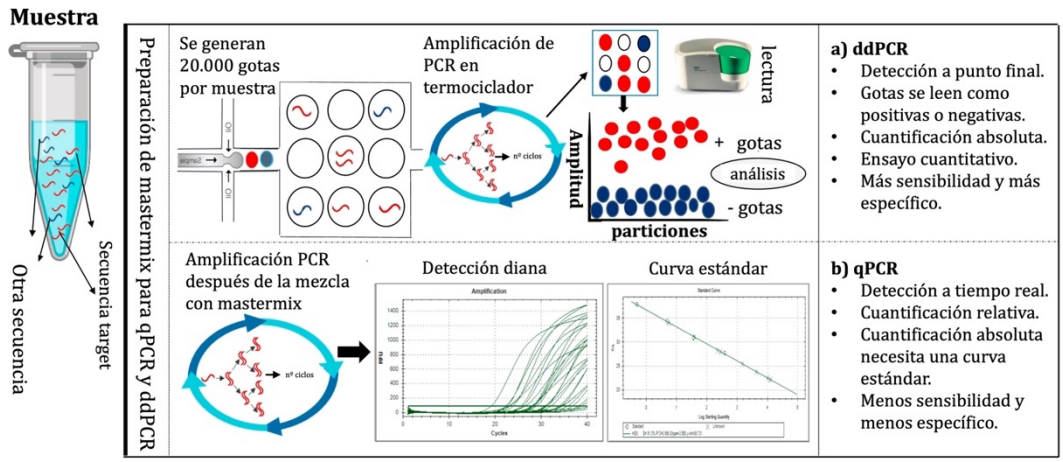

Figura 17. Flujo de trabajo comparando ddPCR y PCR en tiempo real. (a) flujo de trabajo de PCR digital en gotas (ddPCR) y detalles de los pasos de procesamiento de muestras; (b) flujo de trabajo de PCR de cuantificación (qPCR), incluidos detalles sobre el análisis de datos *(Modificado de Nyaruaba et al., 2019).*

Posteriormente las gotas de cada muestra se transfieren cuidadosamente (para proteger la integridad de las gotitas) a una placa de reacción de ddPCR de 96 pocillos, específica para realizar la amplificación del material genético en cada microgota mediante una reacción de PCR (Figura 17a). Después de la amplificación, se procede a la lectura de las gotas a través de un equipamiento específico que funciona como un

citómetro de flujo analizando cada gota y determinando si ha ocurrido una reacción o no en base a sondas o fluoróforos marcados que están unidos a la secuencia diana (Baker, 2012; Gutiérrez-Aguirre et al., 2015). Finalmente, los datos se analizan utilizando un programa específico (Kuypers & Jerome, 2017) en que los resultados obtenidos se interpretan de acuerdo al número de gotas y gráfica obtenido estableciendo los siguientes valores: Positivo ≥ 2, negativo = 0 y área gris > 0 < 1 (Cao et al., 2020).

La ddPCR utiliza los mismos cebadores y sondas que la PCR a tiempo real, pero presenta una mayor Se y precisión en la cuantificación (Baker, 2012; Whale et al., 2012), así lo demuestran estudios previos comparativos en unas mismas muestras a partir de FFPE (Hillemann et al., 2006; Larenas-Muñoz et al., 2022). Además, tiene una menor influencia de inhibidores presentes en la muestra (Dingle et al., 2014; Gutiérrez-Aguirre et al., 2015) y una mayor tolerancia a variaciones en los reactivos y condiciones de reacción (Huggett & Whale, 2013). Estas características hacen que la ddPCR sea especialmente útil en aplicaciones donde se requiere una alta exactitud en la cuantificación o cuando existe una escasa cantidad de ADN diana (Dreo et al., 2014; Gutiérrez-Aguirre et al., 2015; Rački et al., 2014) como es el caso de muchas muestras de animales con TB (Huggett & Whale, 2013; Nyaruaba et al., 2019). Por otro lado, en las aplicaciones estándar, la PCR en tiempo real no puede distinguir un número igual o inferior a dos copias de la diana de interés, a diferencia de la (Baker, 2012), la cual en una gotita puede contener una o más dianas (Nyaruaba et al., 2019).

A pesar de tener múltiples aplicaciones, la ddPCR no está exenta de limitaciones, ya que depende de una instrumentación bastante compleja, lo que conlleva a un elevado coste, haciéndola más difícil de aplicar especialmente en países en desarrollo (Huggett et al., 2015; Huggett & Whale, 2013; Nyaruaba et al., 2019). Por lo tanto, su uso está enfocado principalmente a investigación en la cual ha demostrado grandes avances.

3.2.3. Diagnóstico histopatológico

La histopatología permite analizar los cambios morfológicos que se producen en los tejidos en el transcurso de una enfermedad (Schöne et al., 2013), siendo una forma

rápida, económica y sencilla para identificar lesiones compatibles con TB. Asimismo, mediante técnicas histoquímicas especiales, como la técnica de Ziehl-Neelsen (ZN), se pueden identificar las micobacterias como BAAR (Cegielski et al., 1997; Courcoul et al., 2014; Gormley et al., 2014; Larenas-Muñoz et al., 2022; Morales et al., 2005; OMSA, 2022).

En el campo de la TB, la histopatología presenta la ventaja de detectar y clasificar lesiones tanto en animales positivos a la prueba de la IDTB como en animales negativos a esta técnica. Esto es especialmente útil cuando estas lesiones son muy pequeñas o no llegan a formar una lesión macroscópica visible (NVL) en los estados iniciales de la enfermedad, lo que podría hacer que pasen desapercibidas durante la inspección en el matadero (Cegielski et al., 1997; Morales et al., 2005). Además, en esta técnica se ha descrito una elevada Se, del 93,6 % (89,9–96,9 %), para el diagnóstico de TBb pero con una Sp del 83,3 % (78,7–87,6 %), menor en comparación con otras técnicas (Byrne et al., 2018; Corner et al., 2012; de la Rua-Domenech et al., 2006; Lorente-Leal et al., 2021; Ramos et al., 2015). Esta baja Sp puede atribuirse a que existen lesiones compatibles con TB, pero causadas por otros agentes como por ejemplo por bacterias pertenecientes a *M. avium subespecie paratuberculosis* (Álvarez et al., 2009; Corpa et al., 2000; Fernández et al., 2017; González et al., 2005; Perez et al., 1996) y otras micobacterias no pertenecientes al CMT (Cardoso-Toset, Gómez-Laguna, et al., 2015; Hernández-Jarguín et al., 2020; Supré et al., 2019).

En general, las lesiones asociadas al CMT han sido descritas en numerosos trabajos (J. A. L. Flynn, 2006; García-Jiménez, Benítez-Medina, et al., 2013; García-Jiménez et al., 2012; Hughes & Tobin, 2022; Hunter et al., 2022; Orme & Ordway, 2016; Pérez de Val et al., 2022; Turner et al., 2003; Wangoo et al., 2005; White et al., 2021) identificando como lesión característica al granuloma tuberculoso (Kemal et al., 2019; Palmer et al., 2022; Ramakrishnan, 2012) (véase la descripción y clasificación del granuloma tuberculoso descritas en el capítulo de inmunopatogenia de la TB).

Si bien la histopatología no ofrece un diagnóstico definitivo, ya que depende del aislamiento del CMT a través del cultivo microbiológico y/o PCR (Gormley et al., 2014;

OMSA, 2022; Romero et al., 2021), se ha demostrado que el uso en paralelo de la histopatología y el cultivo de la lesión, permiten identificar a los animales infectados (Courcoul et al., 2014; Varello et al., 2008). Por otro lado, cuando se ha usado en paralelo con la qPCR, los valores de Se y Sp mejoran sustancialmente, obteniendo valores de Se de hasta 98,0 % y Sp de 95,7 % (Cardoso-Toset, Gómez-Laguna, et al., 2015).

En cuanto a la técnica de ZN, ésta se ha utilizado históricamente para detectar BAAR, aunque es posible que en lesiones paucibacilares (baja cantidad de bacilos), ~~es~~ al tener una escasa cantidad de micobacterias no se detecten BAAR, lo que se traduce en niveles de Se y Sp reducidos con valores promedios de 33,9 % y 100 % respectivamente (Varello et al., 2008). En base a esto, se sabe que lesiones paucibacilares son frecuentes de observar en el bovino (Palmer et al., 2007, 2019; Wangoo et al., 2005), porcino (Cardoso-Toset, Gómez-Laguna, et al., 2015; García-Jiménez, Salguero, et al., 2013) y la cabra (Bezos, 2011; M. Gutiérrez et al., 1998). Por el contrario, otras especies como los primates , felinos , mustélidos (tejones) o marsupiales (zarigüeya australiana) suelen observarse lesiones pluribacilares (alta carga bacilar) (Hunter et al., 2022; O'Halloran et al., 2019; OMSA, 2022).

En el manual terrestre de los animales, la OMSA (2022) acepta la histopatología como un método de diagnóstico de TB con el objetivo de demostrar la ausencia de infección en la población, contribuir en los programas de control y erradicación y para confirmar casos clínicos. Recientemente en España, se ha incorporado oficialmente (MAPA, 2023c) el estudio histopatológico como parte del diagnóstico de la TB para los programas de control y erradicación en el caso de: "*Reses de seguimiento procedentes de pruebas de IDTB comparada de rutina o del Procedimiento de actuaciones y movimientos de ganado ante la aparición de animales reaccionantes en rebaños T3H sin sospecha de enfermedad en zonas de baja prevalencia de tuberculosis 2023*". Para esto, se describe que las muestras de animales, procedentes de establecimientos T3 o T3H, serán sometidas al estudio histopatológico o bien a PCR directa, no siendo necesarias pruebas adicionales si no se detectan lesiones histológicas compatibles o el resultado de la PCR es negativo (MAPA, 2023c). Para realizar la técnica, las muestras se

seleccionan de acuerdo a lo descrito en el manual para toma y envío de muestras para el diagnóstico del CMT (Romero et al., 2021).

4. MALDI – imaging: una aproximación a la histología molecular en tuberculosis

Las células contienen toda la información relativa a los cambios morfológicos, genéticos y proteómicos, lo que las convierte en la base óptima para el diagnóstico de enfermedades (Rauser et al., 2010). No obstante, comprender por completo este hecho resulta desafiante con las técnicas tradicionales de evaluación histológica (Morrison & DeNicola, 1993), inmunohistoquímica (Sukswai & Khoury, 2019), los análisis genómicos (Datta et al., 2015) o proteómicos tras microdisección láser (Gutstein & Morris, 2007). Así, en la última década, dentro de las técnicas disponibles en el campo de la proteómica, la imagenología por espectrometría de masas (MALDI-MSI, del inglés *Matrix-Assisted Laser Desorption/Ionization Mass Spectrometry Imaging*) se está utilizado para estudiar la expresión de perfiles de una amplia gama de analitos en los que se incluyen proteínas (Chaurand et al., 2008), péptidos (Beine et al., 2016; Schober et al., 2012), metabolitos (Signor et al., 2007), lípidos (Fernández-Vega et al., 2020; Signor et al., 2007), fármacos (Blanc et al., 2018; Römpp et al., 2011), entre otros (Oppenheimer et al., 2010; Rico Santana, 2015). Para esto, se considera la distribución espacial de estos analitos en el tejido objeto de estudio (Beine et al., 2016), integrando esta técnica con la histología tradicional (Chaurand et al., 2004; Norris & Caprioli, 2013).

La técnica de MALDI-MSI consiste en la colocación de un corte de tejido en un portaobjetos de vidrio sobre el que se le aplica una matriz que absorbe la energía láser y ayuda a la ionización. Seguidamente, un láser UV de alta energía ioniza las moléculas que se aceleran hacia un espectrómetro de masas, donde se separan según su relación masa/carga (*m/z*). La información de masas y abundancia de los iones generados se registran en un detector en función de su posición espacial en la muestra, y se asocia con las coordenadas espaciales de la muestra, lo cual permite la generación de un mapa de distribución molecular, donde se pueden identificar y cuantificar diferentes especies

moleculares en función de su localización en el tejido (Beine et al., 2016; Tuck et al., 2021) (Figura 18).

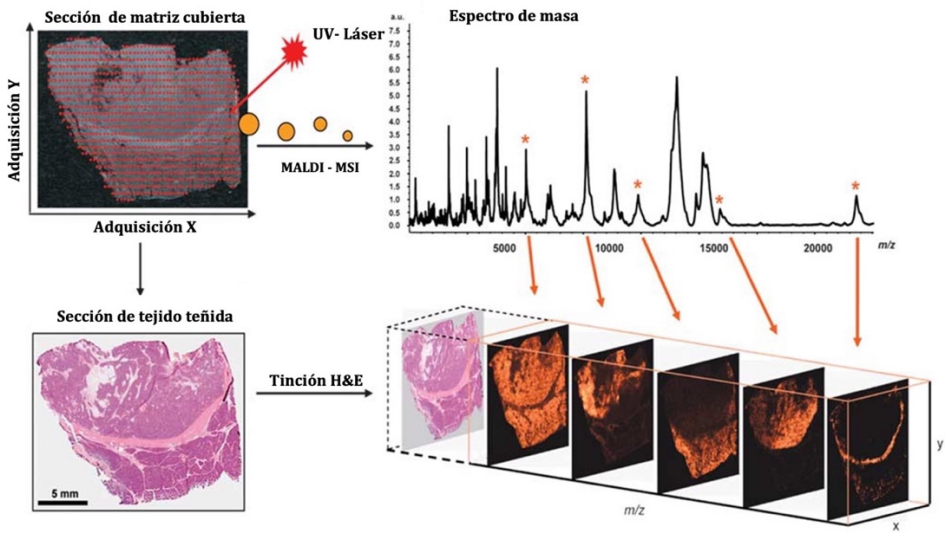

Figura 18. Flujo de trabajo de la técnica MALDI-MSI*. (Modificado de Aichler & Walch, 2015).*

La técnica de MALDI-MSI ofrece varias ventajas en comparación con otras pruebas diagnósticas, especialmente en el campo de la investigación. Así, MALDI-MSI permite hacer una visualización de la distribución espacial de moléculas en una muestra y un análisis no selectivo, permitiendo la detección de múltiples compuestos en paralelo (Beine et al., 2016; Denti et al., 2022; Maier et al., 2013; Sawyer et al., 2023) sin necesidad de conocimiento previo sobre qué se busca. Además, no necesita utilizar tinciones ni marcadores específicos para visualizar estas moléculas (Maier et al., 2013; Walch et al., 2008; Walther & Mann, 2010). Permite identificar moléculas desconocidas lo que hace que sea especialmente valioso en la investigación biomédica (Beine et al., 2016; Tuck et al., 2021). Sin duda una de las principales ventajas, y tal vez lo más atractivo es que MALDI-MSI puede proporcionar información adicional y complementaria a otras pruebas diagnósticas dentro de las que se encuentra principalmente la histopatología, lo que incluye información estructural y visual sobre los tejidos (Chaurand et al., 2004; Deutskens et al., 2011; Norris & Caprioli, 2013;

Wisztorski et al., 2010). En la IHQ, se puede visualizar la distribución de otras moléculas como lípidos y metabolitos (Claes et al., 2023), así como en la inmunofluorescencia (Sawyer et al., 2023) y en combinación con microdisección láser (Datta et al., 2015; Marakalala et al., 2016; Xu et al., 2009). También ha sido de utilidad en secuenciación de ADN y ARN para estudiar la expresión génica (Berggren et al., 2002; Rode et al., 2009) y en el análisis de proteínas y péptidos mediante la combinación de espectrometría de masas en tándem (MS/MS) para identificar proteínas específicas (Jørgensen et al., 2005; Vaysse et al., 2017). Probablemente en la actualidad el mayor uso es en farmacocinética y toxicología para rastrear distribución y metabolismo de fármacos y toxinas en tejidos (Blanc et al., 2018; Prideaux et al., 2011; Römpp et al., 2011; Wu et al., 2022).

A pesar de las múltiples ventajas que ofrece está técnica, algunos de los inconvenientes que posee es la falta de reproducibilidad y significancia de los resultados (Albrethsen, 2007; Rico Santana, 2015), además de ser una técnica cara que requiere de equipos especializados, así como personal capacitado para analizar los datos (Aichler & Walch, 2015; Maier et al., 2013; Rico Santana, 2015). El tiempo de análisis de las muestras es mayor en comparación con otras técnicas y adicionalmente en el procesamiento de las muestras son muy sensibles a la contaminación, puesto que pequeñas impurezas en la matriz o muestras pueden afectar los resultados y reducir la precisión de la técnica (Maier et al., 2013; Vaysse et al., 2017). Finalmente, si bien no es una desventaja, un detalle importante a considerar es que la técnica de MALDI-MSI es una técnica de aproximación diagnóstica, por lo que requiere la validación de sus resultados con otra técnica de diagnóstico (Rauser et al., 2010; Walch et al., 2008).

Desde hace una década hasta la actualidad la técnica de MALDI-MSI se ha aplicado mayoritariamente en la investigación clínica, clasificación de tumores, identificación de biomarcadores, histología molecular y, metabolismo entre otras áreas de interés (Fernández-Vega et al., 2020; Liu et al., 2010; Manzanares-Meza et al., 2017; Oppenheimer et al., 2010; Sallam, 2015). En el contexto de la TB, esta herramienta ya ha sido empleada en la búsqueda de factores de virulencia de *M. tuberculosis* (Madacki et al., 2019) así como en estudios de biomarcadores y resistencia de antibióticos en

humanos (Blanc et al., 2018). En esta última temática es donde se ha utilizado con mayor frecuencia para visualizar la distribución de fármacos y metabolitos en tejidos biológicos. En conejos, se ha utilizado para estudiar la distribución de moxifloxacino (fármaco antituberculoso) a lo largo del tiempo post-administración en muestras de pulmones con lesiones granulomatosas (Prideaux et al., 2011). En humanos, se ha demostrado en pulmones con presencia de granulomas tuberculosos que la rifampicina y pirazinamida penetran eficazmente los granulomas acumulándose en el caseum necrótico donde residen los bacilos tuberculosos persistentes, lo cual contribuye ampliamente a la mejora en el resultado del tratamiento en TB (Prideaux et al., 2015). Por otro lado, y siguiendo esta misma línea, estudios recientes se han centrado en identificar genes expresados diferencialmente (DEG, del inglés *differentially expressed genes*) y redes génicas asociadas a través de proteínas identificadas por MALDI-MSI (Udhaya et al., 2021). Así como, las cascadas de señalización implicadas en la resistencia del CMT frente a múltiples fármacos (Blanc et al., 2018; Prideaux et al., 2011). En otro estudio de TB, Marakala et al. (2016) determinaron la Ontología Genética (GO, del inglés *Gene Ontology*) a través del proteoma de granulomas tuberculosos mediante un análisis combinado con microdisección láser con el objetivo de seleccionar diferentes áreas del granuloma. Los resultados a nivel de la inmunopatogenia sugieren que la capacidad del huésped para contener a la micobacteria y restringir el daño tisular es un fenómeno localizado que sucede en granulomas de forma individual.

Es por esto, que la implementación de MALDI-MSI en cortes de tejidos de animales infectados con CMT permitiría identificar numerosas moléculas expresadas diferencialmente en los granulomas tuberculosos ayudando a comprender su papel y los posibles mecanismos en los que están involucradas en el desarrollo de esta enfermedad.

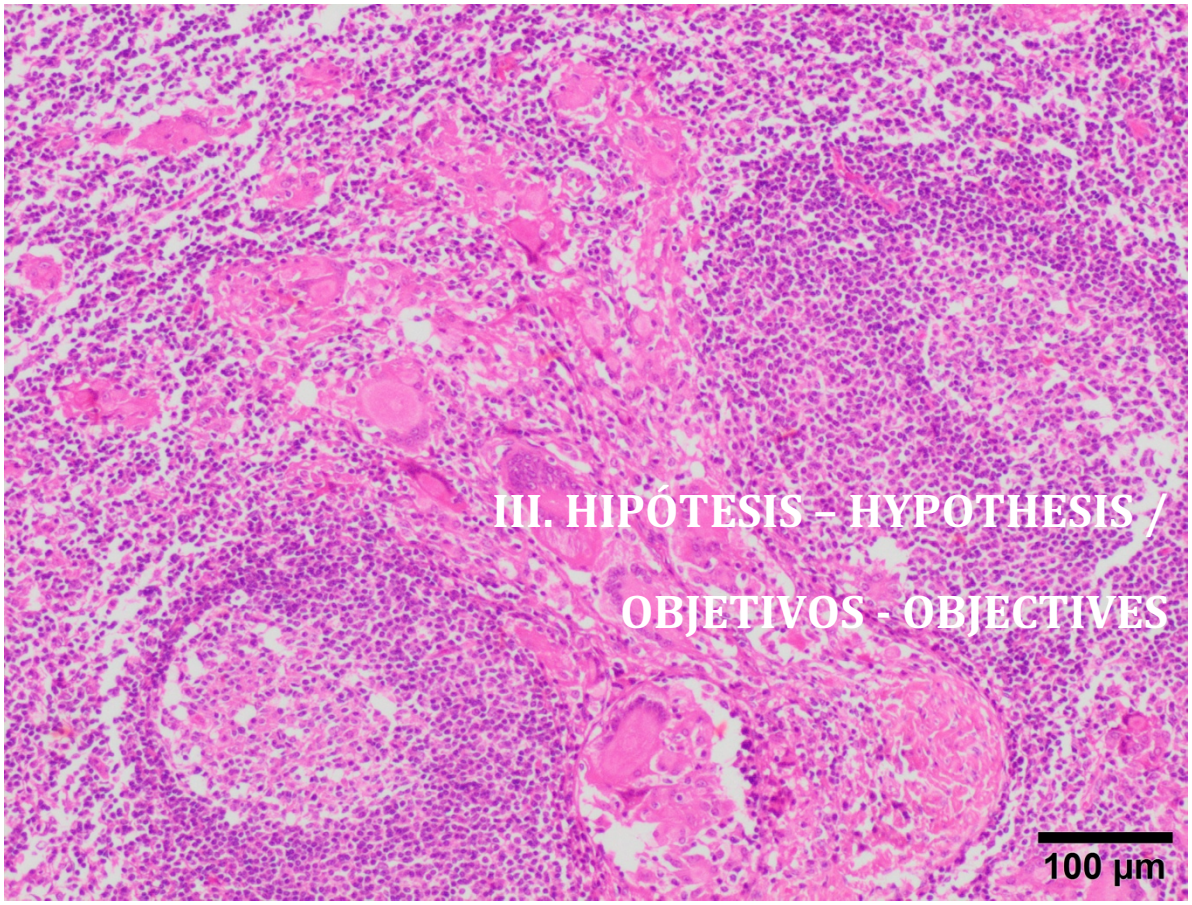

III. HIPÓTESIS – HYPOTHESIS / OBJETIVOS - OBJECTIVES

HIPOTÉSIS

La histopatología aplicada simultáneamente junto a las pruebas de diagnóstico oficial de la tuberculosis bovina, podrían mejorar la detección de animales positivos a la enfermedad. Además, esta técnica junto a la inmunohistoquímica y la histología molecular pueden resultar de gran valor para avanzar en el conocimiento de la inmunopatogenia de la tuberculosis animal.

OBJETIVOS

El objetivo general de esta tesis doctoral consiste en la puesta en valor de la histología como herramienta diagnóstica de tuberculosis, así como, valorar la utilidad de la histología molecular tanto de cara al diagnóstico como al estudio de la inmunopatogenia de la tuberculosis animal, con la finalidad de mejorar la sensibilidad y especificidad de las técnicas actuales y a su vez de los programas de control y erradicación de esta enfermedad.

Objetivo 1: Evaluar la importancia del estudio histopatológico frente a otras técnicas diagnósticas implementadas en el programa de control y erradicación de tuberculosis bovina.

> **Estudio 1:** The role of histopathology as a complementary diagnostic tool in the monitoring of bovine tuberculosis.

Objetivo 2: Evaluar la expresión de marcadores de células mieloides (CD172a y MAC387) y la polarización de macrófagos M1 (iNOS, CD68 y CD107a) y M2 (Arg1 y CD163) en los nódulos linfáticos de bovino y porcino para el estudio de la inmunopatogenia de la tuberculosis.

> **Estudio 2:** Monitoring the immune response of macrophages in tuberculous granuloma through the expression of CD68, iNOS and HLA-DR in naturally infected beef cattle.

Estudio 3: Macrophage polarization in lymph node granulomas from cattle and pigs naturally infected with *Mycobacterium tuberculosis* complex.

Objetivo 3: Estudiar los diferentes estadios de evolución de los granulomas tuberculosos mediante la técnica de espectrometría de masas con imagen por láser de desorción/ionización asistida por matriz (MALDI-Imaging) y detección de nuevos analitos involucrados en la patogenia de esta enfermedad.

Estudio 4: Proteomic analysis of granulomas from cattle and pigs naturally infected with *Mycobacterium tuberculosis* complex by MALDI-MSI.

HYPOTHESIS

Histopathology applied simultaneously with the official diagnostic tests for bovine tuberculosis could improve the detection of animals positive for the disease. In addition, this technique together with immunohistochemistry and molecular histology may be of great value in advancing the understanding of the immunopathogenesis of animal tuberculosis.

OBJECTIVES

The main objective of this doctoral thesis is to enhance the value of histology as a diagnostic tool for tuberculosis, as well as to assess the usefulness of molecular histology for both diagnosis and the study of the immunopathogenesis of animal tuberculosis, with the aim of improving the sensitivity and specificity of current techniques and, in turn, the control and eradication programmes for this disease.

Objective 1: To evaluate the importance of the histopathological study compared to other diagnostic techniques implemented in the programme for the control and eradication of bovine tuberculosis.

> **Study 1:** The role of histopathology as a complementary diagnostic tool in the monitoring of bovine tuberculosis.

Objective 2: To evaluate the expression of myeloid cell markers (CD172a and MAC387) and the polarisation of M1 (iNOS, CD68 and CD107a) and M2 (Arg1 and CD163) macrophages in bovine and porcine lymph nodes to study the immunopathogenesis of tuberculosis.

> **Study 2:** Monitoring the immune response of macrophages in tuberculous granuloma through the expression of CD68, iNOS and HLA-DR in naturally infected beef cattle.

Study 3: Macrophage polarization in lymph node granulomas from cattle and pigs naturally infected with *Mycobacterium tuberculosis* complex.

Objective 3: To study the different stages of evolution of tuberculous granulomas by matrix-assisted laser desorption ionisation/desorption imaging (MALDI-Imaging) mass spectrometry and detection of new analytes involved in the pathogenesis of this disease.

Study 4: Proteomic analysis of granulomas from cattle and pigs naturally infected with *Mycobacterium tuberculosis* complex by MALDI-MSI.

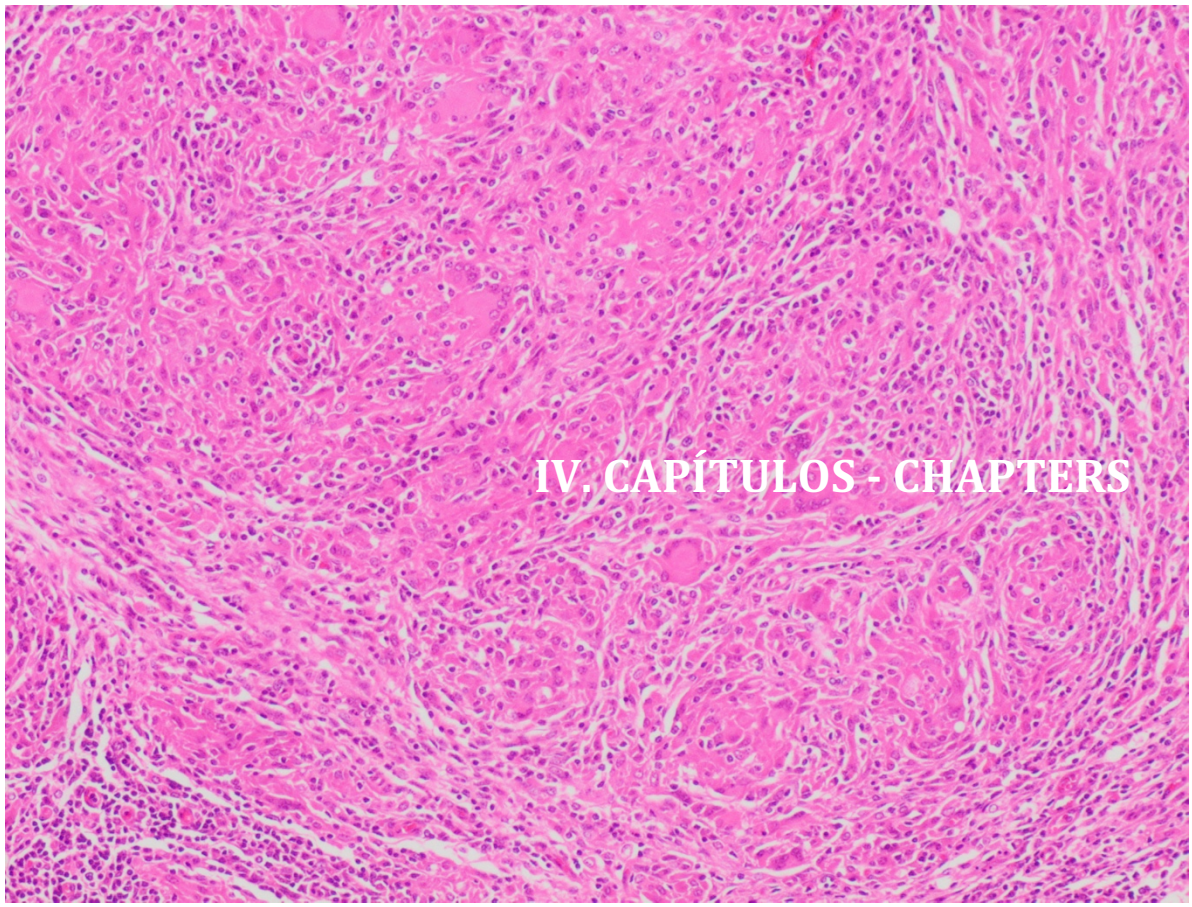

IV. CAPÍTULOS - CHAPTERS

Capítulo I

Estudio 1 / Study 1

Objetivo 1 / Objective 1

Estudio 1: The Role of Histopathology as a Complementary Diagnostic Tool in the Monitoring of Bovine Tuberculosis

Fernanda Larenas-Muñoz [1], José M. Sánchez-Carvajal [1], Ángela Galán-Relaño [2], Inés Ruedas-Torres [1], Eduardo Vera-Salmoral [1,2], Lidia Gómez-Gascón [2], Alfonso Maldonado Librado Carrasco [1], Carmen Tarradas [2], Inmaculada Luque [2], Irene M. Rodríguez-Gómez [1†] and Jaime Gómez-Laguna [1†]*

Publicado en Frontiers in Veterinary Science, 2022, 9, 816190, JIF: 3.2 (Q1)

Objetivo 1: Evaluar la importancia del estudio histopatológico frente a otras técnicas diagnósticas implementadas en el programa de control y erradicación de tuberculosis bovina.

Objective 1: Evaluate the importance of the histopathological study compared with other diagnostic techniques implemented in the bovine tuberculosis control and eradication programme.

The Role of Histopathology as a Complementary Diagnostic Tool in the Monitoring of Bovine Tuberculosis

Fernanda Larenas-Muñoz [1], José M. Sánchez-Carvajal [1], Ángela Galán-Relaño [2], Inés Ruedas-Torres [1], Eduardo Vera-Salmoral [1,2], Lidia Gómez-Gascón [2], Alfonso Maldonado Librado Carrasco [1], Carmen Tarradas [2], Inmaculada Luque [2], Irene M. Rodríguez-Gómez [1†] and Jaime Gómez-Laguna [1†]*

[1] Department of Anatomy and Comparative Pathology and Toxicology, University of Córdoba, International Excellence Agrifood Campus 'CeiA3', Córdoba, Spain,

[2] Department of Animal Health, University of Córdoba, International Excellence Agrifood Campus 'CeiA3', Córdoba, Spain

†These authors have contributed equally to this work and share senior authorship

*Correspondence: Fernanda Larenas-Muñoz

ep2lamuf@uco.es

Abstract

The diagnosis of bovine tuberculosis (bTB) is based on the single intradermal tuberculin test (SIT), interferon gamma, and compulsory slaughter of reactor animals. Culture and PCR from fresh tissue are regarded as gold standard techniques for *post-mortem* confirmation, with the former being time-consuming and presenting moderate to low sensitivity and the latter presenting promising results. Histopathology has the advantage to identify and categorize lesions in both reactor and non-reactor animals. Therefore, this study aims to highlight the role of histopathology in the systematic diagnosis of bTB to shorten the time to disclose positive animals. Blood (212) and lymph node (681) samples were collected for serological, bacteriological, and histopathological analyses from a total of 230 cattle subjected to the Spanish bTB eradication program. Seventy one lymph nodes and 59 cattle yielded a positive result to bacteriology, with 59 lymph nodes and 48 cattle presenting a positive result in real-time PCR from fresh tissue. Roughly 19% (40/212) of sera samples gave a positive result to ELISA. Tuberculosis like lesions (TBLs) were observed in 11.9% (81/681) of the lymph nodes and 30.9% (71/230) of cattle. Noteworthy, TBLs were evidenced in 18 out of 83 SIT^- and realtime PCR and bacteriology negative animals, with 11/18 disclosing a positive result to Ziehl-Neelsen technique and two of them to ddPCR from paraffin blocks targeting IS*6110*. Six out of these 11 ZN^+ corresponded with mesenteric LN and were confirmed positive to paratuberculosis. Histopathology yielded a sensitivity of 91.3% (CI_{95} 83.2– 99.4%) and a specificity of 84.4% (CI_{95} 78.6–89.3%) with good agreement (κ= 0.626) when compared with real-time PCR. Our results confirm that histopathology allows a rapid confirmation of real-time PCR and bacteriology, emphasizing its contribution to bTB control and monitoring.

Keywords: bovine tuberculosis, histopathology, diagnostic tests, tuberculosis like lesions, sensitivity, specificity

1. Introduction

Bovine tuberculosis (bTB) is a chronic infectious zoonotic disease mainly caused by either *Mycobacterium bovis* or *M. caprae,* and other members of the *Mycobacterium tuberculosis* complex (MTC) that affects various species of mammals (1). BTB is a significant economic threat to farm businesses in the form of trading restriction and slaughtering of reactor animals within the eradication campaign framework (1, 2). In many countries, the eradication program has faced important challenges in its struggle against bTB due to the persistence of non-reactive positive animals in the farm and wildlife reservoirs, limiting their progress toward the eradication of this disease from cattle, the main source of infection for humans (1, 3). Therefore, the development of rapid and accurate diagnostic techniques and protocols for the detection and culling of MTC-infected animals is one of the cornerstones of success to control and eradicate bTB in cattle and other species (4–6).

In the European Union (UE), the current bTB control program is mostly based on the single intradermal tuberculin test (SIT) and interferon gamma release assays to disclose reactor animals, followed by compulsory slaughter of these animals and livestock movement restrictions measures (7). The microbiological culture has been traditionally considered as the gold standard technique for bTB diagnosis (8, 9). However, it is reported as a time-consuming technique with a moderate to low sensitivity (Se), delaying the turnaround time to make a decision for 3 months (9).

Nowadays, the diagnostic tests available for bTB are imperfect because of limited Se and specificity (Sp) (5, 10, 11). The standard interpretation of SIT leads to a Se of 68–96.8% and a Sp of 75.5– 98.8% (11), while the gamma interferon test presents a higher estimated Se, between 73.0–100%, and Sp ranging from 85.0 to 99.6% (11, 12). BTB-ELISA test, validated by World Organization for Animal Health (OIE), presents a high variability of Se, ranging from 45.0 to 98.6% and Sp from 52.5 to 100% (13), although better estimates have been reported with alternative cocktails of antigens or

different methodological approaches (14). In the case of *post-mortem* techniques, bacteriology presents average Se and Sp values of 78.1% (72.9–82.8%) and 99.1% (97.1–100%), respectively (15). On the other hand, real-time PCR directly from fresh tissue samples has been recently reported as a promising diagnostic tool with a moderate to high values of Se and Sp (16, 17).

Histopathology has the advantage to identify and categorize lesions in both reactor and non-reactor animals even when they are unnoticed during the visual inspection at the slaughterhouse. This technique presents an average Se of 93.6% (89.9–96.9%) for the diagnosis of bTB but with less Sp than other techniques, on average 83.3% (78.7–87.6%) (16). This approach must be followed by a definitive diagnosis that is dependent on the isolation of *M. bovis*, but it is worth to note that the use in parallel of histopathology and culture of lesion has shown to provide an effective way of identifying infected animals (15). Moreover, identification of microscopic lesions in no grossly affected tissues or tuberculosis-like lesions (TBL) in anergic animals can be achieved by means of histopathology. In this sense, a rapid confirmation of bTB in tuberculosis-free herds is pivotal to prevent the spread of the disease, with the combination of different diagnostic tools representing a smart approach to obtain an efficient diagnosis improving its control. Therefore, this study aimed (i) to highlight the role of histopathology in the systematic diagnosis of bTB to shorten the time to disclose positive animals, but also (ii) to evaluate the histopathology as a complementary tool to be used with real-time PCR targeting IS*6110* and microbiological culture to confirm positive animals.

2. Materials and methods

2.1 *Study Population*

A total of 230 cattle, subjected to the surveillance and monitoring for bTB in the framework of the Spanish national eradication program (18) between October 2018 and December 2019 were included in this study. According to their SIT test result, the 230 cattle were classified as SIT positive (SIT^+, bovine PPD ≥ 4 mm or SIT inconclusive 2 mm > bovine PPD > 4 mm) and SIT negative (SIT^-, ≤ 2 mm bovine PPD), belonging to each group of 139 (60.4%) and 91 (39.6%) animals, respectively. SIT inconclusive results were considered as positive.

Blood samples and samples from retropharyngeal, tracheobronchial, mediastinal, and mesenteric lymph nodes (LNs) were collected along the slaughter line and kept refrigerated until arrival to the laboratory. Tracheobronchial and mediastinal LNs were processed as a pool (tracheobronchial mediastinal LN) since volume sample was not enough when independently processed. Due to the logistics of the slaughterhouse and the timing of slaughtering, it was not always possible to collect blood and LN samples from the 230 cattle. Thus, a total of 212 blood samples for the serological analysis and 227, 226, and 228 samples from retropharyngeal, tracheobronchial-mediastinal, and mesenteric LNs, respectively, were collected. From each LN, samples were divided in two parts. One part was fixed in 10% neutral-buffered formalin for the histopathological analysis and the second part was processed to obtain a tissue homogenate for bacteriological culture.

2.2 Bacteriological Culture

Every LN sample was individually homogenized with a tissue homogenizer (Fisherbrand, Fisher Scientific, Madrid, Spain) to obtain a uniform mixture and stored at −20°C until use (17). Briefly, 4–7 g of each LN tissue sample were placed into a 15 ml

tube (Falcon™; Corning, Madrid, Spain) with the same volume (w/v: 1/1) of 0.85% sterile NaCl and grinded until a homogeneous mixture was obtained. Tissue homogenate was used for selective bacterial culture according to the protocol carried out in a previous study (17). Briefly, the homogenate was decontaminated with an equal volume of 0.75% (w/v: 1/1) hexadecyl pyridinium chloride solution in agitation for 30 min. Samples were centrifuged for 30 min at 1,500 × *g*. Pellets were collected with swabs and cultured in liquid media (MGIT™ 960; Becton Dickinson, Madrid, Spain) using an automatized BD Bactec™ MGIT™ System (Becton Dickinson, Spain). Culture was considered positive when isolates were identified as MTC by real-time PCR (19). Individually, an animal was considered positive when at least one out of the three LN samples was positive.

2.3 Real-Time PCR From Fresh Tissue Targeting IS6110

Deoxyribonucleic acid extraction from homogenized tissue samples and subsequent real-time PCR targeting IS*6110* was performed in a parallel study from our research group (17). Briefly, DNA Extract Vacunek (VK; Bizkaia, Spain) was performed according to manufacturer's instructions with modifications. Specific primers (IS*6110*-forward: 5′GGTAGCAGACCTCACCTATGTGT-3′; IS*6110*-reverse: 5′-AGGCGTCGGTGACAAAGG-3′) and a probe (IS*6110*-probe: 5′-FAM-CACGTAGGCGAACCC-MGBNFQ-3′) targeting a conserved region of IS*6110* transposon were used for the realtime PCR (16, 17, 20) by using the QuantiFast ᴿ Pathogen PCR + IC Kit (QIAGEN, Hilden, Germany). Real-time PCR was carried out using the QuantiFast ᴿ Pathogen PCR + IC Kit (QIAGEN, Hilden, Germany) with amplifications run in duplicate in the MyiQTM2 Two-Color qPCR Detection System (Bio-Rad, Hercules, CA, USA) under the following cycling conditions: 95°C for 5 min, followed by 45 cycles of 95°C for 15 s and 60°C for 30 s. Following the manufacturer's guidelines, an exogenous inhibition heterologous control (internal amplification control, IAC) supplied with the kit was included. Complete inhibition of amplification was considered when IAC did not amplify, while partial inhibition was considered when it showed a quantification cycle

(Cq) > 33. An inter-run calibrator with a known Cq value of 32 was introduced in each assay to self-control intra-assay repeatably and accuracy. The limit of detection for this real-time PCR is from 10 to 100 genomic equivalents, and the cut-off is established at Cq < 38 (17).

2.4 Blood Samples and Antibody Detection

Sera was obtained from blood by centrifugation at 6,000 × *g* for 10 min and stored at −20°C until analysis. The presence of specific antibodies against *M. bovis* was determined by using a commercial ELISA kit (IDEXX, *Mycobacterium bovis* Antibody Test kit, Westbrook, Maine, USA) following manufacturer's instructions.

2.5 Histopathology

Formalin-fixed LNs were routinely processed and embedded in paraffin. All samples were stained with hematoxylin-eosin (H&E) for their histopathological analysis. Histopathological findings were microscopically evaluated, and samples were classified as positive if TBLs were observed. TBLs were considered as those consistent with tuberculous granuloma, pyogranuloma, or scattered Langhans-type multinucleated giant cells (MNGCs). Tuberculosis (TB) granuloma were classified into 4 different stages as previously reported (21). Briefly, stage I (initial) granulomas are characterized by the presence of abundant epithelioid macrophages with lymphocytes, neutrophils, and, at times, MNGCs. Stage II (solid) granulomas are characterized by epithelioid macrophages surrounded by a thin connective tissue capsule. Infiltrates of neutrophils and lymphocytes may be present along with MNGCs. In addition, the necrosis, if present, is minimal. Stage III (necrotic) granulomas are characterized by a necrotic center surrounded by a zone of epithelioid macrophages with or without MNGCs and lymphocytes and encapsulated with fibrous connective tissue. Stage IV (necrotic and mineralized) granulomas are characterized by coalescent granulomas with a complete fibrous encapsulation, extensive central necrosis, and mineralization

surrounded by epithelioid macrophages and MNGCs (21). For each LN sample, all granulomas were staged, and a specific stage was given to the sample according to the most represented stage. Pyogranulomas were characterized by a necrotic core with abundant neutrophils surrounded by epithelioid cells and a rim of connective tissue with infiltrate of mononuclear cells. Tissue with normal histological characteristics and no lesion compatible with TBL was considered as negative.

Additional sections from those samples containing TBLs were carried out and stained with Ziehl-Neelsen (ZN) technique for the identification of acid-fast bacilli (AFB). A sample was considered positive for ZN when one or more AFB were detected in at least one high-power field magnification (HPF, 100x) of the sample and, according to the results, the lesions were classified as paucibacillary if it was observed with 1 to 10 AFB bacilli, or pluribacillary if ≥ 11 AFB were observed per HPF (22, 23). Those lesions that yielded a negative result to ZN technique were also subjected to periodic acid-Schiff (PAS) and Gram staining to rule out the presence of fungal structures and bacterial colonies, respectively.

Furthermore, fresh tissue samples from LNs with TBL and a negative result to SIT, real-time PCR from fresh tissue targeting IS*6110,* and culture were subjected to *Mycobacterium avium* subspecies *paratuberculosis* (MAP) detection by using the PCR MAPTB-VK kit (Vacunek S.L., Bizkaia, Spain). DNA template from fresh tissue was run in duplicate for each sample in the MyiQ™2 Two-Color real-time PCR Detection System (BioRad, Hercules, CA, USA) following manufacturer's guidelines. A sample was considered as positive when the Cq value was < 40.

2.6 DNA Extraction From Formalin-Fixed Paraffin Embedded (FFPE) Samples

Deoxyribonucleic acid extraction from the paraffin blocks and subsequent real-time PCR were performed from SIT, real-time PCR (from fresh tissue), and bacteriology

negative samples, but were positive to the histopathological detection of TBL, independent of their result to ZN technique.

Deoxyribonucleic acid extraction from formalin-fixed paraffine embedded (FFPE) samples was performed using NucleoSpin ® DNA FFPE XS kit (Macherey-Nagel, Germany) according to the manufacturer's guidelines with some modifications. In brief, 7 sections of 10 µm thickness were obtained from each tissue block and collected in a sterile microcentrifuge tube of 1.5 ml. A new blade was used for each tissue block to avoid cross contamination. Tissue sections were dewaxed by three incubation steps in xylene at 60°C and 700 rpm for 2 min, followed by two washes with 100% ethanol to remove residual xylene. After dewaxing, tissues were incubated with an open lid at 60°C for 10–12 min to dry the pellet. The tissue was digested in the lysis buffer FL with 20 µl of proteinase K and incubated at 56°C and 700 rpm overnight. Thereafter, Decrosslink Buffer was added and incubated at 90°C and 250 rpm for 30 min, followed by ethanol precipitation. The solution was transferred into a spin column and washed following manufacturer's instructions. DNA was eluted in 60 µl of Elution Buffer. Residual ethanol DNA was removed by incubation at 90°C and 250 rpm for 8 min.

2.6 Real-Time PCR From FFPE Targeting IS*6110*

Deoxyribonucleic acid templates from FFPE samples were diluted up to a final concentration of 150 ng/µl, and amplifications were run in duplicate for each sample in the MyiQ™2 Two-Color real-time PCR Detection System (Bio-Rad, Hercules, CA, USA) following the similar conditions as above mentioned for real-time PCR from fresh tissue.

2.7 Droplet Digital PCR (ddPCR) for Detection of MTC in FFPE Samples

In order to use a technology with a higher Se than real-time PCR for detecting traces of DNA, a droplet digital PCR (ddPCR) targeting IS*6110* was run in the FFPE samples mentioned above. Indeed, we used the same specific primers and probe targeting a

conserved region of IS*6110*. According to Bio-Rad ddPCR system guidelines, each reaction was prepared in a final volume of 20 µl, including 10 µl of ddPCR Supermix for probe (No dUTP), 1.6 µl of IS*6110*-forward (10 mM), 0.8 µl of IS*6110*-reverse (10 mM), 0.6 µl of IS*6110*-probe (FAM-labeled, 10 mM), 4 µl of DNA template, and 3 µl of nuclease-free water. Afterwards, the droplets were generated on the droplet generator according to the manufacturer's instructions. These droplets were carefully transferred to a specific 96-well ddPCR reaction plate (Bio-Rad, Hercules, CA, USA). After heat-sealing, amplifications were run in the C1000 Touch thermal cycler (Bio-Rad, Hercules, CA, USA) under the following cycling conditions: 95°C for 10 min, followed by 40 cycles of 94°C for 30 s and 59°C (annealing/extension) for 1 min, and finally 98°C for 10 min. The temperature ramping rate was set at 2°C/s. Thereafter, the droplets were stored in darkness at 4°C for 12 h. A QX200 Droplet Reader (Bio-Rad, Hercules, CA, USA) was used to read and count the droplets, and the data were then analyzed by using the QuantaSoft Analysis Program (Bio-Rad, Hercules, CA, USA). Samples were disclosed as MTC-positive when the number of positive droplets was ≥ 2. In contrast, samples were MTC-negative if the number of positive droplets was 0, and a droplet number of 0–1 was defined as the'gray area' (24).

3. Statistical Analysis

Culture and real-time PCR were considered as gold standard tests for *post-mortem* diagnosis of bTB (5). Thus, the results of the histopathological study were compared with bacteriological culture and real-time PCR from fresh tissue results to estimate diagnostic Se and Sp and positive and negative predictive values (PPV/NPVs) by using WinEpi 2.0 (Faculty of Veterinary, University of Zaragoza, Spain; http://www.winepi.net/uk/index. htm). Cohen's kappa coefficient (κ) analysis was conducted to assess the agreement between two raters. Analysis results were categorized into six categories based on kappa values: no agreement (κ≤ 0), slight (0.01 <κ≤ 0.20), weak (0.21 <κ≤ 0.40), moderate (0.41 <κ≤ 0.60), good (0.61 <κ≤ 0.80), and very good (0.81 <κ≤ 1.00) agreement (WinEpi software 2.0).

4. Results

4.1 Bacteriological Culture

Seventy-one LNs yielded a positive result to bacteriological culture. Among these samples, the majority of them corresponded to the tracheobronchial-mediastinal LN (40 out of 71; 56.3%), followed by the retropharyngeal LN (22 out of 71; 31.0%) and, in a lesser extent, the mesenteric LN (9 out of 71; 12.7%) (**Table 1**). Analyzing the results per animal and considering that an animal was positive when at least one of its 3 LNs resulted positive to bacteriology, 59 out of 230 cattle (25.6%) gave a positive result to bacteriological culture, whereas 171 animals (74.3%) were negative. Eleven animals were positive for more than one LN. From them, 5 cattle were positive for both retropharyngeal and tracheobronchial-mediastinal LNs. Another 5 cattle were positive for tracheobronchial-mediastinal and mesenteric LNs, while only one animal (1 out of 11) was positive for the 3 examined LNs.

4.2 Real-Time PCR From Fresh Tissue Targeting IS6110

Fifty-nine out of 681 LNs yielded a positive result to real-time PCR from fresh tissue. Among these samples, the majority of them corresponded to the tracheobronchial-mediastinal LN (36 out of 59; 61.1%), followed by the retropharyngeal LN (18 out of 59; 30.5%) and, in a lesser extent, the mesenteric LN (5 out of 59; 8.5%) (**Table 1**). Analyzing the results per animal and as mentioned above, taking into account that an animal was positive when at least one of its 3 LNs resulted positive to realtime PCR, 59 out of 230 cattle (25.7%) gave a positive result to bacteriological culture, whereas 171 animals (74.3%) were negative. Eleven animals were positive for more than one LN, and from them, seven cattle were positive for both retropharyngeal and tracheobronchial-mediastinal LNs. Another three cattle were also positive for tracheobronchial-mediastinal and mesenteric LNs, while only one animal (1 out of 59) was positive for the 3 examined LNs.

4.3 Serological Analysis

Forty out of 212 sera samples (18.9%) gave a positive result to the ELISA test, while the remaining samples were negative (**Table 2**). Eighteen ELISA$^+$ samples belonged to SIT$^+$/MTC$^+$/PCR$^+$ cattle (18/39; 46.2%), with 19 ELISA$^+$ animals corresponding to cattle positive to any of these three techniques (**Table 2**). Only 3 out of 76 SIT$^-$/MTC$^-$/PCR$^-$ animals (3.9%) presented specific antibodies against *M. bovis*.

TABLE 1 | Results of *Mycobacterium tuberculosis* complex (MTC) culture and real-time PCR IS*6110* considering the examined lymph node.

	Lymph nodes (LN)	Positive	Negative	Total
MTC		(*n* = 71)	(*n* = 610)	(*n* = 681)
	Retropharyngeal LN	22/71 (31.0%)	205/610 (33.6%)	227/681 (33.3%)
	Tracheobronchial-mediastinal LN	40/71 (56.3%)	186/610 (31.0%)	226/681 (33.2%)
	Mesenteric LN	9/71 (12.7%)	219/610 (35.9%)	228/681 (33.5%)
Real-time PCR IS*6110*		(n = 59)	(n = 622)	(n = 681)
	Retropharyngeal LN	18/59 (30.5%)	209/622 (33.6%)	227/681 (33.3%)
	Tracheobronchial-mediastinal LN	36/59 (61.0%)	190/622 (30.5%)	226/681 (33.2%)
	Mesenteric LN	5/59 (8.5%)	223/622 (35.9%)	228/681 (33.5%)

LN, Lymph node

4.4 Histopathological Findings

Tuberculosis-like lesions were observed in 81 out of 681 (11.9%) examined LNs and were distributed as TB granuloma in 60 samples (60 out of 81; 74.1%), pyogranuloma in 5 samples (5 out of 81; 6.2%), and scattered Langhans-type MNGCs in 16 samples (16 out of 81; 19.7%) (**Figure 1**, **Table 3**). TB granulomas were highly represented in the tracheobronchial-mediastinal LN, followed by the retropharyngeal LN (33 out of 38, 86.8%; and 16 out of 21, 76.2%, respectively). The presence of scattered Langhans-type MNGCs was another type of TBL frequently observed in the mesenteric LN (9 out of 22; 40.9%). Seventy one out of 230 cattle (30.9%) presented TBL. Nine animals were positive for more than one LN, and from them, 2 cattle were positive for both retropharyngeal and tracheobronchial-mediastinal LNs and tracheobronchial-mediastinal and mesenteric LNs. Another 4 cattle were positive for tracheobronchial-mediastinal and mesenteric LNs, while only one animal (1 out of 9) was positive for the 3 examined LNs (**Figure 2**). Ziehl-Neelsen technique was performed to determine the presence of AFB in samples with TBL (**Table 4**). Sixty-one out of 81 samples (75.3%) with TBL yielded a positive result to ZN technique, mainly corresponding to TB granuloma (54 out of 81; 66.7%). Only 6 out of 16 samples with Langhans-type MNGCs presented a ZN^+ result (37.5%), and just 1 sample out of 5 (20.0%) with pyogranuloma. As depicted in **Table 5**, from all ZN^+ LNs, 43 showed a paucibacillary form (**Figure 3A**) (22 in tracheobronchial-mediastinal LN, 15 in retropharyngeal LN and 6 in mesenteric LN), whereas 18 showed a pluribacillary form (**Figure 3B**) (8 in mesenteric LN, 7 in tracheobronchial-mediastinal LN, and 3 in retropharyngeal LN). Nineteen out of the 81 TBL samples were positive for ZN (13 paucibacillary and 8 pluribacillary) and negative for SIT, MTC, and PCR. Neither bacterial colonies by H&E and Gram staining nor fungal structures by PAS staining were evidenced in ZN^- samples.

Tuberculosis-like lesions were identified in a total of 61 cattle, with 53 animals presenting a positive result to SIT, MTC, and/or PCR. Noteworthy, TBL were identified

in all animals with a positive result to bacteriology or to PCR, independently of the SIT result, except in 15 out of 59 MTC^+ animals and 6 out of 48 PCR^+ animals in which histopathological lesions were not observed (**Table 6**). Interestingly, when the histopathology was compared to SIT and bacteriological culture results per animal, 18 out of 83 SIT^-, MTC^-, and PCR^- animals presented TBL. Among them, 8 showed TB granuloma, 1 pyogranuloma, and 9 Langhans-type MNGCs. In these animals, ZN results evidenced the presence of AFB in 5 out of 8 TB granuloma and 6 out of 9 Langhans-type MNCGs. The pyogranuloma was negative for ZN. As mentioned above, neither bacterial colonies nor fungal structures were evidenced by H&E, Gram, and PAS staining. Remarkably, MAP was detected in 6 of these samples by real-time PCR, all of them belonging to mesenteric LNs with pluribacillary ZN staining. Among the animals which presented other types of lesions other than TBL, 2 of them presented parasitic migration, 1 choristoma, 10 psammoma bodies, and 2 with inflammatory infiltration.

Furthermore, the relationship between ZN staining (paucibacillar vs. pluribacillar patterns) and the stage of TB granuloma with respect to the result to the different techniques (SIT, ELISA, bacteriology, and real-time PCR) was also analyzed. A total of 54 TB granulomas with a ZN result were included in this study. These samples corresponded to 40 granulomas with a paucibacillar ZN staining and 14 granulomas with a pluribacillar staining. Paucibacillary granulomas were distributed as follows: 1 stage I granuloma, 2 stage II granulomas, 8 stage III granulomas, and 29 stage IV granulomas. Pluribacillary granulomas consisted of 6 stage I granulomas, 5 stage III granulomas, and 3 stage IV granulomas. No stage II granuloma was found.

According to this distribution, paucibacillar stage IV granulomas prevailed in our study and corresponded to cattle positive to at least two of the analyzed techniques: 10 $SIT^+/ELISA^+/MTC^+/PCR^+$ animals; 1 $SIT^+/ELISA^+/MTC^-/PCR^+$ animal; 1 $SIT^+/ELISA^+/MTC^-/PCR^-$ animal; 10 $SIT^+/ELISA^-/ MTC^+/PCR^+$ animals; and 3 $SIT^+/MTC^+/PCR^+$ animals. Two stage IV granulomas yielded a negative result to SIT, bacteriology, and PCR (no serum was available for ELISA). In this line, paucibacillary

stage III granulomas belonged to cattle with positive result to at least three of the analyzed techniques, namely, 3 $SIT^+/ELISA^+/MTC^+/PCR^+$ animals, 4 $SIT^+/ELISA^-/MTC^+/PCR^+$ animals, and 1 $SIT^+/MTC^+/PCR^+$ animal. The low number of animals in which stage I and stage II granulomas prevailed did not allow analyzing their relationship with regards to the other techniques

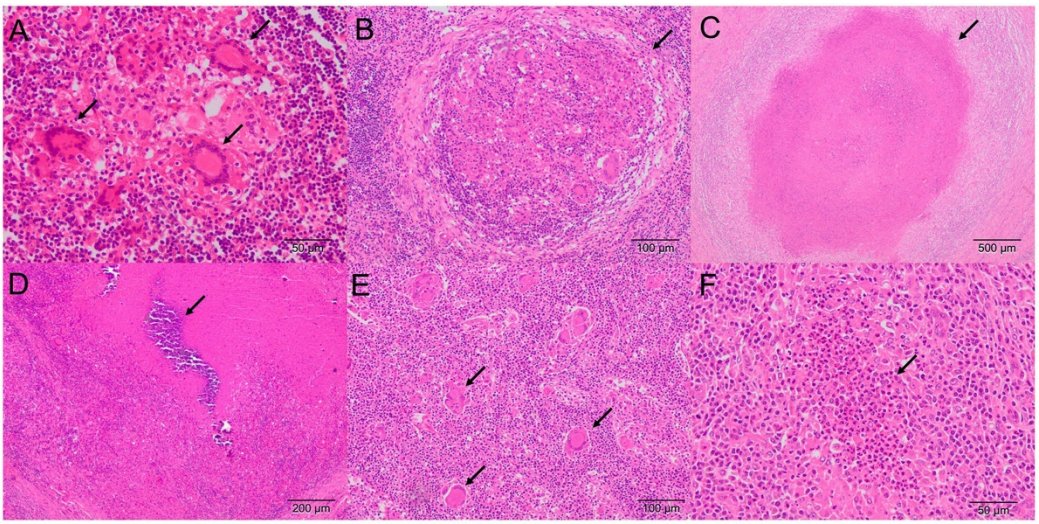

FIGURE 1 | Microscopic lesion of TBLs in LNs (H&E) *(A) Tracheobronchial-mediastinal LN. Stage I granuloma showing clustered epithelioid macrophages with multinucleated giant cells (MNGCs; arrows) (B) Retropharyngeal LN. Stage II granuloma with abundant epithelioid macrophages, lymphocytes, MNGCs, and a fibrous capsule (arrow) (C) Mesenteric LN. Stage III granuloma showing a complete fibrous capsule and central necrosis with little mineralization (arrow) (D) Tracheobronchial-mediastinal LN. Stage IV coalescent granuloma with a complete fibrous encapsulation, extensive central necrosis, and mineralization (arrow) (E) Mesenteric LN. Multiple scattered Langhans-type MNGCs (arrows). (F) Retropharyngeal LN. Pyogranuloma with polymorphonuclear cells (arrow), apoptotic bodies, and abundant necrotic center.*

TABLE 2 | Distribution of ELISA results from the 212 animals according to their intradermal skin test (SIT), culture (MTC) and real-time PCR results.

	SIT⁺ (n = 128)				**SIT⁻ (n = 84)**				
	MTC⁺ (n = 47)		**MTC⁻ (n = 81)**		**MTC⁺ (n = 7)**		**MTC⁻ (n = 77)**		**Total**
	PCR⁺	**PCR⁻**	**PCR⁺**	**PCR⁻**	**PCR⁺**	**PCR⁻**	**PCR⁺**	**PCR⁻**	
ELISA⁺	18/39	2/8	1/2	16/79	0/2	0/5	0/1	3/76	40/212
	(46.2 %)	(25.5 %)	(50.0 %)	(20.3 %)	(0.0 %)	(0.0 %)	(0.0 %)	(3.9 %)	(18.9 %)
ELISA⁻	21/39	6/8	1/2	63/79	2/2	5/5	1/1	73/76	172/212
	(53.8 %)	(75.0 %)	(50.0 %)	(79.7 %)	(100.0 %)	(100.0 %)	(100.0 %)	(96.1 %)	(81.1 %)

SIT, Single Intradermal Tuberculin Test; MTC, Culture of *Mycobacterium tuberculosis* complex; PCR, real-time PCR of targeting IS*6110*; (+), Positive; (-), Negative

Pluribacillar granulomas, independently of their stage, corresponded to animals positive to at least three of the analyzed techniques, with one stage I and one stage IV granuloma being positive only to SIT. Four stage I granulomas belonged to animals negative to SIT, bacteriology, and PCR (no serum was available for ELISA).

4.5 Estimates of Sensitivity and Specificity and Agreement of Histopathology With Respect to the Reference Techniques

Table 7 shows the results of Se, Sp, and κ. Estimates of Se and Sp were calculated for SIT, ELISA, and histopathology with respect to the bacteriological culture and real-time PCR IS*6110* from fresh tissues.

Single intradermal tuberculin test results presented good Se (86.4%; CI_{95}: 77.7-95.2%) but low Sp (48.5%; CI_{95}: 41.0-56.0%) compared with bacteriological culture. The PPV and NPV were 36.7% (CI_{95}: 28.7-44.7%) and 91.2% (CI_{95}: 85.4-97.0%), respectively. When compared with real-time PCR, the Se and Sp of SIT were 93.8% and 48.4%, respectively, and the PPV and NPV were 32.4% (CI_{95}: 24.6-40.2%) and 96.7% (CI_{95}: 93.0-100.4%), with a weak agreement (κ= 0.248) among techniques.

Enzyme-linked immunosorbent assay results presented low Se (37%; CI_{95}: 24.2-49.9%) but good Sp (87%; CI_{95}: 82.2-92.5%). The PPV and NPV were 50% (CI_{95}: 34.5-65.5%) and 80.2% (CI_{95}: 74.3-86.1%), respectively. When compared with real-time PCR from fresh tissue, the Se and Sp of ELISA were 43.2% and 87.5%, respectively, and the PPV and NPV were 47.5% (CI_{95}: 32.0-63.0%) and 85.5% (CI_{95}: 80.2-90.7%), with a weak agreement (κ= 0.317) among techniques.

TABLE 3 | Distribution of microscopic lesions in different lymph nodes.

Histopathological lesions	TBL (n = 81; 81/681; 11.9 %)					
	TB Granuloma (n = 60)	Pyogranuloma (n = 5)	Giant Cell (n = 16)	Other lesions (n = 17)	No lesion (n = 583)	Total
Retropharyngeal LN	16/81 (19.7 %)	2/81 (2.5 %)	3/81 (3.7 %)	3/17 (17.6 %)	203/583 (34.8 %)	227
Tracheobronchial-mediastinal LN	33/81 (40.7 %)	1/81 (1.2 %)	4/81 (4.9 %)	1/17 (5.9 %)	187/583 (32.1 %)	226
Mesenteric LN	11/81 (13.6 %)	2/81 (2.5 %)	9/81 (11.1 %)	13/17 (76.5 %)	193/583 (33.1 %)	228

TBL, Tuberculosis-like lesions; TB, tuberculous; LN, Lymph node.

TABLE 4 | Relationship between microscopic lesions and the presence of acid-fast bacilli (AFB) in different lymph nodes.

	TBL (n = 81; 100 %)						
	TB Granuloma (n = 60; 74.1 %)		Giant cells (n = 16; 19.7 %)		Pyogranuloma (n = 5; 6.2 %)		Total
	ZN^+ (n = 54)	ZN^- (n = 6)	ZN^+ (n = 6)	ZN^- (n = 10)	ZN^+ (n = 1)	ZN^- (n = 4)	(n = 81)
Retropharyngeal LN	16/54 (26.7 %)	0/6 (0.0 %)	1/6 (6.2 %)	2/10 (12.5 %)	1/1 (20.0 %)	1/4 (20.0 %)	21/81
Tracheobronchial-mediastinal LN	29/54 (48.3 %)	4/6 (6.7 %)	0/6 (0.0 %)	4/10 (25.0 %)	0/1 (0.0 %)	1/4 (20.0 %)	38/81
Mesenteric LN	9/54 (15.0 %)	2/6 (3.3 %)	5/6 (31.2 %)	4/10 (25.0 %)	0/1 (0.0 %)	2/4 (40.0 %)	22/81

TBL, Tuberculosis-like lesions; ZN, Ziehl-Neelsen; LN, Lymph node.

Regarding histopathology, it presented an acceptable Se (74.6%; CI_{95}: 63.5-85.7%) and Sp (84.2%; CI_{95}: 78.7-89.7%). The PPV and NPV were 62.0% (CI_{95}: 50.7-73.3%) and 90.6% (CI_{95}: 86.0-95.1%), respectively, with a moderate agreement ($\kappa = 0.551$). On the other hand, the comparison of histopathology with the results of real-time PCR showed a Se of 87.5% (CI_{95} 78.1-96.9%) and a Sp of 84.1% (CI_{95} 78.7–89.4%) with PPV and NPV of 59.2% (CI_{95}: 47.7-70.6%) and 96.2% (CI_{95}: 93.399.2%), respectively. A good agreement ($\kappa = 0.608$) was observed among techniques.

4.6 Real-Time PCR From FFPE Targeting IS6110

Eighteen out of 83 SIT^-, MTC^-, and PCR^- (from fresh tissue) animals presented TBL and were subsequently subjected to realtime PCR analysis directly from the paraffin blocks. One sample was not available for the study because the paraffin block was already exhausted. One sample out of seventeen (5.9%) was positive by means of real-time PCR targeting IS*6110*. The IAC amplified in all samples without partial inhibition. The real-time PCR-positive result belonged to a tracheobronchial-mediastinal LN in a sample that showed TB granuloma in histopathology as TBL and paucibacillary lesion in ZN technique. This animal only presented lesion in this LN.

4.7 Droplet Digital PCR (ddPCR) Targeting IS6110

In addition, ddPCR was carried out from paraffin blocks of the 17 SIT^-, MTC^-, and PCR^- samples with TBL. Only 2 out of 17 samples (11.7%) were positive by ddPCR targeting IS*6110*, with one of them coinciding with the sample positive to real-time PCR from FFPE (**Figure 4**). The other $ddPCR^+$ result belonged to a tracheobronchial-mediastinal LN that showed MNGCs in histopathology to be TBL and had a negative result to ZN technique, without lesion in any other LN in the same animal. No sample was observed in the "gray area."

5. DISCUSSION

Improving the diagnosis of bTB in cattle is a cornerstone in control and eradication programs against this disease, being fundamental in the rapid and effective identification of infected animals. Current diagnostic tests for bTB present a low to moderate Se, therefore, the combination of different diagnostic tests, both *ante-mortem* and *post-mortem*, represents a smart approach to improve the diagnosis against MTC.

Histopathology is an early, rapid, and economic technique that allows us to identify and grade microscopic lesions associated with MTC infection. In addition, it visualizes the presence of mycobacteria within these lesions by additional techniques (ZN staining). Hence, its combination with reference techniques, such as bacteriological culture and real-time PCR, deserves more attention. In the present study, 212 sera samples and 681 LNs (227 retropharyngeal, 226 tracheobronchial-mediastinal and 228 mesenteric LNs) were collected from 230 slaughtered cattle from the national bTB control and eradication program. A higher number of culture positive samples and TBL were obtained from the tracheobronchial-mediastinal LN, followed by the retropharyngeal LN. These results are in agreement with the exposure of cattle to contaminated aerosols as the main route of entry of *M. bovis* (8, 9, 25). Interestingly, one cattle presented culture positive and PCR positive results together with TBL only in the mesenteric LN, which suggests the ingestion of food and/or water contaminated with *M. bovis* (9, 25–28). Although a systematic sampling of LNs is included in the bTB eradication programs (7), the veterinary inspection and sampling at the slaughterhouse is usually limited to head and thoracic cavity LNs from a logistic perspective due to the speed of the slaughter chain. This is one of the main limitations of the current study due to the lack of a more systematic sampling of LNs. However, our results highlight the importance of including mesenteric LNs in the routine sampling to avoid false negative animals limiting the persistence and spread of mycobacterium in negative herds.

Enzyme-linked immunosorbent assay has been considered for *ante-mortem* diagnosis with its simplicity as main advantage, but presenting a low Se (64.6%), which is primarily associated with a delayed development of humoral immunity (around 3 – 12 weeks) (9). In our study, from the total of MTC^+ animals, approximately one third were $ELISA^+$ (20 out of 54; 37.0%), which led to a low Se. The use of ELISA for bTB diagnosis has been argued by many authors for its utility to detect anergic animals (9). In our case, only 3 out of 77 animals (5.9%) were $ELISA^+$ and $SIT^-/MTC^-/PCR^-$. However, these animals did not present TBL. In addition, 15 out of 76 $SIT^-/MTC^-/PCR^-$ animals presented TBL, but disclosed a negative result to ELISA, pointing out that the contribution of the ELISA test for bTB diagnosis is not significant in the conditions of the present study.

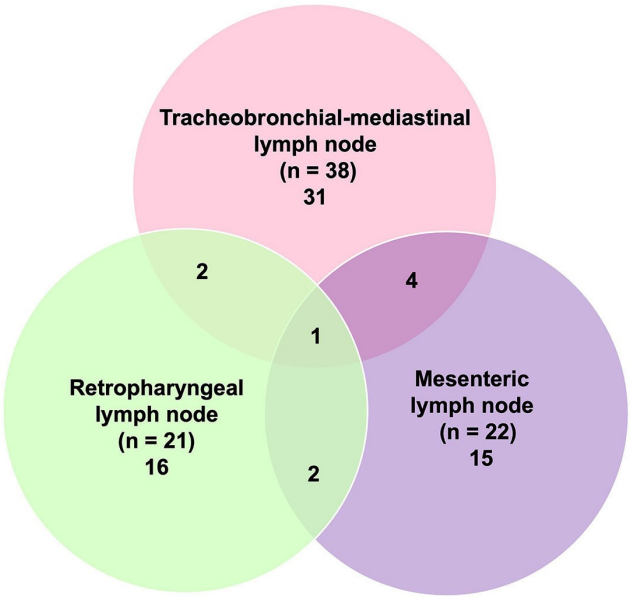

FIGURE 2 | Distribution of tuberculosis-like lesions (TBLs) (n = 81) according to the affected lymph node (LN).

Histopathology allows the identification of lesions compatible with TBL and lesions other than those caused by mycobacteria. The predominant TBL observed in our study was the TB granuloma. It is noteworthy that other TBL, such as pyogranuloma or

Langhans-type MNGCs, were observed. Pyogranulomas may be caused by the concomitant infection of mycobacteria and pyogenic bacteria, such as *Streptococcus* spp. or *Trueperella pyogenes* (29, 30). MNGCs are grossly unnoticed and, interestingly, in our study, were observed in 16 out of 81 LNs of cattle with TBL, being observed more frequently in the mesenteric LNs (9 out of 81; 11.1%). Six out of these 9 mesenteric LNs with Langhans-type MNGCs belonged to $SIT^-/MTC^-/PCR^-$ cattle and presented a positive result to MAP PCR and a pluribacillar (5 LNs) or paucibacillar (1 LN) pattern with ZN staining. Therefore, these cases were consistent with field cases of paratuberculosis, not with an infection by MTC, and emphasize the interest of performing a differential diagnosis when monitoring lesions in LNs from the digestive system (31). Other lesions, including parasitic migration, hemosiderosis, and psammoma bodies, among others, were also observed. Frequently, reactive LNs cannot be grossly differentiated with certainty into those with or without TBL (5, 13, 30). Besides the use of histopathology to confirm the microscopic diagnosis of a TBL, the presence of AFB can also be evidenced through the ZN technique as stated above. Usually, paucibacillary lesions are observed in cattle, however, AFB may not be detected although *M. bovis* is isolated in the bacteriological culture from the same sample (9, 11, 21). ZN^+ mycobacteria are frequently observed in giant cells or in areas of necrosis (32, 33), with the presence of at least one mycobacterium being enough to consider a result as positive. In the present study, ZN technique yielded positive results in a similar percentage (61/81; 75.3%) as described by others (33), with most of the samples preferably presenting importantly in SIT+ cases to allow a faster confirmation of bTB diagnosis. Interestingly, 8 SIT−/MTC−/PCR− animals presented TB granuloma, with 5 of them disclosing a positive result to ZN but negative to ELISA, evidencing the capability of this technique to identify infected animals negative to the reference techniques. Indeed, real-time PCR and ddPCR from FFPE tissues were able to amplify MTC from one of these TB granulomas, which presented a paucibacillary ZN staining, supporting this statement. The implication of a foreign body reaction, bacteria or fungi was ruled out by the histopathological characteristics of the lesion, Gram, and PAS staining, respectively, along with the participation of MAP by real-time PCR. Therefore,

these animals may correspond with anergic and/or immunosuppressed animals, with a low bacterial load, corroborating the role of the histopathological study to identify TBL in a rapid fashion (approximately 48 h), allowing an early diagnostic approach. Nonetheless, a more complete differential diagnosis would allow discarding the involvement of any other potential microorganism in these lesions.

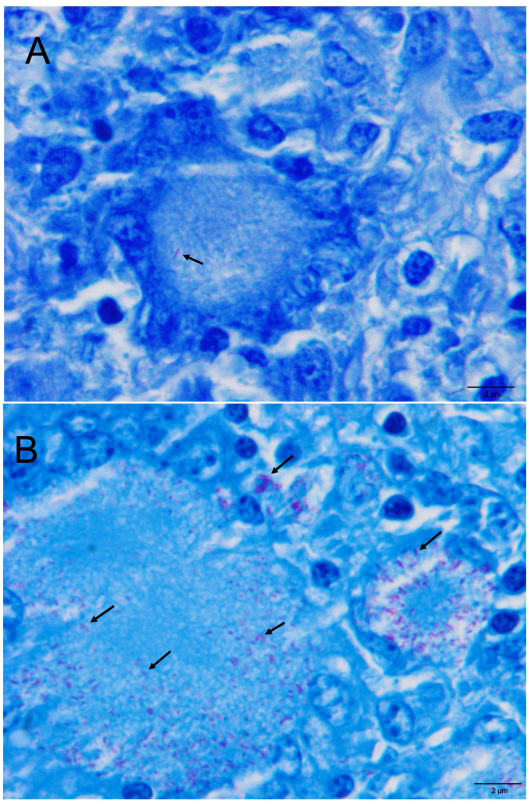

FIGURE 3 | (A) Retropharyngeal LN. Paucibacillary lesion. The arrowhead shows acid fast bacilli (AFB) within cytoplasm of a Langhans-type MNGCs (Ziehl-Neelsen, ZN) (B). Mesenteric LN. Pluribacillary lesion. *Numerous AFB within the cytoplasm of Langhans-type MNGCs and epithelioid cells (ZN).*

TABLE 5 | Classification of the lesions according to the Ziehl-Neelsen (ZN) staining and the number of AFB, paucibacillary or pluribacillary, in the different lymph nodes.

	ZN$^+$ (n = 61; 75.3 %)		**ZN$^-$ (n = 20; 24.7 %)**	**Total**
	Paucibacillary	Pluribacillary		
Retropharyngeal LN	15/43 (24.6 %)	3/18 (4.9 %)	3/20 (15.0 %)	21
Tracheobronchial-mediastinal LN	22/43 (46.6 %)	7/18 (4.9 %)	9/20 (45.0 %)	38
Mesenteric LN	6/43 (11.5 %)	8/18 (11.5 %)	8/20 (40.0 %)	22

LN, Lymph node; ZN, Ziehl-Neelsen; (+), Positive; (−), Negative.

Regarding pyogranulomas, only 1 out of 5 was found to be ZN$^+$, characterized by a pluribacillary lesion and corresponding with an MTC$^+$ and PCR$^+$ animal. On the other hand, one SIT$^-$/MTC$^-$/PCR$^-$ animal presented a TBL consisting with a pyogranuloma. However, this lesion was ZN$^-$ and the animal also yielded a negative result to ELISA, indicating that it might be a disease other than tuberculosis (23).

Analyzing the stage of the granuloma and the ZN pattern with respect to the different methods analyzed in our study, paucibacillar stage IV granulomas were overrepresented with respect to other stages or pluribacillar granulomas. This result highlights the advanced stages of the infection observed in our study, corresponding probably with around 6 months post-infection or later according to previous results (34). Our results do not draw a clear association of granuloma stage or pauci-/pluri-bacillary pattern and the results to the different techniques since most of the animals with different stages of granuloma yielded a positive result to SIT, bacteriological culture, and PCR. Only ELISA results presented a random distribution independently of the stage of the granuloma and ZN pattern. However, it is of interest to remark that in some cases, although in a low proportion, paucibacillar stage IV or pluribacillar stage I granulomas were detected in cattle, negative to all the techniques under study. The number of animals with TB granuloma included in our study together with the distribution of animals according to the stage of the granuloma and ZN pattern did not

allow us to examine the relationship between the number of AFB and the results to the different diagnostic methods.

Single intradermal tuberculin test-positive/MTC⁻/PCR⁻/ TBL⁺ animals (8 out of 86; 9.3%) may be associated with several factors, such as a very low bacterial load, the encapsulation of the granulomas (35), the decontamination process of the microbiological culture (8), or as suggested by Cassidy and coauthors (31), with animals that have eliminated the infection but have been sensitized to the disease. Although co-infection with other pathogens or exposure to other mycobacterial species, including members of the *M. avium* complex (MAP) and environmental mycobacteria, can affect SIT test performance and generate SIT false positives (5, 10, 36), the evidence of TBL together with ZN positive results allow confirming SIT positivity in our case. Nonetheless, according to our results, special caution should be taken when evaluating mesenteric LNs with Langhans type MNGCs as the sole lesion.

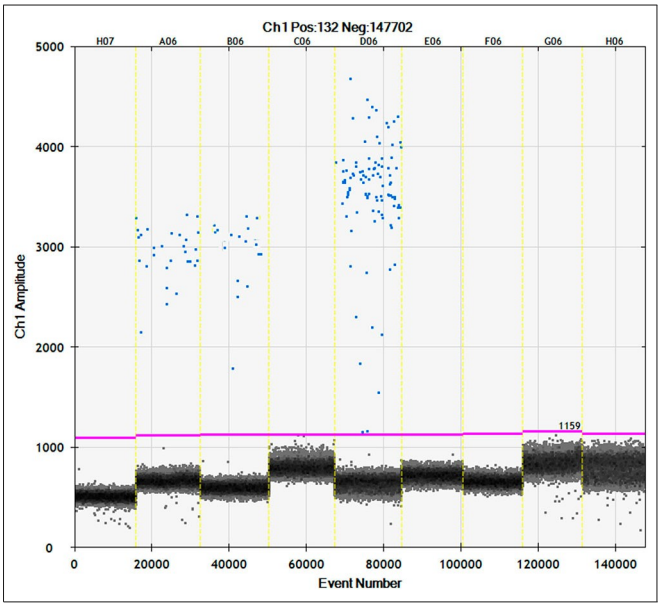

FIGURE 4 | Channel 1 results for droplet separation based on simplex assays. Droplet separation based the IS6110 simplex assay results*. Positive droplets were observed at an amplitude of about 3,000 while negative droplets were observed at an amplitude of about 1,100.*

TABLE 6 | Distribution of the results collected from the 230 animals which were positive or negative to single intradermal skin test and subclassified by culture of MTC and real-time PCR targeting IS*6110 vs.* histopathological lesions.

Histopathological lesions	SIT+ (139)				SIT- (91)			
	MTC+ (n = 51)		MTC- (n = 88)		MTC+ (n = 8)		MTC- (n = 83)	
	PCR+	PCR-	PCR+	PCR-	PCR+	PCR-	PCR+	PCR-
TB Granuloma	40/43 (93.0 %)	0/8 (0.0 %)	1/2 (50.0 %)	3/86 (34.9 %)	0/2 (0.0 %)	1/6 (1.7 %)	0/1 (0.0 %)	8/82 (9.8 %)
Giant cell	0/43 (0.0 %)	0/8 (0.0 %)	0/2 (0.0 %)	4/86 (4.6 %)	0/2 (0.0 %)	2/6 (3.3 %)	0/1 (0.0 %)	9/82 (10.9 %)
Pyogranuloma	1/43 (2.3 %)	0/8 (0.0 %)	0/2 (0.0 %)	1/86 (1,7 %)	0/2 (0.0 %)	0/6 (0.0 %)	0/1 (0.0 %)	1/82 (1.2 %)
Other lesion	0/43 (0.0 %)	0/8 (0.0 %)	0/2 (0.0 %)	11/86 (12.8 %)	0/2 (0.0 %)	0/6 (0.0 %)	0/1 (0.0 %)	4/82 (4.9 %)
No lesion	2/43 (4.7 %)	8/8 (0.0 %)	1/2 (50.0 %)	67/86 (77.9 %)	2/2 (100.0 %)	3/6 (50.0 %)	1/1 (100.0 %)	60/82 (73.2 %)

TB, Tuberculous; SIT, Single intradermal Tuberculin Test; MTC, Culture of Mycobacterium tuberculosis complex; PCR, real-time PCR of targeting IS6110; (+), Positive; (-), Negative.

TABLE 7 | Estimates of sensitivity and specificity of the diagnostic techniques compared to against MTC culture as gold standard either alone or in parallel combination together with real-time PCR targeting IS*6110*.

		Sensitivity (Se)		Specificity (Sp)			
	Diagnostic test	**%**	**CI_{95} %**	**%**	**CI_{95} %**	**κ**	**Agreement**
MTC culture	SIT	86.4	(77.7 - 95.2)	48.5	(41.0 – 56.0)	0.242	Weak
	ELISA	37	(24.2 - 49.9)	87.3	(82.2 - 92.5)	0.256	Weak
	Histopathology (H&E)	74.6	(63.5 - 85.7)	84.2	(78.7 – 89.7)	0.551	Moderate
Real time PCR IS6110	SIT	93.8	(86.9 - 100.6)	48.4	(41.1 - 55.6)	0.248	Weak
	ELISA	43.2	(28.5 - 57.8)	87.5	(82.5 - 92.5)	0.317	Weak
	Histopathology (H&E)	87.5	(78.1 – 96.9)	84.1	(78.7 - 89.4)	0.608	Good

SIT, Single intradermal tuberculin test; H&E, Hematoxylin and eosin staining; MTC, Mycobacterium tuberculosis Complex.

According to the inherent difficulties described above for each one of these techniques to detect bTB in cattle when used in single, the diagnostic performance of SIT, ELISA, and histopathology compared with respect to bacteriology displayed a low to moderate Se and Sp and a weak to moderate agreement among tests. However, when histopathology was compared with real-time PCR from fresh tissues, it presented a higher Se and a good agreement among both techniques (κ= 0.608), evidencing the suitability of including histopathology as a complimentary diagnostic tool which may help improving bTB diagnosis and disease control.

6. Conclusions

Our results confirm that histopathology is a valuable diagnostic tool with an acceptable Se (87.5%) and Sp (84.1%) to be used alone or together with SIT, real-time PCR, and bacteriological culture. Furthermore, histopathology allows not only a rapid confirmation of SIT, PCR, and culture positive results, but also detecting positive animals that yield negative results to these techniques. For these reasons, this tool should be systematically included in bTB surveillance and eradication programs.

Data availability statement

The raw data supporting the conclusions of this article will be made available by the authors, without undue reservation.

Ethics statement

Ethical review and approval was not required for the animal study because no purpose killing of animals was performed for this study, so no ethical or farmer's consent approval was required.

Author contributions

JG-L, LC, IL, and CT conceived, designed, and performed the project. JS-C, AG-R, IR-T, EV-S, and FL-M helped in the sample collection. JS-C, AG-R, and LG-G made the laboratory experiments. AM helped in statistical analysis. FL-M wrote the manuscript.

IR-T and JG-L reviewed the manuscript. LC and JG-L contributed to the reagents, materials, and analysis tools. All authors contributed to the article and approved the submitted version.

Funding

This work was supported by the research project New Measures and Techniques to Control Bovine Tuberculosis in Andalusia (Financial support for Operational Groups of the European Innovation Partnership for Agricultural Productivity and Sustainability (EIP-AGRI) (GOP2I-CO-160010). FL-M was supported by a doctoral grant from ANID (National Research and Development Agency) (Doctoral grant Chile/2019/72200324).

Acknowledgments

We express our appreciation to Alberto Alcántara and Marta Ordóñez-Martínez for their technical assistance and the technical support offered by the Animal Health and Production Laboratory of Córdoba (Spain).

References

1. Rodriguez-Campos S, Smith NH, Boniotti MB, Aranaz A. Overview and phylogeny of Mycobacterium tuberculosis complex organisms: implications for diagnostics and legislation of bovine tuberculosis. *Res Vet Sci*. (2014) 97:S5–19. doi: 10.1016/j.rvsc.2014.02.009
2. Mohamed A. Bovine tuberculosis at the human–livestock– wildlife interface and its control through one health approach in the Ethiopian Somali Pastoralists: a review. *One Heal*. (2020) 9:100113. doi: 10.1016/j.onehlt.2019.100113
3. OIE. World Organisation for Animal Health. Infection with mycobacterium tuberculosis complex. In Autor, editor. Terrestrial Animal Health Code. 28th ed. Paris: World Organisation for Animal Health (2019). p. 1–6.

4. Adams LG. In vivo and in vitro diagnosis of Mycobacterium bovis infection. OIE Rev Sci Tech. (2001) 20:304–24. doi: 10.20506/rst.20.1. 1267

5. de la Rua-Domenech R, Goodchild AT, Vordermeier HM, Hewinson RG, Christiansen KH, Clifton-Hadley RS. Ante mortem diagnosis of tuberculosis in cattle: a review of the tuberculin tests, γ-interferon assay and other ancillary diagnostic techniques. Res Vet Sci. (2006) 81:190– 210. doi: 10.1016/j.rvsc.2005.11.005

6. Reviriego Gordejo FJ, Vermeersch JP. Towards eradication of bovine tuberculosis in the European Union. *Vet Microbiol*. (2006) 112:101–9. doi: 10.1016/j.vetmic.2005.11.034

7. EU. REGLAMENTO DELEGADO (UE) 2020/689 DE LA COMISIÓN de17 de diciembre de 2019 por por el que se completa el Reglamento (UE) 2016/429 del Parlamento Europeo y del Consejo en lo referente a las normas de vigilancia, los programas de erradicación y el estatus. D Of la Unión Eur (2020) 2019

8. Corner LAL, Gormley E, Pfeiffer DU. Primary isolation of Mycobacterium bovis from bovine tissues: conditions for maximising the number of positive cultures. *Vet Microbiol*. (2012) 156:162–71. doi: 10.1016/j.vetmic.2011.10.016

9. Ramos DF, Silva PEA, Dellagostin OA. Diagnosis of bovine tuberculosis: review of main techniques. *Braz J Biol*. (2015) 75:830–7. doi: 10.1590/1519-6984.23613

10. Byrne AW, Graham J, Brown C, Donaghy A, Guelbenzu-Gonzalo M, McNairJ. et al. Modelling the variation in skin-test tuberculin reactions, post-mortem lesion counts and case pathology in tuberculosis-exposed cattle: effects of animal characteristics, histories and co-infection. *Transbound Emerg Dis*. (2018) 65:844–58. doi: 10.1111/tbed.12814

11. Schiller I, Oesch B, Vordermeier HM, Palmer MV, Harris BN, Orloski KA, et al. Bovine tuberculosis: a review of current and emerging diagnostic techniques in view of their relevance for disease control and eradication. *Transbound Emerg Dis*. (2010) 57:205–20. doi: 10.1111/j.1865-1682.2010.01148.x

12. Nuñez-Garcia J, Downs SH, Parry JE, Abernethy DA, Broughan JM, Cameron AR. et al. Meta-analyses of the sensitivity and specificity of ante-mortem and post-

mortem diagnostic tests for bovine tuberculosis in the UK and Ireland. *Prev Vet Med*. (2018) 153:94–107. doi: 10.1016/j.prevetmed.2017. 02.017

13. Bezos J, Casal C, Romero B, Schroeder B, Hardegger R, Raeber AJ, et al. Current ante-mortem techniques for diagnosis of bovine tuberculosis. *Res Vet Sci*. (2014) 97:S44–52. doi: 10.1016/j.rvsc.2014.04.002

14. Fontana S, Pacciarini M, Boifava M, Pellesi R, Casto B, Gastaldelli M, et al. Development and evaluation of two multi-antigen serological assays for the diagnosis of bovine tuberculosis in cattle. *J Microbiol Methods*. (2018) 153:118–26. doi: 10.1016/j.mimet.2018.09.013

15. Courcoul A, Moyen JL, Brugère L, Faye S, Hénault S et al. Estimation of sensitivity and specificity of bacteriology, histopathology and PCR for the confirmatory diagnosis of bovine tuberculosis using latent class analysis. *PLoS ONE*. (2014) 9: 0090334. doi: 10.1371/journal.pone.0090334

16. Lorente-Leal V, Liandris E, Castellanos E, Bezos J, Domínguez L, de Juan L, et al. Validation of a real-time PCR for the detection of mycobacterium tuberculosis complex members in Bovine tissue samples. *Front Vet Sci*. (2019) 6:1–9. doi: 10.3389/fvets.2019.00061

17. Sánchez-Carvajal, JM, Galán-Relaño Á, Ruedas-Torres I, Jurado-MartosF, Larenas-Muñoz et al. Real-Time PCR validation for *Mycobacterium tuberculosis complex detection targeting IS 6110* directly from bovine lymph nodes. *Front in Vet Sci*. (2021) 8:643111. doi: 10.3389/fvets.2021.64 3111

18. España. Real Decreto 2611/1996, de 20 de diciembre, por el que se regulan los programas nacionales de erradicación de enfermedades de los animales. Bol Of del Estado (1996) 21 diciembre 1996 1–37.

19. Thierry D, Brisson-Noel A, Vincent-Levy-Frebault V, Nguyen S, Guesdon JL, Gicquel, B. Characterization of a Mycobacterium tuberculosis insertion sequence, IS6110, and its application in diagnosis. *J Clin Microbiol*. (1990) 28:2668–73. doi: 10.1128/jcm.28.12.2668-2673.1990

20. Michelet L, de Cruz K, Karoui C, Tambosco J, Moyen JL, Hénault S. Second line molecular diagnosis for bovine tuberculosis to improve diagnostic schemes. *PloS ONE*. (2018) 13:e0207614. doi: 10.1371/journal.pone.02 07614

21. Wangoo A, Johnson L, Gough J, Ackbar R, Inglut S, Hicks D, et al. Advanced granulomatous lesions in Mycobacterium bovis-infected cattle are associated with increased expression of type I procollagen, γδ (WC1+) T cells and CD 68+ cells. *J Comp Pathol*. (2005) 133:223–34. doi: 10.1016/j.jcpa.2005. 05.001

22. García-Jiménez WL, Salguero FJ, Fernández-Llario P, Martínez R, Risco D, Gough J. Immunopathology of granulomas produced by Mycobacterium bovis in naturally infected wild boar. *Vet Immunol Immunopathol*. (2013) 156:54–63. doi: 10.1016/j.vetimm.2013.09.008

23. Johnson LK, Liebana E, Nunez A, Spencer Y, Clifton-Hadley R, Jahans K, et al. Histological observations of bovine tuberculosis in lung and lymph node tissues from British deer. *Vet J*. (2008) 175:409–12. doi: 10.1016/j.tvjl.2007.04.021

24. Sánchez-Carvajal J, Vera-Salmoral E, Cuéllar-Gómez R, Galán-Relaño A, Carrasco L, Ruedas-Torres I, et al. Evaluation of droplet digital PCR targeting IS6110 to detect *Mycobacterium tuberculosis complex* DNA in microbiological culture and fresh tissue samples. *Proceedings of the 5th Congress of the European Association of Veterinary Laboratory Diagnosticians (EAVLD)*. (2021) Nov, virtual meeting.

25. Good M, Bakker D, Duignan A, Collins, DM. The history of *in vivo* tuberculin testing in bovines: Tuberculosis, a "One Health" issue. *Front Vet Sci*. (2018) 5:59. doi: 10.3389/fvets.2018.00059

26. Thoen CO, RG Barletta. Pathogenesis of Mycobacterium bovis. In: Thoen CO, Steele JH, Glisdorf M.J, editors. *Mycobacterium bovis Infection in Animals and Humans.* 2a ed. United States: Blackwell Publishing (2006). p. 18–33.

27. Caswell JL, KJ Williams. Respiratory system. In: Maxie M, editor. *Pathology of Domestic Animals*, *Vol 2*. 6th ed. Philadelphia: Elsevier Limited (2016). p. 591.

28. Corner LAL, Murphy D, Gormley E. Mycobacterium bovis infection in the eurasian badger (Meles meles): the disease, pathogenesis, epidemiology and control. *J Comp Pathol*. (2011) 144:1–24. doi: 10.1016/j.jcpa.2010.10.003

29. Cardoso-Toset F, Gómez-Laguna J, Amarilla SP, Vela AI, Carrasco L, Fernández-Garayzábal JF, et al. Multi-Etiological nature of tuberculosis like lesions in condemned pigs at the slaughterhouse. *PLoS ONE*. (2015) 10:e0139130. doi: 10.1371/journal.pone.0139130

30. Pollock JM, Neill SD. Mycobacterium bovis infection and tuberculosis in cattle. *Vet J*. (2002) 163:115–27. doi: 10.1053/tvjl.2001.0655

31. Cassidy, J.P. The pathology of bovine tuberculosis: time for an audit. *Vet J*. (2008) 176:263–4. doi: 10.1016/j.tvjl.2007.09.001

32. Gómez-Laguna J, Carrasco L, Ramis G, Quereda JJ, Gómez S, Pallarés FJ. Use of real-time and classic polymerase chain reaction assays for the diagnosis of porcine tuberculosis in formalin-fixed, paraffin-embedded tissues. *J Vet Diagnostic Investig*. (2010) 22:123–7. doi: 10.1177/1040638710022 00126

33. Gutiérrez Cancela MM, García Marín JF. Comparison of Ziehl-Neelsen staining and immunohistochemistry for the detection of Mycobacterium bovis in bovine and caprine tuberculous lesions. *J Comp Pathol*. (1993) 109:361–70. doi: 10.1016/S0021-9975(08)80299-X

34. Palmer MV, Waters WR, Thacker TC. Lesion development and immunohistochemical changes in granulomas from cattle experimentally infected with Mycobacterium bovis. *Vet Pathol*. (2007) 44:863–74. doi: 10.1354/vp.44-6-863

35. Menin Á, Fleith R, Reck C, Marlow M, Fernandes P, Pilati C, et al. Asymptomatic cattle naturally infected with Mycobacterium bovis present exacerbated tissue pathology and bacterial dissemination. *PLoS ONE*. (2013) 8:18–21. doi: 10.1371/journal.pone.0053884

36. Buddle BM, Livingstone PG, De Lisle GW. Advances in antemortem diagnosis of tuberculosis in cattle. *N Z Vet J*. (2009) 57:173–80. doi: 10.1080/00480169.2009.36899

Conflict of Interest: The authors declare that the research was conducted in the absence of any commercial or financial relationships that could be construed as a potential conflict of interest.

Publisher's Note: All claims expressed in this article are solely those of the authors and do not necessarily represent those of their affiliated organizations, or those of the publisher, the editors and the reviewers. Any product that may be evaluated in this article, or claim that may be made by its manufacturer, is not guaranteed or endorsed by the publisher.

Capítulo II

Estudio 2 / Study 2

Objetivo 2 / Objective 2

Estudio 2: Monitoring the immune response of macrophages in tuberculous granuloma through the expression of CD68, iNOS and HLA-DR in naturally infected beef cattle

Mohamed G. Hamed1, Jaime Gómez-Laguna2, Fernanda Larenas-Muñoz2, Abdelzaher Z. Mahmoud3, Fatma Abo Zakaib Ali1 and Sary Kh. Abd-Elghaffar4

Aceptado para publicar en BMC Veterinary Research , 2023, JIF: 1.31 (Q1)

Objetivo 2: Evaluar la expresión de marcadores de células mieloides (CD172a y MAC387) y la polarización de macrófagos M1 (iNOS, CD68 y CD107a) y M2 (Arg1 y CD163) en los nódulos linfáticos de bovino y porcino para el estudio de la inmunopatogenia de la tuberculosis.

Objective 2: Evaluate the expression of myeloid cell markers (CD172a and MAC387) and the polarisation of M1 (iNOS, CD68 and CD107a) and M2 (Arg1 and CD163) macrophages in bovine and porcine lymph nodes to study the immunopathogenesis of tuberculosis.

Monitoring the immune response of macrophages in tuberculous granuloma through the expression of CD68, iNOS and HLA-DR in naturally infected beef cattle

Mohamed G. Hamed[1], Jaime Gómez-Laguna[2], Fernanda Larenas-Muñoz[2], Abdelzaher Z. Mahmoud[3], Fatma Abo Zakaib Ali[1] and Sary Kh. Abd-Elghaffar[4]

[1]Department of Pathology and Clinical Pathology, Faculty of Veterinary Medicine, Sohag University, Sohag 82524, Egypt.

[2]Department of Anatomy and Comparative Pathology and Toxicology, Pathology and Immunology Group (UCO-PIG), UIC Zoonosis y Enfermedades Emergentes ENZOEM, University of Córdoba, International Excellence Agrifood Campus 'CeiA3', 14014 Córdoba, Spain.

[3]Department of Pathology and Clinical Pathology, Faculty of Veterinary Medicine, Assuit University, Assiut, Egypt.

[4]Department of Pathology and Clinical Pathology, Faculty of Veterinary Medicine, Badr Univerisity, Assiut, Egypt.

Corresponding author: Mohamed G. Hamed.

E-mail address: Mohamed.gamal@vet.sohag.edu.eg (Mohamed G. Hamed.)

Abstract

Bovine tuberculosis still represents a universal threat that creates a wider range of public and animal health impacts. One of the most important steps in the pathogenesis of this disease and granuloma formation is the phagocytosis of tuberculous bacilli by macrophages. Mycobacteria replicate in macrophages, which are crucial to the pathophysiology of mycobacterial infections; however, scarce information is available about the dynamics of the granuloma-stage immunological response. Therefore, immunohistochemistry was used in this work to evaluate the expression of CD68, iNOS, and HLA-DR in different stages of TB granulomas from naturally infected cattle with tuberculosis. Two thousand, one hundred and fifty slaughtered beef cattle were examined during the period from September 2020 to March 2022. Sixty of them showed gross tuberculous pulmonary lesions and samples were collected from all of them for histopathological examination and Ziehl-Neelsen (ZN) staining. Selected samples were subjected to an immunohistochemical study of CD68, iNOS, and HLA-DR expression by macrophages according to granuloma stages. Immunohistochemical analysis revealed that the immunolabeling of CD68+, iNOS+, and HLA-DR+ macrophages significantly reduced as the stage of granuloma increased from stage I to stage IV ($P<0.003$, $P<0.002$, and $P<0.002$, respectively). The distribution of immunolabeled macrophages was similar for the three markers, with immunolabeled macrophages distributed throughout early-stage granulomas (I, II), and surrounding the necrotic core in late-stage granulomas (III, IV). Our results suggest a polarization to the pro-inflammatory environment and increased expression of CD68+, iNOS+, and HLA-DR+ macrophages in the early stages of granulomas (I, II), which may play a protective role in the immune response of naturally infected beef cattle with tuberculosis.

Keywords: tuberculosis, granuloma, macrophage, CD68, iNOS, HLA-DR.

Introduction

Mycobacterium tuberculosis complex (MTC) is the primary cause of bovine tuberculosis (bTB), which affects a variety of domestic, wild animal species, and humans [1]. Cattle are considered the main reservoir of the disease, which also poses a zoonotic risk, infecting humans. Animals with TB are significantly less productive, which results in significant economic losses [2, 3]. According to the World Health Organization (WHO), the disease causes 3 million human deaths and 8 million new cases caused by Mycobacterium tuberculosis each year [4]. The disease geographic distribution disproportionately varies within countries and across the globe, and poverty is the strongest predictor of incidence [5]. In Africa, where insufficient diagnosis and treatment are exceedingly widespread, the disease has a particularly high incidence rate, accounting for 25% of all global TB cases [6]. Sudan is one of the developing countries where tuberculosis is a major public health issue, with an estimated 29,000 cases in 2019 [7]. The most characteristic lesion of bovine tuberculosis is the formation of granulomas in target organs, more significantly in the lungs, lymph nodes, intestines, kidneys, and others [8, 9].

Experimental infections have made it possible to qualitatively classify granulomas into four stages (I-IV) in cattle based on size, cellular composition, and the presence or absence of necrosis, fibrosis, and mineralization in granulomas during the course of bovine tuberculosis infection [10, 11] which has also been characterized in natural infections [12, 13]. Despite the granuloma's significance as a physical barrier in the immune response against *M. bovis*, the dynamics of the granuloma-stage immunological response are scarcely understood [14]. Mycobacterial immunity is predominantly a cell-mediated immune (CMI) response that involves the activation of macrophages, dendritic cells, and T helper type 1 (Th1) cells that are controlled by cytokines [15, 16]. Mycobacteria are phagocytosed by and replicate in macrophages, which are crucial to the pathophysiology of mycobacterial infections. In this sense, the quantity and location of macrophages have been reported to vary as the granuloma developed. Macrophages make up a significant proportion of the cell population within stage I and stage II granulomas, however, they often form a thin rim around the necrotic

core in stage III and stage IV granulomas and are less prevalent in the outermost layers of the connective tissue capsule of the granuloma [11].

Macrophages are one of the first immune cells to interact with inhaled bacilli, and they can suppress bacterial growth through phagocytosis, phagolysosome fusion and acidification, lysosomal proteolytic enzymes, and the production of reactive oxygen and nitrogen species with antimicrobial properties [17]. Two distinct phenotypes can be found within the granuloma. Firstly, mycobacteria are eliminated more quickly by activated macrophages within a pro-inflammatory environment. Secondly, an anti-inflammatory milieu leads to an alternative activation of macrophages, intended to preserve tissue integrity and support tissue repair [18]. Interestingly, whereas a proinflammatory environment is found close to the necrotic center, anti-inflammatory signals are situated more peripherally close to the capsular region in human tuberculous granulomas [19]. Nonetheless, there is scarce information about how this spatial distribution in bovine tuberculosis.

CD68 has been widely employed as a pan-macrophage marker or an M1 marker [20-22]. CD68 is a member of the family of molecules known as lysosome-associated membrane proteins, consisting of a glycosylated type I membrane protein and being connected to the phagocytic activity of the cell [23]. Inducible nitric oxide synthase (iNOS), a marker for classically activated macrophages (M1), is one of the most intriguing markers regarding macrophage polarization [24, 25]. For the generation of Nitric oxide (NO), which can eradicate mycobacterial species. When iNOS is stimulated, inactivates mycobacteria by making highly reactive nitrogen intermediates (peroxynitrite) [26]. iNOS uses arginine as a substrate. iNOS is known to be crucial for the management of *M. tuberculosis* infection in mice [27, 28] and *M. bovis* in bovine [27, 28]. L-arginine is converted by the enzyme iNOS into L-citrulline and NO in the presence of oxygen, which is linked to the elimination of the infection and the destruction of intracellular mycobacteria [24, 29, 30]. Another marker of interest to characterize macrophage subpopulations is class II MHC antigens (MHC-II). MHC-II is crucial for controlling immunological responses and antigen presentation, particularly for T cell-mediated immune response [21]. The expression of MHC-II can be assessed

by an antibody against HLA-DR, which has specificity for the α–a chain of human MHC-II and cross-reacts with bovine tissues [31, 32].

Understanding the immunopathogenesis of bovine tuberculosis requires extensive research and new approaches. Therefore, comprehension of host-pathogen interactions at the granuloma level is crucial. In the current study, immunohistochemistry (IHC) was used to investigate the expression of CD68, iNOS, and HLA-DR within different stages of TB granulomas in naturally tuberculosis-infected cattle. The role and spatial distribution of immunolabeled macrophages are also discussed.

Materials and Methods

Animals, postmortem examination, and specimen collection

Regular visits to the Middle East and Wadyna slaughterhouses were carried out from September 2020 to March 2022. A routine postmortem examination of 2,150 male beef cattle (Zebu) aged from 2 to 3 years was carried out with particular attention to tuberculous affections. The current study was conducted on beef cattle imported from Sudan. The prevalence of zoonotic human bTB is seven cases/100,000 population/year in Sudan [33]. Sixty out of 2,150 animals presented gross tuberculosis-like lesions (TBL) and tissue samples from tracheobronchial and mediastinal lymph nodes were collected from each animal.

Histopathological examinations

Tracheobronchial and mediastinal tissue samples from the 60 animals with TBLs were subjected to histopathological examination and granuloma staging. Tissue samples were fixed in 10 % neutral buffered formalin for 24 to 72 h, embedded in paraffin, sectioned into 4 µm sections, and stained with hematoxylin-eosin (H&E) and Ziehl-Neelsen (ZN) acid-fast stain. A sample was considered positive for ZN when one or more acid-fast bacilli (AFB) were noticed in at least one high-power field

magnification (HPF, 100x) of the sample and accordingly the lesions were classified as paucibacillary (1 to 10 AFB per HPF), or pluribacillary (≥ 11 AFB per HPF) [34]. Granulomas were classified into four different stages (stages I to IV) according to the previously described criteria [10, 13].

Immunohistochemical examinations

For the immunohistochemical study, the tuberculous granuloma was considered as the experimental unit. Five representative samples for each of the four stages of granuloma were selected, all of them presenting a positive result to ZN staining. The avidin-biotin-peroxidase complex (ABC Vector Elite; Vector Laboratories) was used to analyze the expression of CD68, iNOS, and HLA-DR antigens in the different stages of the granulomas. Briefly, 4 μm tissue sections were deparaffinized and rehydrated through graded alcohols, followed by blocking endogenous peroxidase activity using 3 % hydrogen peroxide in methanol for 30 min in darkness. Table 1 shows the antigen recovery method and primary and secondary antibodies. After antigen retrieval, sections were washed with phosphate buffer saline (PBS) (pH 7.4) and incubated with blocking solution for 30 min at room temperature in a humidity chamber. Primary antibody was applied and incubated overnight at 4 °C. To establish the absence of non-specific binding, a negative control was included replacing the primary antibody with the corresponding blocking solution, depending on the antibody. Following a PBS wash, the appropriate biotinylated secondary antibody was applied for 30 min, followed by the Avidin-Biotin-Peroxidase Complex (Vector Laboratories), which was then incubated for 1 h at room temperature in darkness. Labeling was visualized by using the NovaREDTM substrate kit (Vector Laboratories). Finally, slides were mounted, dehydrated, and counterstained with Harris hematoxylin.

Immunohistochemistry evaluation

The immunolabeled sections were examined by light microscopy. In each slide, immunolabeled cells were identified within the different stages of tuberculous granuloma. The percentage of area covered by immunolabelled cells was determined by digital image analysis (Image J software) after setting the thresholds. Necrotic or mineralized areas in stage III and stage IV granulomas were not included in the analysis, as described previously [11]. The results are expressed as the percentage of the positively immunolabeled area within the total area of the granuloma.

Statistical analysis

The results of the immunohistochemical analyses were expressed as the mean and standard deviation (SD) and the results were compared between the different stages of granuloma. A P value < 0.05 was considered statistically significant. The analyses were conducted using GraphPad Prism 5.0 software (GraphPad Prism software 5.0, Inc., San Diego, CA, USA). One-way analysis of variance (ANOVA) and Tukey's multiple comparison post hoc test was used to compare expression between different stages of granuloma.

Results

Pathological examination

Sixty out of the 2,150 examined cases presented tuberculous lesions (2.79 %). Based on gross observations, these lesions were grouped into 9 (15.00 %) cases diagnosed as generalized tuberculosis and 51 (85.00 %) cases diagnosed as localized tuberculosis. Affected lungs, pleura, and peritoneum of generalized cases were characterized by miliary tuberculosis with a large number of small gray to white-yellowish miliary nodules resembling pearls (Fig. 1A and 1B). However, in the localized cases, variably sized multinodular lesions were detected, with cheesy necrotic material or creamy inspissated pus when sectioned (Fig. 1C and 1D). According to the

histopathological examination the granulomas were classified into 4 stages (I, II, II, I, and IV) (Fig. 2A-2D). A total of 515 granulomas were evaluated from tracheobronchial and mediastinal lymph nodes. The distribution of the 515 cattle granulomas according to the granuloma stage was: 110/515 (21.35 %) stage I; 122/515 (23.68 %) stage II; 98/515 (19.0 %) stage III, and 185/515 (35.92 %) stage IV. Forty-two out of 60 animals (70 %) yielded a positive result with the ZN technique, with 35 cases showing a paucibacillary form, whereas 7 cases showed a pluribacillary form (Fig. 2F). AFB was mainly demonstrated within macrophages, multinucleated giant cells (MNGCs) and the necrotic center of granulomas (Fig. 2E and 2F).

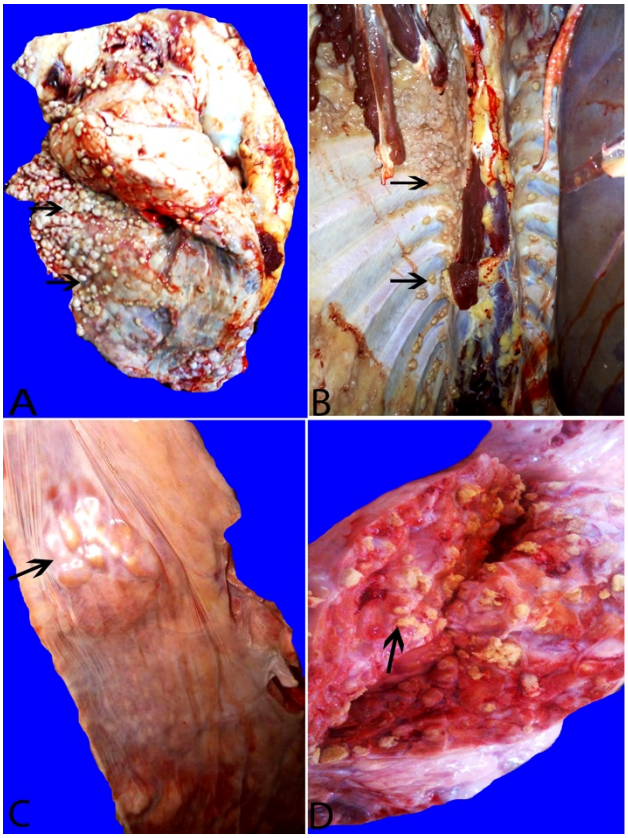

Fig. 1: Lung of cattle: (A&B): large number of small gray to white yellowish tubercles (pearl tuberculosis) above visceral and the parietal pleura (arrows). (C&D): multiple nodular lesions (C, arrow); cut sections revealed cheesy necrotic material (D, arrows) with calcification.

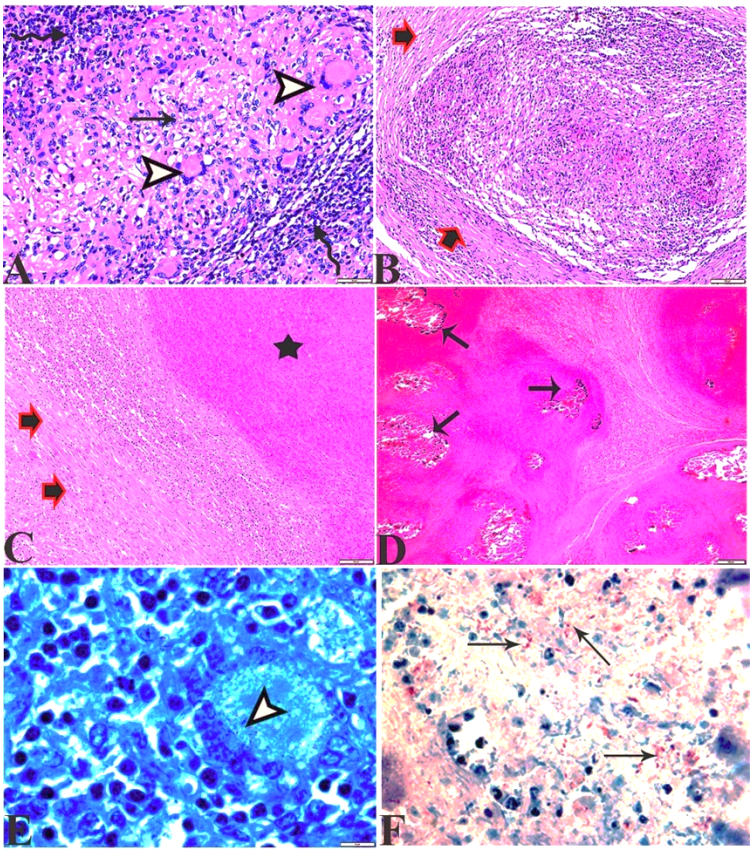

Fig. 2: Histological sections of bronchial lymph nodes showing the four stages of granulomas from naturally infected beef cattle with bovine tuberculosis. (A): Stage I granuloma, epithelioid cell (arrow), and multinucleated giant cells (arrowheads) surrounded by lymphocytes (zigzag arrows). (Hx & E. Bar = 50 µm). (B): Stage II granuloma (solid), increased numbers of epithelioid macrophages can be seen, encircled by thin layer of C.T. (arrows), and central caseous necrosis is not formed (Hx & E, Bar = 100 µm). (C): Stage III granuloma showing fully formed C.T. (arrows) and central caseated area (star) with little mineralization (Hx& E, Bar = 100 µm). (D): Stage IV granuloma with an extensive central caseated area, mature C.T capsule, and extensive multiple mineralizations (arrows) (Hx& E, Bar = 200 µm). (E): Intracellular acid-fast bacilli present inside the multinucleated giant cell (ZN stain) (arrowhead). (F): a large number of acid-fast bacilli (arrows) were detected in the center necrotic area of the granuloma.

Distribution of CD68 immunolabeled cells

Immunohistochemistry for CD68 showed diffuse cytoplasmic expression in macrophages, epithelioid macrophages, and Langhans MNGCs in all stages of granuloma. The intensity of staining was strong in stage I and stage II granulomas. The location of these cells differed between stages, thus, while CD68+ macrophages were dispersed throughout stage I and stage II granulomas (Fig. 3A and 3B), in stages III and IV there was an obvious rim of positively stained macrophages surrounding the necrotic center (Fig. 3C and 3D). The number of CD68+ cells decreased as granuloma development occurred (** = P <0.003) (Fig. 4).

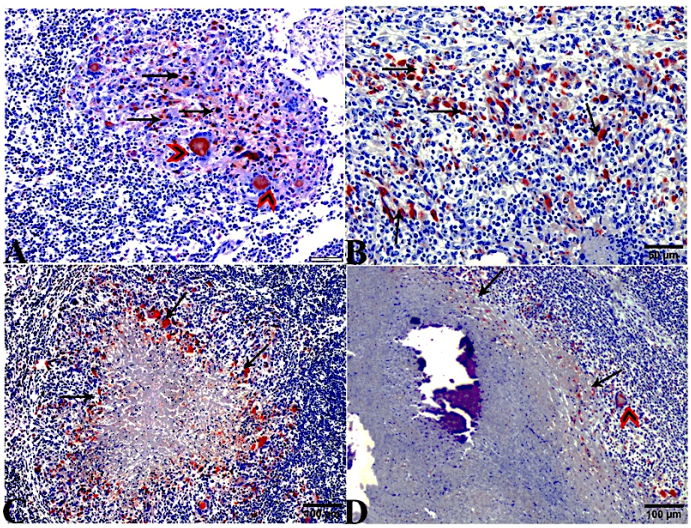

Fig. 3: Expression of macrophages (CD68+). CD68+ staining in (A): stage I and (B): stage II granulomas in the lymph node of beef cattle naturally infected with Mycobacterium. Heavy positive staining can be observed within the cytoplasm of macrophages (arrows) and multi-nucleated giant cells (arrowheads). (IHC, 50 µm). (C): Scattered CD68+ macrophage cells can be detected within the rim of inflammatory cells surrounding the necrotic center of the stage III granuloma (arrows). (D): Expression of CD68+ macrophages in a stage IV granuloma (arrows). (IHC, 100 µm). The expression of CD68+ macrophages can be seen within the cytoplasm of a few epithelioid, macrophages, and multi-nucleated giant cells surrounding the necrotic center. (IHC, 100 µm).

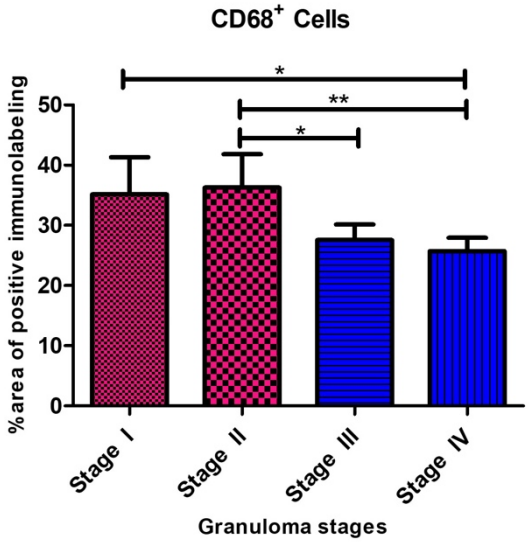

Fig. 4: CD68+ Cells. The CD68+ immunolabeling fraction was higher in the early-stage granulomas compared with the late stages, with a significant difference between stage II and stages III and stage IV (** = P <0.003).

Table 1: Summary of immunohistochemical methodology.

Marker	Primary antibody	Dilution	Blocking fluid	Secondary antibody	Antigen retrieval
CD68	Monoclonal mouse anti-human CD68 (clone EBM 11; Dako Cytomation)	1: 50	BSA 5 %	Polyclonal goat anti-mouse immunoglobulin biotinylated. (1: 200)	Protease from *Bacillus licheniformis* 0.64 % in PBS for 8 minutes
iNOS	Rabbit polyclonal Ab (NeoMarkers, Fremont CA)	1: 500	NGS 10 %	Goat anti-rabbit immunoglobulin biotinylated. (1: 200)	Citrate buffer pH 6 in autoclave at 121 ºC for 10 minutes
HLA-DR	Monoclonal -mouse anti human HLA-DR antigen Alpha-chain (clone TAL.1B5; Dako Cytomation)	1: 20	BSA 5 %	Polyclonal goat anti-mouse immunoglobulin biotinylated. (1: 200)	Citrate buffer pH 3.2 in microwave for 5 min at 540 w followed by 5 min at 140 w

Distribution of iNOS immunolabelled cells

Anti-iNOS antibody was used to identify M1 macrophages iNOS-positive cells consisting of macrophages, epithelioid cells, and MNGCs, with an intense cytoplasmic expression observed especially in the latter. The intensity of immunolabelling was higher in stage I and stage II granulomas, mainly within epithelioid macrophages and MNGCs in the center of the granuloma (Fig. 5A and 5B), whereas stage III and stage IV granulomas showed a rim of iNOS+ macrophages surrounding the necrotic center (Fig. 5C and 5D). Regarding the kinetics of expression of iNOS, the mean frequency of positive cells was higher in the early stages of granulomas compared to the late stages of granulomas (** =P < 0.01; stage I vs stage IV granulomas) (Fig. 6).

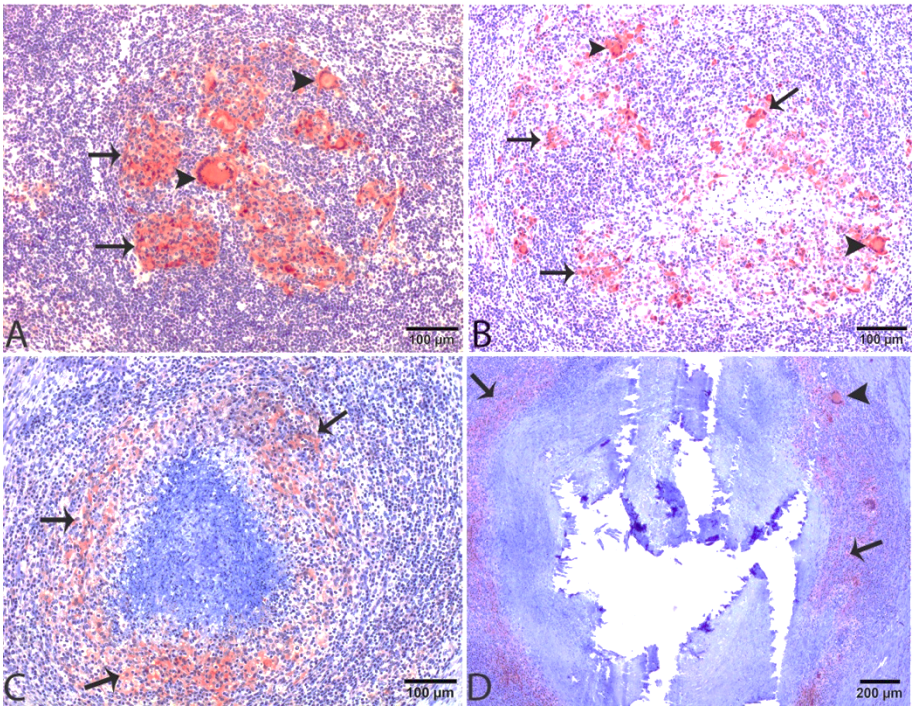

Fig. 5: Expression of iNOS+ immunolabeling in (A): stage I (arrows) and (B): stage II granulomas in the lymph node of beef cattle naturally infected with Mycobacterium. Strong positive expression was observed within the cytoplasm of macrophages (arrows) and multi-nucleated giant cells (arrowheads). (IHC, 100 µm). (C): iNOS+ macrophages forming a peripheral rim surrounding the necrotic center of

the stage III granuloma (arrows). (D) Expression of iNOS+ macrophages in a stage IV granuloma (arrows). (IHC, 100 μm). The expression of iNOS+ macrophages can be seen surrounding the necrotic center in the outer layer of the granuloma (IHC, 200 μm).

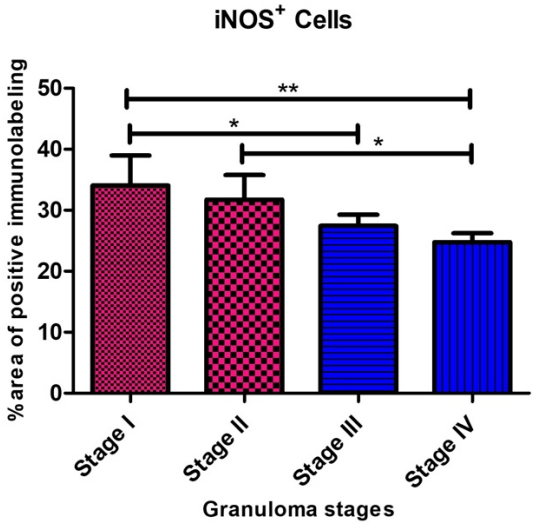

Fig. 6: iNOS+ Cells. The iNOS+ immunolabeling fraction was higher in the early-stage granulomas compared with the late stages, with a significant difference between stage I and stage IV (** =P <0.002).

Distribution of HLA-DR immunolabeled cells

Anti-HLA-DR antibody was used to identify activated macrophages. The expression of HLA-DR was observed in all stages of granuloma with differences in the distribution of immunolabeled cells and percentage of positive area in each stage of granuloma. HLA-DR immunolabeling was observed as diffuse intracytoplasmic within abundant epithelioid macrophages and MNGCs distributed throughout stage I and stage II granulomas (Fig.7A and 7B). In advanced granuloma stages, central caseous necrosis with mineralization was rimmed predominantly by HLA-DR+ macrophages and MNGCs, but also at the peripheral margin of the granuloma (Fig.7C and 7D). The

number of HLA-DR+ cells showed similar kinetics to iNOS+ cells and decreased as granuloma development occurred (** =P <0.0020) (Fig. 8).

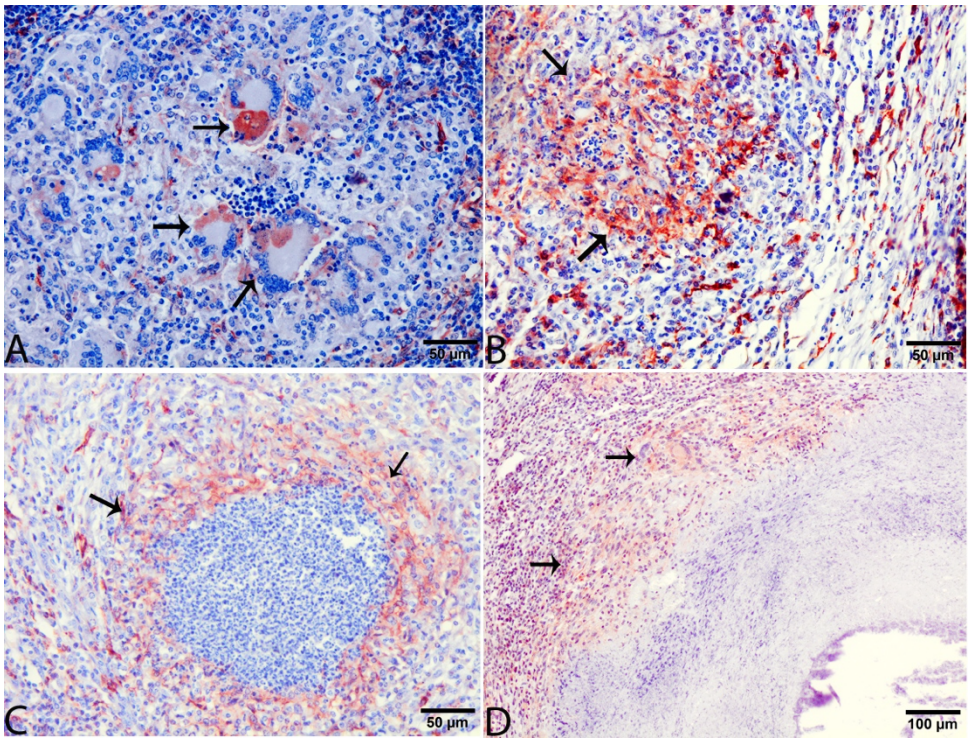

Fig. 7: Expression of macrophages (HLA-DR+). HLA-DR+ immunolabeling in stage I and II granulomas showing: (A&B): strong positive expression observed within the cytoplasm of macrophages (arrows), and multi-nucleated giant cells (arrowheads) respectively. (IHC, 50 µm). (C): HLA-DR+ macrophages immunolabeling forming a peripheral rim surrounding the necrotic center of the stage III granuloma (arrows). (D): Expression of HLA-DR+ macrophages (arrows), in a stage IV granuloma. (IHC, 100 µm). The expression of HLA-DR+ macrophages can be seen surrounding the necrotic center in the outer layer of the granuloma. (IHC, 100 µm).

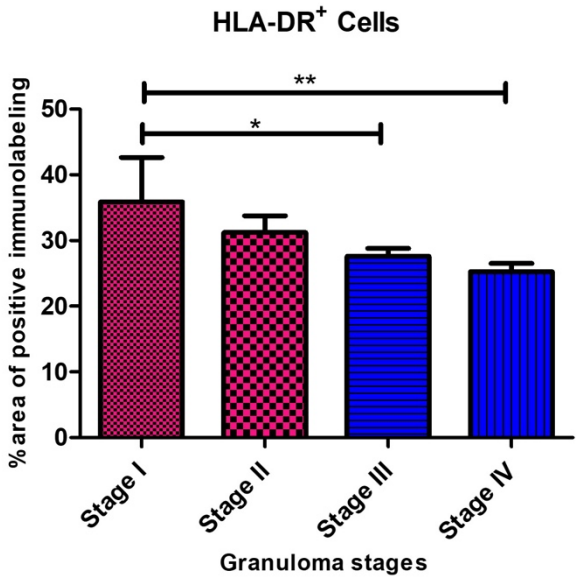

Fig. 8: HLA-DR+ Cells. The mean percentage of the immunolabeling fraction of HLA-DR+ macrophages significantly decreased as the stage of granuloma increased from stage I to stage IV showing similar kinetics as iNOS+ cells. The HLA-DR+ immunolabeling fraction was higher in the early-stage granulomas compared with the late stages, with a significant difference between stage I and stage II both with respect to stage IV) (** =P <0.002).

Discussion

Bovine TB is a chronic, progressive, infectious, and contagious disease caused by *M. tuberculosis* complex [35]. It is characterized by gross and microscopic lesions (tubercles), however, the antemortem diagnosis of this disease is difficult due to the chronicity of the infection and the modulation of the immune response. A state of anergy and a suppressed cell-mediated immune response may occur in animals in the more advanced stages of the disease, rendering them insensitive to the traditional cell-mediated diagnostic tests (i.e., tuberculin and gamma-interferon) [36]. Post-mortem examination allows the identification of the mycobacteria by different techniques,

although there are several factors affecting the sensibility of this diagnosis for example, the relatively high proportion of small lesions which could not be detected in routine inspection. In our study, all cattle examined by visual inspection and histopathology exhibited characteristic gross tubercles and microscopic granulomas, respectively.

Regarding zoonotic diseases, such as bTB, meat inspection and identification of gross lesions at the slaughterhouse are of special importance. Our findings revealed a prevalence of bovine tuberculosis of 2.79 % in the imported beef cattle that were under investigation. This finding nearly agrees with previous studies [37, 38], but differs from others with a higher prevalence (11.6-24 %) [39-41]. The low prevalence observed in our study may be attributable to the low number of tissues inspected at the slaughterhouse, or depend on other diagnostic techniques, variation in the number of examined animals [41] as well as the lack of detection of small lesions in a routine inspection. In addition, our study was mainly carried out on imported beef cattle considered as a species or subspecies of domestic cattle, zebu, which is relatively resistant to bTB [42]. However, a more recent study showed no difference between Zebu and Holstein-Friesian cattle [43]. Indeed, some of the previous studies with a higher prevalence rate were conducted on animals belonging to other breeds than zebu [39, 40]. Therefore, our findings support that the slaughterhouse meat inspection procedures represent a critical point for the identification of TBL gross lesions at the slaughterhouse. It is advisable to enhance meat inspection procedures such as multiple slicing of organs and lymph nodes in young calves (< 8 months [44, 45].

In this study, most of the tuberculosis cases were diagnosed as localized tuberculosis (51, 85%), especially in a pulmonary form where the lesion was frequently seen in the lungs and lymph nodes of the thoracic cavity (complete primary complex). This finding revealed that these imported cattle harbored already the infection from the country of origin. It has been described that chronically infected animals showing severe gross pathology may be unresponsive to the tuberculin test yielding a false negative result [9, 46]. Therefore, it is very important to use additional diagnostic tools to confirm the bTB status of imported beef cattle. The polymerase chain reaction (PCR) is a powerful technique that is considered one of the most widely used techniques in

the diagnosis of *Mycobacterium tuberculosis* complex infections through the amplification of different targets, such as IS6110 [47]. In addition, a histopathological examination is a diagnostic tool with an acceptable sensitivity (87.5%) and specificity (84.1%) which can be used both to confirm the diagnosis obtained by skin intra-dermal tuberculin test and to identify true positive animals which disclose negative results to the other techniques [13]. However, these techniques are currently applied postmortem which impedes having a diagnosis before the movement of animals.

To further comprehend the function and distribution of macrophages in calves naturally infected with tuberculosis, this study used macroscopic lesions, histological assessment of granulomas, and immunohistochemistry analyses. Our findings show that the frequency of immunolabeled cells against these markers progressively reduced from stage I to stage IV granuloma. However, other authors have mentioned a lack of changes or even an increase in the number of CD68+ cells with lesion progress in cattle [10, 12, 26]. CD68 expression was observed within the cytoplasm of macrophages, epithelioid macrophages, and Langhans MNGCs at all stages of granuloma. The number of CD68+ cells dropped as the granuloma developed. CD68 belongs to the lysosomal/endosomal-associated membrane glycoprotein (LAMP) family, which is involved in antigen processing and presentation during phagocytosis [48]. This could be associated with the role of phagocytic activity of macrophages and MNGCs in the early immune response for protection and elimination of the mycobacteria and might indicate a decrease in the phagocytic activity in the later stages of the disease.

iNOS expression followed a similar trend as CD68+ cells, with iNOS+ macrophages seen as dispersed throughout stages I and II granulomas and in a distinct ring encircling the necrotic core in stages III and IV granulomas. Similar kinetics for iNOS+ and CD68+ macrophages have been reported in previous studies [11, 26]. It is hypothesized that increased nitric oxide (NO) production by iNOS+ macrophages is crucial for the management and eradication of mycobacteria during infection [11, 26]. NO inactivates mycobacteria by producing highly reactive nitrogen intermediates [26]. Therefore, NO generation during tuberculosis may increase due to the increased iNOS+ macrophage population. The NO decreased the number of bacteria and cleared the

infection [24, 26], more importantly in early-stage granulomas. Furthermore, the similar kinetics observed concerning CD68 expression support a decrease of macrophage (M 1) polarization from the early stages to the later stages of the disease.

According to Heppner et al. (2015) [21], HLA-DR is a macrophage marker crucial for controlling immunological responses and antigen presentation, particularly for T cell-mediated reactions. Our findings showed that early-stage granulomas (I, II) had higher expression of HLA-DR+ and iNOS+ than late-stage granulomas (III, IV). Increased iNOS expression has been associated with higher levels of IFN-γ in granulomas of calves who received the BCG, favoring those with a better host immune response against mycobacteria [26]. IFN-γ is a Th1 cytokine known to stimulate or activate macrophages, developing mycobactericidal mechanisms [49]. The parallel increase in the expression of CD68, iNOS, and HLA-DR in early-stage granulomas and their progressive decrease in late-stage granulomas indicate a shift in the immune response along the infection, from a more effective proinflammatory immune response to a tolerogenic response which allows the persistence of the disease. Furthermore, the similar kinetics observed with respect to iNOS expression support a decrease of macrophage (M 1) polarization from the early stages to the later stages of the disease.

Conclusion

This study elucidated the role and expression of CD68+, iNOS+, and HLA-DR+ macrophages in different stages of the granuloma in naturally infected cattle. The increased expression of CD68+, iNOS+, and HLA-DR+ macrophages in early-stage granulomas (I, II) compared with late-stage granulomas (III, IV) suggests that macrophages are initially polarized to pro-inflammatory macrophages, playing a protective role in the immune response during the early stages of the disease in naturally infected beef cattle.

List of abbreviations

ABC: avidin-biotin-peroxidase complex

ANOVA: Analysis of variance

AFB: acid-fast bacilli

bTB: bovine tuberculosis

CMI: cell-mediated immune

H&E: hematoxylin-eosin

HLA-DR: Human leucocytic antigen-DR

HPF: high-power field magnification

iNOS: Inducible nitric oxide synthase

MHC-II: class II MHC antigens

MNGCs: multinucleated giant cells

NO: Nitric oxide

PBS: phosphate buffer saline

PCR: polymerase chain reaction

SD: standard deviation

TBL: Tuberculosis-like lesions

Th1: T helper type 1

WHO: World Health Organization

ZN: Ziehl-Neelsen

Acknowledgments

We express our appreciation to Islam Sayed Ali for his assistance in sample collection from the slaughterhouses.

Author Contributions

M.G.H, J.G. L, F.L.M, A.Z.M, F.A. A, and S.KH. A: involved in the conception of the idea, and methodology design, performed data analysis and interpretation, and prepared the manuscript for publication and revision. All authors read and approved the final version of the manuscript.

Funding

This study was not supported by any funding

Data availability

The data supporting this study's findings are available on request from the corresponding author.

Declarations

Ethics approval and consent to participate.

The current study was performed in compliance with the Guidelines of the Egyptian regulations for imported animals. All experimental protocols and procedures were conducted by the ethical committee guidelines of the Faculty of Veterinary Medicine, Sohag University. The ethical approval number is Soh. Un. Vet/0007R

Competing interests

The authors declare that they have no competing interests.

Consent for publication:

Not applicable.

References

1. Rodriguez-Campos S, Smith NH, Boniotti MB, Aranaz A: Overview and phylogeny of *Mycobacterium tuberculosis* complex organisms: implications for diagnostics and legislation of bovine tuberculosis. Research in veterinary science 2014, 97:S5-S19.

2. Biet F, Boschiroli ML, Thorel MF, Guilloteau LA: Zoonotic aspects of Mycobacterium bovis and *Mycobacterium avium*-intracellulare complex (MAC). Veterinary research 2005, 36(3):411-436.

3. Gelalcha BD, Zewude A, Ameni G: Tuberculosis caused by *Mycobacterium* bovis in a sheep flock colocated with a tuberculous dairy cattle herd in Central Ethiopia. Journal of Veterinary Medicine 2019, 2019.

4. W.H.O.: World Health Organization report. In: Fact sheet No 104. 2016: http://www.who.int/mediacentre/factsheets/who104/en/print.html.

5. Trauer JM, Dodd PJ, Gomes MGM, Gomez GB, Houben RM, McBryde ES, Melsew YA, Menzies NA, Arinaminpathy N, Shrestha S: The importance of heterogeneity to the epidemiology of tuberculosis. Clinical infectious diseases 2019, 69(1):159-166.

6. Adebisi YA, Agumage I, Sylvanus TD, Nawaila IJ, Ekwere WA, Nasiru M, Okon EE, Ekpenyong AM, Lucero-Prisno III DE: Burden of tuberculosis and challenges facing its eradication in West Africa. International Journal of Infection 2019, 6(3).

7. Organization WH: Global tuberculosis report 2021: supplementary material. 2022.

8. Domingo M, Vidal E, Marco A: Pathology of bovine tuberculosis. Research in veterinary science 2014, 97:S20-S29.

9. Stear MJ: OIE Manual of Diagnostic Tests and Vaccines for Terrestrial Animals (Mammals, Birds and Bees) 5th Edn. Volumes 1 & 2. World Organization for Animal Health 2004. ISBN 92 9044 622 6.€ 140. Parasitology 2005, 130(6):727-727.

10. Wangoo A, Johnson L, Gough J, Ackbar R, Inglut S, Hicks D, Spencer Y, Hewinson G, Vordermeier M: Advanced granulomatous lesions in *Mycobacterium bovis*-infected cattle are associated with increased expression of type I procollagen, γδ (WC1+) T cells and CD 68+ cells. Journal of comparative pathology 2005, 133(4):223-234.

11. Aranday-Cortes E, Bull N, Villarreal-Ramos B, Gough J, Hicks D, Ortiz-Peláez A, Vordermeier H, Salguero F: Upregulation of IL-17 A, CXCL 9 and CXCL 10 in Early-Stage Granulomas Induced by M ycobacterium bovis in Cattle. Transboundary and emerging diseases 2013, 60(6):525-537.

12. Tulu B, Martineau HM, Zewude A, Desta F, Jolliffe DA, Abebe M, Balcha TT, Belay M, Martineau AR, Ameni G: Cellular and cytokine responses in the granulomas of asymptomatic cattle naturally infected with *Mycobacterium bovis* in Ethiopia. Infection and Immunity 2020, 88(12):e00507-00520.

13. Larenas-Muñoz F, Sánchez-Carvajal JM, Galán-Relaño Á, Ruedas-Torres I, Vera-Salmoral E, Gómez-Gascón L, Maldonado A, Carrasco L, Tarradas C, Luque I: The Role of Histopathology as a Complementary Diagnostic Tool in the Monitoring of Bovine Tuberculosis. Frontiers in Veterinary Science 2022, 9.

14. Rusk RA, Palmer MV, Waters WR, McGill JL: Measuring bovine γδ T cell function at the site of *Mycobacterium bovis* infection. Veterinary immunology and immunopathology 2017, 193:38-49.

15. Widdison S, Schreuder L, Villarreal-Ramos B, Howard C, Watson M, Coffey T: Cytokine expression profiles of bovine lymph nodes: effects of *Mycobacterium bovis* infection and bacille Calmette–Guérin vaccination. Clinical & Experimental Immunology 2006, 144(2):281-289.

16. Thacker TC, Palmer MV, Waters WR: Associations between cytokine gene expression and pathology in *Mycobacterium bovis* infected cattle. Veterinary immunology and immunopathology 2007, 119(3-4):204-213.

17. Davis JM, Ramakrishnan L: The role of the granuloma in expansion and dissemination of early tuberculous infection. Cell 2009, 136(1):37-49.

18. Italiani P, Boraschi D: From monocytes to M1/M2 macrophages: phenotypical vs. functional differentiation. Frontiers in immunology 2014, 5:514.

19. Marakalala MJ, Raju RM, Sharma K, Zhang YJ, Eugenin EA, Prideaux B, Daudelin IB, Chen P-Y, Booty MG, Kim JH: Inflammatory signaling in human tuberculosis granulomas is spatially organized. Nature medicine 2016, 22(5):531-538.

20. Holness CL, Simmons DL: Molecular cloning of CD68, a human macrophage marker related to lysosomal glycoproteins. 1993.

21. Heppner FL, Ransohoff RM, Becher B: Immune attack: the role of inflammation in Alzheimer disease. Nature Reviews Neuroscience 2015, 16(6):358-372.

22. Sisino G, Bouckenooghe T, Aurientis S, Fontaine P, Storme L, Vambergue A: Diabetes during pregnancy influences Hofbauer cells, a subtype of placental macrophages, to acquire a pro-inflammatory phenotype. Biochimica et Biophysica Acta (BBA)-Molecular Basis of Disease 2013, 1832(12):1959-1968.

23. Song L, Lee C, Schindler C: Deletion of the murine scavenger receptor CD68 [S]. Journal of lipid research 2011, 52(8):1542-1550.

24. Mattila JT, Ojo OO, Kepka-Lenhart D, Marino S, Kim JH, Eum SY, Via LE, Barry CE, Klein E, Kirschner DE: Microenvironments in tuberculous granulomas are delineated by distinct populations of macrophage subsets and expression of nitric oxide synthase and arginase isoforms. The Journal of Immunology 2013, 191(2):773-784.

25. Lisi L, Ciotti GMP, Braun D, Kalinin S, Curro D, Russo CD, Coli A, Mangiola A, Anile C, Feinstein D: Expression of iNOS, CD163 and ARG-1 taken as M1 and M2 markers of microglial polarization in human glioblastoma and the surrounding normal parenchyma. Neuroscience letters 2017, 645:106-112.

26. Salguero F, Gibson S, Garcia-Jimenez W, Gough J, Strickland T, Vordermeier H, Villarreal-Ramos B: Differential cell composition and cytokine expression within lymph node granulomas from BCG-vaccinated and non-vaccinated Cattle Experimentally Infected with *Mycobacterium bovis*. Transboundary and emerging diseases 2017, 64(6):1734-1749.

27. MacMicking JD, North RJ, LaCourse R, Mudgett JS, Shah SK, Nathan CF: Identification of nitric oxide synthase as a protective locus against tuberculosis. Proceedings of the National Academy of Sciences 1997, 94(10):5243-5248.

28. Scanga CA, Mohan VP, Tanaka K, Alland D, Flynn JL, Chan J: The inducible nitric oxide synthase locus confers protection against aerogenic challenge of both clinical and laboratory strains of *Mycobacterium tuberculosis* in mice. Infection and immunity 2001, 69(12):7711-7717.

29. Peranzoni E, Marigo I, Dolcetti L, Ugel S, Sonda N, Taschin E, Mantelli B, Bronte V, Zanovello P: Role of arginine metabolism in immunity and immunopathology. Immunobiology 2008, 212(9-10):795-812.

30. Fang FC: Antimicrobial reactive oxygen and nitrogen species: concepts and controversies. Nature Reviews Microbiology 2004, 2(10):820-832.

31. Cooperman LS, Garovoy MR, Sondel PM: Association of the HLA-DR2/DR4 phenotype with skin test responses to bovine dermal collagen: A potential interaction of two MHC alleles in regulating an immune response. Human immunology 1986, 17(4):471-479.

32. Kumar A, Sherlin HJ, Ramani P, Natesan A, Premkumar P: Expression of CD 68, CD 45 and human leukocyte antigen-DR in central and peripheral giant cell granuloma, giant cell tumor of long bones, and tuberculous granuloma: An immunohistochemical study. Indian Journal of Dental Research 2015, 26(3):295.

33. Müller B, Dürr S, Alonso S, Hattendorf J, Laisse CJ, Parsons SD, Van Helden PD, Zinsstag J: Zoonotic *Mycobacterium bovis*–induced tuberculosis in humans. Emerging infectious diseases 2013, 19(6):899.

34. García-Jiménez W, Salguero F, Fernández-Llario P, Martínez R, Risco D, Gough J, Ortiz-Peláez A, Hermoso-de-Mendoza J, Gómez L: Immunopathology of granulomas produced by *Mycobacterium bovis* in naturally infected wild boar. Veterinary immunology and immunopathology 2013, 156(1-2):54-63.

35. O'Reilly LM, Daborn C: The epidemiology of *Mycobacterium bovis* infections in animals and man: a review. Tubercle and Lung disease 1995, 76:1-46.

36. de la Rua-Domenech R, Goodchild A, Vordermeier H, Hewinson R, Christiansen K, Clifton-Hadley R: Ante mortem diagnosis of tuberculosis in cattle: a review of the tuberculin tests, γ-interferon assay and other ancillary diagnostic techniques. Research in veterinary science 2006, 81(2):190-210.

37. Moussa I, Kh FM, Marwah M, Nasr E, Atef MS, Mounir MS-B, Hatem M: Comparison between the conventional and modern techniques used for identification of *Mycobacterium tuberculosis* complex. African Journal of Microbiology Research 2011, 5(25):4338-4343.

38. Nasr EA, Marwah M, Melika LF, Tammam AA, Gorge SF: Comparison of tuberculin skin test and lateral flow rapid test for detection of bovine tuberculosis in dairy cattle. Journal of Applied Veterinary Sciences 2016, 1(1):21-27.

39. El-Sabban M, Lotfy O, Hammam H, Dimitri R, Gergis S: Bovine tuberculosis and its extent of spread as a source of infection to man and animals in Arab Republic of Egypt. In: The International Conference on Animal Tuberculosis in Africa & Middle East, Cairo (Egypt), 28-30 Apr 1992: 1995; 1995.

40. Nawal AH, Mohey AH, Alaa AG, Yasser AG: Bovine tuberculosis in a dairy cattle farm as a threat to public health. African Journal of Microbiology Research 2009, 3(8):446-450.

41. Ameni G, Erkihun A: Bovine tuberculosis on small-scale dairy farms in Adama Town, central Ethiopia, and farmer awareness of the disease. Revue Scientifique et Technique-Office International des Epizooties 2007, 26(3):711-720.

42. Dechassa T: Gross pathological lesions of bovine tuberculosis and efficiency of meat inspection procedure to detect-infected cattle in Adama municipal abattoir. Journal of Veterinary Medicine and Animal Health 2014, 6(2):48-53.

43. Alcaraz-López OA, Flores-Villalva S, Cortéz-Hernández O, Vigueras-Meneses G, Carrisoza-Urbina J, Benítez-Guzmán A, Esquivel-Solís H, Werling D, Salguero Bodes FJ, Vordemeier M: Association of immune responses of Zebu and

Holstein-Friesian cattle and resistance to mycobacteria in a BCG challenge model. Transboundary and Emerging Diseases 2021, 68(6):3360-3365.

44. Corner L: Post mortem diagnosis of *Mycobacterium bovis* infection in cattle. Veterinary microbiology 1994, 40(1-2):53-63.

45. Whipple DL, Bolin CA, Miller JM: Distribution of lesions in cattle infected with *Mycobacterium bovis.* Journal of Veterinary Diagnostic Investigation 1996, 8(3):351-354.

46. Mekonnen GA, Conlan AJ, Berg S, Ayele BT, Alemu A, Guta S, Lakew M, Tadesse B, Gebre S, Wood JL: Prevalence of bovine tuberculosis and its associated risk factors in the emerging dairy belts of regional cities in Ethiopia. Preventive veterinary medicine 2019, 168:81-89.

47. Sánchez-Carvajal JM, Galán-Relaño Á, Ruedas-Torres I, Jurado-Martos F, Larenas-Muñoz F, Vera E, Gómez-Gascón L, Cardoso-Toset F, Rodríguez-Gómez IM, Maldonado A: Real-Time PCR validation for *Mycobacterium tuberculosis* complex detection targeting IS 6110 directly from bovine lymph nodes. Frontiers in Veterinary Science 2021, 8:643111.

48. Chistiakov DA, Killingsworth MC, Myasoedova VA, Orekhov AN, Bobryshev YV: CD68/macrosialin: not just a histochemical marker. Laboratory investigation 2017, 97(1):4-13.

49. Palmer M, Waters W, Thacker T: Lesion development and immunohistochemical changes in granulomas from cattle experimentally infected with *Mycobacterium bovis*. Veterinary pathology 2007, 44(6):863-874.

Capítulo II

Estudio 2 / Study 2

Objetivo 2 / Objective 2

Estudio 2: Macrophage polarization in lymph node granulomas from cattle and pigs naturally infected with *Mycobacterium tuberculosis* complex

Fernanda Larenas-Muñoz[a*], Mohamed G. Hamed[b], Inés Ruedas-Torres[a], José María Sánchez-Carvajal[a], Javier Domínguez[c], Francisco José Pallarés[a], Librado Carrasco[a], Irene M. Rodríguez-Gómez[a†], Jaime Gómez-Laguna[a†]

Aceptado para publicar en Veterinary Pathology, 2023, JIF: 2.4 (Q1)

Objetivo 2: Evaluar la expresión de marcadores de células mieloides (CD172a y MAC387) y la polarización de macrófagos M1 (iNOS, CD68 y CD107a) y M2 (Arg1 y CD163) en los nódulos linfáticos de bovino y porcino para el estudio de la inmunopatogenia de la tuberculosis.

Objective 2: Evaluate the expression of myeloid cell markers (CD172a and MAC387) and the polarisation of M1 (iNOS, CD68 and CD107a) and M2 (Arg1 and CD163) macrophages in bovine and porcine lymph nodes to study the immunopathogenesis of tuberculosis.

Macrophage polarization in lymph node granulomas from cattle and pigs naturally infected with *Mycobacterium tuberculosis* complex

Fernanda Larenas-Muñoz[a*], Mohamed G. Hamed[b], Inés Ruedas-Torres[a], José María Sánchez-Carvajal[a], Javier Domínguez[c], Francisco José Pallarés[a], Librado Carrasco[a], Irene M. Rodríguez-Gómez[a†], Jaime Gómez-Laguna[a†]

[a] Department of Anatomy and Comparative Pathology and Toxicology, Pathology and Immunology Group (UCO-PIG), UIC Zoonosis y Enfermedades Emergentes ENZOEM, University of Córdoba, International Excellence Agrifood Campus 'CeiA3', 14014 Córdoba, Spain

[b] Department of Pathology and Clinical Pathology, Faculty of Veterinary Medicine, University of Sohag, 82524 Sohag, Egypt

[c] Department of Biotechnology, INIA, CSIC, 28040 Madrid, Spain

†These authors have contributed equally to this work and share senior authorship

*Correspondence: Fernanda Larenas-Muñoz

ep2lamuf@uco.

Abstract

Animal tuberculosis is caused by members of the *Mycobacterium tuberculosis* complex (MTC), being the tuberculous granuloma the main characteristic lesion. The macrophage is the main cell subset involved in the development of tuberculous granuloma, presenting a wide plasticity and, leading towards the polarization to classically activated or pro-inflammatory macrophages (M1) or to alternatively activated or anti-inflammatory macrophages (M2). Thus, this study aimed to analyze macrophage polarization in granulomas from cattle and pig lymph nodes from naturally MTC-infected animals. Tuberculous granulomas were microscopically categorized into four stages and a panel of myeloid cells (CD172a/MAC387), M1 macrophage polarization (iNOS/CD68/CD107a) and M2 macrophage polarization (Arg1/CD163) markers were analyzed by immunohistochemistry. CD172a and MAC387 followed the same kinetics, having the latter greater expression in late-stage granulomas in pigs. From the M1 panel, the expression of iNOS and CD68 prevailed in cattle in comparison to pig, being the expression higher in early-stage granulomas. CD107a staining was only observed in porcine granulomas, with a higher expression in stage I granulomas. For M2 panel, $Arg1^+$ cells were significantly higher in pigs than in cattle, particularly in late-stage granulomas. Quantitative analysis of $CD163^+$ cells showed similar kinetics in both species with a consistent frequency of immunolabeled cells throughout the different stages of the granuloma. Our results indicate that M1 macrophage polarization prevails in cattle during early-stage granulomas (I and II), whereas M2 phenotype is observed in later stages. Contrary, and mainly due to the expression of Arg1, M2 macrophage polarization is predominant in pigs in all granuloma stages.

Keywords: Animal tuberculosis, granuloma, macrophages, polarization, cattle, pig

1. Introduction

Animal tuberculosis (TB) is a chronic progressive infectious disease affecting a wide range of domestic and wildlife animals, as well as humans.[33] The disease is caused by bacteria belonging to the *Mycobacterium tuberculosis* complex (MTC).[27] The characteristic lesion of the disease is the tuberculous granuloma,[37,38] which is classified into four different stages of development in both cattle and pigs, with the macrophage being the target cell for mycobacteria replication and leading to the transition to epithelioid cells and the formation of Langhans-type multinucleated giant cells (MNGCs).[5,30,38]

The interaction between different cellular components reflects the crosstalk between the host's immune response and pathogen virulence factors. Despite the importance of tuberculous granuloma,[30] the mechanisms triggered off during the pathogenesis of this disease are not still well understood. Subsequently to the infection by MTC, the initial immunologic events include cytokine- and chemokine-mediated recruitment of monocytes, neutrophils, and macrophages.[18] Then, macrophages may act as a functional element to control or overcome the infection, cooperating with activated T cells to establish the granuloma.[26]

The cytokine microenvironment in the granuloma can guide macrophage polarization adopting different functional responses according to the stimuli and signals.[17,23,36] Thus, two main macrophage subpopulations may be identified, the classically activated (M1) pro-inflammatory macrophages and the alternatively activated (M2) anti-inflammatory macrophages. M1 macrophages are polarized by Th1 cytokines, such as interferon-γ (IFN-γ) and tumor necrosis factor-α (TNF-α), and lipopolysaccharide (LPS),[17,23] displaying a high capacity for antigen presentation as well as secreting high levels of pro-inflammatory cytokines, nitric oxide (NO), reactive oxygen species, and antimicrobial peptides together with low levels of interleukin (IL)-10.[28,36] In human, M1 macrophage polarization is

characterized by the upregulation of CD80/CD86, CD68, major histocompatibility complex class -II (MHC-II), IL-1R, Toll-like receptor (TLR)-2, TLR-4, inducible nitric oxide synthase (iNOS), IL-12 and secretion of low levels of IL-10.[24,36] Nevertheless, some of these markers, such as CD68 and MHC-II, have been also proposed as general markers for macrophages in the mouse model,[22] thus the role of these markers may vary according to several factors, such as the species, age or stimulus. Other markers, such as CD107a, also known as lysosome-associated membrane protein-1 (LAMP-1), has not been profoundly analyzed in the field of macrophage polarization; however, since it is associated with a Th1 response following LPS stimulation, it may lead to M1 polarization in specific scenarios. By contrast, M2 macrophage polarization is mediated by anti-inflammatory Th2 cytokines, such as IL-4 and IL-13, through the IL-4 receptor alpha (IL-4Rα), or IL-10 (through a different receptor and glucocorticoids)[17,23,36] and can be further divided into at least four different subsets according to the activating stimulus (M2a to M2d). M2 macrophages are characterized in human and/or mice by the up-regulation of several surface molecules such as arginase 1 (Arg1), CD163, CD206, IL-1R, TLR1 and TLR8, and downregulation of CD14, among others.[24,36]

Despite M1/M2 dichotomy, macrophage polarization is not fixed as their plasticity allows them to change during inflammation and disease.[28] In this line, macrophage polarization has been simplified in TB studies in different animal models, identifying M1 macrophages as those which express iNOS, and M2 macrophages as those expressing Arg1,[13,26,30] however, studies comparing the expression of different macrophage polarization markers and their location within the tuberculous granuloma in different animal species are scarce. Therefore, the aim of this study was to compare the expression and distribution of macrophage polarization related markers in granulomas from cattle and pig lymph nodes (LNs) from naturally MTC-infected animals.

2. Materials and methods

2.1. Animals and tissue samples

This study is part of a large project from cattle subjected to the surveillance and monitoring for bovine TB (bTB) in the framework of the Spanish national eradication program.[35] Samples from pigs belong to a study where animals were condemned at the slaughterhouse because of the presence of generalized tuberculosis-like lesions (TBL).[6] Ethical review and approval were not required for the animal study since no purpose killing of animals was performed for this study.

Samples for bacteriological, histopathological, immunohistochemical and PCR studies were collected along the slaughter-line and consisted of retropharyngeal and tracheobronchial LNs from five cattle and mandibular LNs from four free-range pigs according to previous reports, respectively.[25,29] All included animals yielded positive results to bacteriological culture and/or real-time PCR against MTC.[6,35] The granuloma was considered as the experimental unit.

2.2. Histopathology

Samples from the different LNs were fixed in 10 % buffered neutral formalin and embedded in paraffin. Four μm sections were stained with hematoxylin and eosin (H&E) for histopathological examination and with the Ziehl-Neelsen (ZN) technique for the identification of acid-fast bacilli (AFB). H&E-stained sections were used to identify microscopic granulomas which were further classified as stage I (initial), stage II (solid), stage III (minimal necrosis) and stage IV (necrosis and mineralization) as published elsewhere.[5,16,29] A minimum of 10 granulomas per stage was required for the subsequent immunohistochemical study. Table 1 shows the breakdown of granulomas included in the study according to ZN technique for cattle and pigs, respectively. A sample was considered positive for ZN when one or

more AFB were detected in at least one high-power field magnification (HPF, 100x) of the granuloma. The total number of AFB present in each granuloma was recorded on a scale of 0 to 3 (0 = no bacilli; 1 = 1–10 bacilli; 2 = 11–50 bacilli, and 3 ≥ 51 bacilli).[15,20]

2.3. Immunohistochemical study

The Avidin–Biotin–Peroxidase complex technique (ABC Vector Elite, Vector Laboratories, Burlingame, CA, USA) was carried out to identify and characterize macrophages (CD172a and MAC387), M1 macrophages (iNOS, CD68 and CD107a) and M2 macrophages (Arg1 and CD163). Briefly, 4 µm tissue sections were deparaffinized and rehydrated through graded alcohols, followed by blocking of the endogenous peroxidase activity using 3 % hydrogen peroxide in methanol for 30 minutes (min) in darkness. Table 2 summarizes antigen recovery method, blocking solution and primary and secondary antibodies details. Primary antibody was applied either neat or diluted and incubated overnight at 4 °C as described in table 2. Additionally, a negative control was included for each antibody. The corresponding biotinylated secondary antibody was applied for 30 min followed by Avidin-Biotin-Peroxidase Complex (Vector Laboratories) for 1 hour at room temperature and darkness. Labeling was visualized by NovaRED™ substrate kit (Vector Laboratories).

2.4. Digital analysis

Immunolabeled slides were subjected to objective digital image analysis to determine the positive percentage (%) of $CD172a^+$, $MAC387^+$, $iNOS^+$, $CD68^+$, $CD107a^+$, $Arg1^+$ and $CD163^+$ immunolabeled cells. The slides were photographed at 100x magnification by camera and light microscopy (Olympus BX43, L'Hospitalet de Llobregat, Barcelona, Spain). Immunolabeled cells were registered for the different stages (I, II, III and IV) of tuberculous granulomas for each slide. All

granulomas present in each slide were included in the study. The slides were digitalized and the whole area of the granuloma was selected as the region of interest (ROI), with the area of immunolabeled cells inside the ROI being calculated by QuPath software version 0.3.0[1] after setting thresholds for each marker and stage of granuloma. For stage III and stage IV granulomas, necrotic or mineralized center were not included in the analysis, as previously described.[38] The results were expressed as the percentage of the area covered by immunolabeled cells within the whole area of the granuloma.

2.5. Statistical analysis

Differences between granuloma stages and species were evaluated using D'Agostino & Pearson's normality test, followed by Mann Whitney *U* nonparametric test or Student's t-unpaired test for parametric data, as appropriate. Figures and data analyses were performed using GraphPad Prism 9.0 software (GraphPad Prism software 9.0, Inc., San Diego, CA, USA). For all data, *P* value lower than 0.05 was considered statistically significant. In the figures, (*) indicates $P \leq 0.05$, (**) $P \leq 0.01$, (***) $P \leq 0.001$ and (****) $P \leq 0.0001$.

3. Results

3.1. Distribution of bovine and porcine granulomas according to stage and ZN technique

A total of 254 granulomas were evaluated from bovine LNs and 101 granulomas from porcine LNs. According to the granuloma stage classification, the distribution of the 254 bovine granulomas was: 142/254 (55.9 %) of stage I; 42/254 (16.5 %) of stage II; 33/254 (13.0 %) of stage III, and 37/254 (14.6 %) of stage IV. In the case of porcine granulomas, the distribution was as follows: 26/101 (25.7 %) stage I;

18/101 (17.8 %) stage II; 34/101 (33.7 %) stage III, and 23/101 (22.8 %) stage IV (table 1).

ZN technique was performed to determine the presence of AFB in each tuberculous granuloma. Accordingly, no AFB were detected in most bovine granulomas (151/254; 59.4 %). One to ten AFB (grade 1) were observed in 79 out of 254 granulomas (31.1 %). Grade 2 (11-50 AFB) and grade 3 (≥ 51 AFB) were present in 18 (7.1 %) and in 6 (2.4 %) out of 254 granulomas, respectively. The number of AFB showed a trend to increase with the stage of the granuloma in bovine samples (table 1). In porcine LNs, 59 out of 101 granulomas (58.4 %) did not present any AFB whereas 1 to 10 AFB (grade 1) were observed in 42 out of 101 granulomas (41.6 %). No porcine granuloma presented more than 10 AFB (grades 2 and 3). In this species, no differences were observed between the number of AFB and the granuloma stage (table 1).

TABLE 1. Number of tuberculous granulomas according to acid-fast bacilli (AFB) counts in each granuloma stage in lymph nodes (LNs) from cattle and pig.

	AFB Scale	Stage I		Stage II		Stage III		Stage IV		Total	
Cattle		(n=142)	%	(n=42)	%	(n=33)	%	(n=37)	%	(n=254)	%
	0 = 0	101	71.1 %	27	64.3 %	11	33.3 %	12	32.4 %	151	59.4 %
	1 = 1-10	37	26.1 %	14	33.3 %	13	39.4 %	15	40.5 %	79	31.1 %
	2 = 11-50	4	2.8 %	1	2.4 %	7	21.2 %	6	16.2 %	18	7.1 %
	3 ≥ 51	0	0.0 %	0	0.0 %	2	6.1 %	4	10.8 %	6	2.4 %
		(n=26)	%	(n=18)	%	(n=34)	%	(n=23)	%	(n=101)	%
Pig	0 = 0	22	84.6 %	10	55.6 %	19	55.9 %	8	34.8 %	59	58.4 %
	1 = 1-10	4	15.4 %	8	44.4 %	15	44.1%	15	65.2 %	42	41.6 %
	2 = 11-50	0	0.0 %	0	0.0 %	0	0.0 %	0	0.0 %	0	0.0 %
	3 ≥ 51	0	0.0 %	0	0.0 %	0	0.0 %	0	0.0 %	0	0.0 %

AFB: Acid-fast bacilli; %: Percentage

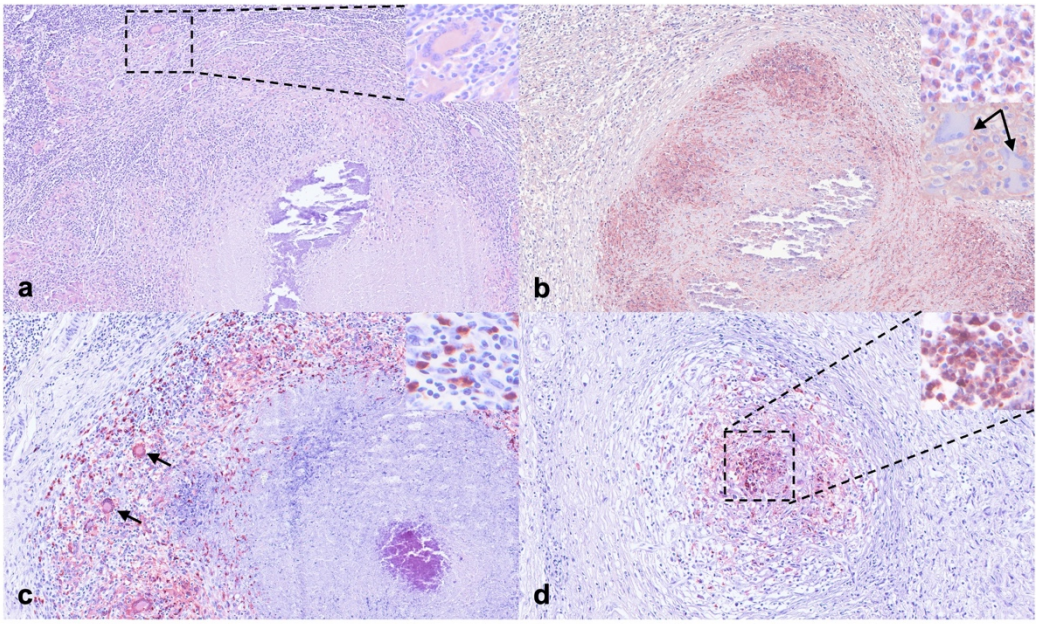

Figure 1. Immunohistochemistry for myeloid cell markers in tuberculous granulomas in cattle and pig lymph nodes*. (a) CD172a⁺ macrophages and epithelioid cells as well as MNGCs within the fibrous capsule of a stage IV granuloma in cattle. Inset: detail of the weak staining within a MNGC. (b) Stage IV granuloma in a pig displaying a marked expression of CD172a in the cells within the surrounding capsule of connective tissue, as well as within the necrotic core. Upper inset: detail of CD172a⁺ cells. Lower inset: detail of two CD172⁻ MNGCs (arrows). (c) MAC387⁺ macrophages, epithelioid cells, MNGCs (arrows) as well as neutrophils within the fibrous capsule of a stage IV granuloma in cattle. Inset: detail of the intense staining within neutrophils. (d) Stage II granuloma in a pig displaying a marked expression of MAC387 in the center of a granuloma highlighting a strong neutrophilic infiltrate. Inset: detail of MAC387⁺ neutrophils.*

3.2 Immunolabeling against CD172a and MAC387 in bovine and porcine granulomas as markers of myeloid cells

CD172a expression showed a diffuse and cytoplasmic pattern with a stronger staining in myeloid cells (including macrophages and epithelioid cells) in both species, while only scattered MNGCs from cattle were weakly stained against this marker (figure 1a, b). The expression was similar within the different granuloma stages in both species, but stage III and stage IV granulomas in pigs showed additional immunolabeling of neutrophils within the necrotic core and within the rim between the necrotic center and the fibrous capsule (figure 1b). Figure 2a shows the frequency of CD172a$^+$ cells, which displayed a similar trend in both species, although a significant increase was observed in stage II granulomas from pigs in comparison to cattle ($P < 0.001$). Moreover, a slight decrease in the frequency of CD172a$^+$ cells was observed in porcine granulomas when progressing from stage II granulomas to later stages ($P < 0.05$).

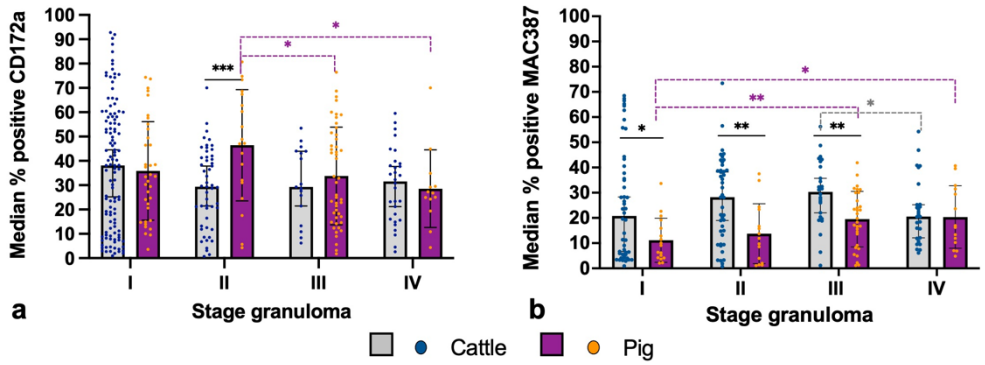

Figure 2. Graphs represent the median percentage of positively stained cells within each granuloma for CD172a (a) and MAC387 (b) in bovine and porcine lymph nodes*. Grey columns and blue points represent bovine tuberculous granulomas and purple columns and orange points represent porcine tuberculous granulomas. Statistical differences are shown as * = P < 0.05, ** = P < 0.01 and, *** = P < 0.001.*

MAC387 expression showed a cytoplasmic staining within macrophages, epithelioid cells, MNGCs and neutrophils in all stages of granulomas from both species (figures 1c, d). In cattle, immunolabeled cells were more numerous in the center of stage I and stage II granulomas in contrast to stages III and IV, where immunolabeled cells, including MNGCs, were distributed surrounding the necrotic center (figure 1c). However, in pigs, the frequency of $MAC387^{+}$ cells was lower, with only few positive cells, mainly neutrophils, in the center of stage I and II granulomas (figure 1d). In stages III and IV, the distribution of immunolabeled cells was like the one observed in cattle. The quantitative analysis of $MAC387^{+}$ cells showed a higher frequency of immunolabeled cells for all stages of granuloma in cattle in comparison to pig, being statistically significant in stages I ($P < 0.05$), II and III ($P < 0.01$). In general, there was a tendency to increase towards the most advanced granuloma stages, particularly in stages II and III in cattle and stages III and IV in pigs (figure 2b).

TABLE 2. Primary and secondary antibodies, suppliers and conditions

Primary antibody (Clone)	Antibody type	Dilution	Supplier	Antigen recovery method	Blocking solution	Secondary antibody**	Cross reactivity
CD172a (BA1C11)	Monoclonal anti-porcine	Neat	In house/ INIA	Citrate pH 3.2 Au	BSA 2%	Anti-Mouse	Cattle[a]; Pig[b]
Myeloid/ Histiocyte Antigen (MAC387)	Monoclonal anti-human	1:100	Dako	Protease*	BSA 2%	Anti-Mouse	Multispecies[c]
iNOS	Polyclonal	1:500	NeoMarker sFremont CA	Citrate pH 6.0 Au	NGS 10%	Anti-Rabbit	Multispecies[c]
CD68 (EBM11)	Monoclonal anti-human	1:100	Dako	Protease*	BSA 2%	Anti-Mouse	Multispecies[c]
CD107a (4E9/11)	Monoclonal anti-porcine	Neat	In house/ INIA	Citrate pH 3.2 Au	BSA 2%	Anti-Mouse	Pig[d]
Arginase 1	Polyclonal	1:100	Invitrogen	Citrate pH 8.5 Mw	BSA 2%	Anti-Goat	Multispecies[c]
CD163 (EDHu-1)	Monoclonal anti-human	1:400	Bio-Rad	Citrate pH 6.0 Au	NGS 10%	Anti-Mouse	Multispecies[c]

iNOS: inducible nitric oxide synthase; IgG: immunoglobulin G; BSA: Bovine serum albumin; NGS: Normal Goat serum; Mw: microwave; Au: autoclave; *Protease from *Bacillus licheniformis* (Sigma-Aldrich, Darmstadt, Germany): 8 min at room temperature; ** Dilution for all secondary antibodies was 1:200; Anti-Mouse: Polyclonal Goat-Anti-Mouse IgG (Dako, Santa Clara, CA, USA); Anti-Goat: Polyclonal Rabbit Anti-Goat IgG (Dako); Anti-Rabbit: Goat Anti-Rabbit IgG (Vector laboratories, Burlingame, CA, USA). [a] Zhang et al., 2012; [b] Domenech et al., 2003; [c] Multispecies cross-reactivity, including bovine and porcine, according to the datasheet.[d] Bullido et al 1997

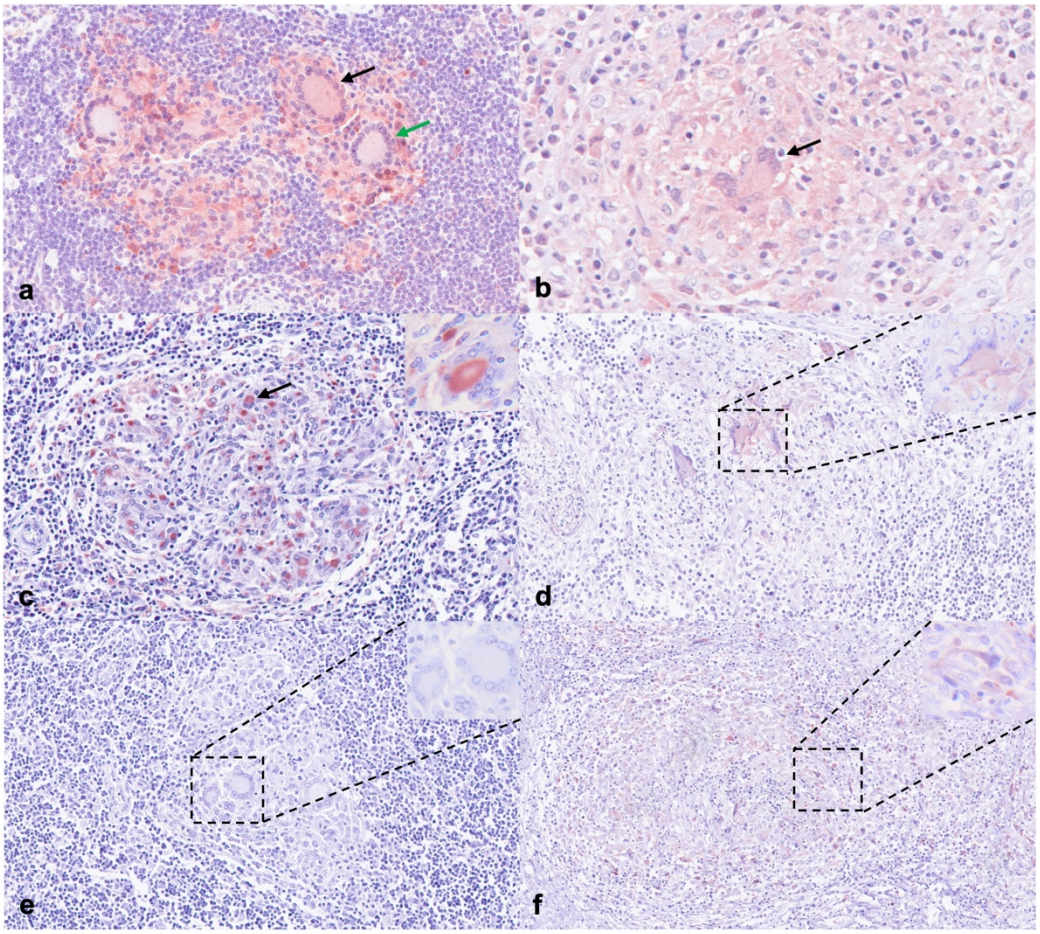

Figure 3. Immunohistochemistry for M1 macrophage markers in tuberculous granulomas in cattle and pig lymph nodes*. (a) Strongly stained iNOS⁺ macrophages, epithelioid cells and MNGCs (black arrow) and weakly stained iNOS⁺. MNGCs (green arrow) of a stage I granuloma in cattle. (b) Stage I granuloma in a pig displaying a weak expression of iNOS in a MNGC (arrow). (c) CD68⁺ macrophages, epithelioid cells and MNGCs (arrow) of a stage II granuloma in cattle. Inset: detail of a MNGC with an intense CD68 cytoplasmic immunolabeling. (d) Weak expression of CD68 in macrophages and epithelioid cells with a more evident staining of MNGCs in a stage II granuloma in a pig. Inset: detail of a CD68⁺ MNGC. (e) Stage I granuloma from cattle showing the lack of cross-reactivity against CD107a. Inset: detail of MNGCs evidencing absence of CD107a staining. (f) CD107a⁺ macrophages epithelioid cells as*

well as MNGCs of a stage II granuloma from a pig. Inset: detail of CD107a⁺ macrophages within the granuloma.

3.3 *Immunolabeling against iNOS, CD68, and CD107a in bovine and porcine tuberculous granulomas as markers of M1 macrophages*

iNOS expression showed a diffuse cytoplasmic staining pattern mainly found in epithelioid cells and MNGCs in all stages of granulomas, with a stronger staining in granulomas from cattle when compared to pigs (figure 3a, b). In stage I and II granulomas, immunolabeled cells were distributed throughout the granuloma, whereas in stage III and stage IV granulomas iNOS⁺ cells consisted of epithelioid cells macrophages and MNGCs forming a rim surrounding the necrotic core and intertwining in the fibrous capsule of the granuloma. Figure 4a shows the quantitative analysis of iNOS staining in granulomas from cattle and pig LNs. Although a similar kinetics was observed in both species, displaying a significant decrease from stage I granulomas towards more advanced stage granulomas (stage IV) ($P < 0.0001$), the median frequency of iNOS⁺ cells was higher in bovine than in porcine (figure 4a).

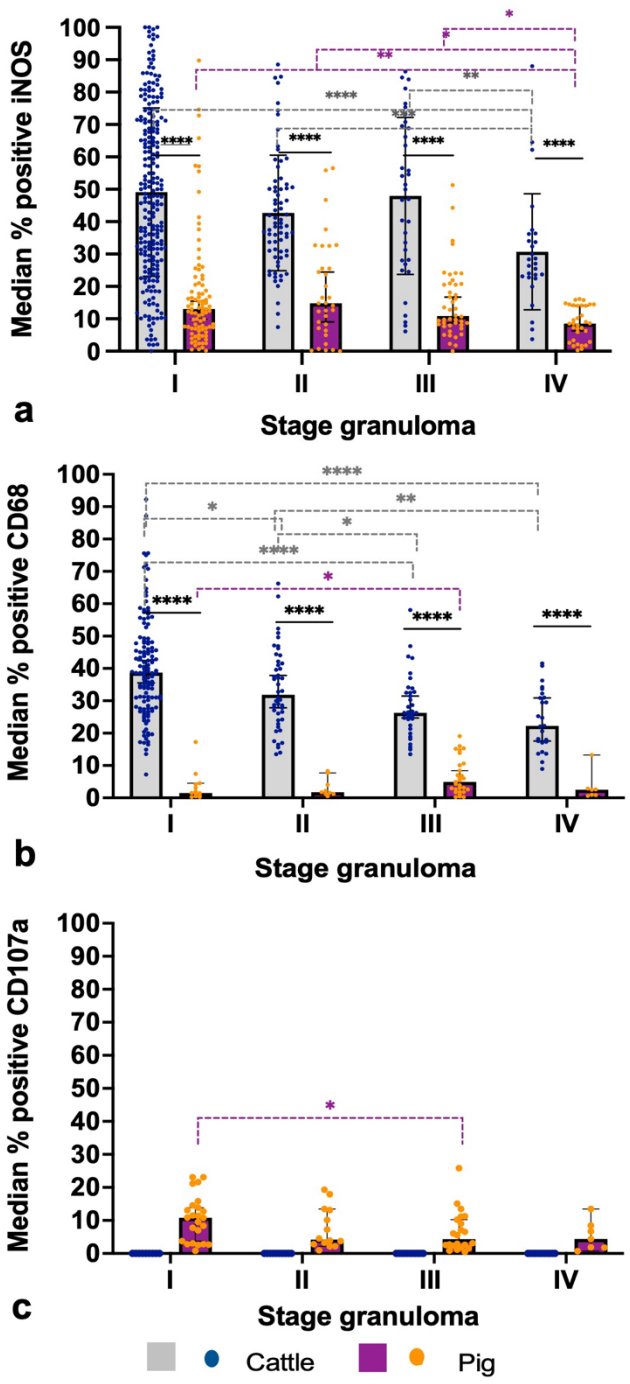

Figure 4. Graphs represent the median percentage of positively stained cells within each granuloma for iNOS (a), CD68 (b) and CD107a (c) in bovine and

porcine lymph nodes. *Grey columns and blue points represent bovine tuberculous granulomas and purple columns and orange points represent porcine tuberculous granulomas. Statistical differences are shown as * = P < 0.05, ** = P < 0.01, *** = P < 0.001 and, **** = P < 0.0001*.

CD68 expression was observed within the cytoplasm of macrophages, MNGCs and epithelioid cells from all granuloma stages (I-IV) in both species (figures 3c, d). However, the staining was weaker in pigs compared to cattle, where MNGCs were strongly labeled. Scattered $CD68^+$ macrophages and epithelioid cells were distributed throughout stage I and II granulomas in cattle also with positive cells, although in less number, within the fibrous capsule of stage III-IV granulomas. In contrast, porcine stage I and II granulomas showed only scattered $CD68^+$ macrophages and MNGCs in the center of the granuloma. $CD68^+$ macrophages and MNGCs were randomly distributed at the border of the necrotic center and within the fibrous capsule in stage III and IV of porcine granulomas, slightly increasing the frequency of positivity as the granuloma stage progressed. The quantitative analysis of $CD68^+$ cells (figure 4b) showed a significantly higher frequency of immunolabeled cells ($P < 0.0001$) in cattle compared to pigs with a progressive decrease from early stages to more advanced stage granulomas, as it was observed for iNOS expression.

CD107a staining was only observed in porcine granulomas; no cross-reactivity was observed in cattle tissue (figures 3e, f). In pigs, granulomas from the different stages (I-IV) showed scattered $CD107a^+$ macrophages and MNGCs, which were mainly found within the granuloma fibrous capsule (figure 3f). The highest frequency of $CD107a^+$ cells was observed in stage I granulomas, displaying a decrease towards more advanced stage granulomas ($P < 0.05$, stage I *vs* stage III granulomas) (figure 4c).

3.2. Immunolabeling against Arg1 and CD163 in bovine and porcine tuberculous granulomas as markers of M2 macrophages

Arg1 staining was expressed in macrophages and MNGCs in both species, with a stronger expression in MNGCs (figures 5a, b). The frequency of $Arg1^+$ cells was significantly higher in pigs than in cattle, notably in stage III granulomas ($P < 0.001$) (figure 6a). In the case of cattle, the frequency of $Arg1^+$ cells was higher in stage I and II granulomas decreasing onwards, whereas a marked increase in the number of $Arg1^+$ cells was observed in porcine stage III and IV granulomas, especially in the former. In late-stage granulomas, positive cells were observed demarcating the necrotic core, particularly in pigs (figure 5b), becoming less numerous towards the periphery.

CD163 expression showed two immunolabeling patterns. A diffuse cytoplasmic staining pattern was seen in epithelioid cells and, inconsistently, in most of the MNGCs, whiles macrophages showed stronger staining in all granuloma stages from cattle (figure 5c) and pigs (figure 5d). In stage I and II granulomas, immunolabeled cells were distributed throughout the granuloma (figure 5c, d). However, in bovine stage III and stage IV granulomas, $CD163^+$ epithelioid cells and macrophages were observed surrounding the necrotic core together with $CD163^+$ MNGCs, whereas in pigs, $CD163^+$ macrophages were mainly observed at the level of the fibrous capsule and in few MNGCs in these stages. The quantitative analysis of $CD163^+$ cells (figure 6b) displayed a similar kinetics in both species with a constant frequency of immunolabeled cells along the different granuloma stages; however, a significantly higher number of cells was observed in cattle compared to pigs in granulomas of stages I, III and IV ($P < 0.01$; $P < 0.001$).

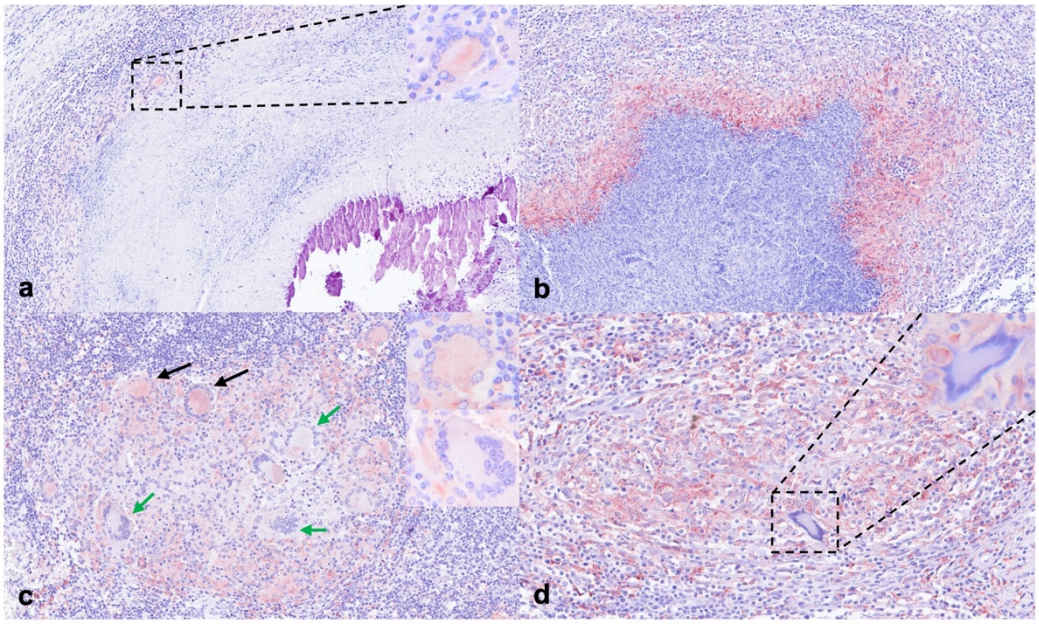

Figure 5. ***Immunohistochemistry for M2 macrophage markers in tuberculous granulomas in cattle and pig lymph node*s**. (a) Weakly stained Arg1^{+} macrophages, epithelioid cells as well as MNGCs within the fibrous capsule of a stage IV granuloma in cattle. Inset: detail of the moderate staining within a MNGC. (b) Stage IV granuloma in a pig displaying a marked expression of Arg1 in the cells within the surrounding rim of the necrotic center of a stage III granuloma. (c) CD163^{+} macrophages, epithelioid cells and MNGCs (black arrows) and CD163^{-} MNGCs (green arrows) in a stage I granuloma in cattle. Upper inset: detail of a CD163^{+} MNGC. Lower inset: detail of a CD163^{-} MNGC. (d) Stage II granuloma in a pig displaying a marked expression of CD163 in the cells within the surrounding capsule of connective tissue and lack of expression in a MNGC. Inset: detail of a CD163^{-} MNGC.

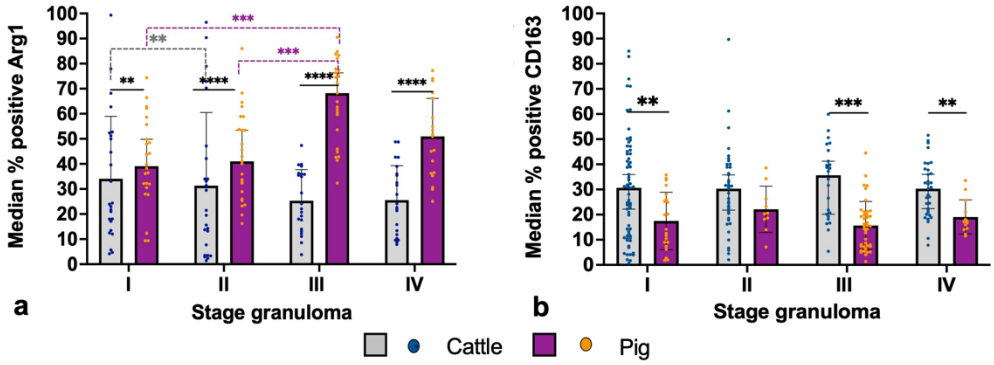

Figure 6. ***Graphs represent the median percentage of positively stained cells within each granuloma for Arg1 (a) and CD163 (b) in bovine and porcine lymph nodes.*** *Grey columns and blue points represent bovine tuberculous granulomas and purple columns and orange points represent porcine tuberculous granulomas. Statistical differences are shown as * = P < 0.05, ** = P < 0.01, *** = P < 0.001 and, **** = P < 0.0001.*

3.3. Evaluation of M1/M2 ratio along granuloma stages in bovine and porcine tuberculous granulomas

To evaluate the polarization to M1 or M2 in bovine and porcine tuberculous granulomas, the ratio between iNOS/Arg1, as representatives of M1 and M2 polarization, respectively, as well as the ratio between the sum of the staining to each one of the M1 (iNOS + CD68 + CD107a) or M2 (Arg1 + CD163) polarization markers used in the present study were calculated. Table 3 summarizes the results of both ratios for each granuloma stage. Our results showed a clear trend to M1 polarization in bovine tuberculous granulomas from stages I to II, which balanced to M2 polarization when progressing to stages III and IV (table 3). Contrary, porcine tuberculous granulomas were governed by a clear M2 polarization along all granuloma stages (table 3).

TABLE 3. Immunohistochemistry ratios according to the analyzed iNOS/Arg1 and M1/M2 macrophage markers in lymph nodes from cattle and pigs.

	iNOS/Arg1		M1/M2 markers	
Granuloma stage	Bovine	Porcine	Bovine	Porcine
I	1.2	0.4	1.4	0.3
II	1.3	0.5	1.3	0.3
III	1.2	0.3	1.0	0.3
IV	0.9	0.2	0.9	0.2

iNOS: inducible nitric oxide synthase; Arg1: Arginase 1; M1: Macrophage type 1; M2: Macrophage type 2.

4. Discussion

The complex interaction between mycobacteria and the host immune system makes it difficult to understand the pathogenesis of TB. Therefore, deepening our understanding of the mechanisms involved in the onset and progression of the tuberculous granuloma throughout the course of infection and its comparison among between different animal species may provide valuable information to advance the knowledge of this disease.

In the present study a high percentage of granulomas was negative to ZN technique, with similar results in both cattle (59.4 %) and pigs (58.4 %), results which are in agreement with those observed in other reports.[6,14,15] Pluribacillary lesions (grade 3) were only observed in cattle towards the more advanced stages of the granuloma (stage III and IV), highlighting an increase in the number of AFB and bacterial load, as it has been previously proposed by others.[30]

Specific markers for myeloid cells (macrophages and epithelioid cells)[9,40] (CD172a, MAC387) were used to characterize the macrophage population along the different granuloma stages, thereafter, selected panels of specific markers for M1 macrophages (iNOS, CD68, CD107a)[4,26,29,34] and M2 macrophages (Arg1, CD163)[10,13,26] were evaluated. Results showed that CD172a was expressed in cattle and pig granulomas similarly, decreasing slightly its expression in advanced stage granulomas (III and IV). Considering its expression in MNGCs, they weakly expressed CD172a in cattle, but no staining was found in the case of pigs. Waters and coauthors (2009)[39] highlighted the expression of this marker as being crucial in the formation of MNGCs in calves. However, from our results, the expression of CD172a does not seem to play a major role in the formation of porcine MNGCs.

MAC387 behaved like CD172a in cattle, while in pigs it evidenced an increasing frequency according to the stage of the granuloma, differing to that reported by García-Jiménez and coauthors (2012; 2013)[15,16] regarding fallow deer and wild boar, in which the percentage of MAC387$^+$ cells decreased towards more advanced stages of granuloma.[15,16] [5] MAC387 was highly expressed in neutrophils of porcine tuberculous granulomas, other marked difference between cattle and pigs in our study, although this cell subset has been also observed in tuberculous granulomas from wild boars and different deer species.[14,15,20] The role of neutrophils in the context of MTC infection is not clearly understood.[3] These cells have been reported to be able to phagocytose and eliminate *Mycobacterium tuberculosis* but they could also supply nutrients to mycobacteria and cause tissue damage through their cellular storage of antimicrobials.[3,11,31] However, when neutrophils fail to kill mycobacteria due to their virulence, the uncontrolled generation of reactive oxidative species within the neutrophils drive them into necrosis.[8] Furthermore, the attraction of other inflammatory cells as well as persistent recruitment of cells to sites of chronic mycobacterial infection by neutrophils will promote the progression to more advanced granuloma stages. [8,11] On the other side, the multi-etiological

nature of lymphadenitis in pigs,[5] where it is common to find TB associated with other bacteria besides mycobacteria, may also give an explanation to the higher participation of neutrophils in pig granulomas. To better understand the function of these cells in the context of tuberculous granulomas, further research needs to be developed.

Markers pointing towards M1 macrophage polarization were highly expressed in cattle, particularly at early-stage granulomas. Specifically for iNOS, our results agree with those previously reported in cattle,[29] deer[15] and wild boar,[14] suggesting an important role for NO in the early stages of the disease as an attempt to eliminate mycobacteria.[19] Since iNOS and Arg1 compete directly for L-arginine, the expression of these molecules is of significance to determine the polarization towards M1 or M2 macrophages, respectively.[13]

CD68 expression followed the same trend as iNOS, but with a stronger expression in MNGCs, as reported elsewhere[29]. However, other authors have reported a lack of changes or even an increase in the number of $CD68^+$ cells when lesions progressed in the same species.[34,38] Interestingly, positive and negative correlations among iNOS and CD68 expression with respect to the count of AFB have been previously reported in bovine paratuberculosis,[12] which may suggest opposite roles for these molecules in cattle for this disease. However, in our study, focused on bTB, both parameters presented similar kinetics, displaying a higher expression in early-stage (paucibacillary) granulomas and decreasing onwards, when a higher number of AFB were observed within late-stage granulomas. Since CD68 play a central role in phagocytosis, and being involved in antigen processing and presentation,[7] our findings point to a lack of activation of macrophages by this pathway in porcine. Furthermore, the similar kinetics observed with respect to iNOS expression in cattle support a decrease of M1 polarization from initial stages to later stages of TB.

The molecule CD107a was weakly expressed in porcine granulomas, showing a slightly higher positivity in stage I granulomas and decreasing in late-stage granulomas, while in cattle no staining was observed, probably due to a lack of cross-reactivity. All in all, the expression of iNOS, CD68 and CD107a support a higher polarization towards M1 macrophages in bovine than porcine granulomas, being more noticeable during the early stages of TB and decreasing with the evolution of the disease, which could give somehow a rationale to understand the persistence of the mycobacteria within the tuberculous granuloma.

M2 polarization was explored by the expression of Arg1 and CD163. Interestingly, Arg1 showed a higher expression in pigs compared to cattle with a higher frequency of $Arg1^+$ cells towards more advanced stages of granuloma. There are scarce number of studies analyzing this marker in TB in livestock, but similar results have been previously observed in mice,[21] macaques[26] and human lungs[32]. The expression of Arg1 has been associated with necrosis in tuberculous granulomas which is supported by the higher expression of this marker in porcine stage III and IV granulomas in our study, stages in which a big necrotic core prevails. In this sense, Arg1 deletion has been associated with a lower mycobacterial count[21] and a higher expression of iNOS[13]. These results are in line with ours, which showed an increase in the number of $Arg1^+$ cells together with a drop in the frequency of $iNOS^+$ cells as well as a trend to pluribacillary granulomas.[10] According to the higher expression of Arg1 in porcine than in bovine granulomas in our study, further studies are warranted to determine the role of these molecules in the immunopathogenesis of TB in both species.

The expression of $CD163^+$ did not display differences along the granuloma stages in both species, however, the expression was higher in cattle than in pigs and slightly higher in more advanced stages of granulomas.[18,22] Mattila and coauthors (2013)[26] observed that granulomas with a necrotic core have a high percentage of $CD163^+$ cells close to the periphery of the granuloma in humans and macaques, as

well as in the surrounding fibrous capsule, similarly to our findings in advanced stages of granulomas in cattle and pigs. This finding suggests a tendency towardsM2 profile in cattle and pigs, particularly at end-stage granulomas. In this line, although a pro-inflammatory status might be beneficial to control the development of the granuloma, once established, the anti-inflammatory response could act to control tissue damage generated by the granuloma itself.

To summarize, this study shows the location and expression of several lineage and M1/M2 macrophage polarization markers in tuberculous granulomas from cattle and pigs naturally infected with MTC. Our results in cattle are somehow in agreement with those previously reported in humans[2] and indicate that M1 macrophage polarization prevails during early granuloma stages (I and II), whereas a M2 phenotype is also observed in later stages. Contrary, and mainly due to the expression of Arg1, M2 macrophage polarization is predominant in pigs. These results are supported and represented in our study by the ratios iNOS/Arg1 and M1/M2 macrophage polarization markers.

Acknowledgements

We express our appreciation to Alberto Alcántara and Marta Ordóñez-Martínez for their technical assistance and the technical support offered by the Animal Health and Production Laboratory of Córdoba (Spain).

Declaration of Conflicting Interests

The author(s) declared no potential conflicts of interest with respect to the research, authorship, and/or publication of this article.

Funding

This work was supported by the research project "New measures and techniques to control Bovine Tuberculosis in Andalusia" (Financial support for Operational Groups of the European Innovation Partnership for Agricultural productivity and Sustainability, EIP-AGRI) (GOP2I-CO-16-0010). Fernanda Larenas-Muñoz is supported by a doctoral grant from ANID (National Research and Development Agency)/Doctoral grant Chile/2019/72200324.

Authors' contributions

JGL and LC conceived, designed, and performed the project. JSC, IRT and FLM helped in the sample collection. FLM, MG-H and JSC performed the laboratory experiments. JD and JGL contributed to the reagents, materials, and analysis tools. FLM wrote the manuscript with contribution from the other authors. IR-T, IMRG, FJP and JGL reviewed the manuscript. All authors contributed to the article and approved the submitted version.

References

1. Bankhead P, Loughrey MB, Fernández JA, et al. QuPath: Open source software for digital pathology image analysis. *Sci Rep*. 2017;7(1):1–7.

2. Barros MHM, Hauck F, Dreyer JH, Kempkes B, Niedobitek G. Macrophage polarisation: An immunohistochemical approach for identifying M1 and M2 macrophages. PLoS One. 2013;8(11):1–11.

3. Borkute RR, Woelke S, Pei G, Dorhoi A. Neutrophils in tuberculosis: Cell biology, cellular networking and multitasking in host defense. Int J Mol Sci. 2021;22(9):4801.

4. Bullido R, Gómez Del Moral M, Alonso F, et al. Monoclonal antibodies specific for porcine monocytes/macrophages: Macrophage heterogeneity in the pig

evidenced by the expression of surface antigens. Tissue Antigens. 1997;49(4):403–413.

5. Cardoso-Toset F, Gómez-Laguna J, Amarilla SP, et al. Multi-etiological nature of tuberculosis-like lesions in condemned pigs at the slaughterhouse. PLoS One. 2015;10(9):1–12.

6. Cardoso-Toset F, Luque I, Amarilla SP, et al. Evaluation of rapid methods for diagnosis of tuberculosis in slaughtered free-range pigs. Vet J. 2015;204(2):232–234.

7. Chistiakov DA, Killingsworth MC, Myasoedova VA, Orekhov AN, Bobryshev Y V. CD68/macrosialin: Not just a histochemical marker. Lab Invest. 2017;97(1):4–13.

8. Corleis B, Korbel D, Wilson R, Bylund J, Chee R, Schaible UE. Escape of Mycobacterium tuberculosis from oxidative killing by neutrophils. Cell Microbiol. 2012;14(7):1109–1121.

9. Domenech N, Rodríguez-Carreño MP, Filgueira P, Alvarez B, Chamorro S, Domínguez J. Identification of porcine macrophages with monoclonal antibodies in formalin-fixed, paraffin-embedded tissues. Vet Immunol Immunopathol. 2003;94(1–2):77–81.

10. Duque-Correa MA, Kühl AA, Rodriguez PC, et al. Macrophage arginase-1 controls bacterial growth and pathology in hypoxic tuberculosis granulomas. Proc Natl Acad Sci U S A. 2014;111(38):E4024–E4032.

11. Eum SY, Kong JH, Hong MS, et al. Neutrophils are the predominant infected phagocytic cells in the airways of patients with active pulmonary TB. Chest. 2010;137(1):122–128.

12. Fernández M, Benavides J, Castaño P, et al. Macrophage Subsets Within Granulomatous Intestinal Lesions in Bovine Paratuberculosis. Vet Pathol. 2017;54(1):82–93.

13. Flynn JL, Chan J, Lin PL. Macrophages and control of granulomatous inflammation in tuberculosis. Mucosal Immunol. 2011;4(3):271–278.

14. García-Jiménez WL, Benítez-Medina JM, Fernández-Llario P, et al. Comparative Pathology of the Natural infections by Mycobacterium bovis and by Mycobacterium caprae in Wild Boar (Sus scrofa). Transbound Emerg Dis. 2013;60(2):102–109.

15. García-Jiménez WL, Fernández-Llario P, Gómez L, et al. Histological and immunohistochemical characterisation of Mycobacterium bovis induced granulomas in naturally infected Fallow deer (Dama dama). Vet Immunol Immunopathol. 2012;149(1–2):66–75.

16. García-Jiménez WL, Salguero FJ, Fernández-Llario P, et al. Immunopathology of granulomas produced by Mycobacterium bovis in naturally infected wild boar. Vet Immunol Immunopathol. 2013;156(1–2):54–63.

17. Gordon S, Martínez FO. Alternative activation of macrophages: Mechanism and functions. Immunity. 2010;32(5):593–604.

18. Gordon S, Plüddemann A, Martinez Estrada F. Macrophage heterogeneity in tissues: Phenotypic diversity and functions. Immunol Rev. 2014;262(1):36–55.

19. Hernández-Pando R, Schön T, Orozco EH, Serafin J, Estrada-Garcióa I. Expression of inducible nitric oxide synthase and nitrotyrosine during the evolution of experimental pulmonary tuberculosis. Exp Toxicol Pathol. 2001;53(4):257–265.

20. Johnson LK, Liebana E, Nunez A, et al. Histological observations of bovine tuberculosis in lung and lymph node tissues from British deer. Vet J. 2008;175(3):409–412.

21. Kasmi KC El, Qualls JE, Pesce JT, et al. Toll-like receptor-induced arginase 1. Nat Immunol. 2009;9(12):1399–1406.

22. Klopfleisch R. Macrophage reaction against biomaterials in the mouse model – Phenotypes, functions and markers. Acta Biomater. 2016;43:3–13.

23. Liu YC, Zou XB, Chai YF, Yao YM. Macrophage polarization in inflammatory diseases. Int J Biol Sci. 2014;10(5):520–529.

24. Ma S, Zhang J, Liu H, Li S, Wang Q. The Role of Tissue-Resident Macrophages in the Development and Treatment of Inflammatory Bowel Disease. Front Cell Dev Biol. 2022;10(May):1–18.

25. Di Marco V, Mazzone P, Capucchio MT, et al. Epidemiological significance of the domestic black pig (Sus scrofa) in maintenance of bovine tuberculosis in sicily. J Clin Microbiol. 2012;50(4):1209–1218.

26. Mattila JT, Ojo OO, Kepka-Lenhart D, et al. Microenvironments in Tuberculous Granulomas Are Delineated by Distinct Populations of Macrophage Subsets and Expression of Nitric Oxide Synthase and Arginase Isoforms. J Immunol. 2013;191(2):773–784.

27. Mohamed A. Bovine tuberculosis at the human–livestock–wildlife interface and its control through one health approach in the Ethiopian Somali Pastoralists: A review. One Health. 2020;9(August 2019):100113.

28. Murray PJ. Macrophage Polarization. Annu Rev Physiol. 2017;79:541–566.

29. Palmer M V., Waters WR, Thacker TC. Lesion development and immunohistochemical changes in granulomas from cattle experimentally infected with Mycobacterium bovis. Vet Pathol. 2007;44(6):863–874.

30. Palmer M V., Kanipe C, Boggiatto PM. The Bovine Tuberculoid Granuloma. Pathogens. 2022;11(1):61.

31. Persson YAZ, Blomgran-Julinder R, Rahman S, Zheng L, Stendahl O. Mycobacterium tuberculosis-induced apoptotic neutrophils trigger a pro-inflammatory response in macrophages through release of heat shock

protein 72, acting in synergy with the bacteria. Microbes Infect. 2008;10(3):233–240.

32. Pessanha AP, Martins RAP, Mattos-Guaraldi AL, Vianna A, Moreira LO. Arginase-1 expression in granulomas of tuberculosis patients. FEMS Immunol Med Microbiol. 2012;66(2):265–268.

33. Rodríguez-Campos S, Smith NH, Boniotti MB, Aranaz A. Overview and phylogeny of Mycobacterium tuberculosis complex organisms: Implications for diagnostics and legislation of bovine tuberculosis. Res Vet Sci. 2014;97(S):S5–S19.

34. Salguero FJ, Gibson S, García-Jiménez W, et al. Differential Cell Composition and Cytokine Expression Within Lymph Node Granulomas from BCG-Vaccinated and Non-vaccinated Cattle Experimentally Infected with Mycobacterium bovis. Transbound Emerg Dis. 2017;64(6):1734–1749.

35. Sánchez-Carvajal JM, Galán-Relaño Á, Ruedas-Torres I, et al. Real-Time PCR Validation for Mycobacterium tuberculosis Complex Detection Targeting IS6110 Directly From Bovine Lymph Nodes. Front Vet Sci. 2021;8.

36. Shapouri-Moghaddam A, Mohammadian S, Vazini H, et al. Macrophage plasticity, polarization, and function in health and disease. J Cell Physiol. 2018;233(9):6425–6440.

37. Tulu B, Martineau HM, Zewude A, et al. Cellular and cytokine responses in the granulomas of asymptomatic cattle naturally infected with mycobacterium bovis in Ethiopia. Infect Immun. 2020;88(12):1–12.

38. Wangoo A, Johnson L, Gough J, et al. Advanced granulomatous lesions in Mycobacterium bovis-infected cattle are associated with increased expression of type I procollagen, γδ (WC1+) T cells and CD 68+ cells. J Comp Pathol. 2005;133(4):223–234.

39. Waters WR, Palmer M V., Nonnecke BJ, et al. Signal regulatory protein α (SIRPα)+ cells in the adaptive response to ESAT-6/CFP-10 protein of tuberculous mycobacteria. PLoS One. 2009;4(7):1–10.

40. Zhang W, Nasu T, Hosaka YZ, Yasuda M. Comparative studies on the distribution and population of immunocompetent cells in bovine hemal node, lymph node and spleen. J Vet Med Sci. 2012;74(4):405–411

Capítulo III

Estudio 3 / Study 3

Objetivo 3 / Objective 3

Estudio 3: Proteomic analysis of granulomas from cattle and pigs naturally infected with *Mycobacterium tuberculosis* complex by MALDI-imaging

Fernanda Larenas-Muñoz[1,*], José María Sánchez-Carvajal[1], Inés Ruedas-Torres[1,2], Carmen Álvarez-Delgado[1], Karola Fristiková[1], Franciso J. Pallarés[1], Librado Carrasco[1], Eduardo Chicano-Gálvez[3], Irene M. Rodríguez-Gómez[1,†], Jaime Gómez-Laguna[1,†]

Enviado para revisión a Molecular and Cellular proteomic 2023..

Objetivo 3: Estudiar los diferentes estadios de evolución de los granulomas tuberculosos mediante la técnica de espectrometría de masas con imagen por láser de desorción/ionización asistida por matriz (MALDI-Imaging) y detección de nuevos analitos involucrados en la patogenia de esta enfermedad.

Objective 3: To study the different stages of evolution of tuberculous granulomas by matrix-assisted laser desorption ionisation/desorption imaging (MALDI-Imaging) mass spectrometry and detection of new analytes involved in the pathogenesis of this disease.

Proteomic analysis of granulomas from cattle and pigs naturally infected with *Mycobacterium tuberculosis* complex by MALDI-imaging

Fernanda Larenas-Muñoz[1,*], José María Sánchez-Carvajal[1], Inés Ruedas-Torres[1,2], Carmen Álvarez-Delgado[1], Karola Fristiková[1], Franciso J. Pallarés[1], Librado Carrasco[1], Eduardo Chicano-Gálvez[3], Irene M. Rodríguez-Gómez[1,†], Jaime Gómez-Laguna[1,†]

[1] Department of Anatomy and Comparative Pathology and Toxicology, Pathology and Immunology Group (UCO-PIG), UIC Zoonosis y Enfermedades Emergentes ENZOEM, University of Córdoba, International Excellence Agrifood Campus 'CeiA3', 14014 Córdoba, Spain

[2] UK Health Security Agency (UKHSA), Porton Down, Salisbury SP4 0JG, United Kingdom

[3] IMIBIC Mass Spectrometry and Molecular Imaging Unit (IMSMI), Maimónides Biomedical Research Institute of Córdoba, Reina Sofia University Hospital, University of Córdoba, 14071 Córdoba, Spain

Revisiting tuberculous granuloma by MALDI-Imaging

[†]Irene Magdalena Rodríguez-Gómez and Jaime Gómez-Laguna shared senior authorship

[*]Corresponding author

E-mail address: ep2lamuf@uco.es (Larenas-Muñoz F.)

Graphical abstract

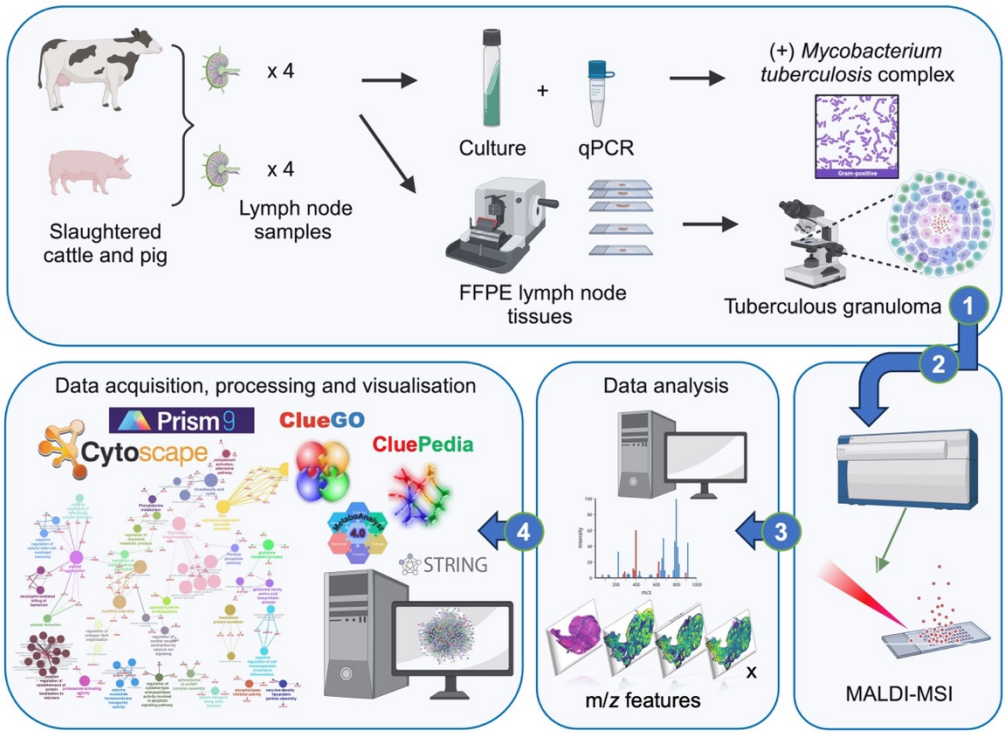

Highlights

- MALDI-MSI reveals the proteome of tuberculous granuloma in cattle and pigs
- Common and species-specific pathways are activated in animal TB.
- Tricarboxylic acid cycle and glycolysis are metabolic routes conserved in both species.
- Activation of complement, apoptosis, IL-4 and IL-17 pathways are identified in cattle and pigs during TB.
- Degranulation of natural killer cells is activated and inhibited in cattle and pigs, respectively.

Abbreviations

ACTN4 : Alpha-actinin-4
AFB : Acid-fast bacilli
ANOVA : Analysis of Variance
AZU1 : Azurocidin 1
BAX : Apoptosis regulator BAX
BPs : Biological Processes
BSA : Bovine serum albumin
C3 : Complement 3
CA : Carbonic hydrogenase
CEACAM1 : Carcinoembryonic antigen-related cell adhesion molecule 1
CORO1A : Coronin-1A
CPS-1 : Carbamoyl phosphate synthase-1
CTSG : Cathepsin G
DENAJC13 : DnaJ heat shock protein family (Hsp40) member C13
DEPs : Differentially expressed proteins
FASN : Fatty acid synthase
FC : Fold-change
FDR : False discovery rate
FWHM : Full-width at half maximum
GO : Gene Ontology
GSN : Isoform 2 of Gelsolin
HCCA : α-cyano-4-hydroxycinnamic acid
HLA-DR : Human leukocyte antigen DR
HRP : Horseradish peroxidase
HTRA2 : Serine protease HTRA2, mitochondrial
IFI30 : Gamma-interferon-inducible lysosomal thiol reductase
IFN-γ : Interferon gamma
IHC : Immunohistochemistry
ISPs : Immune System Processes
KEGG : Kyoto Encyclopedia of Genes and Genomes
LNs : Lymph nodes
m/z : Mass-to-charge
MALDI : Matrix-assisted laser desorption/ionization
MAP2K1 : Dual specificity mitogen-activated protein kinase kinase 1

MMP9 : Matrix metalloproteinase-9
MMPs : Matrix metalloproteinases
MPO : Myeloperoxidase
MSI : Mass spectrometry imaging
MTC : *Mycobacterium tuberculosis* complex
MYO1D : Unconventional myosin-Id
MYO5C : Unconventional myosin-Vc
NH_4HCO_3 : Ammonium bicarbonate
NK : Natural killer
PBS : Phosphate buffered saline
PPI : Protein-protein interaction
RAB21 : Ras-related protein Rab-21
RAB27A : Ras-related protein Rab-27A
ROI : Regions of interest
sPLS-DA : Sparse Partial Least Squares Discriminant Analysis
TB : Tuberculosis
TIC : Total ion current
TBL : Tuberculosis-like lesions
TBST : Tris Buffered Saline Buffer with Tween 20
TCA : Tricarboxylic acid cycle
VAMP : Vesicle associated membrane protein
WOAH : World Organization for Animal Health
ZN : Ziehl-Neelsen

Abstract

Matrix-assisted laser desorption/ionization mass spectrometry imaging (MALDI-MSI) has recently gained prominence for its ability to provide molecular and spatial information in tissue sections. This technology has the potential to uncover novel insights into proteins and other molecules in biological and immunological pathways activated along diseases with a complex host-pathogen interaction, such as animal tuberculosis. Thus, the present study conducted a data analysis of protein signature in granulomas of cattle and pigs naturally infected with *Mycobacterium tuberculosis* complex (MTC), identifying biological and immunological signalling pathways activated throughout the disease. Lymph nodes from four pigs and cattle, positive for MTC by bacteriological culture and/or real-time PCR, were processed for histopathological examination and MALDI-MSI. Protein identities were assigned using the MaTisse database, and protein-protein interaction networks were visualised using the STRING database. Gene Ontology (GO) analysis was carried out to determine biological and immunological signalling pathways in which these proteins could participate together with KEGG analysis. Distinct proteomic profiles between cattle and pig granulomas were displayed. Noteworthy, the GO analysis revealed also common pathways among both species, such as "Complement activation, alternative pathway" and "Tricarboxylic acid cycle", which highlights pathways that are conserved among different species infected by MTC. In addition, species-specific terms were identified in the current study, such as "Natural killer cell degranulation" in cattle or those related to platelet and neutrophils recruitment and activation in pigs. Overall, this study provides insights into the immunopathogenesis of tuberculosis in cattle and pigs, opening new areas of research and highlighting the importance, among others, of the complement activation pathway and the regulation of natural killer cell and neutrophil-mediated immunity in this disease.

1. Introduction

Animal tuberculosis (TB) is a chronic disease caused by bacteria belonging to *Mycobacterium tuberculosis* complex (MTC), which has a major global impact due to its importance in public health and the large associated economic losses [1–4]. Currently, the World Organization for Animal Health (WOAH) considers all mammalian species susceptible to TB, with the ability of any member of the MTC to induce a highly similar disease [5]. The tuberculous granuloma serves as a pathological hallmark during the development of the disease [6, 7]. According to the multi-host dimension of TB [5, 8, 9] different animal models have been used to unravel the host immune response [10–15]. However, the interaction between host and mycobacterium is complex, with numerous gaps in our understanding of the pathogenesis of this disease. Therefore, the use of new methodological approaches is encouraged to improve the understanding of the mechanisms involved in the development of TB.

Matrix-assisted laser desorption/ionization mass spectrometry imaging (MALDI-MSI) has emerged as a novel methodology for this purpose, being capable of simultaneously detecting biomolecules by their molecular weight, such as proteins, lipids, metabolites, and other biological macromolecules, together with their spatial tissue distribution [16–18]. In this sense, MALDI-MSI has been mostly applied to clinical research, tumour classification, biomarkers identification, molecular histology and metabolism, among other areas of interest [19, 20]. In the context of TB, this tool has been already employed in the search of *Mycobacterium tuberculosis* virulence factors [21] as well as in biomarker and drug resistance studies in humans [15].

The multi-host character of animal TB [5, 8, 9] highlights the likely activation of common pathways in the different animal species infected by mycobacteria belonging to MTC [14, 21–23]; nonetheless, structural peculiarities have also been reported in concrete species [7, 10, 11, 13, 14, 24], therefore species-specific pathways are equally expected to be activated along this disease.

The flexibility of MALDI-MSI has allowed the detection of analytes in different tissues and structures [17, 18], such as the identification of the cytokine environment in

granulomas from humans and rabbits [14]. Thus, the confirmation of specific molecules involved in the activation of specific pathways will enlighten the pathogenesis of the disease, as well as the recognition of biomarkers of interest for its diagnosis and control. Therefore, the present study aims to compare the protein signature in granulomas from lymph nodes of cattle and pigs naturally infected by MTC, identifying the potential participation of these proteins in biological and immunological pathways activated along the disease, together with those differentially expressed in both species.

2. Experimental procedures

Ethical review and approval were not required for this animal study since no purposed killing of animals was addressed.

2.1 Animals and tissue samples

For this study, samples from bovine and porcine lymph nodes (LNs) from the Spanish national programme for surveillance and monitoring of bovine TB and from free-range pig carcasses completely condemned at the slaughterhouse due to the presence of generalised tuberculosis-like lesions (TBL) were used [24, 25]. Samples, which corresponded to tracheobronchial and mandibular LNs from four cattle and pigs, respectively, were fixed in 10 % neutral buffered formalin for histopathological and histomolecular studies (MALDI-MSI). All included animals resulted positive for MTC by bacteriological culture and/or real-time PCR [24, 25]. The tuberculous granuloma was considered the experimental unit.

2.2 Histopathology

Four-µm sections were stained with H&E for histopathological examination. Additionally, another set of sections was stained with Ziehl-Neelsen (ZN) technique for the identification of acid-fast bacilli (AFB). H&E-stained sections were used to identify microscopic TBL, identifying a total of 220 and 78 granulomas in the LNs from cattle and pig naturally infected with MTC, respectively. The cellular composition of granulomas was similar in both species, but a higher presence of neutrophils in the centre of the granuloma and infiltrating the connective tissue of the surrounding capsule was

observed in porcine granulomas. ZN technique was considered positive by detecting at least one AFB in at least one high-power field magnification (HPF, 100x). Positive samples were classified as paucibacillary (1 - 10 AFB) or pluribacillary (≥ 11 AFB) [26]. All samples from both species showed AFB positivity, displaying a paucibacillary pattern in both bovine and porcine granulomas, apart from one cattle in which a pluribacillary pattern was also observed.

2.3 MALDI-MSI technique

2.3.1 Sample preparation for MALDI-MSI

Three-µm sections of each sample were mounted onto an indium tin oxide slide (576352, Sigma-Aldrich, Germany) previously coated with poly-L-lysine (P1274-25mg, Sigma-Aldrich). Following this, a standard deparaffination/rehydration protocol was carried out as follows: two washes of 10 minutes (min) in xylene, one wash of 5 min in absolute ethanol, 96 % and 70 %, followed by 2 additional washes of 5 min each in 10 mM ammonium bicarbonate (NH_4HCO_3). Subsequently, antigen retrieval was performed by heating the rehydrated tissues with 100 mM Tris pH 9 at 98 ºC for 30 min. Samples were allowed to cool at room temperature until reaching a minimum temperature of 50 ºC, and then subjected to three additional 3 min washing steps with 10 mM NH_4HCO_3 prior to on-tissue digestion.

2.3.2 On-tissue digestion and matrix deposition

On-tissue digestion was carried out by spraying four layers of trypsin (V5111, Promega, Madison, WI, USA) at a concentration of 0.1 µg/µL in 25 mM NH_4HCO_3 and 10 % trifluoroethanol (Sigma-Aldrich), maintaining a constant flow of 10 µL/min using a SunCollect sprayer (Sunchrom, Friedrichsdorf, Germany). Afterwards, samples were incubated overnight at 37 ºC within a saturated humid chamber. Following the completion of the on-tissue digestion, the slides were vacuum-dried for 30 min before matrix deposition. A matrix solution containing 7 mg/mL with 60 % acetonitrile (Fisher Chemical, USA) and 0.2 % trifluoroacetic acid α-cyano-4-hydroxycinnamic acid (HCCA, Sigma-Aldrich) was employed to cover the tissues. Additional internal calibrants

namely, bradikynin F1-7, angiotensin II and glu-fibrinopeptide (Sigma-Aldrich) were added to the matrix solution.

The final matrix solution was applied using the Suncollect sprayer in eight layers as follows: the first layer at 10 µL/min, the second layer at 20 µL/min, the third to eighth layers at 30 µL/min, all at a z axis equal to 27.05. Upon completion, the slides underwent vacuum drying for an additional 30 min.

2.3.3 Sample processing for MALDI-MSI

Imaging measures were carried out in positive ionization mode using an UltrafleXtreme mass spectrometer (Bruker Daltonics, Germany).

The m/z range for all samples was set from 700 to 2500 m/z. Laser intensity global attenuator was fixed to 20 % and the number of shots per pixel to 600. Digitizer was fixed to 2.50GS/s, real-time smoothing was set to medium and base line offset adjustment was fixed to 3.2 % or 4.2 mV. Voltage parameters were adjusted for each sample to ensure a resolution (FWHW) >15000 at glu-fibrinopeptide reference mass peak. For mass spectrometer calibration purposes, 4 reference peaks previously mixed with the HCCA matrix were used. Those peaks were 757.3998 $[M+H]^+$ (bradikynin F-1,7), 842.508 $[M+H]^+$ (trypsin autolysis peak), 1046.5420 $[M+H]^+$ (angiotensin II) and 1570.6770 $[M+H]^+$ (glu-fibrinopeptide). Calibration was done fixing a maximum peak tolerance error of 50 ppm and quadratic mode was used for peak adjustment.

All datasets were acquired using the FlexImaging software (version Bruker, Germany) with a lateral resolution of 100 µm for all samples, enough to allow a correct analysis distinguishing different histological features. Tissue samples were analysed in a random order to prevent any possible bias due to factors such as variation in mass spectrometer sensitivity or matrix influence.

2.3.4 Data analysis

For MALDI-MSI generation, SCILS® analysis software (Bruker, Germany) was first used to export the entire acquired tissue areas to imzml file format to share them in

ProteomeXchange public repository [27]. Later, the same dataset was used to perform a “virtual microdissection” of regions of interest (ROI) containing granulomas by doing bisecting k-means segmentation of the entire scanned tissue area. After this microdissection, each ROI was saved as imzml file format. Thereafter, the Cardinal R package (v3.0.1) was used [28] to analyse the granulomas dataset. Data files were normalised by total ion current (TIC) and all spectra underwent baseline subtraction to remove noise, resampling via peak-picking to lower data dimensionality and smoothing to remove tissue and measurement artefacts. Then, a mean spectrum for each granuloma was extracted for statistical analysis. The Cardinal package was used to generate molecular images based on the viridis linear colour scale, identifying the more intense positive signal intensity of the peptide in question in an intense yellow colour.

After data generation, m/z features obtained from granulomas in cattle and pigs, meaning common m/z found in granulomas from both species and m/z from each individual species, were evaluated. For this purpose, the online Venn Diagram platform of the University of Ghent, Belgium, was used (https://bioinformatics.psb.ugent.be/webtools/Venn/). Afterwards, the reference MaTisse database [29] was used to assign identity of putative proteins to the molecular weight of each m/z with a margin of +/- 0.025 m/z or 30 ppm. The gene coding for each selected protein was then identified on the UniProt platform (https://www.uniprot.org/).

Statistical analysis was performed with MetaboAnalyst 4.0 software (https://www.metaboanalyst.ca/) using a one-way Analysis of Variance (ANOVA) test. Data sets were structured according to developer’s instructions. Datasets were previously normalised including sample median normalisation, logarithmic transformation, and auto-scaling. Sparse Partial Least Squares Discriminant Analysis (sPLS-DA) was used to represent the separation between the groups. Besides, a hierarchical clustering and heatmap that allowed visualisation of the MALDI-MSI analysis were also performed. All software used in our analysis have an open access from their corresponding author repositories.

2.4 Construction of protein-protein interaction (PPI) network

The interaction between identified proteins from cattle and pigs' granuloma was visualised by PPI networks using the STRING database (Search Tool for the Retrieval of Interacting Genes) [30] through Cytoscape software [31]. STRING protein is an online tool, which integrates information from multiple protein-protein association databases and provides interaction predictions [30]. Only consistent interactions were considered for a cut-off point ≤ 0.4.

2.5 GO analysis

For the visualisation of protein molecular interaction networks, the Cytoscape software (version 3.91) was used [31]. Functional analysis of proteins involved in granulomas from cattle and pigs was performed with the plugins ClueGO (version 2.5.9) and CluePedia (version 1.5.9) [32, 33] for detailed information of pathways. Plugins for ClueGO describing Biological Processes (BPs), Immune System Processes (ISPs), and Kyoto Encyclopaedia of Genes and Genomes (KEGG) pathways integrated with GO were used together as an enrichment step. Significantly represented pathways were visualised into ClueGO functionally grouped networks. Regarding this, following instructions [34], the *Homo sapiens* organism was selected for having the most extensive mapped genes and different levels of specificity were used. Specific pathways with GO levels tree interval 7 – 15 and GO term/pathways selection with a minimum of 3 proteins/term and at least 15 % of coverage from the total associated proteins were selected. To carry out GO analysis from common proteins between both species, GO levels tree interval 3 – 8 and GO term/pathways selection with a minimum of 3 proteins/term and at least 3 % of coverage from the total associated proteins were selected. Differentially expressed proteins (DEPs) were obtained from the dataset, showing the DEPs whose pathways were statistically significant ($P < 0.05$). For analysis, a log2 fold-change (FC) was performed with the data obtained to evaluate differentially expressed m/z after MALDI-MSI, considering a false discovery rate (FDR) < 0.001 and a log2 FC ≥ 2, to determine those m/z that were expressed in a differential way between both species with statistical significance. The differentially expressed m/z were visualised in a

volcano plot which was performed using GraphPad Prism 9.0 software (GraphPad Prism software 9.0, Inc., San Diego, CA, USA).

For GO a Kappa score ≤ 0.4 was used to define term-term interactions (edges) and functional groups based on shared proteins between the terms on the network. The $P < 0.05$ was calculated using a right-sided hypergeometric test with Bonferroni step down correction for multiple testing.

2.6 Validation of MALDI-MSI results by immunohistochemistry

Immunohistochemistry (IHC) against the proteins complement 3 (C3) in bovine, human leukocyte antigen – DR (HLA-DR) in pig and matrix metalloproteinase 9 (MMP9) in both species was used to validate MALDI-MSI results. Four µm tissue sections were deparaffinised with xylene and rehydrated with graded alcohols followed by blocking endogenous peroxidase activity with 3 % hydrogen peroxide in methanol for 30 min. For antigen retrieval, the samples were heated in citrate buffer (10 mM, 0.05 % Tween 20, pH 6.0) for C3, HLA-DR (10 mM, pH 3.2) and MMP9 (10 mM, pH 6.0). After this, sections were incubated with 2 % BSA blocking solution for 30 min. Primary antibodies [anti-C3c rabbit polyclonal antibody (Abcam, Cambridge, United Kingdom) with a 1:100 dilution in 2 % BSA, anti-human HLA-DR mouse monoclonal antibody, clone TAL. 1B5 (Dako, Copenhagen, Denmark) with a 1:25 dilution in 2 % BSA, and anti-MMP9 rabbit polyclonal antibody (Thermo Fischer Scientific, Hsinchu, Taiwan) with a 1:100 dilution in 2 % BSA] were applied and incubated overnight at 4 ºC. For C3 immunolabelling, HRP kit (Technology Inc., MA, USA) was applied and incubated 30 min after washes with 1X tris-buffered saline with 0.1 % Tween 20 (TBST). Visualisation was performed with DAB (Dako). For HLA-DR and MMP9 immunolabelling, biotinylated goat anti-mouse (Dako) and goat anti-rabbit IgG (Vector laboratories, Burlingame, CA, USA) secondary antibodies were diluted 1:200 in 2 % BSA respectively and applied for 30 minutes after washing in PBS. Then, avidin–biotin-peroxidase complex (ABC Vector Elite, Vector Laboratories) was applied and incubated for 1 hour at room temperature. Immunolabelling was visualised by application of NovaRED™ substrate

kit (Vector Laboratories). The slides were counterstained with Harris' haematoxylin, dehydrated, and mounted with EUKITT® mounting medium (Sigma-Aldrich).

2.7 Experimental Design and Statistical Rationale

The samples were taken from a retrospective study, considering a total of 4 routinely slaughtered cattle and pigs. After veterinary inspection, LNs were collected and processed for histopathology and microbiological culture for MTC detection. The final samples were used as described in the experimental setup and consisted of a retrospective targeted sampling, with samples being positive for MTC according to the gold standard technique for TB diagnosis (microbiological culture) and with tuberculous granuloma at histopathology. The tuberculous granuloma was considered as the experimental unit, then we used WinEpi 2.0 (Faculty of Veterinary, University of Zaragoza, Spain; http://www.winepi.net/uk/index.htm) with a confidence level of 95 % and a 12.00 % margin of error in order to determine the sample size obtaining a minimum sample size 67 granulomas for each species. In the case of MALDI-MSI analysis all the slides were performed in triplicate.

For MALDI MSI and GO terms statistical data are shown in the different sections of this study. The differences were considered statistically significant when $P \leq 0.05$.

3. Results

3.1 Identification of the matrix proteome from granulomas in cattle and pigs

After MALDI-MSI analysis, a total of 4,168 m/z features were obtained from cattle and pig granulomas, showing two clearly separated groups according to the clustering and distribution of the features within each species when evaluated by principal component analysis (sPLS-DA) (Figure 1A). These m/z were distributed as follows: 1,438 m/z in cattle granulomas, 1,898 m/z in porcine granulomas, and 416 m/z shared between both species (Figure 1B). After comparison of the molecular weight from each m/z with the reference MaTisse database, a total of 433 potential proteins out of the 1,438 specific m/z were identified in cattle, 732 potential proteins out of the 1,898

specific m/z in porcine and 115 potential proteins out of the 416 m/z were identified as shared between both species.

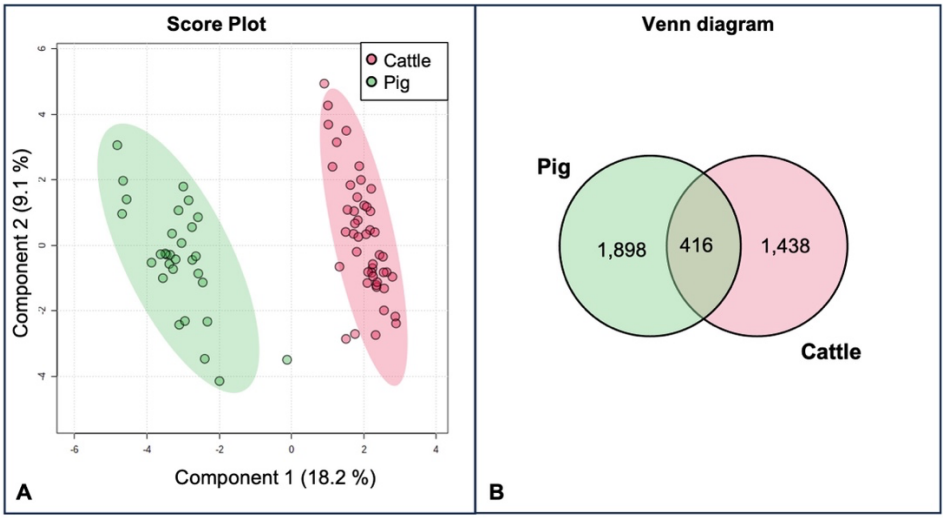

Figure 1. (A) Principal component (sPLS-DA) 2D-plot. Scattered red and green dots corresponded to bovine and porcine granulomas, respectively, distributed according to their protein signature*. A clear separation between bovine and pig granulomas is evident. The explained variances for each component are shown in brackets.* ***(B)*** *Venn diagram, showing the distribution of m/z features present in cattle and pig, obtained from MALDI-MSI analysis and identifying species-specific m/z as well as those common m/z features among both species.*

3.2 Construction of PPI network and functional annotation analysis in cattle

Figure 2A shows the PPI network in cattle, where an interaction of 323 nodes and 1,971 edges were obtained by the STRING database. Following, a functional-enrichment analysis based on the GO database was performed to explore BPs and ISPs together with KEGG analysis. Twenty-two significantly enriched GO terms with a $P < 0.05$ were identified (Figure 2B). These terms were clustered into 15 different groups according to their expression level and were represented according to the percentage of proteins per group (Figure 2C). The results of the GO analysis showed that most of the m/z in cattle were mainly involved in the citrate cycle (TCA cycle) (KEGG:00020),

tricarboxylic acid cycle (GO:0006099), regulation of complement activation (GO:0030449), natural killer cell degranulation (GO:0043320), nitrogen metabolism (KEGG:00910), regulation of cysteine-type endopeptidase activity involved in apoptotic signalling pathway (GO:2001267), vesicle transport along actin filament (GO:0030050), complement activation, alternative pathway (GO:0006957) and regulation of early endosome to late endosome transport (GO:2000641), among others. Table 1 shows these terms associated with their corresponding putative proteins identified in cattle. All terms identified in bovine granulomas together with the proteins included within each term can be consulted in Supplementary table 1.

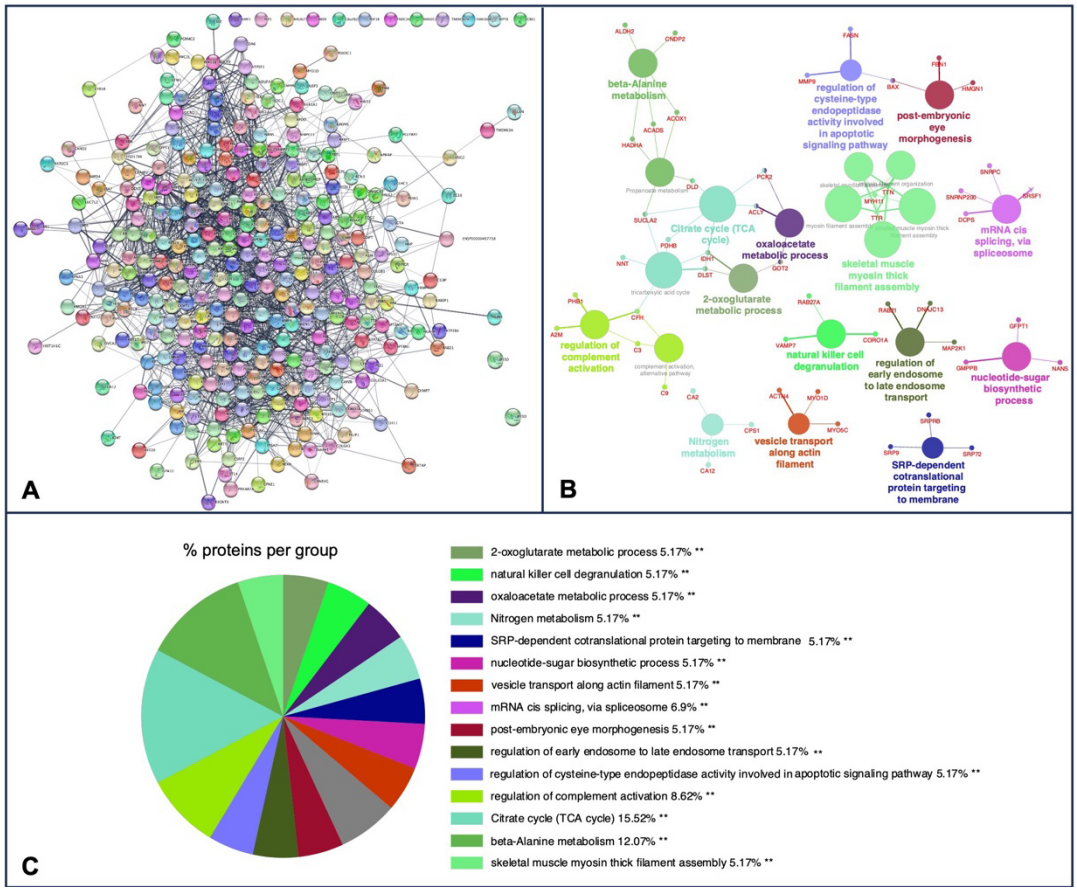

Figure 2. (A) PPI network of 323 overlapped nodes and 1,971 edges from bovine specific m/z features obtained by the STRING database and visualised by Cytoscape. (B) Functional network from cattle specific m/z features was visualised in Cytoscape with ClueGo and CluePedia*, incorporating Biological Processes (BP), Immune System Processes (ISPs) and Kyoto Encyclopedia of Genes and Genomes (KEGG) for enrichment of the pathways. Terms are displayed as nodes (coloured circles), with node size being directly proportional to P ≤ 0.05. Terms are linked by edges (lines) based on their kappa score. Only statistically significant terms have been considered. (**C**) Sector diagram representing the proportion of proteins associated with the top functional groups expressed in a pie chart according to GO terms specific to each group. A value of P ≤ 0.05 shows significantly enriched GO terms. ** P ≤ 0.01.*

Table 1. Summary list with the terms from Gene Ontology (GO) Biological Processes (BPs), Immune System Processes (ISPs) and Kyoto Encyclopedia of Genes and Genomes (KEGG) and their specific m/z identified in cattle.

GO Term	No. proteins	% Associated proteins	Associated proteins found
Citrate cycle (TCA cycle)	7	23.33	[ACLY, DLD, DLST, IDH1, PCK2, PDHB, SUCLA2]
Tricarboxylic acid cycle	6	17.65	[CFH, DLST, IDH1, NNT, PDHB, SUCLA2]
Regulation of complement activation	4	18.18	[A2M, C3, CFH, PHB1]
Natural killer cell degranulation	3	23.08	[CORO1A, RAB27A, VAMP7]
Nitrogen metabolism	3	17.65	[CA12, CA2, CPS1]
Regulation of cysteine-type endopeptidase activity involved in apoptotic signalling pathway	3	16.67	[BAX, FASN, MMP9]
Vesicle transport along actin filament	3	15.79	[ACTN4, MYO1D, MYO5C]
Complement activation, alternative pathway	3	15.00	[C3, C9, CFH]
Regulation of early endosome to late endosome transport	3	15.00	[DNAJC13, MAP2K1, RAB21]

No.: number.

* For the complete list see Supplementary table 1

3.3 Construction of PPI network and functional annotation analysis in pigs

In pig granulomas, a higher number of m/z were observed in the PPI network, which showed the interaction of 447 nodes and 3,994 edges (Figure 3A). Afterwards, according to the GO functional-enrichment (BPs and ISPs categories) and KEGG analyses, most of the m/z were significantly enriched within 61 different terms (Figure 3B), which merged into 29 different groups (Figure 3C). The main terms, in which these proteins were involved, were glycolysis/gluconeogenesis (KEGG:00010), platelet aggregation (GO:0070527), tricarboxylic acid cycle (GO:0006099), neutrophil-mediated killing of bacterium (GO:0070944), regulation of cysteine-type endopeptidase activity involved in apoptotic signalling pathway (GO:2001267), negative regulation of natural killer cell mediated cytotoxicity (GO: 0045953), negative regulation of natural killer cell mediated immunity (GO:0002716), platelet formation (GO:0030220) and complement activation, alternative pathway (GO:0006957). Table 2 shows these terms associated with the putative proteins identified in each term. An extensive description of all terms identified in pig granulomas with the proteins included for each term is detailed in Supplementary table 2.

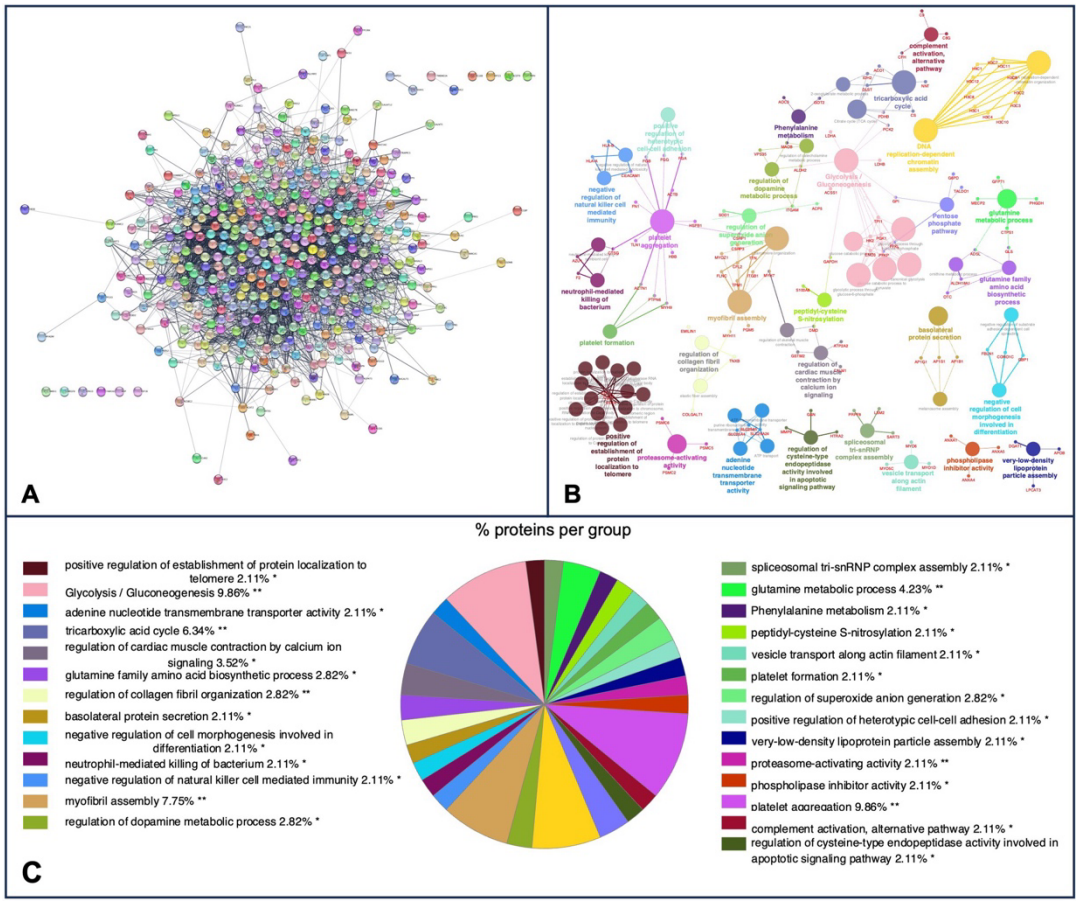

Figure 3. (A) PPI network of 447 overlapped nodes and 3,994 edges from pig specific m/z features obtained by the STRING database and visualised by Cytoscape. (B). Functional network from pig specific m/z features was visualised in Cytoscape with ClueGo and CluePedia, incorporating Biological Processes (BPs), Immune System Processes (ISPs) and Kyoto Encyclopedia of Genes and Genomes (KEGG) for enrichment of the pathways. *Terms are displayed as nodes (coloured circles), with node size being directly proportional to P ≤ 0.05. Terms are linked by edges (lines) based on their kappa score. Only statistically significant terms have been considered. (**C**) Sector diagram representing the proportion of proteins associated with the top functional groups expressed in a pie chart according to GO terms specific to each group. A value of P ≤ 0.05 shows significantly enriched GO terms. *P ≤ 0.05; ** P ≤ 0.01.*

Table 2. Summary list with terms from Gene Ontology (GO) Biological processes (BPs), immune system processes (ISPs) and Kyoto Encyclopedia of Genes and Genomes (KEGG) and their specific m/z identified in pigs.

GO Term	No. proteins	% Associated proteins	Associated proteins found
Glycolysis/gluconeogenesis	14	20.90	[ACSS1, ALDH2, ENO3, GAPDH, GPI, HK2, LDHA, LDHB, PCK2, PDHB, PFKL, PFKP, PGK1, TPI1]
Platelet aggregation	14	18.42	[ACTB, ACTN1, CEACAM1, CSRP1, CTSG, FGA, FGB, FGG, FN1, HBB, HSPB1, MYH9, PTPN6, TLN1]
Tricarboxylic acid cycle	7	20.59	[ACO1, CFH, CS, DLST, IDH2, NNT, PDHB]
Neutrophil-mediated killing of bacterium	3	25	[AZU1, CTSG, F2]
Regulation of cysteine-type endopeptidase activity involved in apoptotic signalling pathway	3	16.67	[GSN, HTRA2, MMP9]
Negative regulation of natural killer cell mediated cytotoxicity	3	15,79	[CEACAM1, HLA-A, HLA-B]
Negative regulation of natural killer cell mediated immunity	3	15	[CEACAM1, HLA-A, HLA-B]
Platelet formation	3	15	[ACTN1, MYH9, PTPN6]
Complement activation, alternative pathway	3	15	[C8G, C9, CFH]

No.: number.

* For the complete list table see Supplementary table 2

3.4 Construction of PPI network and functional annotation analysis from common m/z identified in both cattle and pigs

A total of 416 m/z were shared in granulomas from both species, in which a PPI network with a total of 71 nodes and 93 edges was obtained (Figure 4A). In the functional analysis of the proteins, after GO functional-enrichment (BPs and ISPs categories) and KEGG analyses, all m/z were significantly enriched in a total of 11 different terms (Figure 4B), which merged into 9 different groups (Figure 4C), highlighting the response to interleukin-4 (GO:0070670), antigen processing and presentation (KEGG:04612), complement and coagulation cascades (KEGG:04610), IL-17 signalling pathway (KEGG:04657), and tricarboxylic acid cycle (GO:0006099). Detail of the 11 terms identified in this part of the study together with their putative proteins are shown in table 3.

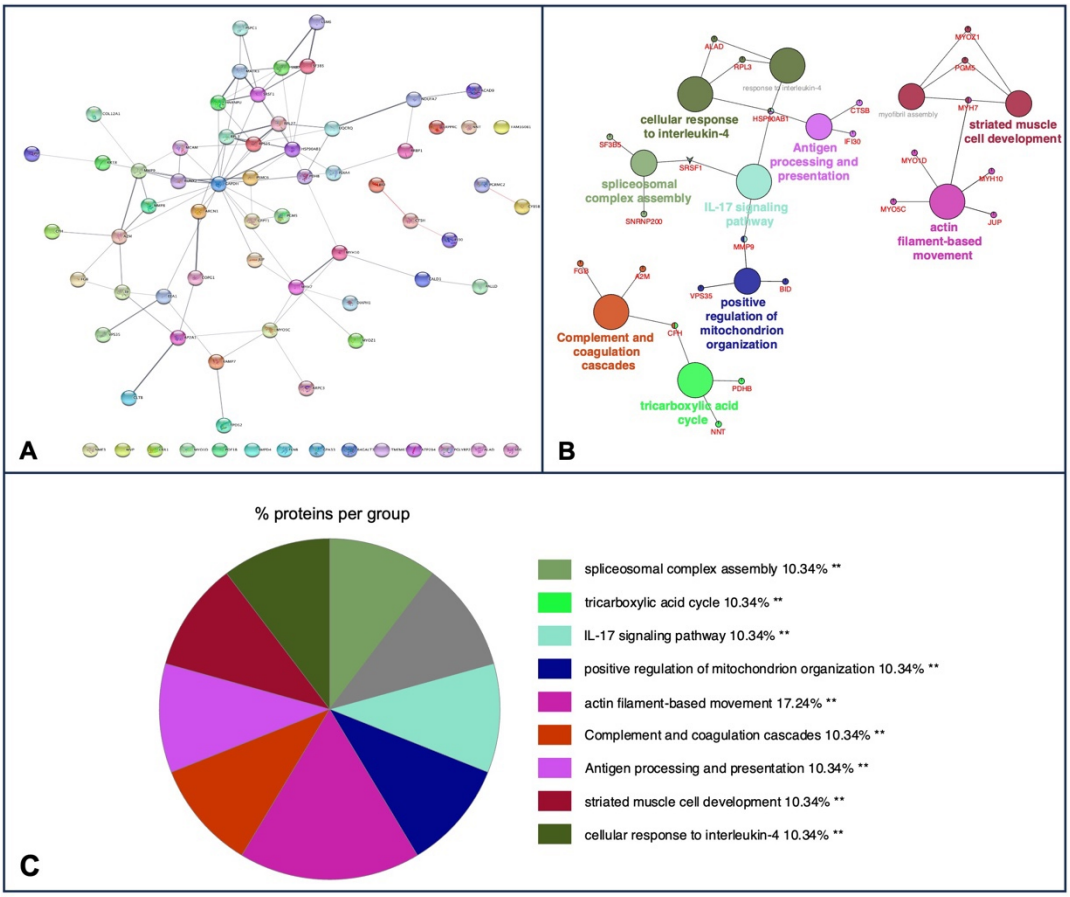

F*igure 4. (A) PPI network of 71 overlapped nodes and 93 edges from common m/z features among bovine and porcine obtained by the STRING database and visualized by Cytoscape. (B) Functional network from cattle and pig common m/z features was visualised in Cytoscape with ClueGo and CluePedia, incorporating Biological Processes (BP), Immune System Processes (ISPs) and Kyoto Encyclopedia of Genes and Genomes (KEGG) for enrichment of the pathways. Terms are displayed by nodes (coloured circles), with node size being directly proportional to P value ≤ 0.05. Terms are linked by edges (lines) based on their kappa score. Only statistically significant terms have been considered. (**C)** Sector diagram representing the proportion of proteins associated with the top functional groups from cattle and pig common m/z expressed in a pie chart according to GO terms specific to each group. A value of P ≤ 0.05 shows significantly enriched GO terms. ** P ≤ 0.01.*

Table 3. List with terms from Gene Ontology (GO) Biological Processes (BPs), Immune System Processes (ISPs) and Kyoto Encyclopedia of Genes and Genomes (KEGG) and their specific m/z which were shared by both cattle and pigs.

GO Term	No. Proteins	% Associated Proteins	Associated Proteins Found
Actin filament-based movement	5	3.65	[JUP, MYH10, MYH7, MYO1D, MYO5C]
Response to interleukin-4	3	76.92	[ALAD, HSP90AB1, RPL3]
Striated muscle cell development	3	42.25	[MYH7, MYOZ1, PGM5]
Spliceosomal complex assembly	3	39.47	[SF3B5, SNRNP200, SRSF1]
Antigen processing and presentation	3	38.46	[CTSB, HSP90AB1, IFI30]
Positive regulation of mitochondrion organization	3	38.46	[BID, MMP9, VPS35]
Complement and coagulation cascades	3	35.29	[A2M, CFH, FGB]
IL-17 signalling pathway	3	31.91	[HSP90AB1, MMP9, SRSF1]
Tricarboxylic acid cycle	3	8.82	[CFH, NNT, PDHB]
Cellular response to interleukin-4	3	8.33	[ALAD, HSP90AB1, RPL3]
Myofibril assembly	3	4.29	[MYH7, MYOZ1, PGM5]

No.: number

3.5 Differentially expressed proteins in cattle and pig granulomas

DEPs in both species were obtained considering a statistical significance of *FDR* < 0.0001 and a log2 FC ≥ 2. Thus, 436 differentially expressed m/z were observed in the study, with 187 DEPs in bovine granulomas and 249 DEPs in porcine (Figure 5). From them, 45 putative proteins in cattle and 57 putative proteins in pigs were identified with the reference MaTisse database.

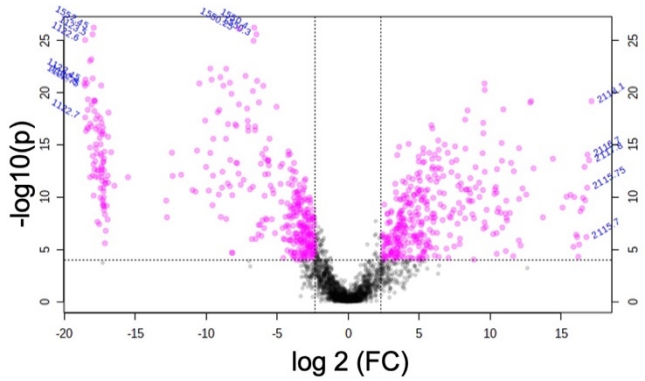

Figure 5. Volcano plot representation of the m/z features obtained from bovine and porcine granulomas by MALDI-MSI. *Magenta dots represent differentially expressed m/z in both species, while black dots correspond to non-differentially expressed m/z (FDR < 0.0001 and log2 FC ≥ 2).*

After GO functional-enrichment (BPs and ISPs categories) and KEGG analyses, the DEPs identified in cattle and pig granulomas were significantly enriched in a total of 7 different terms (Figure 6A). In cattle, all the m/z were associated with one single representative term, Glycolysis/gluconeogenesis (KEGG:00010) (Figure 6B); whereas DEPs from pig granulomas were included within 6 representative terms, highlighting antigen processing and presentation (KEGG:04612), selective autophagy (GO:0061912), structural constituent of cytoskeleton (GO:0005200), spliceosomal

complex assembly (GO:0000245), and organic hydroxy compound catabolic process (GO:1901616) (Figure 6C) (Table 4).

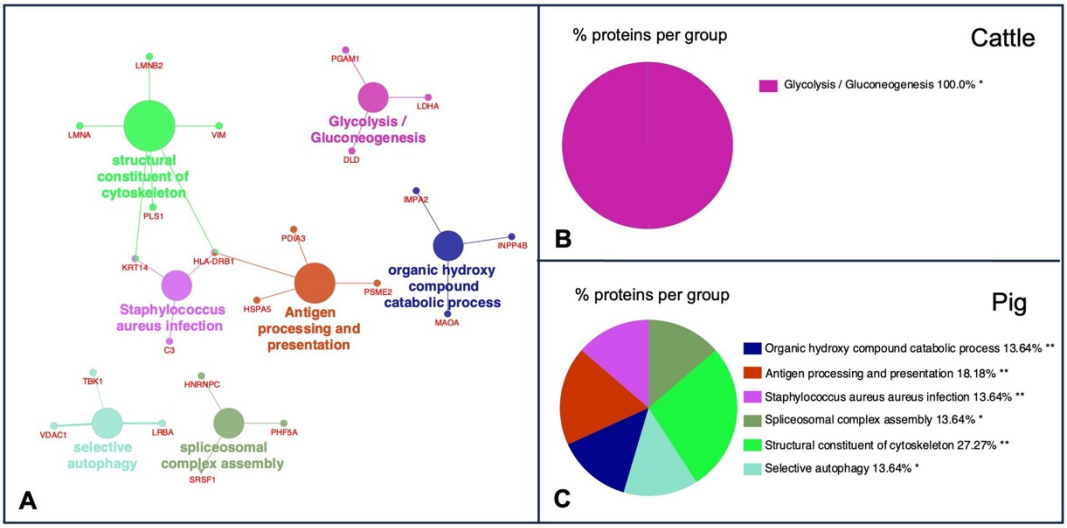

Figure 6. (**A**). Functional network from cattle and pig differentially expressed m/z features was visualised in Cytoscape with ClueGo and CluePedia, incorporating Biological Processes (BPs), immune system processes (ISPs) and Kyoto Encyclopedia of Genes and Genomes (KEGG) for enrichment of the pathways. Terms are displayed by nodes (coloured circles), with node size being directly proportional to *P* value ≤ 0.05. Terms are linked by edges (lines) based on their kappa score. Only statistically significant terms have been considered. (**B-C**). Sector diagram representing the proportion of proteins associated with the top functional groups from cattle (**B**) and pig (**C**) differentially expressed m/z displayed in a pie chart according to GO terms specific to each group. $P \leq 0.05$ shows significantly enriched GO terms. *$P < 0.05$; **$P \leq 0.01$.

Table 4. List of terms of Gene Ontology (GO) Biological Processes (BPs), Immune System Processes (ISPs) and Kyoto Encyclopedia of Genes and Genomes (KEGG) and their specific m/z from differentially expressed proteins in cattle and pigs.

GO Term	No. proteins	% Associated proteins	Associated proteins found
Cattle			
Glycolysis/gluconeogenesis	3	44.78	[DLD, LDHA, PGAM1]
Pig			
Antigen processing and presentation	4	51.28	[HLA-DRB1, HSPA5, PDIA3, PSME2]
Structural constituent of cytoskeleton	4	35.71	[HLA-DRB1, KRT14, LMNA, LMNB2]
Spliceosomal complex assembly	3	39.47	[HNRNPC, PHF5A, SRSF1]
Organic hydroxy compound catabolic process	3	35.29	[IMPA2, INPP4B, MAOA]
Selective autophagy	3	34.48	[LRBA, TBK1, VDAC1]
Staphylococcus aureus infection	3	31.25	[C3, HLA-DRB1, KRT14]

No.: number

3.6 Confirmation of MALDI-MSI results by IHC.

Figure 7 shows the H&E image together with the spatial distribution of C3, HLA-DR and MMP9 by MALDI-MSI together with the protein expression of each molecule by IHC in different representative animals from the corresponding species. C3 (m/z = 2217.25) was mainly expressed in the periphery of the granulomas from cattle (Figure 7B); in accordance with the MALDI-MSI image, C3 immunolabelling was found in the cytoplasm of epithelioid macrophages and multinucleated giant cells of granulomas with lack of expression at the necrotic core (Figure 7C). In the case of HLA-DR (m/z = 1963.95) (Figure 7D-F), the spatial distribution and pattern of expression was like C3 but in pig granulomas (Figure 7E). Most immunolabelled cells corresponded to epithelioid macrophages organising the granuloma and located close to the necrotic core (Figure 7F). For MMP9 (m/z = 959.404) spatial distribution in bovine (Figure 7G-I) and porcine (Figure 7J-L) granulomas, epithelioid macrophages, multinucleated giant cells, neutrophils and fibroblasts from the periphery of granulomas were immunolabelled in both species (Figures 7I and 7L).

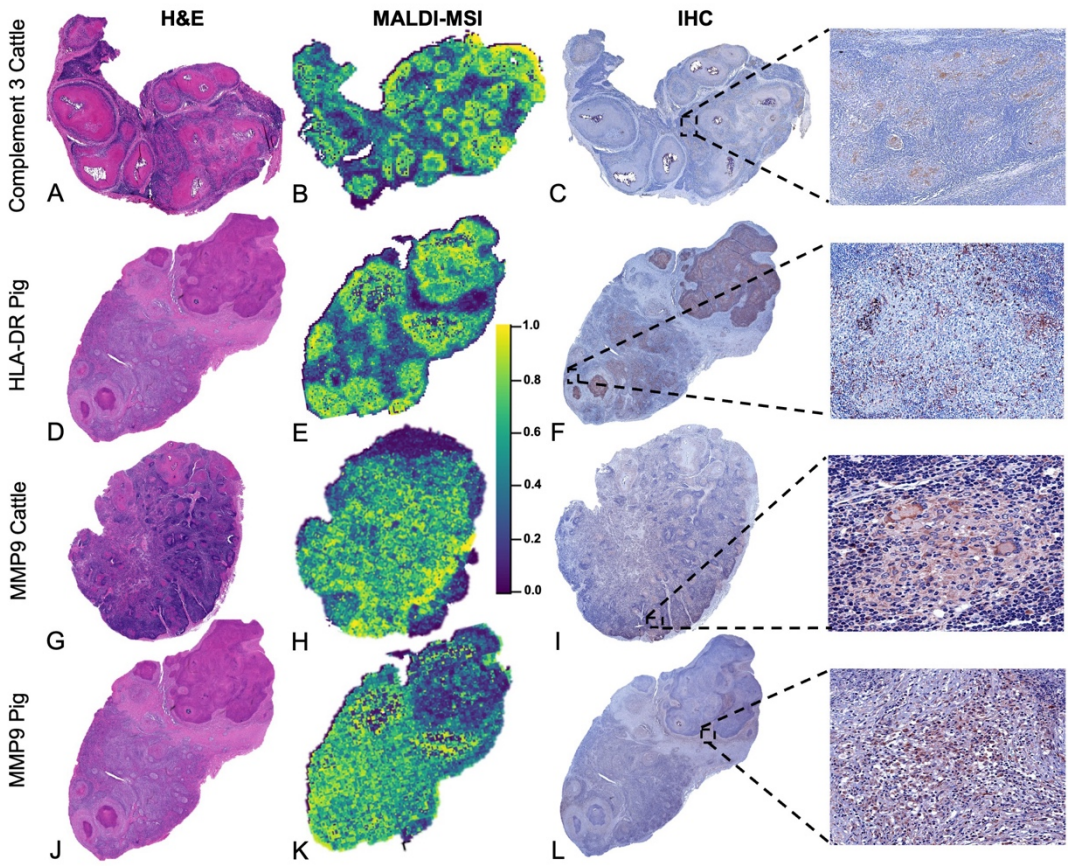

Figure 7. Spatial distribution according to selected m/z features in bovine and porcine granulomas and validation by immunohistochemistry. (A, D, G, J) *Sub-gross H&E-stained sections from a lymph node with multiple granulomas belonging to cattle or pig, as specified.* ***(B, E, H, K)*** *Distribution pattern of C3 (m/z = 2217.25) in a bovine LN, HLA-DR (m/z = 1963.90) in a porcine LN and MMP9 (m/z = 959.40) in bovine and porcine LNs, respectively. C3 and HLA-DR were homogeneously distributed throughout granulomas, whereas MMP9 was absent in the necrotic centre of granulomas. (C, F, I, L) Immunolabelling against the three selected molecules in the different granulomas in each species to confirmate MALDI-MSI results.*

4. Discussion

New high throughput sequencing techniques are emerging as tools of interest to decipher host-pathogen interactions within the context of major diseases, such as TB. In this sense, the combination of sequencing strategies together with tissue morphology, like MALDI-MSI, can provide valuable information to deepen in the pathogenesis of diseases, improving the understanding on how specific lesions are developed. In the current study, a proteomic analysis in tuberculous granulomas from cattle and pig LNs was performed to gain more information on the pathways involved in the regulation of the host response to the disease in each species.

Although a different number of cattle and pig granulomas were included in the present study (220 *vs* 78 granulomas), a similar number of m/z was identified in both species (1,438 m/z from cattle granulomas *vs* 1,898 m/z from pig granulomas) which allowed us to perform a robust comparison among cattle and porcine. From the beginning of the study, after principal component analysis, a clear separation between bovine and porcine granulomas according to the expressed m/z in each species was observed, which already pointed to a different protein signature in granulomas according to the species.

Although specific m/z were identified in each species, some GO-enriched terms also matched in both. This was the case of the term "Complement activation, alternative pathway" (tables 1 and 2) represented in both species by the proteins complement 9 (C9) and complement factor H (CFH) as well as by the proteins C3 specifically in bovine and complement C8 gamma chain (C8G) in porcine. Opsonophagocytic activity mediated by C3 or C3b has been reported to be enhanced in TB caused by either *M. tuberculosis* [35] or *Mycobacterium bovis* in wild boar, suggesting a role in bacterial clearance, which might be due to the production of IL-1β and other cytokines by innate immune cells, stimulating the production of C3 [36]. The expression of different molecules of the alternative pathway of complement activation in both species points to the activation of common pathways with species-specific peculiarities. Another term represented in both species was "Regulation of cysteine-type endopeptidase activity

involved in apoptotic signalling pathway", including MMP9 in both species, but also the proteins FASN and BAX in bovine and GSN and HTRA2 in porcine. Among them, matrix metalloproteinases (MMPs) are significant mediators of the inflammatory response and tissue destruction in TB [37], being MMP9 specifically involved in macrophage recruitment and tissue remodelling, which allows the formation of the granuloma [38–40]. Furthermore, MMP9 has been highlighted as a specific biomarker for the diagnosis of TB in cattle [41, 42], which could be also the case for porcine according to our results. The same applies to several pathways related to the regulation of the metabolism, such as the GO terms "Tricarboxylic acid cycle" (TCA) and "Glycolysis/gluconeogenesis" which were commonly represented in both species, but again being represented by different proteins. Our findings support a central role for these terms in the metabolism, model proposed by Xu et al. (2022) for *M. tuberculosis*, since amino acids, such as arginine, are synthesized from TCA using carbon metabolites from glycolysis as an energy source, which support the significant role of these pathways in TB in bovine and porcine. Interestingly, and in conjunction with these previous GO terms, "Nitrogen metabolism" was another term activated in cattle, involving proteins such as carbonic hydrogenase-like proteins (CA12, CA2) and carbamoyl phosphate synthase-1 (CPS-1), which has been shown to play a relevant role in mycobacterial nutrition and survival [43].

Regarding specific terms activated in cattle, the GO term "Natural killer cell degranulation" included the proteins VAMP27, CORO1A and RAB27A. Degranulation of natural killer (NK) cells involves the release of their granules, containing cytotoxic proteins, such as perforin and granzyme, which trigger the target cells to undergo apoptosis [44]. In TB, the release of these granules has been found to control mycobacterial growth, being essential for inhibiting mycobacterial replication [45]. On the contrary, "Negative regulation of natural killer cell mediated immunity" as well as "Negative regulation of natural killer cell mediated cytotoxicity" (HLA-A, HLA-B, CEACAM1) were activated among porcine GO terms, referring to a set of mechanisms that downregulate or inhibit the activity of NK cells, through downregulation of activating receptors on the surface of NK cells or upregulation of inhibitory receptors [44]. These pathways may act as a

double-edged sword. On one hand, they contribute to maintain immune homeostasis and avoid autoimmunity, thereby preventing excessive inflammation and tissue damage [46]. However, on the other hand, these pathways can be exploited by pathogens to evade the immune system and establish chronic infections, such as TB. Further studies need to be conducted to explore the role of NK cells during TB in swine.

Other specific GO terms identified in cattle included "Vesicle transport along actin filament" (ACTN4, MYO1D, MYO5C) and "Regulation of early endosome to late endosome transport" (DNAJC13, MAP2K1, RAB21), built through proteins that participate in endosomal protein and vesicular trafficking. Actin filaments and endosomes are important in TB infection, as they play a critical role in the intracellular trafficking and survival of mycobacteria within host cells [47–49]. In addition, an alteration of actin filaments could impede the process of nitric oxide synthase induction and inhibit enzyme activity in activated macrophages, thus increasing the survival of mycobacteria within macrophages [48]. Therefore, we could deduce that the integrity of actin filaments for the transport of early endosomes plays an important role in the destruction of mycobacteria [49].

Noteworthy, specific GO terms were activated only in porcine, such as "Platelet formation" and "Platelet aggregation". Platelets are capable to initiate and accelerate a rapid innate immune response against *M. tuberculosis*, activating monocytes and leading to the expression of activation markers, such as MMPs, as well as phagocytosis and tissue injury [50], in which thrombocytosis and increased severity of the disease may be critical [51]. Furthermore, "Neutrophil-mediated killing of bacterium" was also represented in pig granulomas in our study, which is consistent with the histological features observed in this species. In TB, neutrophils are fundamental mediators of the innate immune response, as they provide protection trying to kill mycobacteria through the release of their granules, notably, the primary (azurophilic) granules, which contain myeloperoxidase (MPO), cathepsin G, elastase, proteinase 3 and defensin, responsible for pathogen clearance [52, 53]. Interestingly, the proteins azurocidin 1 (AZU1) and cathepsin G (CTSG) were identified in our study within this GO term. Previous

studies in cattle have shown active phagocytosis of *M. bovis* by neutrophils, however, neutrophils failed to kill mycobacteria, proposing a potential role for autophagy [54]. Remarkably, in the context of mycobacterial infection, neutrophils have been reported to act as a "Trojan horse" with infected neutrophils serving as vehicles, transporting mycobacterial organisms to distant sites, thereby causing systemic dissemination of the bacteria [23, 52, 54].

The GO terms represented by common m/z in both species (table 3) included "Response to interleukin-4" and "IL-17 signalling pathway", while the first has an anti-inflammatory function, the second has proinflammatory activity [55]. IL-4 has been highlighted as a marker of virulence and protective immune response during TB in cattle, being associated with animals with mild lesions compared to those with severe lesions [56]. This supports the idea that IL-4 acts to attenuate the adverse effect of exacerbated IFN-γ (interferon gamma) driven inflammation in host tissues [57]. Similar results have been seen in BCG-immunised wild boars, suggesting implications for the development of vaccines against TB in wild boar and other wildlife species [58]. Furthermore, it has been shown that cattle with macroscopic lesions developed higher IL-17 expression in later stages of the disease compared to animals without lesions [57], indicating that IL-17 is an important proinflammatory cytokine in the immune response against mycobacterial infection with predictive prognostic value in TB in cattle [22, 57] .

The GO term "Antigen processing and presentation" contained within its proteins cathepsin B (CTSB) and gamma-interferon-inducible lyosomal thiol reductase (IFI30). Cathepsins are proteolytic enzymes with a key role in lysosomes formation, contributing to pathogen clearance either directly by pathogen killing or indirectly by participating in antigen presentation. In this sense, a decrease in cathepsin B has been associated with an increased survival of intracellular mycobacteria [59]. Furthermore, cathepsin B has been reported to be pivotal in granuloma immunopathology during TB [60].

In addition, DEPs among both species were analysed. Due to the low number of DEPs identified with the MaTisse database, only the term "Glycolysis/gluconeogenesis"

was recognised among GO terms in cattle. Interestingly, gluconeogenesis is known as essential for mycobacteria survival in the host [61], with a central role of phosphoenolpyruvate carboxykinase for *M. tuberculosis* infections and survival [62]. The differential expression of this term in granulomas from cattle indicate a key role of this metabolic pathway in bovine for the metabolism of mycobacteria from MTC. In the case of pigs, among the GO terms represented from DEPs "Antigen processing and presentation" and "Structural constituent of cytoskeleton" were found, sharing the protein major histocompatibility complex class II, DR beta 1 (HLA-DRB1), which is directly involved in the processing and presentation of mycobacterial antigens, crucial to control this infection [63]. Noteworthy, the term "Antigen processing and presentation" was commonly represented in both species, although HLA-DRB1 was only significantly expressed in porcine granulomas. Furthermore, the GO term "Selective autophagy" was also identified from DEPs in porcine which is in connexion with the role proposed for neutrophils during TB [64] as well as with the higher infiltrate of neutrophils observed in granulomas from pigs in the present study. Autophagy plays a crucial role in maintaining cellular homeostasis and dysregulation of this process has been linked to various diseases such as TB, with suppression of this pathway increasing bacterial survival in macrophages as well as a worse prognosis and increased severity of the disease [65].

5. Conclusions

New high throughput sequencing techniques, combined with tissue morphology analysis, such as MALDI-MSI, offer a significant advantage for studying the pathogenesis of diseases such as TB. In this study, a proteomic analysis was carried out on cattle and pig tuberculous granulomas identifying some GO-enriched terms shared among both species, such as "Tricarboxylic acid cycle", "Complement activation, alternative pathway" and "Regulation of cysteine-type endopeptidase activity involved in apoptotic signalling pathway", which highlights pathways that are conserved among different species infected by MTC. Furthermore, species-specific terms identified in the current study, such as "Natural killer cell degranulation" in cattle or those related to platelet and neutrophils recruitment and activation in pigs, provide new insights into host-

pathogen interaction in TB in different species and highlights the importance of studying proteomics in understanding this disease.

Acknowledgements

We express our appreciation to Alberto Alcántara and Marta Ordóñez-Martínez for their technical assistance, the technical support offered by the Animal Health and Production Laboratory of Córdoba (Spain) and the technical support offered by Consuelo Gómez-Díaz and Carlos A. Fuentes-Almagro from the Proteomics Unit (SCAI-UCO), University of Córdoba and the staff from IMIBIC Mass Spectrometry and Molecular Imaging Unit, Maimónides Biomedical Research Institute of Córdoba, Reina Sofia University Hospital, University of Córdoba, 14071 Córdoba, Spain

Data availability

The mass spectrometry proteomics data have been deposited to the ProteomeXchange Consortium (http://proteomecentral.proteomexchange.org) via the PRIDE [66] partner repository with the dataset identifier PXD045377.

CRediT author statement.

LC: Conceptualisation; Resources; Writing - Review & Editing; Supervision; Funding acquisition. **JG-L**: Conceptualisation; Methodology; Resources; Writing - Review & Editing; Supervision; Funding acquisition. **IR-G**: Conceptualisation; Methodology; Writing - Review & Editing; Supervision. **FL-M**: Formal analysis; Investigation; Writing - Original Draft; Visualisation. **JS-C**: Investigation; Writing - Review & Editing. **IR-T**: Investigation; Writing - Review & Editing. **CA-D**: Validation; Writing - Review & Editing. **KF**: Validation; Writing - Review & Editing. **FJ-P**: Validation; Writing - Review & Editing. **EC-G**: Formal analysis; Data Curation; Writing - Review & Editing.

Conflict of interest

The authors declare that they have no competing interest.

Funding

This work was supported by the investigation project "New measures and techniques to control Bovine Tuberculosis in Andalusia" (Financially supported by Operational Groups of the European Innovation Partnership for Agricultural productivity and Sustainability, EIP-AGRI) (GOP2I-CO-16-0010). Fernanda Larenas-Muñoz is supported by a doctoral grant from ANID (National Research and Development Agency)/Doctoral grant Chile/2019/72200324. Inés Ruedas-Torres and José María Sánchez-Carvajal are supported by a "Margarita Salas" contract from the Spanish Ministry of Universities.

Supplemental data

This article contains supplemental data, containing supplemental figures and supplemental tables.

Finally, for editor and reviewers, you can find raw data available via ProteomeXchange with identifier PXD045377".

Username: reviewer_pxd045377@ebi.ac.uk

Password: mtamqfCc

References

1. González Llamazares, O.R, Gutiérrez Martín, C.B, Aranaz Martín A., Liébana Criado E., Domínguez Rodríguez, L. and Rodríguez Ferri, E.F. (1999) Comparison of different methods for diagnosis of bovine tuberculosis from tuberculin-or interferon-γ-reacting cattle in Spain. J Appl Microbiol. 87, 465–71.

2. Good, M., Bakker, D., Duignan, A. and Collins D.M. (2018) The history of in vivo tuberculin testing in bovines: Tuberculosis, a "One Health" issue. Front Vet Sci. 5 APR:59. https://doi.org/10.3389/fvets.2018.00059

3. Mohamed, A. (2020). Bovine tuberculosis at the human–livestock–wildlife interface and its control through one health approach in the Ethiopian Somali Pastoralists: A review. One Health, 9, 100113.

4. Rodriguez-Campos, S., Smith, N.H., Boniotti, M.B. and Aranaz, A. (2014) Overview and phylogeny of Mycobacterium tuberculosis complex organisms: Implications for diagnostics and legislation of bovine tuberculosis. Res Vet Sci. 97, S5–19.

5. World organization for animal health (WOAH). Tuberculosis de los mamíferos (Infección por el complejo Mycobacterium tuberculosis). In: Terrestrial Animal Health Code. 2022. p. 1–24.

6. Kemal, J., Sibhat, B., Abraham, A., Terefe, Y., Tulu, K.T., Welay, K, et al. (2019) Bovine tuberculosis in eastern Ethiopia: Prevalence, risk factors and its public health importance. BMC Infect Dis. 19, 1–9.

7. Palmer, M.V., Kanipe, C. and Boggiatto, P.M. (2022) The Bovine Tuberculoid Granuloma. Pathogens. 11, 61.

8. de Lisle, G.W., Mackintosh, C.G. and Bengis, R.G. (2001) Mycobacterium bovis in free-living and captive wildlife, including farmed deer. Rev Sci Tech. 20, 86–111.

9. Malone, K.M. and Gordon, S.V. (2017) Mycobacterium tuberculosis Complex Members Adapted to Wild and Domestic Animals. Adv Exp Med Biol. 1019, 135–54.

10. Padilla-Carlin, D.J, McMurray, D.N. and Hickey, A.J. (2008) The guinea pig as a model of infectious diseases. Comp Med. 58, 324–40.

11. Silva Miranda, M., Breiman, A., Allain, S., Deknuydt, F. and Altare, F. (2012) The tuberculous granuloma: An unsuccessful host defence mechanism providing a safety shelter for the bacteria? Clin Dev Immunol. 2012, 139127.

12. Young, D. (2009) Animal models of tuberculosis. Eur J Immunol. 39, 2011–2014.

13. Flynn, J.A.L. (2006) Lessons from experimental Mycobacterium tuberculosis infections. Microbes Infect. 8, 1179–1188.

14. Marakalala, M.J., Raju, R.M., Sharma, K., Zhang, Y.J., Eugenin, A., Prideaux, B., et al. (2016) Inflammatory signaling in human tuberculosis granulomas is spatially organized. Nat Med. 22, 531–538.

15. Blanc, L., Lenaerts, A., Dartois, V. and Prideaux, B. (2018) Visualization of Mycobacterial Biomarkers and Tuberculosis Drugs in Infected Tissue by MALDI-MS Imaging. Anal Chem. 90, 6275–6282.

16. Walther, T.C. and Mann, M. (2010) Mass spectrometry – based proteomics in cell biology. Journal of cell biology. 190, 491–500.

17. Schöne, C., Höfler, H. and Walch, A. (2013) MALDI imaging mass spectrometry in cancer research: Combining proteomic profiling and histological evaluation. Clin Biochem. 46, 539–545.

18. Aichler, M. and Walch, A. (2015) MALDI Imaging mass spectrometry: Current frontiers and perspectives in pathology research and practice. Laboratory Investigation. 95, 422–431.

19. Manzanares-Meza, L.D., Gutiérrez-Román, C.I. and Medina-Contreras, O. (2017) MALDI imaging: beyond classic diagnosis. Bol Med Hosp Infant Mex. 74, 212–718.

20. Fernández-Vega, A., Chicano-Gálvez, E., Prentice, B.M., Anderson, D., Priego-Capote, F., López-Bascón, M.A, et al. (2020) Optimization of a MALDI-Imaging protocol for studying adipose tissue-associated disorders. Talanta. 219, 121184.

21. Madacki, J., Mas Fiol, G. and Brosch, R. (2019) Update on the virulence factors of the obligate pathogen Mycobacterium tuberculosis and related tuberculosis-causing mycobacteria. journal of molecular epidemiology and evolutionary genetics in infectious diseases. 72, 67–77.

22. Waters, W.R., Maggioli, M.F., Palmer, M.V., Thacker, T.C., McGill, J.L., Vordermeier, H.M., et al. (2016) Interleukin-17A as a Biomarker for Bovine Tuberculosis. Clinical and Vaccine Immunology.23,168–180.

23. Warren, E., Teskey, G. and Venketaraman, V. (2017) Effector mechanisms of neutrophils within the innate immune system in response to Mycobacterium tuberculosis infection. J Clin Med. 6,15.

24. Cardoso-Toset, F., Gómez-Laguna, J., Amarilla, S.P., Vela, A.I., Carrasco, L., Fernández-Garayzábal, J.F., et al. (2015) Multi-etiological nature of tuberculosis-like lesions in condemned pigs at the slaughterhouse. PLoS One. 10, 1–12.

25. Sánchez-Carvajal, J.M., Galán-Relaño, Á., Ruedas-Torres, I., Jurado-Martos, F., Larenas-Muñoz, F., Vera, E., et al. (2021) Real-Time PCR Validation for Mycobacterium tuberculosis Complex Detection Targeting IS6110 Directly From Bovine Lymph Nodes. Front Vet Sci. 8, 643111.

26. Larenas-Muñoz, F., Sánchez-Carvajal, J.M., Galán-Relaño, Á., Ruedas-Torres, I., Vera-Salmoral, E., Gómez-Gascón, L., et al. (2022) The Role of Histopathology as a Complementary Diagnostic Tool in the Monitoring of Bovine Tuberculosis. Front Vet Sci. 9, 816190.

27. Deutsch, E.W., Csordas, A., Sun, Z., Jarnuczak, A., Perez-Riverol, Y., Ternent, T., et al. (2017) The ProteomeXchange consortium in 2017: Supporting the cultural change in proteomics public data deposition. Nucleic Acids Res. 45, D1100–D1106.

28. Bemis, K.D., Harry, A., Eberlin, L.S., Ferreira, C., Van De Ven, S.M., Mallick, P., et al. (2015) Cardinal: An R package for statistical analysis of mass spectrometry-based imaging experiments. Bioinformatics. 31, 2418–2420.

29. Maier, S.K., Hahne, H., Gholami, A.M., Balluff, B., Meding, S., Schoene, C., et al. (2013) Comprehensive identification of proteins from MALDI imaging. Molecular and Cellular Proteomics. 12, 2901–2910.

30. Doncheva, N.T., Morris, J.H., Gorodkin, J. and Jensen, L.J. (2019) Cytoscape StringApp: Network Analysis and Visualization of Proteomics Data. J Proteome Res. 18, 623–632.

31. Shannon, P., Markiel, A., Ozier, O., Baliga, N.S., Wang, J.T., Ramage, D., et al. (2003) Cytoscape: A Software environment for integrated models of biomolecular interaction networks. Genome Res. 13, 2498–24504.

32. Bindea, G., Galon, J. and Mlecnik, B. (2013) CluePedia Cytoscape plugin: Pathway insights using integrated experimental and in silico data. Bioinformatics. 29, 661–663.

33. Bindea, G., Mlecnik, B., Hackl, H., Charoentong, P., Tosolini, M., Kirilovsky, A., et al. (2009) ClueGO: A Cytoscape plug-in to decipher functionally grouped gene ontology and pathway annotation networks. Bioinformatics. 25, 1091–1093.

34. Mlecnik, B., Galon, J. and Bindea, G. (2019) Automated exploration of gene ontology term and pathway networks with ClueGO-REST. Bioinformatics. 35, 3864–3866.

35. Jagatia, H. and Tsolaki, A.G. (2021) The role of complement system and the immune response to tuberculosis infection. Medicina (Kaunas). 57, 84.

36. De La Fuente, J., Gortázar, C. and Juste, R. (2016) Complement component 3: A new paradigm in tuberculosis vaccine. Expert Rev Vaccines.15, 275–277.

37. Sheen, P., O'Kane, C.M., Chaudhary, K., Tovar, M., Santillan, C., Sosa, J., et al. (2009) High MMP-9 activity characterises pleural tuberculosis correlating with granuloma formation. European Respiratory Journal. 33, 134–141.

38. Ragno, S., Romano, M., Howell, S., Pappin, D.J.C., Jenner, P.J., Colston. M.J. (2001) Changes in gene expression in macrophages infected with Mycobacterium tuberculosis: a combined transcriptomic and proteomic approach. Immunology. 104, 99–108.

39. Rivera-Marrero, C.A., Schuyler, W., Roser, S., Ritzenthaler, J.D., Newburn, S.A., Roman, J. (2002) M. tuberculosis induction of matrix metalloproteinase-9: the role of mannose and receptor-mediated mechanisms. American journal of physiology. 282, 546–555.

40. Taylor, J.L., Hattle, J.M, Dreitz, S.A, Troudt, J.L.M, Izzo, L.S., Basaraba, R.J., et al. (2006) Role for matrix metalloproteinase 9 in granuloma formation during pulmonary Mycobacterium tuberculosis infection. Infect Immun. 74, 6135–6144.

41. Klepp, L.I, Eirin, M.E., Garbaccio, S., Soria, M., Bigi, F. and Blanco, F.C. (2019) Identification of bovine tuberculosis biomarkers to detect tuberculin skin test and IFNγ release assay false negative cattle. Res Vet Sci. 122, 7–14.

42. Klepp, L.I., Colombatti, M.A., Moyano, R.D., Romano, M.I., Malovrh, T., Ocepek, M, et al. (2023) Assessment of tuberculosis biomarkers in paratuberculosis-infected cattle. J Vet Res. 67, 55–60.

43. Xu, Y., Pooja and Borah, K. (2022) Mycobacterium tuberculosis carbon and nitrogen metabolic fluxes. Biosci Rep. 42, BSR20211215.

44. Vivier, E., Tomasello, E., Baratin, M., Walzer, T and Ugolini, S. (2008) Functions of natural killer cells. Nature Immunology. 9, 503–510.

45. Liu, C.H., Liu, H. and Ge, B. (2017) Innate immunity in tuberculosis: Host defense vs pathogen evasion. Cell Mol Immunol. 14, 963–975.

46. Hallett, W.H.D. and Murphy, W.J. (2006) Positive and negative regulation of Natural Killer cells: Therapeutic implications. Seminars in Cancer Biology.16, 367–382.

47. Layre, E. (2020) Trafficking of Mycobacterium tuberculosis Envelope Components and Release Within Extracellular Vesicles: Host-Pathogen Interactions Beyond the Wall. Front Immunol. 11, 1230.

48. Guérin, I. and de Chastellier, C. Pathogenic Mycobacteria Disrupt the Macrophage Actin Filament Network. Infect Immun. 68, 2655–2662.

49. DePina, A.S. and Langford, G.M. (1999) Vesicle transport: The role of actin filaments and myosin motors. Microsc Res Tech.47, 93–106.

50. Kirwan, D.E., Chong, D.L.W. and Friedland, J.S. (2021) Platelet Activation and the Immune Response to Tuberculosis. Front Immunol. 12, 631696.

51. Ünsal, E., Aksaray, S., Köksal, D. and Şipit, T. (2005) Potential role of interleukin 6 in reactive thrombocytosis and acute phase response in pulmonary tuberculosis. Postgrad Med J. 81, 604–607.

52. Alcantara, C.A., Glassman, I., Nguyen, K.H., Parthasarathy, A. and Venketaraman, V. (2023) Neutrophils in Mycobacterium tuberculosis. Vaccines (Basel). 11, 631.

53. Hilda, J.N., Das, S., Tripathy, S.P. and Hanna, L.E. (2020) Role of neutrophils in tuberculosis: A bird's eye view. Innate Immunity. 26, 240–247.

54. Wang, J., Zhou, X., Pan, B., Yang, L., Yin, X., Xu, B., et al. (2013) Investigation of the effect of Mycobacterium bovis infection on bovine neutrophils functions. Tuberculosis. 93, 675–687.

55. Mansouri, F., Heydarzadeh, R. and Yousefi, S. (2018) The association of interferon-gamma, interleukin-4 and interleukin-17 single-nucleotide polymorphisms with susceptibility to tuberculosis. APMIS. 126, 227–233.

56. Thacker, T.C., Palmer, M. V. and Waters, W.R. (2007) Associations between cytokine gene expression and pathology in Mycobacterium bovis infected cattle. Vet Immunol Immunopathol. 119, 204–213.

57. Blanco, F.C, Bianco, M.V., Meikle, V., Garbaccio, S., Vagnoni, L., Forrellad, M., et al. (2011) Increased IL-17 expression is associated with pathology in a bovine model of tuberculosis. Tuberculosis. 91, 57–63.

58. de la Lastra, J.M.P., Galindo, R.C, Gortázar, C., Ruiz-Fons, F., Aranaz, A., de la Fuente J. (2009) Expression of immunoregulatory genes in peripheral blood mononuclear cells of European wild boar immunized with BCG. Vet Microbiol. 134, 334–339.

59. Pires, D., Marques, J., Pombo, J.P., Carmo, N., Bettencourt, P., Neyrolles, O., et al. (2016) Role of Cathepsins in Mycobacterium tuberculosis Survival in Human Macrophages. Sci Rep. 6, 32247.

60. Kakegawa, H., Matano, Y., Inubushi, T. and Katunuma, N. (2004) Significant accumulations of cathepsin B and prolylendopeptidase in inflammatory focus of

delayed-type hypersensitivity induced by Mycobacterium tuberculosis in mice. Biochem Biophys Res Commun. 316, 78–84.

61. Ganapathy, U., Marrero, J., Calhoun, S., Eoh, H., De Carvalho, L.P.S., Rhee, K., et al. (2015) Two enzymes with redundant fructose bisphosphatase activity sustain gluconeogenesis and virulence in *Mycobacterium tuberculosis*. Nat Commun. 6, 7912.

62. Marrero, J., Rhee, K.Y., Schnappinger, D., Pethe, K. and Ehrt, S. (2010) Gluconeogenic carbon flow of tricarboxylic acid cycle intermediates is critical for *Mycobacterium tuberculosis* to establish and maintain infection. Proc Natl Acad Sci U S A. 107, 9819–9824.

63. Harding, C.V. and Boom W.H. (2010) Regulation of antigen presentation by *Mycobacterium tuberculosis*: A role for Toll-like receptors. Nat Rev Microbiol. 8, 296–307.

64. Wang, J., Zhou, X., Pan, B., Yang, L., Yin, X,. Xu, B., et al. (2013) Investigation of the effect of Mycobacterium bovis infection on bovine neutrophils functions. Tuberculosis. 93, 675–687.

65. Lam, A., Prabhu, R., Gross, C.M., Riesenberg, L.A., Singh, V. and Aggarwal, S. (2017) Role of apoptosis and autophagy in tuberculosis. Am J Physiol Lung Cell Mol Physiol. 313, 218–229.

66. Perez-Riverol, Y., Bai, J., Bandla, C., García-Seisdedos, D., Hewapathirana, S., Kamatchinathan, S., et al. (2022) The PRIDE database resources in 2022: A hub for mass spectrometry-based proteomics evidences. Nucleic Acids Res. 50, D543–D552.

Supplementary tables

Table S-1. Table lists with all terms of Gene Ontology (GO) Biological Processes (BPs), Immune System Processes (ISPs) and Kyoto Encyclopedia of Genes and Genomes (KEGG) and their specific m/z identified in cattle.

GO Term	No. Proteins	% Associated Proteins	Associated Proteins Found
Citrate cycle (TCA cycle)	7	23.33	[ACLY, DLD, DLST, IDH1, PCK2, PDHB, SUCLA2]
Tricarboxylic acid cycle	6	17.65	[CFH, DLST, IDH1, NNT, PDHB, SUCLA2]
Beta-alanine metabolism	5	16.13	[ACADS, ACOX1, ALDH2, CNDP2, HADHA]
Propanoate metabolism	5	15.63	[ACADS, ACOX1, DLD, HADHA, SUCLA2]
Regulation of complement act vation	4	18.18	[A2M, C3, CFH, PHB1]
mRNA cis splicing, via splicec some	4	16.67	[DCPS, SNRNP200, SNRPC, SRSF1]
Skeletal muscle myosin thick fi ament assembly	3	75.00	[MYH11, TTN, TTR]
Striated muscle myosin thick fi ament assembly	3	75.00	[MYH11, TTN, TTR]
Myosin filament assembly	3	60.00	[MYH11, TTN, TTR]
Myosin filament organization	3	50.00	[MYH11, TTN, TTR]
Post-embryonic eye morphoge nesis	3	37.50	[BAX, FBN1, HMGN1]
Skeletal myofibril assembly	3	30.00	[MYH11, TTN, TTR]
Oxaloacetate metabolic proces:	3	27.27	[ACLY, GOT2, PCK2]
Natural killer cell degranulatio	3	23.08	[CORO1A, RAB27A, VAMP7]
Nitrogen metabolism	3	17.65	[CA12, CA2, CPS1]

Srp-dependent cotranslational protein targeting to membrane	3	16.67	[SRP72, SRP9, SRPRB]
Regulation of cysteine-type en dopeptidase activity involved i apoptotic signalling pathway	3	16.67	[BAX, FASN, MMP9]
Vesicle transport along actin fi ament	3	15.79	[ACTN4, MYO1D, MYO5C]
Complement activation, alterna tive pathway	3	15.00	[C3, C9, CFH]
Nucleotide-sugar biosynthet process	3	15.00	[GFPT1, GMPPB, NANS]
Regulation of early endosome t late endosome transport	3	15.00	[DNAJC13, MAP2K1, RAB21]
2-oxoglutarate metabolic pro cess	3	1.00	[DLST, GOT2, IDH1]

No.: number.

Table S-2. Table lists with all terms of Gene Ontology (GO) Biological Processes (BPs), Immune System Processes (ISPs) and Kyoto Encyclopedia of Genes and Genomes (KEGG) and their specific m/z identified in pigs.

GO Term	No. Proteins	% Associated Proteins	Associated Proteins Found
Platelet aggregation	14	18.42	[ACTB, ACTN1, CEACAM1, CSRP1, CTSG, FGA, FGB, FGG, FN1, HBB, HSPB1, MYH9, PTPN6, TLN1]
Glycolysis/gluconeogenesis	14	20.90	[ACSS1, ALDH2, ENO3, GAPDH, GPI, HK2, LDHA, LDHB, PCK2, PDHB, PFKL, PFKP, PGK1, TPI1]
DNA replication-dependent chromatin assembly	11	34.38	[H3C1, H3C10, H3C11, H3C12, H3C2, H3C3, H3C4, H3C6, H3C7, H3C8, H4C1]
Myofibril assembly	11	15.71	[CFL2, CSRP1, CSRP3, FLNC, ITGB1, MYH11, MYH7, MYOZ1, PGM5, TPM1, TTN]
DNA replication-dependent chromatin organization	11	34.38	[H3C1, H3C10, H3C11, H3C12, H3C2, H3C3, H3C4, H3C6, H3C7, H3C8, H4C1]
Sarcomere organization	9	20.00	[CFL2, CSRP1, CSRP3, FLNC, ITGB1, MYH7, MYOZ1, TPM1, TTN]
Tricarboxylic acid cycle	7	20.59	[ACO1, CFH, CS, DLST, IDH2, NNT, PDHB]
Canonical glycolysis	6	25.00	[ENO3, HK2, PFKL, PFKP, PGK1, TPI1]
Glucose catabolic process to pyruvate	6	25.00	[ENO3, HK2, PFKL, PFKP, PGK1, TPI1]
Glycolytic process through glucose-6-phosphate	6	23.08	[ENO3, HK2, PFKL, PFKP, PGK1, TPI1]
Glycolytic process through fructose-6-phosphate	6	22.22	[ENO3, HK2, PFKL, PFKP, PGK1, TPI1]

Citrate cycle (TCA cycle)	6	20.00	[ACO1, CS, DLST, IDH2, PCK2, PDHB]
Glucose catabolic process	6	18.75	[ENO3, HK2, PFKL, PFKP, PGK1, TPI1]
Glutamine metabolic process	6	1.93	[ADSL, CTPS1, GFPT1, GLS, MECP2, PHGDH]
Pentose phosphate pathway	5	16.67	[G6PD, GPI, PFKL, PFKP, TALDO1]
Glutamine family amino acid biosynthetic process	4	21.05	[ADSL, ALDH18A1, GLS, OTC]
Regulation of dopamine metabolic process	4	20.00	[ALDH2, ITGAM, MAOB, VPS35]
Regulation of catecholamine metabolic process	4	20.00	[ALDH2, ITGAM, MAOB, VPS35]
Regulation of superoxide anion generation	4	16.00	[ACP5, CSRP1, ITGAM, SOD1]
Regulation of cardiac muscle contraction by calcium ion signalling	4	15.38	[ATP2A2, CALM1, DMD, GSTM2]
Basolateral protein secretion	3	75.00	[AP1B1, AP1G1, AP1S1]
Proteasome-activating activity	3	50.00	[PSMC2, PSMC5, PSMC6]
Regulation of collagen fibril organization	3	42.86	[COLGALT1, EMILIN1, TNXB]
Positive regulation of establishment of protein localization to telomere	3	30.00	[CCT2, CCT7, CCT8]
Very-low-density lipoprotein particle assembly	3	27.27	[APOB, DGAT1, LPCAT3]

Regulation of establishment of protein localization to telomere	3	27.27	[CCT2, CCT7, CCT8]
Regulation of protein localization to Cajal body	3	27.27	[CCT2, CCT7, CCT8]
Positive regulation of protein localization to Cajal body	3	27.27	[CCT2, CCT7, CCT8]
Elastic fiber assembly	3	25.00	[EMILIN1, MYH11, TNXB]
Regulation of establishment of protein localization to chromosome	3	25.00	[CCT2, CCT7, CCT8]
Neutrophil-mediated killing of bacterium	3	25.00	[AZU1, CTSG, F2]
Protein localization to nuclear body	3	25,00	[CCT2, CCT7, CCT8]
Positive regulation of protein localization to chromosome, telomeric region	3	25.00	[CCT2, CCT7, CCT8]
Protein localization to Cajal body	3	25.00	[CCT2, CCT7, CCT8]
Spliceosomal tri-snrnp complex assembly	3	23.08	[LSM2, PRPF8, SART3]
ATP transmembrane transporter activity	3	23.08	[SLC25A24, SLC25A4, SLC25A5]
Ornithine metabolic process	3	23.08	[ADSL, ALDH18A1, OTC]
Negative regulation of cell morphogenesis involved in differentiation	3	21.43	[CORO1C, FBLN1, GBP1]
Neutrophil-mediated killing of symbiont cell	3	21.43	[AZU1, CTSG, F2]

Negative regulation of substrate adhesion-dependent cell spreading	3	21.43	[CORO1C, FBLN1, GBP1]
Regulation of protein localization to chromosome, telomeric region	3	21.43	[CCT2, CCT7, CCT8]
Protein localization to nucleoplasm	3	21.43	[CCT2, CCT7, CCT8]
Phospholipase inhibitor activity	3	20.00	[ANXA1, ANXA4, ANXA5]
Positive regulation of heterotypic cell-cell adhesion	3	20.00	[FGA, FGB, FGG]
Regulation of skeletal muscle contraction	3	18.75	[DMD, GSTM2, MYH7]
Positive regulation of telomerase RNA localization to Cajal body	3	18.75	[CCT2, CCT7, CCT8]
Phenylalanine metabolism	3	18.75	[AOC3, GOT2, MAOB]
Establishment of protein localization to telomere	3	17.65	[CCT2, CCT7, CCT8]
ATP transport	3	16.67	[SLC25A24, SLC25A4, SLC25A5]
Regulation of cysteine-type endopeptidase activity involved in apoptotic signalling pathway	3	16.67	[GSN, HTRA2, MMP9]
Adenine nucleotide transmembrane transporter activity	3	15.79	[SLC25A24, SLC25A4, SLC25A5]
Purine ribonucleotide transmembrane transporter activity	3	15.79	[SLC25A24, SLC25A4, SLC25A5]

Vesicle transport along actin filament	3	15.79	[MYO1D, MYO5C, MYO6]
Negative regulation of natural killer cell mediated cytotoxicity	3	15,79	[CEACAM1, HLA-A, HLA-B]
Regulation of telomerase RNA localization to Cajal body	3	15.79	[CCT2, CCT7, CCT8]
Negative regulation of natural killer cell mediated immunity	3	15.00	[CEACAM1, HLA-A, HLA-B]
2-oxoglutarate metabolic process	3	15.00	[DLST, GOT2, IDH2]
Complement activation, alternative pathway	3	15.00	[C8G, C9, CFH]
Peptidyl-cysteine S-nitrosylation	3	15.00	[DMD, GAPDH, S100A8]
Platelet formation	3	15.00	[ACTN1, MYH9, PTPN6]
Melanosome assembly	3	15,00	[AP1B1, AP1G1, AP1S1]

No.: number.

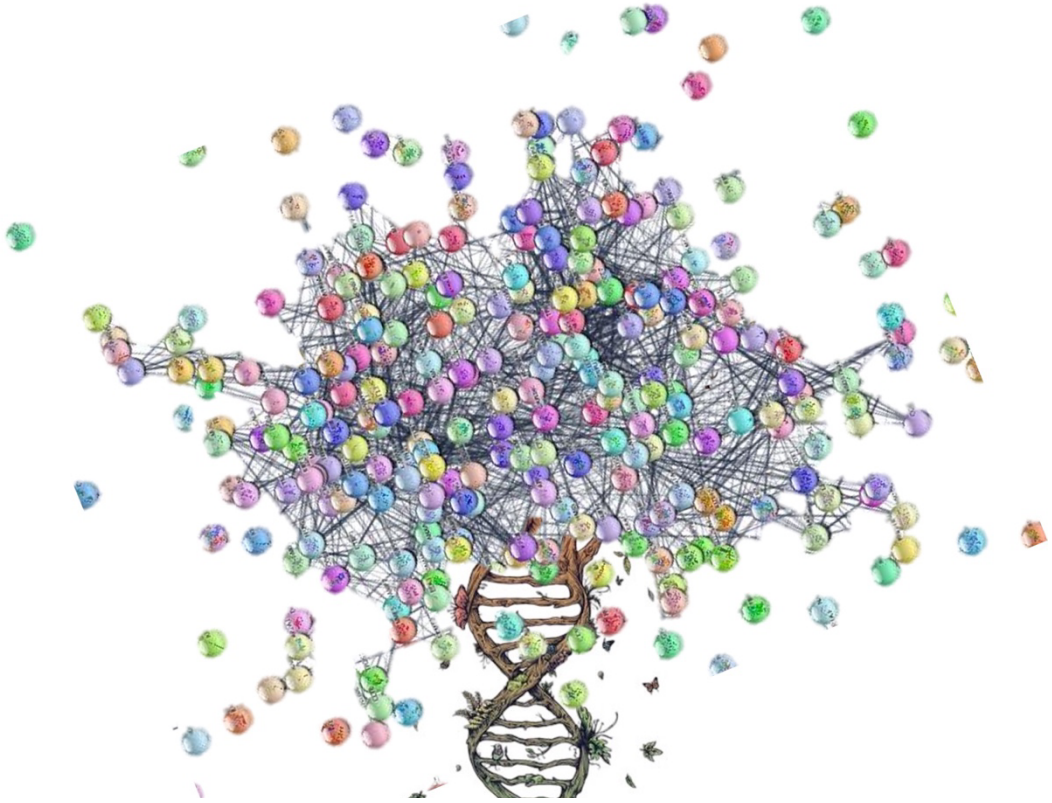

V. DISCUSIÓN GENERAL - GENERAL DISCUSSION

DISCUSIÓN GENERAL

A pesar de los avances en el diagnóstico y tratamiento de la TB, ésta sigue siendo una enfermedad de gran repercusión a nivel mundial, con un gran alcance tanto en salud pública como en salud animal, manteniéndose en la actualidad dentro de las enfermedades infecciosas con mayor impacto económico en la industria ganadera, lo que afecta especialmente a países vulnerables y en vías de desarrollo. Además, el carácter multihospedador de la TB y la compleja interacción hospedador-patógeno hacen que aparezcan importantes desafíos en la inmunopatogenia de la enfermedad debido a las diferencias en la respuesta inmunitaria, la transmisión interespecie y los desafíos diagnósticos. De este modo, los esfuerzos globales se centran actualmente en la detección temprana, la prevención y el control de la enfermedad con el fin de disminuir su propagación, así como, la implementación de nuevas técnicas diagnósticas en los programas de control y erradicación.

En esta tesis doctoral titulada "Aportaciones de la histopatología y de la histología molecular al diagnóstico e inmunopatogenia de la tuberculosis animal" se profundiza en la importancia del estudio histopatológico como técnica complementaria en el diagnóstico de la TB, la expresión de diferentes marcadores relacionados con la activación de macrófagos, como célula diana de esta enfermedad, mediante técnicas de inmunohistoquímica y la utilidad de la histología molecular, a través de la herramienta MALDI-MSI, en la detección de nuevos analitos involucrados en la patogenia de la TB en el bovino y el porcino. Estas tres grandes áreas de trabajo persiguen mejorar la Se y Sp de las técnicas actuales y a su vez contribuir a comprender mejor los mecanismos inmunopatogénicos que puedan ayudar a mejorar el diagnóstico y prevenir la propagación de la enfermedad a través de las medidas de los programas de control y erradicación de esta enfermedad.

En el primer estudio de esta tesis doctoral, se evaluó la utilidad de la histopatología como herramienta de diagnóstico *postmortem* de la TBb al utilizarla combinada en paralelo con otras herramientas diagnósticas, como el cultivo microbiológico o la PCR, o bien de forma individual. Nuestros resultados han permitido identificar el NL

traqueobronquial/mediastínico como el principal NL en el que se evidenciaron lesiones compatibles con TB, seguido del NL retrofaríngeo, lo que destaca la exposición a aerosoles como la principal vía de infección en esta especie (Corner et al., 2012; Ramos et al., 2015; Thoen et al., 2006). Sin embargo, también se observaron lesiones compatibles con TB en el NL mesentérico, indicando que la vía digestiva también tiene que ser considerada como puerta de entrada de micobacterias del CMT, aunque sea menos frecuente (Cardoso-Toset, Gómez-Laguna, et al., 2015; Caswell & Williams, 2016; Corner et al., 2011; Neill et al., 1994; Ramos et al., 2015; Thoen & Barletta, 2006). Estos resultados destacan la importancia de incluir el NL mesentérico en el muestreo de rutina en mataderos para evitar resultados falsos negativos.

El estudio histopatológico resultó ser de especial utilidad para la identificación de lesiones compatibles con TB en animales IDTB$^-$/CMT$^-$/PCR$^-$, destacando la importancia de la histopatología en el diagnóstico al identificar animales falsos negativos por las otras técnicas, ya que en varias de estas muestras se consiguió detectar BAAR mediante la técnica de ZN así como ADN del CMT mediante ddPCR. La histopatología presentó una buena concordancia (κ = 0,608) con respecto a la PCR a tiempo real, mostrando una alta Se (87,5 %) y una buena Sp (84,1 %), lo que la posiciona como una herramienta complementaria útil para mejorar el diagnóstico y control de la TBb.

Además de poner de manifiesto la utilidad de la histopatología como herramienta de diagnóstico de la TBb, los otros dos objetivos de esta tesis doctoral se centraron en evidenciar el uso de la histología, inmunohistoquímica e histología molecular para profundizar en la inmunopatogenia e identificación de moléculas clave de esta enfermedad. De este modo, utilizando el granuloma tuberculoso como unidad experimental y el macrófago como célula diana de la TB (Cardoso-Toset, Gómez-Laguna, et al., 2015; García-Jiménez, Benítez-Medina, et al., 2013; Palmer et al., 2022), se llevó a cabo un estudio comparado de la polarización de macrófagos M1 y M2 en NLs de bovinos y porcinos utilizando un panel de anticuerpos frente a células mieloides (CD172a/MAC387), y marcadores específicos para macrófagos M1 (iNOS/CD68/CD107a) y macrófagos M2 (Arg1/CD163) evaluando su expresión a

través de inmunohistoquímica. Nuestros resultados muestran que la expresión del marcador CD172a presenta un comportamiento similar en macrófagos de granulomas bovinos y porcinos, dibujando una discreta disminución en granulomas de estadios más avanzados (estadios III y IV), mientras que la expresión del marcador MAC387 presentó un aumento en granulomas de estadios avanzados en porcino, diferente a lo publicado por otros autores (García-Jiménez et al., 2012; García-Jiménez et al., 2013), lo que indicaría posibles diferencias en la respuesta inmunitaria frente a la TB entre las dos especies. Además, MAC387 se expresó intensamente en neutrófilos de granulomas tuberculosos porcinos, sin embargo, la función de estos en el contexto de la TB es poco comprendida (Borkute et al., 2021) y su función presenta cierta controversia, ya que si bien pueden fagocitar micobacterias del CMT, también podrían aportar nutrientes a las mismas y causar daños titulares (Borkute et al., 2021; Eum et al., 2010; Persson et al., 2008).

Los marcadores asociados a la polarización de macrófagos M1 (iNOS, CD68 y CD107a) se expresaron de manera más marcada en granulomas de la especie bovina, especialmente en los granulomas de estadios tempranos (estadios I y II), disminuyendo la frecuencia de células positivas en granulomas de estadios más avanzados. Estos resultados coinciden con lo descrito en otros estudios para la iNOS en otras especies (García-Jiménez, et al., 2013; García-Jiménez et al., 2012; Palmer et al., 2007), y sugiere un papel importante del óxido nítrico en el intento de eliminar las micobacterias (Hernández-Pando et al., 2001). La expresión de CD68 siguió la misma tendencia que la de iNOS, habiéndose descrito correlaciones positiva y negativa, respectivamente, entre la expresión de iNOS y CD68 con respecto al recuento de BAAR en la paratuberculosis bovina (Fernández et al., 2017). Sin embargo, en nuestro estudio, centrado en la TB, ambos parámetros presentaron una cinética similar, mostrando una mayor expresión en los granulomas de estadios tempranos (paucibacilares) y disminuyendo su expresión en granulomas de estadio III y IV en los que se observó un mayor número de BAAR, lo que además sugiere una disminución de la polarización M1 desde las etapas iniciales hasta las etapas posteriores de la TB. A pesar de que el marcador CD107a se expresó débilmente en estadios iniciales de los

granulomas en la especie porcina, la expresión de iNOS, CD68 y CD107a apoyan una mayor polarización hacia macrófagos M1 en los granulomas bovinos que en los porcinos, siendo más notable durante las primeras etapas de la infección con el CMT, lo que podría favorecer la persistencia de micobacterias dentro del granuloma.

En cuanto a la polarización M2, la Arg1 mostró una mayor expresión en los granulomas de porcino en comparación con los de bovino, especialmente en los estadios más avanzados, habiéndose descrito resultados similares en otras especies (Kasmi et al., 2009; Mattila et al., 2013; Pessanha et al., 2012). La mayor expresión de Arg1 en porcinos en estadios más avanzados de los granulomas, podría contribuir al control del daño tisular, el cual es generado por el propio granuloma (Bezos, 2011; P. J. Murray, 2017; Pesce et al., 2009). Sin embargo, la molécula CD163 no mostró diferencias significativas entre los distintos estadios de los granulomas en cada una de las especies, pero sí entre ambas especies, siendo mayor su expresión en el ganado bovino que en el porcino y aumentando ligeramente en los granulomas de estadios más avanzados. Esto sugiere que el granuloma tuberculoso en el ganado porcino tiende a tener un perfil M2, sobre todo en los granulomas de estadios III y IV, lo que podría por un lado ser beneficioso para controlar el daño tisular relacionado con los granulomas, pero por otro lado podría indicar incapacidad a la hora de controlar la replicación de la micobacteria, dando lugar a granulomas con formas pluribacilares.

Los resultados obtenidos en este segundo estudio ponen de relieve que en el ganado bovino existe una mayor polarización de macrófagos M1 durante los primeros estadios del granuloma (I y II), que evolucionaría hacia un fenotipo M2 en estadios posteriores. Por el contrario, y debido principalmente a la expresión de Arg1, la polarización de macrófagos M2 predominaría en el ganado porcino.

El tercer objetivo de esta tesis doctoral se centró en estudiar la firma proteica de los granulomas tuberculosos en bovinos y porcinos mediante la técnica MALDI-MSI para identificar rutas de señalización comunes, así como, rutas específicas para cada especie. El análisis de componentes principales mostró una clara separación entre los granulomas de ambas especies según las masas expresadas, lo que indicaría un perfil

proteico diferente según la especie. Aunque se identificaron masas específicas en cada especie, las distintas masas dieron lugar a la representación en algunos casos de los mismos términos en cada especie tras el análisis de ontología. En ambas especies se observó representado el término "Activación del complemento, vía alternativa", lo que indicaría que este mecanismo podría desempeñar un papel importante en la eliminación bacteriana, debido al aumento de la actividad opsonofagocítica (Bezos, 2009; Carroll et al., 2009; Jagatia & Tsolaki, 2021; Krocova et al., 2020), lo que podría estar más desarrollado en el porcino/jabalí en el control de la enfermedad Además, las vías relacionadas con el metabolismo, como el "Ciclo del ácido tricarboxílico" (TCA) y la "Glucólisis/gluconeogénesis", fueron comunes en ambas especies, demostrando la importancia en el metabolismo de la micobacteria, ya que aminoácidos como la arginina, se sintetizan a partir de TCA utilizando como fuente de energía metabolitos del carbono obtenidos a partir de la glucólisis (Xu et al., 2022). Además, en el ganado bovino otro término representado fue el “Metabolismo del nitrógeno”. Lo cual coincide con la expresión de iNOS y Arg1 observado mediante inmunohistoquímica en el segundo estudio, ya que se ha visto que la micobacteria puede aumentar la expresión de Arg1, lo que conlleva a una competencia con iNOS por el sustrato (L-arginina) y a una drástica reducción del óxido nítrico (Kasmi et al., 2009). Del mismo modo, se ha visto que *M. tuberculosis* utiliza estrategias metabólicas flexibles, como el metabolismo del glucógeno y la regulación del TCA, para adaptarse a diversas condiciones nutricionales, incluida su interacción con los macrófagos en el contexto de la infección (Borah et al., 2021), donde se ha observado que para la obtención de la fuente de energía, los macrófagos M1 dependen del glucógeno, mientras que los macrófagos M2 dependen de la mitocondria y del TCA (Ahmad et al., 2022).

Los granulomas bovinos mostraron una activación específica de la "Degranulación de las células natural killer", mientras que los granulomas porcinos mostraron una activación de las vías implicadas en la ”Formación de plaquetas” y “Agregación de plaquetas”, entre otras, lo que puede indicar distintas vías de iniciar y activar la respuesta inmunitaria innata frente al CMT (Kirwan et al., 2021). Además, la “Regulación de la actividad de la endopeptidasa de tipo cisteína implicada en la vía de

señalización apoptótica" se ha observado en ambas especies, pero con activación de proteínas diferentes. Por otro lado, la "Respuesta a la IL-4" y la "Vía de señalización de la IL-17" fueron compartidas entre ambas especies, mostrando actividades opuestas, ya que la primera tiene una función antiinflamatoria, mientras que la segunda tiene actividad proinflamatoria (Mansouri et al., 2018). Sin embargo, en ambas especies se ha identificado la proteína de choque térmico HSP 90-β (HSP90AB1). En otros estudios se ha visto que estas proteínas participan en la polarización de macrófagos M2 para proteger a las bacterias de la presión inmunitaria del hospedador (Lopes et al., 2014; Y. Zhang et al., 2020). Teniendo en cuenta estos antecedentes, sería interesante estudiar la expresión de ésta y de otras moléculas asociadas en granulomas de ambas especies para estudiar su asociación con la polarización de los macrófagos y la resolución de la enfermedad. En este sentido, se ha visto que los macrófagos polarizados M2 expresan niveles más altos de IL-4 (Gunassekaran et al., 2021). Por consiguiente, es evidente que la polarización de los macrófagos es un mecanismo crucial de virulencia con la contribución de múltiples moléculas efectoras por parte del hospedador y del patógeno (Ahmad et al., 2022).

Estos resultados aportan información valiosa sobre las diferencias y similitudes en las firmas proteicas y las rutas de señalización en los granulomas tuberculosos de las especies bovina y porcina. La clara separación entre las dos especies basada en la expresión de proteínas sugiere que la respuesta inmunitaria y la progresión de la enfermedad en la TB pueden tener características específicas de cada especie. La activación compartida de ciertos términos de ontología indica la implicación de rutas comunes en la eliminación de la bacteria y la respuesta inmunitaria. La comprensión de la respuesta inmunitaria específica de cada especie puede tener implicaciones para el desarrollo de enfoques diagnósticos y estrategias de control específicas de la TB tanto en el ganado bovino como en el ganado porcino. Sin embargo, se necesitan más investigaciones para explorar las funciones específicas de estas rutas en la patogenia de la TB en cada especie.

En conjunto, en esta tesis doctoral destaca la importancia del uso de la histopatología como herramienta diagnóstica en el control de la TB, desde su uso más simple en la confirmación de lesiones macroscópicas en animales positivos a la IDTB, cultivo microbiológico y/o PCR desde tejido, hasta el importante valor añadido que tiene al identificar lesiones microscópicas en animales sin lesiones visibles durante la inspección y resultado negativo a las técnicas de diagnóstico de referencia. Por otro lado, la aplicación de herramientas de histología molecular en estudios de inmunopatogenia a través de inmunohistoquímica y de técnicas más avanzadas y novedosas como MALDI-MSI, permite la identificación de nuevas moléculas de interés así como analizar la distribución espacial de estas moléculas en estructuras y células concretas del tejido.

En general, el uso combinado de la histopatología, la inmunohistoquímica y MALDI-MSI permite una evaluación integral para el análisis de muestras de tejido, mejorando la precisión, la detección temprana de enfermedades como la TB y el avance de la investigación en nuevas áreas. El análisis comparado entre distintas especies mediante herramientas como MALDI-MSI, ofrece una identificación especie específica, siendo útil en la comprensión de la inmunopatogenia y el desarrollo de estrategias terapéuticas frente a la TB, así como, la identificación de diferentes rutas metabólicas implicadas en el desarrollo de la enfermedad. Aunque por el momento la información es limitada y los estudios son escasos, los resultados obtenidos sugieren una aplicación novedosa para considerar y profundizar en el desarrollo a futuro de nuevos estudios en el campo de la TB en distintas especies animales.

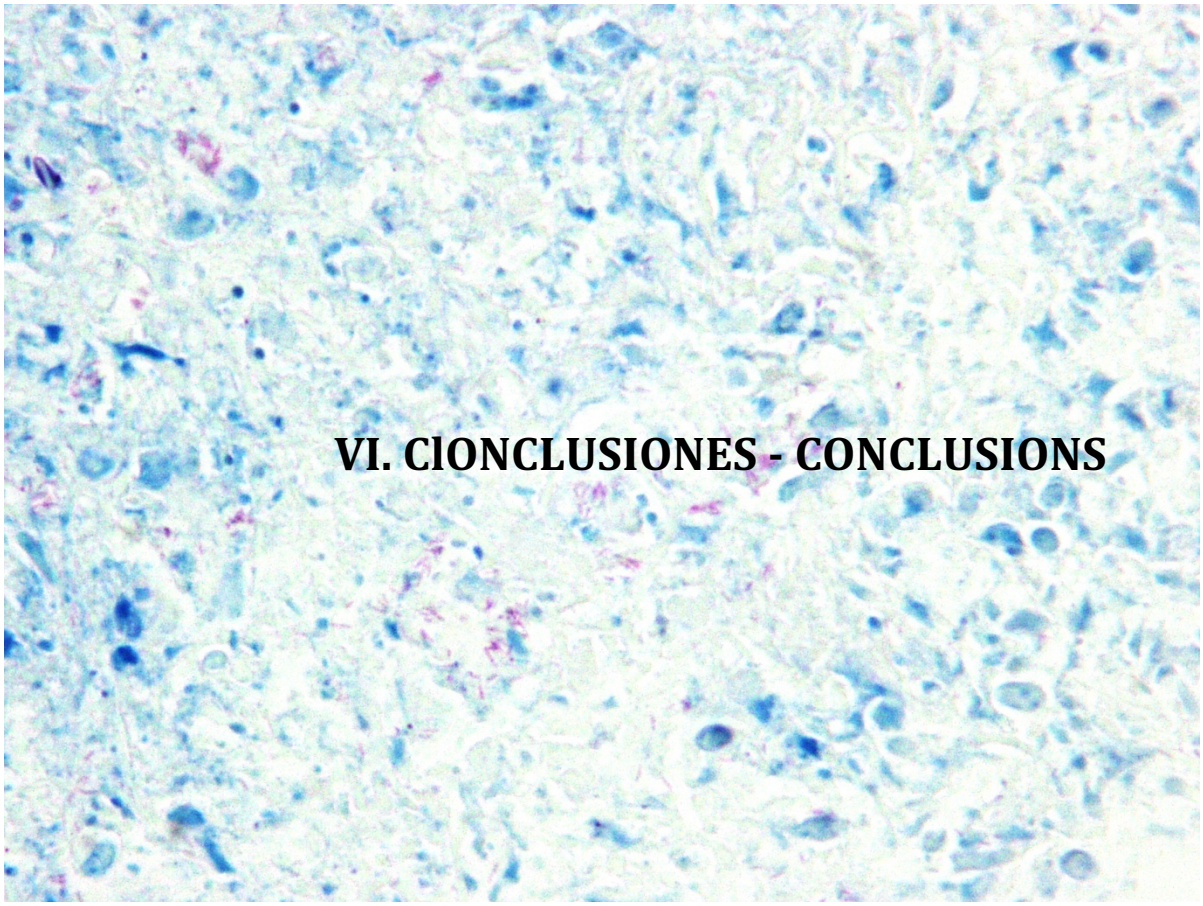

VI. ClONCLUSIONES - CONCLUSIONS

Primera conclusión: La histopatología es una herramienta de diagnóstico valiosa con una Se (87,5 %) y Sp (84,1 %) aceptables para ser utilizada de manera individual o combinada en paralelo junto con la IDTB, PCR a tiempo real y el cultivo bacteriológico. Además, la histopatología permite no sólo confirmar rápidamente los resultados positivos de la IDTB, PCR y el cultivo, sino también detectar animales positivos que dan resultados negativos a estas técnicas. Por estas razones, esta herramienta debería incluirse sistemáticamente en los programas de vigilancia y erradicación de la TBb.

Segunda conclusión: Nuestros resultados en NLs de ganado bovino indican que la polarización de macrófagos M1 prevalece durante los estadios iniciales del granuloma (I y II), mientras que progresa a un fenotipo M2 a medida que los granulomas evolucionan a estadios posteriores. Por el contrario, y debido principalmente a la expresión de Arg1, la polarización de macrófagos M2 es predominante en los granulomas del ganado porcino. Estos resultados se apoyan en nuestro estudio por la ratio iNOS/Arg1 y la ratio entre los marcadores de polarización de macrófagos M1 y M2 (M1/M2).

Tercera conclusión: El análisis proteómico de granulomas tuberculosos de ganado bovino y porcino identifica rutas de señalización compartidas entre ambas especies infectadas por el CMT, como "Activación del complemento, vía alternativa", "Regulación de la actividad endopeptidasa de tipo cisteína implicada en la vía de señalización apoptótica" y "Ciclo del ácido tricarboxílico". Además, este análisis permite identificar términos específicos de especie, como "Degranulación de células natural killer" en bovinos o los relacionados con el reclutamiento y la activación de plaquetas y neutrófilos en ganado porcino, permitiendo profundizar en el conocimiento sobre la interacción hospedador-patógeno en la TB en diferentes especies y destacando la importancia del estudio proteómico para comprender esta enfermedad.

First conclusion: The histopathology is a valuable diagnostic tool with an acceptable Se (87.5%) and Sp (84.1%) to be used alone or together with SIT, real-time PCR, and bacteriological culture. Furthermore, histopathology allows not only a rapid confirmation of SIT, PCR, and culture positive results, but also detecting positive animals that yield negative results to these techniques. For these reasons, this tool should be systematically included in bTB surveillance and eradication programs.

Second conclusion: Our results in NLs, indicate that M1 macrophage polarization prevails during early granuloma stages (I and II) in cattle, whereas a M2 phenotype is also observed in later stages. Contrary, and mainly due to the expression of Arg1, M2 macrophage polarization is predominant in pigs. These results are supported and represented in our study by the ratios iNOS/Arg1 and M1/M2 macrophage polarization markers.

Third conclusion: The proteomic analysis carried out on cattle and pig tuberculous granulomas identifies some GO-enriched terms shared among both species infected by MTC, such as “Complement activation, alternative pathway”, “Regulation of cysteine-type endopeptidase activity involved in apoptotic signaling pathway” and “Tricarboxylic acid cycle”. Furthermore, this analysis allows the identification of species-specific terms, such as “Natural killer cell degranulation” in cattle or those related to platelet and neutrophils recruitment and activation in pigs, providing new insights into host-pathogen interaction in TB in different species and highlighting the importance of studying proteomics in understanding this disease.

VII. REFERENCIAS – REFERENCES

Abebe, F. (2019). Synergy between Th1 and Th2 responses during Mycobacterium tuberculosis infection: A review of current understanding. International Reviews of Immunology, 38(4), 172–179. https://doi.org/10.1080/08830185.2019.16328 42

Ackermann, M. R. (2021). Inflammation and Healing. In J. F. Zachary (Ed.), James F. Zachary - Pathologic Basis of Veterinary Disease (pp. 104–170). Elsevier.

Adams, D. 0. (1974). The structure of mononuclear phagocytes differentiating in vivo I. sequential fine and histologic studies of the Effect of Bacillus Calmette-Guerin (BCG). American Journal of Pathology, 76(1), 17–48.

Ahmad, F., Rani, A., Alam, A., Zarin, S., Pandey, S., Singh, H., Hasnain, S. E., & Ehtesham, N. Z. (2022). Macrophage: A cell with many faces and functions in tuberculosis. Frontiers in Immunology, 13, 747799. https://doi.org/10.3389/fimmu.2022.747799

Aichler, M., & Walch, A. (2015). MALDI Imaging mass spectrometry: Current frontiers and perspectives in pathology research and practice. Laboratory Investigation, 95(4), 422–431. https://doi.org/10.1038/labinvest.2014.156

Albrethsen, J. (2007). Reproducibility in protein profiling by MALDI-TOF mass spectrometry. Clinical Chemistry, 53(5), 852–858. https://doi.org/10.1373/clinchem.2006. 082644

Alexander, K. A., Laver, P. N., Michel, A. L., Williams, M., van Helden, P. D., Warren, R. M., & van Pittius, N. C. G. (2010). Novel mycobacterium tuberculosis complex pathogen, M. Mungi. Emerging Infectious Diseases, 16(8), 1296–1299. https://doi.org/10.3201/eid1608.100314

Álvarez, J. (2008). Complejo Mycobacterium avium, diagnóstico, caracterización molecular e interferencia con el diagnóstico de la tuberculosis. Universidad Complutence de Madrid.

Álvarez, J., de Juan, L., Romero, B., Castellanos, E., Bezos, J., & Rodríguez, L. (2015). Epidemiología y diagnóstico de la tuberculosis bovina. 1–43.

Álvarez, J., de Juan, L., Bezos, J., Romero, B., Sáez, J. L., Gordejo, F. J. R., Briones, V., Moreno, M. Á., Mateos, A., Domínguez, L., & Aranaz, A. (2008a). Interference of paratuberculosis with the diagnosis of tuberculosis in a goat flock with a natural mixed infection. Veterinary Microbiology, 128(1–2), 72–80. https://doi.org/10.1016/j.vetmic.2007.08.034

Álvarez, J., de Juan, L., Bezos, J., Romero, B., Sáez, J. L., Gordejo, F. J. R., Briones, V., Moreno, M. Á., Mateos, A., Domínguez, L., & Aranaz, A. (2008b). Interference of paratuberculosis with the diagnosis of tuberculosis in a goat flock with a natural mixed infection. Veterinary Microbiology, 128(1–2), 72–80. https://doi.org/10.1016/j.vetmic.2007.08.034

Álvarez, J., de Juan, L., Bezos, J., Romero, B., Sáez, J. L., Marqués, S., Domínguez, C., Mínguez, O., Fernández-Mardomingo, B., Mateos, A., Domínguez, L., & Aranaz, A. (2009). Effect of paratuberculosis on the diagnosis of bovine tuberculosis in a cattle herd with a mixed infection using interferon-gamma detection assay. Veterinary Microbiology, 135(3–4), 389–393. https://doi.org/10.1016/j.vetmic.2008.09.060

Álvarez, J., Perez, A., Bezos, J., Marqués, S., Grau, A., Saez, J. L., Mínguez, O., De Juan, L., & Domínguez, L. (2012). Evaluation of the sensitivity and specificity of bovine tuberculosis diagnostic tests in naturally infected cattle herds using a Bayesian approach. Veterinary Microbiology, 155(1), 38–43. https://doi.org/10.1016/j.vetmic.2011.07.034

Andersson, H., Andersson, B., Eklund, D., Ngoh, E., Persson, A., Svensson, K., Lerm, M., Blomgran, R., & Stendahl, O. (2014). Apoptotic neutrophils augment the inflammatory response to Mycobacterium tuberculosis infection in human macrophages. PLoS ONE, 9(7). https://doi.org/10.1371/journal.pone.0101514

Angkawanish, T., Morar, D., van Kooten, P., Bontekoning, I., Schreuder, J., Maas, M., Wajjwalku, W., Sirimalaisuwan, A., Michel, A., Tijhaar, E., & Rutten, V. (2013). The elephant interferon gamma assay: A contribution to diagnosis of

tuberculosis in elephants. Transboundary and Emerging Diseases, 60(Suppl 1), 53–59. https://doi.org/10.1111/tbed.12098

Aranaz, A., Cousins, D., Mateos, A., & Domínguez, L. (2003). Elevation of Mycobacterium tuberculosis subsp. caprae Aranaz et al. 1999 to species rank as Mycobacterium caprae comb. nov., sp. nov. International Journal of Systematic and Evolutionary Microbiology, 53(6), 1785–1789. https://doi.org/10.1099/ijs.0.02532-0

Aranaz, A., De Juan, L., Bezos, J., Álvarez, J., Romero, B., Lozano, F., Paramio, J. L., López-Sánchez, J., Mateos, A., & Domínguez, L. (2006). Assessment of diagnostic tools for eradication of bovine tuberculosis in cattle co-infected with Mycobacterium bovis and M. avium subsp. paratuberculosis. Veterinary Research, 37(4), 593–606. https://doi.org/10.1051/vetres:2006021

Aranday-Cortes, E., Bull, N. C., Villarreal-Ramos, B., Gough, J., Hicks, D., Ortiz-Peláez, Á., Vordermeier, H. M., & Salguero, F. J. (2013). Upregulation of IL-17A, CXCL9 and CXCL10 in early-stage granulomas induced by Mycobacterium bovis in cattle. Transboundary and Emerging Diseases, 60(6), 525–537. https://doi.org/10.1111/j.1865-1682.2012.01370.x

Arcos, J., Sasindran, S. J., Fujiwara, N., Turner, J., Schlesinger, L. S., & Torrelles, J. B. (2011). Human lung hydrolases delineate Mycobacterium tuberculosis –macrophage interactions and the capacity to control infection. The Journal of Immunology, 187(1), 372–381. https://doi.org/10.4049/jimmunol.1100823

Aspatwar, A., Gong, W., Wang, S., Wu, X., & Parkkila, S. (2022). Tuberculosis vaccine BCG: the magical effect of the old vaccine in the fight against the COVID-19 pandemic. International Reviews of Immunology, 41(2), 283–296. https://doi.org/10.1080/08830185.2021.1922685

Aung, Y. W., Faksri, K., Sangka, A., Tomanakan, K., & Namwat, W. (2023). Heteroresistance of Mycobacterium tuberculosis in the sputum detected by droplet digital PCR. Biology, 12(4). https://doi.org/10.3390/biology12040525

Ayele, W. Y., Neill, S. D., Zinsstag, J., Weiss, M. G., & Pavlik, I. (2004). Bovine tuberculosis: An old disease but a new threat to Africa. The International Journal of Tuberculosis and Lung Disease, 8(8), 924–937.

Baker, M. (2012). Digital PCR hits its stride. Nature Methods, 9(6), 541–544. https://doi.org/10.1038/nmeth.2027

Balseiro, A., Gortázar, C., & Sáez LLorente, J. L. (2020). Tuberculosis animal: Una aproximación desde la perspectiva de la ciencia y la administración (P. y Alimentación. Ministerio de Agricultura, Secretaría General Técnica. Centro de publicaciones., & Centro de publicaciones, Eds.). https://cpage.mpr.gob.es/

Barberis, I., Bragazzi, N. L., Galluzzo, L., & Martini, M. (2017). The history of tuberculosis: From the first historical records to the isolation of Koch's bacillus. Journal of Preventive Medicine and Hygiene, 58(1), E9–E12.

Barbier, Maxime., & Wirth, Thierry. (2016). The evolutionary history, demography, and spread of the Mycobacterium tuberculosis complex. Microbiology Spectrum, 4(4). https://doi.org/10.1128/microbiolspec.tbtb2-0008-2016

Beine, B., Diehl, H. C., Meyer Helmut E, & Henkel Corinna. (2016). Tissue MALDI mass spectrometry imaging (MALDI MSI) of peptides. In Reinders Jörg (Ed.), Proteomics in Systems Biology Methods and Protocols Methods in Molecular Biology (Vol. 1394, pp. 129–150). Humana Press. https://doi.org/10.1007/978-1-4939-3341-9_10

Berggren, W. T., Takova, T., Olson, M. C., Eis, P. S., Kwiatkowski, R. W., & Smith, L. M. (2002). Multiplexed gene expression analysis using the invader RNA assay with MALDI-TOF mass spectrometry detection. Analytical Chemistry, 74(8), 1745–1750. https://doi.org/10.1021/ac011167t

Bermejo, M. C., Clavera, I., Michel De La Rosa, F. J., & Marín, B. (2007). Epidemiología de la tuberculosis. Anales Del Sistema Sanitario de Navarra, 30(2), 7–19.

Beste, D. J. V., Espasa, M., Bonde, B., Kierzek, A. M., Stewart, G. R., & McFadden, J. (2009). The genetic requirements for fast and slow growth in mycobacteria. PLoS ONE, 4(4). https://doi.org/10.1371/journal.pone.0005349

Bezos, J. (2009, January 28). Reconocimiento antigénico y respuesta inmune innata en la tuberculosis bovina. Revista VISAVET Divulgación . www.visavet.es/es/articulos/reconocimiento-antigenico-respuesta-inmune-innata-tuberculosis-bovina.php

Bezos, J. (2011). Tuberculosis caprina: estudio de la respuesta inmune y aportaciones a su diagnóstico. Centro de vigilancia Sanitaria Veterinaria (VISAVET).

Bezos, J., Álvarez, J., Romero, B., Aranaz, A., & Juan, L. de. (2012). Tuberculosis in goats: Assessment of current in vivo cell-mediated and antibody-based diagnostic assays. Veterinary Journal, 191(2), 161–165. https://doi.org/10.1016/j.tvjl.2011.02.010

Bezos, J., Álvarez, J., Romero, B., de Juan, L., & Domínguez, L. (2014). Bovine tuberculosis: Historical perspective. In Research in Veterinary Science (Vol. 97, Issue S, pp. S3–S4). Elsevier B.V. https://doi.org/10.1016/j.rvsc.2014.09.003

Bezos, J., Romero, B., de Juan, L., González, S., & Saéz, J. (2019). Realización de las pruebas de intradermotuberculinización y gamma-interferón. In Manuales de procedimientos sanitarios, VISAVET (2nd ed.). VISAVET, Universidad Complutence de Madrid. www.visavet.es/data/mapa/manual_procedimiento_IDTB_IFN_2019.pdf

Bezos, J., Roy, Á., Infantes-Lorenzo, J. A., González, I., Venteo, Á., Romero, B., Grau, A., Mínguez, O., Domínguez, L., & de Juan, L. (2018). The use of serological tests in combination with the intradermal tuberculin test maximizes the detection of tuberculosis infected goats. Veterinary Immunology and Immunopathology, 199, 43–52. https://doi.org/10.1016/j.vetimm.2018.03.006

Bezos, Javier., Casal, Carmen., Romero, Beatriz., Schroeder, Bjoern., Hardegger, Roland., Raeber, A. J., López, Lissette., Rueda, Paloma., & Domínguez, Lucas. (2014).

Current ante-mortem techniques for diagnosis of bovine tuberculosis. Research in Veterinary Science, 97(S), S44–S52. https://doi.org/10.1016/j.rvsc.2014. 04.002

Biberstein, E. L. (1994). Especies de Mycobacterium: Agentes de las tuberculosis de los animales. In E. L. Biberstein & Y. C. Zee (Eds.), Tratado de microbiología veterinaria (pp. 229–240). Acribia.

Blanc, L., Lenaerts, A., Dartois, V., & Prideaux, B. (2018). Visualization of mycobacterial biomarkers and tuberculosis drugs in infected tissue by MALDI-MS Imaging. Analytical Chemistry, 90(10), 6275–6282. https://doi.org/10.1021/acs.analchem.8b00985

Bolin, C. A., Whipple, D. L., Khanna, K. V, Risdahl, J. M., Peterson, P. K., & Molitor, T. W. (1997). Infection of swine with Mycobacterium bovis as a model of human tuberculosis. Journal of Infectious Diseases, 176(6), 1559–1566. https://doi.org/10.1086/514155

Borah, K., Mendum, T. A., Hawkins, N. D., Ward, J. L., Beale, M. H., Larrouy-Maumus, G., Bhatt, A., Moulin, M., Haertlein, M., Strohmeier, G., Pichler, H., Forsyth, V. T., Noack, S., Goulding, C. W., McFadden, J., & Beste, D. J. V. (2021). Metabolic fluxes for nutritional flexibility of Mycobacterium tuberculosis. Molecular Systems Biology, 17(5). https://doi.org/10.15252/msb.202110280

Borkute, R. R., Woelke, S., Pei, G., & Dorhoi, A. (2021). Neutrophils in tuberculosis: Cell biology, cellular networking and multitasking in host defense. International Journal of Molecular Sciences, 22(9), 4801. https://doi.org/10.3390/ijms 22094801

Braian, C., Hogea, V., & Stendahl, O. (2013). Mycobacterium tuberculosis-induced neutrophil extracellular traps activate human macrophages. Journal of Innate Immunity, 5(6), 591–602. https://doi.org/10.1159/000348676

Buddle, B. M., Livingstone, P. G., & De Lisle, G. W. (2009). Advances in ante-mortem diagnosis of tuberculosis in cattle. New Zealand Veterinary Journal, 57(4), 173–180. https://doi.org/10.1080/00480169.2009.36899

Byrne, A. W., Graham, J., Brown, C., Donaghy, A., Guelbenzu-Gonzalo, M., McNair, J., Skuce, R. A., Allen, A., & McDowell, S. W. (2018). Modelling the variation in skin-test tuberculin reactions, post-mortem lesion counts and case pathology in tuberculosis-exposed cattle: Effects of animal characteristics, histories and co-infection. Transboundary and Emerging Diseases, 65(3), 844–858. https://doi.org/10.1111/tbed.12814

Cao, Z., Wu, W., Wei, H., Gao, C., Zhang, L., Wu, C., & Hou, L. (2020). Using droplet digital PCR in the detection of Mycobacterium tuberculosis DNA in FFPE samples. International Journal of Infectious Diseases, 99, 77–83. https://doi.org/10.1016/j.ijid.2020.07.045

Cardona, P. J. (2016). The progress of therapeutic vaccination with regard to tuberculosis. Frontiers in Microbiology, 7, 1536. https://doi.org/10.3389/ fmicb.2016.01536

Cardona, P. J. (2017). What we have learned and what we have missed in tuberculosis pathophysiology for a new vaccine design: Searching for the 'pink swan'. Frontiers in Immunology, 8(MAY). https://doi.org/10.3389/fimmu.2017.00556

Cardona, P. J. (2018). Pathogenesis of tuberculosis and other mycobacteriosis. Enfermedades Infecciosas y Microbiologia Clinica, 36(1), 38–46. https://doi.org/10.1016/j.eimc.2017.10.015

Cardoso, M. A., Cardoso, R. F., Hirata, R. D. C., Hirata, M. H., Leite, C. Q. F., Santos, A. C. B., Siqueira, V. L. D., Okano, W., Rocha, N. S., & Lonardoni, M. V. C. (2009). Direct detection of Mycobacterium bovis in bovine lymph nodes by PCR. Zoonoses and Public Health, 56(8), 465–470. https://doi.org/10.1111/j.1863-2378.2008.01199.x

Cardoso-Toset, F., Gómez-Laguna, J., Amarilla, S. P., Vela, A. I., Carrasco, L., Fernández-Garayzábal, J. F., Astorga, R. J., & Luque, I. (2015). Multi-etiological nature of tuberculosis-like lesions in condemned pigs at the slaughterhouse. PLoS ONE, 10(9), 1–12. https://doi.org/10.1371/journal.pone.0139130

Cardoso-Toset, F., Luque, I., Amarilla, S. P., Gómez-Gascón, L., Fernández, L., Huerta, B., Carrasco, L., Ruiz, P., & Gómez-Laguna, J. (2015). Evaluation of rapid methods for diagnosis of tuberculosis in slaughtered free-range pigs. Veterinary Journal, 204(2), 232–234. https://doi.org/10.1016/j.tvjl.2015.01.022

Cardoso-Toset, F., Luque, I., Carrasco, L., Jurado-Martos, F., Risalde, M. Á., Venteo, Á., Infantes-Lorenzo, J. A., Bezos, J., Rueda, P., Gortázar, C., Domínguez, L., Domínguez, M., & Gomez-Laguna, J. (2016). Evaluation of four ELISA assays to diagnose Mycobacterium tuberculosis complex infection in pigs. 8th European Symposium of Porcine Health Management. http://hdl.handle.net/10261/175668

Cardoso-Toset, F., Luque, I., Carrasco, L., Jurado-Martos, F., Risalde, M. Á., Venteo, Á., Infantes-Lorenzo, J. A., Bezos, J., Rueda, P., Tapia, I., Gortázar, C., Domínguez, L., Domínguez, M., & Gomez-Laguna, J. (2017). Evaluation of five serologic assays for bovine tuberculosis surveillance in domestic free-range pigs from southern Spain. Preventive Veterinary Medicine, 137, 101–104. https://doi.org/10.1016/j.prevetmed.2016.12.016

Carroll, M. V., Lack, N., Sim, E., Krarup, A., & Sim, R. B. (2009). Multiple routes of complement activation by Mycobacterium bovis BCG. Molecular Immunology, 46(16), 3367–3378. https://doi.org/10.1016/j.molimm.2009.07.015

Casal, C., Infantes, J. A., Risalde, M. A., Díez-Guerrier, A., Domínguez, M., Moreno, I., Romero, B., de Juan, L., Sáez, J. L., Juste, R., Gortázar, C., Domínguez, L., & Bezos, J. (2017). Antibody detection tests improve the sensitivity of tuberculosis diagnosis in cattle. Research in Veterinary Science, 112, 214–221. https://doi.org/10.1016/j.rvsc.2017.05.012

Cassidy, J. P. (2008). The pathology of bovine tuberculosis: Time for an audit. In Veterinary Journal (Vol. 176, Issue 3, pp. 263–264). https://doi.org/10.1016/j.tvjl.2007.09.001

Cassidy, J. P., Bryson, D. G., Pollock, J. M., Evans, R. T., Forster, F., & Neill, S. D. (1998). Early lesion formation in cattle experimentally infected with Mycobacterium bovis. Journal of Comparative Pathology, 119(1), 27–44. https://doi.org/10.1016/s0021-9975(98)80069-8

Castets, M., Boisvert, H., Grumbach, F., Brunel, M., & Rist, N. (1968). Tuberculosis bacilli of the african type: Preliminary note. Revue de Tuberculose et de Pneumologie, 32(2), 179–184.

Caswell, J. L., & Williams, K. J. (2016). Respiratory System. In M. Grant Maxie (Ed.), Pathology of Domestics Animals (6th ed., Vol. 2, pp. 465–591).

Cegielski, J. P., Devlin, B. H., Morris, A. J., Kitinya, J. N., Pulipaka, U. P., Lema, L. E. K., Lwakatare, J., & Reller, L. B. (1997). Comparison of PCR, culture, and histopathology for diagnosis of tuberculous pericarditis. Journal of Clinical Microbiology, 35(12), 3254–3257. https://doi.org/10.1128/jcm.35.12.3254-3257.1997

Chaurand, P., Latham, J. C., Lane, K. B., Mobley, J. A., Polosukhin, V. V., Wirth, P. S., Nanney, L. B., & Caprioli, R. M. (2008). Imaging mass spectrometry of intact proteins from alcohol-preserved tissue specimens: Bypassing formalin fixation. Journal of Proteome Research, 7(8), 3543–3555. https://doi.org/10.1021/pr800286z

Chaurand, P., Schwartz, S. A., Billheimer, D., Xu, B. J., Crecelius, A., & Caprioli, R. M. (2004). Integrating Histology and Imaging Mass Spectrometry. Analytical Chemistry, 76(4), 1145–1155. https://doi.org/10.1021/ac0351264

Chen, B., Jiang, Y., Cao, X., Liu, C., Zhang, N., & Shi, D. (2021). Droplet digital PCR as an emerging tool in detecting pathogens nucleic acids in infectious diseases. Clinica Chimica Acta, 517, 156–161. https://doi.org/10.1016/j.cca.2021.02.008

Chen, R., Mias, G. I., Li-Pook-Than, J., Jiang, L., Lam, H. Y. K., Chen, R., Miriami, E., Karczewski, K. J., Hariharan, M., Dewey, F. E., Cheng, Y., Clark, M. J., Im, H., Habegger, L., Balasubramanian, S., O'Huallachain, M., Dudley, J. T., Hillenmeyer, S., Haraksingh, R., … Snyder, M. (2012). Personal omics profiling reveals dynamic molecular and medical phenotypes. Cell, 148(6), 1293–1307. https://doi.org/10.1016/j.cell.2012.02.009

Claes, B. S. R., Krestensen, K. K., Yagnik, G., Grgic, A., Kuik, C., Lim, M. J., Rothschild, K. J., Vandenbosch, M., & Heeren, R. M. A. (2023). MALDI-IHC-Guided in-depth spatial proteomics: Targeted and untargeted MSI combined. Analytical Chemistry, 95(4), 2329–2338. https://doi.org/10.1021/acs.analchem.2c04220

Collins, D. M., & Stephens, D. M. (1991). Identification of an insertion sequence, IS1081, in Mycobacterium bovis. FEMS Microbiology Letters, 83(1), 11–16. https://doi.org/10.1111/j.1574-6968.1991.tb04380.x

Comer, L. A. (1994). Post mortem diagnosis of Mycobacterium bovis infection in cattle. Veterinary Microbiology, 40(1–2), 53–63. https://doi.org/10.1016/0378-1135(94)90046-9.

Corner, L. A. L. (2006). The role of wild animal populations in the epidemiology of tuberculosis in domestic animals: How to assess the risk. Veterinary Microbiology, 112(2–4), 303–312. https://doi.org/10.1016/j.vetmic.2005.11.015

Corner, L. A. L., Gormley, E., & Pfeiffer, D. U. (2012). Primary isolation of Mycobacterium bovis from bovine tissues: Conditions for maximising the number of positive cultures. Veterinary Microbiology, 156(1–2), 162–171. https://doi.org/10.1016/j.vetmic.2011.10.016

Corner, L. A. L., Murphy, D., & Gormley, E. (2011). Mycobacterium bovis infection in the Eurasian Badger (Meles meles): The disease, pathogenesis, epidemiology and control. Journal of Comparative Pathology, 144(1), 1–24. https://doi.org/10.1016/j.jcpa.2010.10.003

Corner, L. A. L., Ni Bhuachalla, D., Gormley, E., & More, S. (2014). The role of badgers in the epidemiology of Mycobacterium bovis infection (tuberculosis) in cattle in the United Kingdom and the Republic of Ireland: current perspectives on control strategies. Veterinary Medicine: Research and Reports, 27. https://doi.org/10.2147/vmrr.s53643

Corpa, J. M., Garrido, J., García Marín, J. F., & Pérez, V. (2000). Classification of lesions observed in natural cases of paratuberculosis in goats. Journal of Comparative Pathology, 122(4), 255–265. https://doi.org/10.1053/jcpa.1999.0368

Cosivi, O., Granje, J. M., Daborn, C. J., Raviglione, M. C., Fujikura, T., Cousins, D., Robinson, R. A., Huchzermeyer, H. F. A. K., de Kantor, I., & Meslin, F. X. (1998). Zoonotic tuberculosis due to Mycobacterium bovis in developing countries. Emerging Infectious Diseases, 4(1), 59–70. https://doi.org/doi.org/10.3201/eid0401.980108

Courcoul, A., Moyen, J. L., Brugère, L., Faye, S., Hénault, S., Gares, H., & Boschiroli, M. L. (2014). Estimation of sensitivity and specificity of bacteriology, histopathology and PCR for the confirmatory diagnosis of bovine tuberculosis using latent class analysis. PLoS ONE, 9(3). https://doi.org/10.1371/journal.pone.0090334

Cousins, D. V. (2001). Mycobacterium bovis infection and control in domestic livestock. Revue Scientifique et Technique (International Office of Epizootics), 20(1), 71–85. https://doi.org/doi.org/10.20506/rst.20.1.1263

Cousins, D. V., Bastida, R., Cataldi, A., Quse, V., Redrobe, S., Dow, S., Duignan, P., Murray, A., Dupont, C., Ahmed, N., Collins, D. M., Butler, W. R., Dawson, D., Rodríguez, D., Loureiro, J., Romano, M. I., Alito, A., Zumarraga, M., & Bernardelli, A. (2003). Tuberculosis in seals caused by a novel member of the Mycobacterium tuberculosis complex: Mycobacterium pinnipedii sp. nov. International Journal of Systematic and Evolutionary Microbiology, 53(5), 1305–1314. https://doi.org/10.1099/ijs.0.02401-0

Crawshaw, T., Daniel, R., Clifton-Hadley, R., Clark, J., Evans, H., Rolfe, S., & De La Rua-Domenech, R. (2008). TB in goats caused by Mycobacterium bovis. Veterinary Record, 163(4), 127. https://doi.org/10.1136/vr.163.4.127

Cronan, M. R., Beerman, R. W., Rosenberg, A. F., Saelens, J. W., Johnson, M. G., Oehlers, S. H., Sisk, D. M., Jurcic Smith, K. L., Medvitz, N. A., Miller, S. E., Trinh, L. A., Fraser, S. E., Madden, J. F., Turner, J., Stout, J. E., Lee, S., & Tobin, D. M. (2016). Macrophage epithelial reprogramming underlies mycobacterial granuloma formation and promotes infection. Immunity, 45(4), 861–876. https://doi.org/10.1016/j.immuni.2016.09.014

Daftary, V. G., Banker, D. D., & Daftary, G. V. (1994). ELISA test for tuberculosis. Indian Journal of Medical Sciences, 48(2), 39–42.

Dalley, D., Davé, D., Lesellier, S., Palmer, S., Crawshaw, T., Hewinson, R. G., & Chambers, M. (2008). Development and evaluation of a gamma-interferon assay for tuberculosis in badgers (Meles meles). Tuberculosis, 88(3), 235–243. https://doi.org/10.1016/j.tube.2007.11.001

Daniel, T. M. (2006). The history of tuberculosis. Respiratory Medicine, 100(11), 1862–1870. https://doi.org/10.1016/j.rmed.2006.08.006

Dannenberg, A. M. (1994). Roles of cytotoxic delayed-type hypersensitivity and macrophage-activating cell-mediated immunity in the pathogenesis of tuberculosis. Immunobiology, 191(4–5), 461–473. https://doi.org/10.1016/S01712985(11)80452-3

Datta, S., Malhotra, L., Dickerson, R., Chaffee, S., Sen, C. K., & Roy, S. (2015). Laser capture microdissection: Big data from small samples. Histology and Histopathology, 30(11), 1255–1269. https://doi.org/10.14670/HH-11-622

de la Rua-Domenech, R., Goodchild, A. T., Vordermeier, H. M., Hewinson, R. G., Christiansen, K. H., & Clifton-Hadley, R. S. (2006). Ante mortem diagnosis of tuberculosis in cattle: A review of the tuberculin tests, γ-interferon assay and other

ancillary diagnostic techniques. Research in Veterinary Science, 81(2), 190–210. https://doi.org/10.1016/j.rvsc.2005.11.005

de Lisle, G. W., Bengis, R. G., Schmitt, S. M., & O;Brien, D. J. (2002). Tuberculosis in free-ranging wildlife: detection, diagnosis and management. Revue Scientifique et Technique (International Office of Epizootics, 21(2), 317–334. https://doi.org/doi.org/10.20506/rst.21.2.1339

de Lisle, G. W., Collins, D. M., Loveday, A. S., Young, W. A., & Julian, A. F. (1990). A report of tuberculosis in cats in new zealand, and the examination of strains of mycobuctetium bovis by dna restriction endonuclease analysis. New Zealand Veterinary Journal, 38(1), 10–13. https://doi.org/10.1080/00480169.1990.35606

Dennis Lo, Y. M., Lun, F. M. F., Chan, A., Tsui, N. B. Y., Chong, K. C., Lau, T. K., Leung, T. Y., Zee, B. C. Y., Cantor, C. R., Chiu, R. W. K., Li, ‡ *, & Shing, K. (2007). Digital PCR for the molecular detection of fetal chromosomal aneuploidy. Roceedings of the National Academy of Sciences of the United States of America, 104(32), 13116–13121. https://doi.org/doi.org/10.1073/pnas.0705765104

Denti, V., Capitoli, G., Piga, I., Clerici, F., Pagani, L., Criscuolo, L., Bindi, G., Principi, L., Chinello, C., Paglia, G., Magni, F., & Smith, A. (2022). Spatial multiomics of lipids, N-glycans, and tryptic peptides on a single FFPE tissue section. Journal of Proteome Research, 21(11), 2798–2809. https://doi.org/10.1021/acs.jproteome.2c00601

Deutskens, F., Yang, J., & Caprioli, R. M. (2011). High spatial resolution imaging mass spectrometry and classical histology on a single tissue section. Journal of Mass Spectrometry, 46(6), 568–571. https://doi.org/10.1002/jms.1926

Devonshire, A. S., O'Sullivan, D. M., Honeyborne, I., Jones, G., Karczmarczyk, M., Pavšič, J., Gutteridge, A., Milavec, M., Mendoza, P., Schimmel, H., Van Heuverswyn, F., Gorton, R., Cirillo, D. M., Borroni, E., Harris, K., Barnard, M., Heydenrych, A., Ndusilo, N., Wallis, C. L., … Huggett, J. F. (2016). The use of digital PCR to improve

the application of quantitative molecular diagnostic methods for tuberculosis. BMC Infectious Diseases, 16(1), 1–10. https://doi.org/10.1186/s12879-016-1696-7

Di Marco, V., Mazzone, P., Capucchio, M. T., Boniotti, M. B., Aronica, V., Russo, M., Fiasconaro, M., Cifani, N., Corneli, S., Biasibetti, E., Biagetti, M., Pacciarini, M. L., Cagiola, M., Pasquali, P., & Marianelli, C. (2012). Epidemiological significance of the domestic black pig (Sus scrofa) in maintenance of bovine tuberculosis in Sicily. Journal of Clinical Microbiology, 50(4), 1209–1218. https://doi.org/10.1128/JCM.06544-11

Dingle, T. C., Sedlak, R. H., Cook, L., & Jerome, K. R. (2014). Tolerance of droplet-digital PCR vs real-time quantitative PCR to inhibitory substances. Clinical Chemistry, 59(11), 1670–1672. https://doi.org/10.1373/clinchem.2013.211045

Dorronsoro, I., & Torroba, L. (2007). Microbiología de la tuberculosis. Anales del Sistema Sanitario de Navarra, 30(2), 67–85. http://scielo.isciii.es/scielo.php?script=sci_arttext&pid=S113766272007000400006&nrm=iso

Dranoff, G. (2004). Cytokines in cancer pathogenesis and cancer therapy. Nature Reviews Cancer, 4(1), 11–22. https://doi.org/10.1038/nrc1252

Dreo, T., Pirc, M., Ramšak, Ž., Pavšič, J., Milavec, M., Žel, J., & Gruden, K. (2014). Optimising droplet digital PCR analysis approaches for detection and quantification of bacteria: A case study of fire blight and potato brown rot. Analytical and Bioanalytical Chemistry, 406(26), 6513–6528. https://doi.org/10.1007/s00216-014-8084-1

Echeverria-Valencia, Gabriela., Flores-Villalva, Susana., & Espitia, C. I. (2018). Virulence factors and pathogenicity of Mycobacterium. In W. Ribón (Ed.), Mycobacterium Research and Development (pp. 231–255). IntechOpen. https://doi.org/10.5772/intechopen.72027

Eum, S. Y., Kong, J. H., Hong, M. S., Lee, Y. J., Kim, J. H., Hwang, S. H., Cho, S. N., Via, L. E., & Barry, C. E. (2010). Neutrophils are the predominant infected phagocytic cells in the airways of patients with active pulmonary TB. Chest, 137(1), 122–128. https://doi.org/10.1378/chest.09-0903

Faurschou, M., & Borregaard, N. (2003). Neutrophil granules and secretory vesicles in inflammation. In Microbes and Infection (Vol. 5, Issue 14, pp. 1317–1327). Elsevier Masson SAS. https://doi.org/10.1016/j.micinf.2003.09.008

Ferguson, J. S., & Schlesinger, L. S. (2000). Pulmonary surfactant in innate immunity and the pathogenesis of tuberculosis. Tubercle and Lung Disease, 80(4–5), 173–184. https://doi.org/10.1054/tuld.2000.0242

Fernández, M., Benavides, J., Castaño, P., Elguezabal, N., Fuertes, M., Muñoz, M., Royo, M., Ferreras, M. C., & Pérez, V. (2017). Macrophage subsets within granulomatous intestinal lesions in bovine paratuberculosis. Veterinary Pathology, 54(1), 82–93. https://doi.org/10.1177/0300985816653794

Fernández-Vega, A., Chicano-Gálvez, E., Prentice, B. M., Anderson, D., Priego-Capote, F., López-Bascón, M. A., Calderón-Santiago, M., Avendaño, M. S., Guzmán-Ruiz, R., Tena-Sempere, M., Fernández, J. A., Caprioli, R. M., & Malagón, M. M. (2020). Optimization of a MALDI-Imaging protocol for studying adipose tissue-associated disorders. Talanta, 219, 121184. https://doi.org/10.1016/j.talanta.2020.121184

Fitzgerald, S. D., & Kaneene, J. B. (2013). Wildlife reservoirs of bovine tuberculosis worldwide: Hosts, pathology, surveillance, and control. Veterinary Pathology, 50(3), 488–499. https://doi.org/10.1177/0300985812467472

Fitzgerald, S. D., Kaneene, J. B., Butler, K. L., Clarke, K. R., Fierke, J. S., Schmitt, S. M., Bruning-Fann, C. S., Mitchell, R. R., Berry, D. E., & Payeur, J. B. (2000). Comparison of postmortem techniques for the detection of Mycobacterium bovis in white-tailed deer (Odocoileus virginianus). Journal of Veterinary Diagnostic Investigation, 12(4), 322–327. https://doi.org/10.1177/104063870001200404

Flores-Villalva, S., Suárez-Güemes, F., Espitia, C., Whelan, A. O., Vordermeier, M., & Gutiérrez-Pabello, J. A. (2012). Specificity of the tuberculin skin test is modified by use of a protein cocktail containing ESAT-6 and CFP-10 in cattle naturally infected with Mycobacterium bovis. Clinical and Vaccine Immunology, 19(5), 797–803. https://doi.org/10.1128/CVI.05668-11

Flynn, J. A. L. (2006). Lessons from experimental Mycobacterium tuberculosis infections. Microbes and Infection, 8(4), 1179–1188. https://doi.org/10.1016/j.micinf.2005.10.033

Flynn, J. L., Chan, J., & Lin, P. L. (2011). Macrophages and control of granulomatous inflammation in tuberculosis. Mucosal Immunology, 4(3), 271–278. https://doi.org/10.1038/mi.2011.14

Gaffney, E., Murphy, D., Walsh, A., Connolly, S., Basdeo, S. A., Keane, J., & Phelan, J. J. (2022). Defining the role of neutrophils in the lung during infection: Implications for tuberculosis disease. Frontiers in Immunology, 13, 984293. https://doi.org/10.3389/fimmu.2022.984293

Garbaccio, S. G., Garro, C. J., Delgado, F. O., Tejada, G. A., Eirin, M. E., Huertas, P. S., Leon, L. A., & Zumárraga, M. J. (2019). Enzyme-linked immunosorbent assay as complement of intradermal skin test for the detection of Mycobacterium bovis infection in cattle. Tuberculosis (Edinburgh, Scotland), 117, 56–61. https://doi.org/10.1016/j.tube.2019.05.006

Garcia, M. A., Yee, J., Bouley, D. M., Moorhead, Roberta., & Lerche, N. W. (2004). Diagnosis of tuberculosis in macaques, using whole-blood in vitro interferon-gamma (PRIMAGAM) testing. Comparative Medicine, 54(1), 86–92.

García, M. de los Á., Sarmiento, M. E., & Acosta, A. (2009). La inmunidad antituberculosa y su aplicación en el desarrollo de candidatos vacunales. VacciMonitor, 18(1), 25–34. https://www.redalyc.org/articulo.oa?id=203414612005

García-Bocanegra, I., Barranco, I., Rodríguez-Gómez, I. M., Pérez, B., Gómez-Laguna, J., Rodríguez, S., Ruiz-Villamayor, E., & Perea, A. (2010). Tuberculosis in alpacas

(Lama pacos) caused by Mycobacterium bovis. Journal of Clinical Microbiology, 48(5), 1960–1964. https://doi.org/10.1128/JCM.02518-09

García-Jiménez, W. L., Benítez-Medina, J. M., Fernández-Llario, P., Abecia, J. A., García-Sánchez, A., Martínez, R., Risco, D., Ortiz-Peláez, A., Salguero, F. J., Smith, N. H., Gómez, L., & Hermoso de Mendoza, J. (2013). Comparative pathology of the natural infections by Mycobacterium bovis and by Mycobacterium caprae in Wild Boar (Sus scrofa). Transboundary and Emerging Diseases, 60(2), 102–109. https://doi.org/10.1111/j.1865-1682.2012.01321.x

García-Jiménez, W. L., Fernández-Llario, P., Gómez, L., Benítez-Medina, J. M., García-Sánchez, A., Martínez, R., Risco, D., Gough, J., Ortiz-Peláez, A., Smith, N. H., Mendoza, J. H. de, & Salguero, F. J. (2012). Histological and immunohistochemical characterisation of Mycobacterium bovis induced granulomas in naturally infected Fallow deer (Dama dama). Veterinary Immunology and Immunopathology, 149(1–2), 66–75. https://doi.org/10.1016/j.vetimm.2012.06.010

García-Jiménez, W. L., Salguero, F. J., Fernández-Llario, P., Martínez, R., Risco, D., Gough, J., Ortiz-Peláez, A., Hermoso-de-Mendoza, J., & Gómez, L. (2013). Immunopathology of granulomas produced by Mycobacterium bovis in naturally infected wild boar. Veterinary Immunology and Immunopathology, 156(1–2), 54–63. https://doi.org/10.1016/j.vetimm.2013.09.008

Ge, G., Jiang, H., Xiong, J., Zhang, W., Shi, Y., Tao, C., & Wang, H. (2021). Progress of the art of macrophage polarization and different subtypes in mycobacterial infection. Frontiers in Immunology, 12, 752657. https://doi.org/10.3389/fimmu.2021.752657

Gholoobi, A., Masoudi-Kazemabad, A., Meshkat, M., & Meshkat, Z. (2014). Comparison of culture and PCR methods for diagnosis of Mycobacterium tuberculosis in different clinical specimens. Jundishapur Journal of Microbiology, 7(2), e8939. https://doi.org/10.5812/jjm.8939

Gibbons, A. (2008). American sssociation of physical anthropologists meeting. Tuberculosis jumped from humans to cows, not vice versa. Science (New York, N.Y., 320(5876), 608. https://doi.org/doi.org/10.1126/science.320.5876.608a

Gómez-Laguna, J., Carrasco, L., Ramis, G., Quereda, J. J., Gómez, S., & Pallarés, F. J. (2010). Use of real-time and classic polymerase chain reaction assays for the diagnosis of porcine tuberculosis in formalin-fixed, paraffin-embedded tissues. Journal of Veterinary Diagnostic Investigation, 22(1), 123–127. https://doi.org/10.1177/104063871002200126

González, J., Geijo, M. V., García-Pariente, C., Verna, A., Corpa, J. M., Reyes, L. E., Ferreras, M. C., Juste, R. A., García Marín, J. F., & Pérez, V. (2005). Histopathological classification of lesions associated with natural paratuberculosis infection in cattle. Journal of Comparative Pathology, 133(2–3), 184–196. https://doi.org/10.1016/j.jcpa.2005.04.007

González Llamazares, O. R., Gutiérrez Martín, C. B., Aranaz Martín, A., Liébana Criado, E., Domínguez Rodríguez, L., & Rodríguez Ferri, E. F. (1999). Comparison of different methods for diagnosis of bovine tuberculosis from tuberculin-or interferon-γ-reacting cattle in Spain. Journal of Applied Microbiology, 87(4), 465–471. https://doi.org/10.1046/j.1365-2672.1999.00823.x

González-Fernández, A., Fernández Mastache, E., & Abalde, L. S. (2005). Linfocitos T y B. Clasificación. Receptores. Generación de diversidad: mecanismos moleculares. Capacidades funcionales. Medicine- Medicine - Programa de Formación Médica Continuada Acreditado, 9(33), 2162–2173. https://doi.org/10.1016/s0211-3449(05)73617-1

Good, M., Bakker, D., Duignan, A., & Collins, D. M. (2018). The history of in vivo tuberculin testing in bovines: Tuberculosis, a 'One Health' issue. Frontiers in Veterinary Science, 5(APR), 59. https://doi.org/10.3389/fvets.2018.00059

Gordon, S., & Martinez, F. O. (2010). Alternative activation of macrophages: Mechanism and functions. Immunity, 32(5), 593–604. https://doi.org/10.1016/j.immuni.2010.05.007

Gormley, E. (2007). Diagnosis of Mycobacterium bovis infection in cattle. Australian Journal of Dairy Technology, 62(2), 101–109. https://doi.org/10.1079/9781780643960.0168

Gormley, E., Corner, L. A. L., Costello, E., & Rodriguez-Campos, S. (2014). Bacteriological diagnosis and molecular strain typing of Mycobacterium bovis and Mycobacterium caprae. Research in Veterinary Science, 97(S), S30–S43. https://doi.org/10.1016/j.rvsc.2014.04.010

Gortázar, C., Vicente, J., Samper, S., Garrido, J. M., Fernández-De-Mera, I. G., Gavín, P., Juste, R. A., Martín, C., Acevedo, P., De La Puente, M., & Höfle, U. (2005). Molecular characterization of Mycobacterium tuberculosis complex isolates from wild ungulates in south-central Spain. Veterinary Research, 36(1), 43–52. https://doi.org/10.1051/vetres:2004051

Greenwald, R., Esfandiari, J., Lesellier, S., Houghton, R., Pollock, J., Aagaard, C., Andersen, P., Hewinson, R. G., Chambers, M., & Lyashchenko, K. (2003). Improved serodetection of Mycobacterium bovis infection in badgers (Meles meles) using multiantigen test formats. Diagnostic Microbiology and Infectious Disease, 46(3), 197–203. https://doi.org/10.1016/S0732-8893(03)00046-4

Gunassekaran, G. R., Poongkavithai Vadevoo, S. M., Baek, M. C., & Lee, B. (2021). M1 macrophage exosomes engineered to foster M1 polarization and target the IL-4 receptor inhibit tumor growth by reprogramming tumor-associated macrophages into M1-like macrophages. Biomaterials, 278, 121137. https://doi.org/10.1016/j.biomaterials.2021.121137

Guta, S., Casal, J., Napp, S., Saez, J. L., Garcia-Saenz, A., Perez De Val, B., Romero, B., Alvarez, J., & Allepuz, A. (2014). Epidemiological investigation of bovine

tuberculosis herd breakdowns in Spain 2009/2011. PLoS ONE, 9(8). https://doi.org/10.1371/journal.pone.0104383

Gutiérrez, M. C., Brisse, S., Brosch, R., Fabre, M., Omaïs, B., Marmiesse, M., Supply, P., & Vincent, V. (2005). Ancient origin and gene mosaicism of the progenitor of Mycobacterium tuberculosis. PLoS Pathogens, 1(1), e5. https://doi.org/10.1371/journal.ppat.0010005

Gutiérrez, M., Tellechea, J., & García Marín, J. F. (1998). Evaluation of cellular and serological diagnostic tests for the detection of Mycobacterium bovis-infected goats. Veterinary Microbiology, 62(4), 281–290. https://doi.org/doi.org/10.1016/S0378-1135 (98)00217-X

Gutiérrez-Aguirre, I., Rački, N., Dreo, T., & Ravnikar, M. (2015). Droplet digital PCR for absolute Quantification of pathogens. In C. Lacomme (Ed.), Methods in molecular biology 1302 (second, pp. 331–347). Humana Press. https://doi.org/doi.org/10.1007/978-1-4939-2620-6_24

Gutstein, H. B., & Morris, J. S. (2007). Laser capture sampling and analytical issues in proteomics. Expert Review of Proteomics, 4(5), 627–637. https://doi.org/10.1586/14789450.4.5.627

Helming, L., & Gordon, S. (2008). The molecular basis of macrophage fusion. Immunobiology, 212(9–10), 785–793. https://doi.org/10.1016/j.imbio.2007.09.012

Hernández-Jarguín, A. M., Martínez-Burnes, J., Molina-Salinas, G. M., de la Cruz-Hernández, N. I., Palomares-Rangel, J. L., Mayagoitia, A. L., & Barrios-García, H. B. (2020). Isolation and histopathological changes associated with non-tuberculous mycobacteria in lymph nodes condemned at a bovine slaughterhouse. Veterinary Sciences, 7(4), 1–10. https://doi.org/10.3390/vetsci7040172

Hernández-Pando, R., Schön, T., Orozco, E. H., Serafin, J., & Estrada-Garcióa, I. (2001). Expression of inducible nitric oxide synthase and nitrotyrosine during the evolution of experimental pulmonary tuberculosis. Experimental and Toxicologic Pathology, 53(4), 257–265. https://doi.org/10.1078/0940-2993-00182

Hilda, J. N., Das, S., Tripathy, S. P., & Hanna, L. E. (2020). Role of neutrophils in tuberculosis: A bird's eye view. Innate Immunity, 26(4), 240–247. https://doi.org/10.1177/1753425919881176

Hillemann, D., Galle, J., Vollmer, E., & Richter, E. (2006). Real-time PCR assay for improved detection of Mycobacterium tuberculosis complex in paraffin-embedded tissues. Journal of Tuberculosis and Lung Disease, 10(3), 340–342.

Hines, N., Payeur, J. B., & Hoffman, L. J. (2006). Comparison of the recovery of Mycobacterium bovis isolates using the BACTEC MGIT 960 system, BACTEC 460 system, and Middlebrook 7H10 and 7H11 solid media. Journal of Veterinary Diagnostic Investigation, 18(3), 243–250. https://doi.org/10.1177/104063870601800302

Huggett, J. F., Cowen, S., & Foy, C. A. (2015). Considerations for digital PCR as an accurate molecular diagnostic tool. Clinical Chemistry, 61(1), 79–88. https://doi.org/10.1373/clinchem.2014.221366

Huggett, J. F., & Whale, A. (2013). Digital PCR as a novel technology and its potential implications for molecular diagnostics. Clinical Chemistry, 59(12), 1691–1693. https://doi.org/10.1373/clinchem.2013.214742

Hughes, E. J., & Tobin, D. M. (2022). Decoding the tuberculous granuloma. Immunity, 55(5), 819–821. https://doi.org/10.1016/j.immuni.2022.04.009

Hunter, L., Hingley-Wilson, S., Stewart, G. R., Sharpe, S. A., & Salguero, F. J. (2022). Dynamics of Macrophage, T and B Cell infiltration within pulmonary granulomas induced by Mycobacterium tuberculosis in two non-human primate models of aerosol infection. Frontiers in Immunology, 12, 776913. https://doi.org/10.3389/fimmu.2021.776913

Jagatia, H., & Tsolaki, A. G. (2021). The role of complement system and the immune response to tuberculosis infection. Medicina (Kaunas, Lithuania), 57(2), 84. https://doi.org/10.3390/medicina57020084

Jiménez-Martín, D., Cano-Terriza, D., Risalde, M. A., Napp, S., Álvarez, J., Fernández-Morente, M., Fernández-Molera, V., Moreno, I., Infantes-Lorenzo, J. A., & García-Bocanegra, I. (2023). Seroepidemiology of tuberculosis in sheep in southern Spain. Preventive Veterinary Medicine, 215, 105920. https://doi.org/10.1016/J.PREVETMED.2023.105920

Johnson, L., Gough, J., Spencer, Y., Hewinson, G., Vordermeier, M., & Wangoo, A. (2006). Immunohistochemical markers augment evaluation of vaccine efficacy and disease severity in bacillus Calmette-Guerin (BCG) vaccinated cattle challenged with Mycobacterium bovis. Veterinary Immunology and Immunopathology, 111(3–4), 219–229. https://doi.org/10.1016/j.vetimm.2006.01.016

Johnson, L. K., Liebana, E., Nunez, A., Spencer, Y., Clifton-Hadley, R., Jahans, K., Ward, A., Barlow, A., & Delahay, R. (2008). Histological observations of bovine tuberculosis in lung and lymph node tissues from British deer. Veterinary Journal, 175(3), 409–412. https://doi.org/10.1016/j.tvjl.2007.04.021

Jørgensen, T. J. D., Bache, N., Roepstorff, P., Gårdsvoll, H., & Ploug, M. (2005). Collisional activation by MALDI tandem time-of-flight mass spectrometry induces intramolecular migration of amide hydrogens in protonated peptides. Molecular and Cellular Proteomics, 4(12), 1910–1919. https://doi.org/10.1074/mcp.M500163-MCP200

Karlson, A. G. (1980). Género Mycobacterium. In I. A. Merchant & R. Packer (Eds.), Bacteriología y virología veterinaria (3a, pp. 453–477). Acribia, S.A.

Karlson, A. G., & Lessel, E. F. (1970). Mycobacterium bovis nom. nov. International Journal of Systematic Bacteriology, 20(3), 273–282. https://doi.org/doi.org/10.1099/00207713-20-3-273

Kasmi, K. C. El, Qualls, J. E., Pesce, J. T., Smith, A. M., Robert, W., Henao-tamayo, M., Basaraba, R. J., König, T., Schleicher, U., Koo, M., Kaplan, G., Fitzgerald, K. A., Tuomanen, E. I., Orme, I. M., Kanneganti, T., Bogdan, C., Wynn, T. A., & Murray,

P. J. (2009). Toll-like receptor-induced arginase 1. Nature Immunology, 9(12), 1399–1406. https://doi.org/10.1038/ni.1671.Toll-like

Kassa, G. M., Abebe, F., Worku, Y., Legesse, M., Medhin, G., Bjune, G., & Ameni, G. (2012). Tuberculosis in goats and sheep in afar pastoral region of ethiopia and isolation of Mycobacterium tuberculosis from goat. Veterinary Medicine International, 2012. https://doi.org/10.1155/2012/869146

Kemal, J., Sibhat, B., Abraham, A., Terefe, Y., Tulu, K. T., Welay, K., & Getahun, N. (2019). Bovine tuberculosis in eastern Ethiopia: Prevalence, risk factors and its public health importance. BMC Infectious Diseases, 19(1), 1–9. https://doi.org/10.1186/s12879-018-3628-1

Khader, S. A., Bell, G. K., Pearl, J. E., Fountain, J. J., Rangel-Moreno, J., Cilley, G. E., Shen, F., Eaton, S. M., Gaffen, S. L., Swain, S. L., Locksley, R. M., Haynes, L., Randall, T. D., & Cooper, A. M. (2007). IL-23 and IL-17 in the establishment of protective pulmonary CD4+ T cell responses after vaccination and during Mycobacterium tuberculosis challenge. Nature Immunology, 8(4), 369–377. https://doi.org/10.1038/ni1449

Kim, O. (2003). Effect of fixation time and freeze-thaw cycles on the molecular analysis of viral DNA. Journal of Veterinary Science, 4(2), 203–204.

Kirwan, D. E., Chong, D. L. W., & Friedland, J. S. (2021). Platelet activation and the immune response to tuberculosis. Frontiers in Immunology, 12, 631696. https://doi.org/10.3389/fimmu.2021.631696

Klopfleisch, R. (2016). Macrophage reaction against biomaterials in the mouse model – Phenotypes, functions and markers. Acta Biomaterialia, 43, 3–13. https://doi.org/10.1016/j.actbio.2016.07.003

Kobayashi, S. D., & DeLeo, F. R. (2009). Role of neutrophils in innate immunity: A systems biology-level approach. Wiley Interdisciplinary Reviews. Systems Biology and Medicine, 1(3), 309–333. https://doi.org/10.1002/wsbm.32

Krocova, Z., Plzakova, L., Pavkova, I., Kubelkova, K., Macela, A., Ozanic, M., Marecic, V., Mihelcic, M., & Santic, M. (2020). The role of B cells in an early immune response to Mycobacterium bovis. Microbial Pathogenesis, 140. https://doi.org/10.1016/j.micpath.2019.103937

Kumar, V., Abbas, A. K., & Aster, J. C. (2015a). Enfermedades del sistema inmunitario. In V. Kumar, A. K. Abbus, & J. C. Aster (Eds.), Robbins y Cotran - Patología estructural de la célula (9th ed., pp. 185–264). Elsevier.

Kumar, V., Abbas, A. K., & Aster, J. C. (2015b). Inflamación y reparación. In V. Kumar, A. K. Abbas, & J. C. Aster (Eds.), Robbins y Cotran - Patología Estructural y funcional (9a ed., pp. 69–109). Elsevier.

Kumar, V., Abbas, A. K., & Aster, J. C. (2021). Robbins y Cotran. Patología estructural y funcional (10th ed.). Elsevier.

Kuypers, J., & Jerome, K. R. (2017). Applications of digital PCR for clinical microbiology. Journal of Clinical Microbiology, 55(6), 1621–1628. https://doi.org/10.1128/JCM.00211-17

Ladero-Auñon, I., Molina, E., Holder, A., Kolakowski, J., Harris, H., Urkitza, A., Anguita, J., Werling, D., & Elguezabal, N. (2021). Bovine neutrophils release extracellular traps and cooperate with macrophages in Mycobacterium avium subsp. paratuberculosis clearance In vitro. Frontiers in Immunology, 12, 645304. https://doi.org/10.3389/fimmu.2021.645304

Larenas-Muñoz, F., Sánchez-Carvajal, J. M., Galán-Relaño, Á., Ruedas-Torres, I., Vera-Salmoral, E., Gómez-Gascón, L., Maldonado, A., Carrasco, L., Tarradas, C., Luque, I., Rodríguez-Gómez, I. M., & Gómez-Laguna, J. (2022). The role of histopathology as a complementary diagnostic tool in the monitoring of bovine tuberculosis. Frontiers in Veterinary Science, 9(9), 816190. https://doi.org/10.3389/fvets.2022.816190

Ledermann, W. (2003). La tuberculosis antes del descubrimiento de Koch Tuberculosis before Koch's discovery. Revista Chilena Infectología, 20, 46–47. https://doi.org/dx.doi.org/10.4067/S0716-10182003020200014

Liébana, E., Aranaz, A., Mateos, A., Vilafranca, M., Gomez-Mampaso, E., Tercero, J. C., Alemany, J., Suarez, G., Domingo, M., & Domínguez, L. (1995). Simple and rapid detection of Mycobacterium tuberculosis complex organisms in bovine tissue samples by PCR. Journal of Clinical Microbiology, 33(1), 33–36. https://doi.org/doi.org/10.1128/jcm.33.1.33-36.1995

Liebana, E., Marsh, S., Gough, J., Nunez, A., Vordermeier, H. M., Whelan, A., Spencer, Y., Clifton-Hardley, R., Hewinson, G., & Johnson, L. (2007). Distribution and activation of T-lymphocyte subsets in tuberculous bovine lymph-node granulomas*. Veterinary Pathology, 44(3), 366–372. https://doi.org/doi.org/10.1354/vp.44-3-366

Lilenbaum, W., & Fonseca, L. S. (2006). The use of Elisa as a complementary tool for bovine tuberculosis control in Brazil. Brazilian Journal of Veterinary Research and Animal Science, 43(2), 256–261. https://doi.org/doi.org/10.11606/issn.1678-4456.bjvras.2006.26507

Lilenbaum, W., Ribeiro, E. R., Souza, G. N., Moreira, E. C., Fonseca, L. S., Ferreira, M. A., & Schettini, J. (1999). Evaluation of an ELISA-PPD for the diagnosis of bovine tuberculosis in field trials in Brazil. Research in Veterinary Science, 66(3), 191–195. https://doi.org/10.1053/rvsc.1998.0229

Lim, J. H., Kim, C. K., & Bae, M. H. (2019). Evaluation of the performance of two real-time PCR assays for detecting Mycobacterium species. Journal of Clinical Laboratory Analysis, 33(1), e22645. https://doi.org/10.1002/jcla.22645

Lipiec, M., Radulski, Ł., & Szulowski, K. (2019). A case of bovine tuberculosis in pigs in Poland - a country free from the disease. Annals of Agricultural and Environmental Medicine, 26(1), 29–32. https://doi.org/10.26444/aaem/ 90979

Liu, C. H., Liu, H., & Ge, B. (2017). Innate immunity in tuberculosis: Host defense vs pathogen evasion. Cellular and Molecular Immunology, 14(12), 963–975. https://doi.org/10.1038/cmi.2017.88

Liu, Y. C., Zou, X. B., Chai, Y. F., & Yao, Y. M. (2014). Macrophage polarization in inflammatory diseases. International Journal of Biological Sciences, 10(5), 520–529. https://doi.org/10.7150/ijbs.8879

Liu, Y., Chen, Y., Momin, A., Shaner, R., Wang, E., Bowen, N. J., Matyunina, L. V, Deette Walker, L., Mcdonald, J. F., Sullards, M. C., & Merrill, A. H. (2010). Elevation of sulfatides in ovarian cancer: An integrated transcriptomic and lipidomic analysis including tissue-imaging mass spectrometry. Molecular Cancer, 9, 186. https://doi.org/10.1186/1476-4598-9-186.

LoBue, P. A., Betacourt, W., Peter, C., & Mosert, K. S. (2003). Epidemiology of Mycobacterium bovis disease in San Diego County, 1994-2000. International Journal of Tuberculosis and Lung Disease, 7(2), 180–185.

Lopes, R. L., Borges, T. J., Araújo, J. F., Pinho, N. G., Bergamin, L. S., Battastini, A. M. O., Muraro, S. P., Souza, A. P. D., Zanin, R. F., & Bonorino, C. (2014). Extracellular mycobacterial DnaK polarizes macrophages to the M2-like phenotype. PLoS ONE, 9(11), e113441. https://doi.org/10.1371/journal.pone.0113441

López, A., & Martinson, S. A. (2021). Respiratory system, thoracic cavities, mediastinum, and pleurae. In J. F. Zachary (Ed.), James F. Zachary- Pathologic Basis of Veterinary Disease (7th ed., pp. 547–642). Elsevier.

Lorente-Leal, V., Liandris, E., Castellanos, E., Bezos, J., Domínguez, L., de Juan, L., & Romero, B. (2019). Validation of a real-time PCR for the detection of Mycobacterium tuberculosis complex members in bovine tissue samples. Frontiers in Veterinary Science, 6, 61. https://doi.org/10.3389/fvets. 2019.00061

Lorente-Leal, V., Liandris, E., Pacciarini, M., Botelho, A., Kenny, K., Loyo, B., Fernández, R., Bezos, J., Domínguez, L., de Juan, L., & Romero, B. (2021). Direct PCR on tissue samples to detect Mycobacterium tuberculosis complex: An alternative to the

bacteriological culture. Journal of Clinical Microbiology, 59(2), 1–14. https://doi.org/10.1128/JCM.01404-20

Lorenz, T. C. (2012). Polymerase chain reaction: Basic protocol plus troubleshooting and optimization strategies. Journal of Visualized Experiments, 63, e3998. https://doi.org/10.3791/3998

Lowe, D. M., Redford, P. S., Wilkinson, R. J., O'Garra, A., & Martineau, A. R. (2012). Neutrophils in tuberculosis: Friend or foe? Trends in Immunology, 33(1), 14–25. https://doi.org/10.1016/j.it.2011.10.003

Lyashchenko, K. P., Greenwald, R., Esfandiari, J., Chambers, M. A., Vicente, J., Gortazar, C., Santos, N., Correia-Neves, M., Buddle, B. M., Jackson, R., O'Brien, D. J., Schmitt, S., Palmer, M. V., Delahay, R. J., & Waters, W. R. (2008). Animal-side serologic assay for rapid detection of Mycobacterium bovis infection in multiple species of free-ranging wildlife. Veterinary Microbiology, 132(3–4), 283–292. https://doi.org/10.1016/j.vetmic.2008.05.029

Lyu, L., Li, Z., Pan, L., Jia, H., Sun, Q., Liu, Q., & Zhang, Z. (2020). Evaluation of digital PCR assay in detection of M.tuberculosis IS6110 and IS1081 in tuberculosis patients plasma. BMC Infectious Diseases, 20(1), 657. https://doi.org/10.1186/s12879-020-05375-y

Ma, S., Zhang, J., Liu, H., Li, S., & Wang, Q. (2022). The role of tissue-resident macrophages in the development and treatment of inflammatory bowel disease. Frontiers in Cell and Developmental Biology, 10, 896591. https://doi.org/10.3389/fcell.2022.896591

Maas, M., van Kooten, P. J. S., Schreuder, J., Morar, D., Tijhaar, E., Michel, A. L., & Rutten, V. P. M. G. (2012). Development of a lion-specific interferon-gamma assay. Veterinary Immunology and Immunopathology, 149(3–4), 292–297. https://doi.org/10.1016/j.vetimm.2012.07.014

Machado, D., Couto, I., & Viveiros, M. (2019). Advances in the molecular diagnosis of tuberculosis: From probes to genomes. Infection, Genetics and Evolution, 72, 93–112. https://doi.org/10.1016/j.meegid.2018.11.021

Madacki, J., Mas Fiol, G., & Brosch, R. (2019). Update on the virulence factors of the obligate pathogen Mycobacterium tuberculosis and related tuberculosis-causing mycobacteria. Infection, Genetics and Evolution, 72, 67–77. https://doi.org/10.1016/j.meegid.2018.12.013

Maier, S. K., Hahne, H., Gholami, A. M., Balluff, B., Meding, S., Schoene, C., Walch, A. K., & Kuster, B. (2013). Comprehensive identification of proteins from MALDI imaging. Molecular and Cellular Proteomics, 12(10), 2901–2910. https://doi.org/10.1074/mcp.M113.027599

Maison, D. P. (2022). Tuberculosis pathophysiology and anti-VEGF intervention. Journal of Clinical Tuberculosis and Other Mycobacterial Diseases, 27, 100300. https://doi.org/10.1016/j.jctube.2022.100300

Malech, H. L., DeLeo, F. R., & Quinn, M. T. (2020). The Role of Neutrophils in the Immune System: An Overview. In M. T. Quinn & F. R. DeLeo (Eds.), Neutrophil (3rd ed., pp. 1–467). Springer Nature. https://doi.org/doi.org/10.1007/978-1-0716-0154-9

Mansouri, F., Heydarzadeh, R., & Yousefi, S. (2018). The association of interferon-gamma, interleukin-4 and interleukin-17 single-nucleotide polymorphisms with susceptibility to tuberculosis. APMIS : Acta Pathologica, Microbiologica, et Immunologica Scandinavica, 126(3), 227–233. https://doi.org/10.1111/apm.12810

Manzanares-Meza, L. D., Gutiérrez-Román, C. I., & Medina-Contreras, O. (2017). MALDI imaging: beyond classic diagnosis. Boletín Médico Del Hospital Infantil de México, 74(3), 212–218. https://doi.org/10.1016/j.bmhimx.2017.03.004

MAPA. (2023a). Programa nacional de erradicación de tuberculosis bovina 2023 (Infección por el complejo Mycobacterium tuberculosis). www.mapa.es

MAPA. (2023b). Tuberculosis. https://www.mapa.gob.es/es/ganaderia/temas/ sanidad-animal-higiene-ganadera/sanidadanimal/enfermedades/tuberculosis/Tuberculosis_bovina.aspx#prettyPhoto

MAPA. (2023c). Manual para la realización de estudios histopatológicos, inmunohistoquímicos y de PCR directa de tejidos para el diagnóstico rápido de la tuberculosis bovina por el complejo Mycobacterium tuberculosis (CMT). www.mapa.gob.es/es/ganaderia/temas/sanidad-animal-higiene-ganadera/manual_est_histopatologicos_inmunohistoqumicos_pcr_diagnostico_tuberculosis_cmt_visavet-santafe2023_tcm30-561053.pdf

Marakalala, M. J., Raju, R. M., Sharma, K., Zhang, Y. J., Eugenin, A., Prideaux, B., Daudelin, I. B., Chen, P., Booty, M. G., Kim, J. H., Eum, S. Y., Via, L. E., Behar, S. M., Iii, C. E. B., Mann, M., Dartois, V., & Rubin, E. J. (2016). Inflammatory signaling in human tuberculosis granulomas is spatially organized. Nature Medicine, 22(5), 531–538. https://doi.org/10.1038/nm.4073.Inflammatory

Marianelli, C., Cifani, N., Teresa Capucchio, M., Fiasconaro, M., Russo, M., La Mancusa, F., Pasquali, P., Di Marco, V., Sperimentale della Sicilia, Z., Pozzo di Gotto, B., Fiasconaro, I., & Marco, D. (2010). A case of generalized bovine tuberculosis in a sheep. Journal of Veterinary Diagnostic Investigation, 22(3), 445–448. https://doi.org/doi.org/10.1177/104063871002200319

Martins, A. (2021, July 18). BCG: 100 años de la vacuna más antigua aún en uso (y por qué es un 'dolor de cabeza' para la ciencia). BBC News Mundo. https://www.bbc.com/mundo/noticias-57866217

Mattila, J. T., Ojo, O. O., Kepka-Lenhart, D., Marino, S., Kim, J. H., Eum, S. Y., Via, L. E., Barry, C. E., Klein, E., Kirschner, D. E., Morris, S. M., Lin, P. L., & Flynn, J. L. (2013). Microenvironments in tuberculous granulomas are delineated by distinct populations of macrophage subsets and expression of nitric oxide synthase and arginase isoforms. The Journal of Immunology, 191(2), 773–784. https://doi.org/10.4049/jimmunol.1300113

McAdam, A. J., Milner, D. A., & Sharpe, A. H. (2015). Enfermedades infecciosas. In V. Kumar, A. K. Abbas, & J. C. Aster (Eds.), Robbins y Cotran- Patología estructural y funcional (9th ed., pp. 390–401). Elsevier.

McClean, C. M., & Tobin, D. M. (2016). Macrophage form, function, and phenotype in mycobacterial infection: Lessons from tuberculosis and other diseases. Pathogens and Disease, 74(7), 1–15. https://doi.org/10.1093/femspd/ftw068

McGill, J. L., Sacco, R. E., Baldwin, C. L., Telfer, J. C., Palmer, M. V., & Ray Waters, W. (2014). The role of gamma delta T cells in immunity to Mycobacterium bovis infection in cattle. Veterinary Immunology and Immunopathology, 159(3–4), 133–143. https://doi.org/10.1016/j.vetimm.2014.02.010

Menin, Á., Fleith, R., Reck, C., Marlow, M., Fernandes, P., Pilati, C., & Báfica, A. (2013). Asymptomatic Cattle Naturally Infected with Mycobacterium bovis Present Exacerbated Tissue Pathology and Bacterial Dissemination. PLoS ONE, 8(1), 18–21. https://doi.org/10.1371/journal.pone.0053884

Michel, A. L., Müller, B., & van Helden, P. D. (2010). Mycobacterium bovis at the animal-human interface: A problem, or not? Veterinary Microbiology, 140(3–4), 371–381. https://doi.org/10.1016/j.vetmic.2009.08.029

Mitchell, G., Chen, C., & Portnoy, D. A. (2016). Strategies used by bacteria to grow in macrophages. Microbiology Spectrum, 4(3), 1128. https://doi.org/10.1128/microbiolspec.mchd-0012-2015

Mohamed, A. (2020). Bovine tuberculosis at the human–livestock–wildlife interface and its control through one health approach in the Ethiopian Somali Pastoralists: A review. One Health, 9, 100113. https://doi.org/10.1016/j.onehlt.2019.100113

Morales, A., Martínez, I., Carlos, A., Álvarez, G., Álvarez, M., & Maldonado, J. (2005). Comparison of Histopathology, Culture and PCR for Diagnosis of Bovine Tuberculosis. Revista Científica, XV (2), 103–108.

Morrison, W. B. & DeNicola, D. B. (1993). Advantages and disadvantages of cytology and histopathology for the diagnosis of cancer. Seminars in Veterinary Medicine and Surgery (Small Animal), 8(4), 222–227.

Mostowy, S., & Behr, M. A. (2005). The origin and evolution of Mycobacterium tuberculosis. Clinics in Chest Medicine, 26(2), 207–216. https://doi.org/10.1016/j.ccm.2005.02.004

Muñoz Mendoza, M., Juan, L. de, Menéndez, S., Ocampo, A., Mourelo, J., Sáez, J. L., Domínguez, L., Gortázar, C., García Marín, J. F., & Balseiro, A. (2012). Tuberculosis due to Mycobacterium bovis and Mycobacterium caprae in sheep. The Veterinary Journal, 191(2), 267–269. https://doi.org/10.1016/J.TVJL.2011.05.006

Muñoz-Mendoza, M., Romero, B., Del Cerro, A., Gortázar, C., García-Marín, J. F., Menéndez, S., Mourelo, J., de Juan, L., Sáez, J. L., Delahay, R. J., & Balseiro, A. (2015). Sheep as a potential source of bovine TB: Epidemiology, pathology and evaluation of diagnostic techniques. Transboundary and Emerging Diseases, 63(6), 635–646. https://doi.org/10.1111/tbed.12325

Murray, J. F., Rieder, H. L., & Finley-Croswhite, A. (2016). The king's evil and the royal touch: The medical history of scrofula. International Journal of Tuberculosis and Lung Disease, 20(6), 713–716. https://doi.org/10.5588/ijtld.16.0229

Murray, P. J. (2017). Macrophage Polarization. Annual Review of Physiology, 79, 541–566. https://doi.org/10.1146/annurev-physiol-022516-034339

Mustafa, T., Wiker, H. G., Mørkve, O., & Sviland, L. (2008). Differential expression of mycobacterial antigen MPT64, apoptosis and inflammatory markers in multinucleated giant cells and epithelioid cells in granulomas caused by Mycobacterium tuberculosis. Virchows Archiv, 452(4), 449–456. https://doi.org/10.1007/s00428-008-0575-z

Naranjo, V., Gortazar, C., Vicente, J., & de la Fuente, J. (2008). Evidence of the role of European Wild boar as a reservoir of Mycobacterium tuberculosis complex.

Veterinary Microbiology, 127(1–2), 1–9. https://doi.org/10.1016/j.vetmic.2007.10.002

Neill, S. D., Bryson, D. G., & Pollock, J. M. (2001). Pathogenesis of tuberculosis in cattle. Tuberculosis, 81(1–2), 79–86. https://doi.org/10.1054/tube.2000.0279

Neill, S. D., Pollock, J. M., Bryson, D. B., & Hanna, J. (1994). Pathogenesis of Mycobacterium bovis infection in cattle. Veterinary Microbiology, 40(1–2), 41–52. https://doi.org/10.1016/0378-1135(94)90045-0.

Norris, J. L., & Caprioli, R. M. (2013). Imaging mass spectrometry: A new tool for pathology in a molecular age. Proteomics - Clinical Applications, 7(11–12), 733–738. https://doi.org/10.1002/prca.201300055

North, R. J., & Jung, Y. J. (2004). Immunity to tuberculosis. Annual Review of Immunology, 22, 599–623. https://doi.org/10.1146/annurev.immunol.22.012703.104635

Núñez-García, J., Downs, S. H., Parry, J. E., Abernethy, D. A., Broughan, J. M., Cameron, A. R., Cook, A. J., de la Rua-Domenech, R., Goodchild, A. V., Gunn, J., More, S. J., Rhodes, S., Rolfe, S., Sharp, M., Upton, P. A., Vordermeier, H. M., Watson, E., Welsh, M., Whelan, A. O., … Greiner, M. (2018). Meta-analyses of the sensitivity and specificity of ante-mortem and post-mortem diagnostic tests for bovine tuberculosis in the UK and Ireland. Preventive Veterinary Medicine, 153, 94–107. https://doi.org/10.1016/j.prevetmed.2017.02.017

Nyaruaba, R., Mwaliko, C., Kering, K. K., & Wei, H. (2019). Droplet digital PCR applications in the tuberculosis world. Tuberculosis, 117, 85–92. https://doi.org/10.1016/j.tube.2019.07.001

Nyaruaba, R., Xiong, J., Mwaliko, C., Wang, N., Kibii, B. J., Yu, J., & Wei, H. (2020). Development and evaluation of a single dye duplex droplet digital PCR assay for the rapid detection and quantification of mycobacterium tuberculosis. Microorganisms, 8(5), 701. https://doi.org/10.3390/microorganisms8050701

O'Halloran, C., Ioannidi, O., Reed, N., Murtagh, K., Dettemering, E., Van Poucke, S., Gale, J., Vickers, J., Burr, P., Gascoyne-Binzi, D., Howe, R., Dobromylskyj, M., Mitchell, J., Hope, J., & Gunn-Moore, D. (2019). Tuberculosis due to Mycobacterium bovis in pet cats associated with feeding a commercial raw food diet. Journal of Feline Medicine and Surgery, 21(8), 667–681. https://doi.org/10.1177/1098612X19848455

Okamoto Yoshida, Y., Umemura, M., Yahagi, A., O'Brien, R. L., Ikuta, K., Kishihara, K., Hara, H., Nakae, S., Iwakura, Y., & Matsuzaki, G. (2010). Essential Role of IL-17A in the Formation of a Mycobacterial Infection-Induced Granuloma in the Lung. The Journal of Immunology, 184(8), 4414–4422. https://doi.org/10.4049/jimmunol.0903332

OMS. (2022). Global Tuberculosis report. http://apps.who.int/bookorders.

OMS. (2023, April 21). Tuberculosis. https://www.who.int/es/news-room/fact-sheets/detail/tuberculosis

OMSA. (2022). Tuberculosis de los mamíferos (infección por el complejo Mycobacterium tuberculosis (pp. 1–24). https://www.woah.org/es/que-hacemos/sanidad-y-bienestar-animal/recopilacion-de-datos-sobre-enfermedades/

Oppenheimer, S. R., Mi, D., Sanders, M. E., & Caprioli, R. M. (2010). Molecular analysis of tumor margins by MALDI mass spectrometry in renal carcinoma. Journal of Proteome Research, 9(5), 2182–2190. https://doi.org/10.1021/pr900936z

Orme, I. M., & Cooper, A. (1999). Cytokine/chemokine cascades in immunity to tuberculosis. Immunology Today, 20(7), 307–312. https://doi.org/10.1016/s0167-5699(98)01438-8

Orme, I. M., & Ordway, D. J. (2016). Mouse and guinea pig models of tuberculosis. Microbiology Spectrum, 4(4), TBTB2-0002-2015. https://doi.org/10.1128/microbiolspec.TBTB2-0002-2015

Palmer, M. V. (2013). Mycobacterium bovis: Characteristics of wildlife reservoir hosts. Transboundary and Emerging Diseases, 60(Suppl 1), 1–13. https://doi.org/10.1111/tbed.12115

Palmer, M. V., Kanipe, C., & Boggiatto, P. M. (2022). The bovine tuberculoid granuloma. Pathogens, 11(1), 61. https://doi.org/10.3390/pathogens11010061

Palmer, M. V., Thacker, T. C., & Waters, W. R. (2016). Multinucleated giant cell cytokine expression in pulmonary granulomas of cattle experimentally infected with Mycobacterium bovis. Veterinary Immunology and Immunopathology, 180, 34–39. https://doi.org/10.1016/j.vetimm.2016.08.015

Palmer, M. V., & Waters, W. R. (2006). Advances in bovine tuberculosis diagnosis and pathogenesis: What policy makers need to know. Veterinary Microbiology, 112(2-4 SPEC. ISS.), 181–190. https://doi.org/10.1016/j.vetmic.2005.11.028

Palmer, M. V., Waters, W. R., & Thacker, T. C. (2007). Lesion development and immunohistochemical changes in granulomas from cattle experimentally infected with Mycobacterium bovis. Veterinary Pathology, 44(6), 863–874. https://doi.org/10.1354/vp.44-6-863

Palmer, M. V., Wiarda, J., Kanipe, C., & Thacker, T. C. (2019). Early pulmonary lesions in cattle infected via aerosolized Mycobacterium bovis. Veterinary Pathology, 56(4), 544–554. https://doi.org/10.1177/0300985819833454

Parra, A., Fernández-Llario, P., Tato, A., Larrasa, J., García, A., Alonso, J. M., Hermoso De Mendoza, M., & Hermoso De Mendoza, J. (2003). Epidemiology of Mycobacterium bovis infections of pigs and wild boars using a molecular approach. Veterinary Microbiology, 97(1–2), 123–133. https://doi.org/10.1016/j.vetmic.2003.08.007

Parsons, S. D. C., Drewe, J. A., van Pittius, N. C. G., Warren, R. M., & van Helden, P. D. (2013). Novel cause of tuberculosis in meerkats, South Africa. Emerging Infectious Diseases, 19(12), 2004–2007. https://doi.org/10.3201/eid1912.130268

Pérez de Val, B., Perea, C., Estruch, J., Solano-Manrique, C., Riera, C., Sanz, A., Vidal, E., & Velarde, R. (2022). Generalized tuberculosis due to Mycobacterium caprae in a red fox phylogenetically related to livestock breakdowns. BMC Veterinary Research, 18(1), 1–6. https://doi.org/10.1186/s12917-022-03454-7

Perez, V., Marin, J. F. G., & Badiola, J. J. (1996). Description and classification of different types of lesion associated with natural paratuberculosis infection in sheep. Journal of Comparative Pathology, 114(2), 107–122. https://doi.org/10.1016/S0021-9975(96)80001-6

Persson, Y. A. Z., Blomgran-Julinder, R., Rahman, S., Zheng, L., & Stendahl, O. (2008). Mycobacterium tuberculosis-induced apoptotic neutrophils trigger a pro-inflammatory response in macrophages through release of heat shock protein 72, acting in synergy with the bacteria. Microbes and Infection, 10(3), 233–240. https://doi.org/10.1016/j.micinf.2007.11.007

Pesce, J. T., Ramalingam, T. R., Mentink-Kane, M. M., Wilson, M. S., Kasmi, K. C. E., Smith, A. M., Thompson, R. W., Cheever, A. W., Murray, P. J., & Wynn, T. A. (2009). Arginase-1-expressing macrophages suppress Th2 cytokine-driven inflammation and fibrosis. PLoS Pathogens, 5(4). https://doi.org/10.1371/journal.ppat.1000371

Pesciaroli, M., Alvarez, J., Boniotti, M. B., Cagiola, M., Di Marco, V., Marianelli, C., Pacciarini, M., & Pasquali, P. (2014). Tuberculosis in domestic animal species. Research in Veterinary Science, 97(suppl), S78–S85. https://doi.org/10.1016/j.rvsc.2014.05.015

Pesciaroli, M., Russo, M., Mazzone, P., Aronica, V., Fiasconaro, M., Boniotti, M. B., Corneli, S., Cagiola, M., Pacciarini, M., Di Marco, V., & Pasquali, P. (2012). Evaluation of the interferon-gamma (IFN-γ) assay to diagnose Mycobacterium bovis infection in pigs. Veterinary Immunology and Immunopathology, 148(3–4), 369–372. https://doi.org/10.1016/j.vetimm.2012.06.020

Pessanha, A. P., Martins, R. A. P., Mattos-Guaraldi, A. L., Vianna, A., & Moreira, L. O. (2012). Arginase-1 expression in granulomas of tuberculosis patients. FEMS Immunology and Medical Microbiology, 66(2), 265–268. https://doi.org/10.1111/j.1574-695X.2012.01012.x

Peterson, P. K., Gekker, G., Hu, S., Anderson, W. R., Teichert, M., Chao, C. C., & Molitor, T. W. (1996). Multinucleated giant cell formation of swine microglia induced by Mycobacterium bovis. Journal of Infectious Diseases, 173(1), 1194–1201. https://doi.org/10.1093/infdis/173.5.1194

Plackett, P., Ripper, J., Corner, L. A., Small, K., de Witte, K., Melville, L., Hides, S., & Wood, P. R. (1989). An ELISA for the detection of anergic tuberculous cattle. Australian Veterinary Journal, 66(1), 15–19. https://doi.org/10.1111/j.1751-0813.1989.tb09706.x

Polena, H., Boudou, F., Tilleul, S., Dubois-Colas, N., Lecointe, C., Rakotosamimanana, N., Pelizzola, M., Andriamandimby, S. F., Raharimanga, V., Charles, P., Herrmann, J. L., Ricciardi-Castagnoli, P., Rasolofo, V., Gicquel, B., & Tailleux, L. (2016). Mycobacterium tuberculosis exploits the formation of new blood vessels for its dissemination. Scientific Reports, 6, 33162. https://doi.org/10.1038/srep33162

Pollock, J. M., & Andersen Peter. (1996). El potencial del antígeno ESAT-6 secretado por micobacterias virulentas para el diagnóstico específico de la tuberculosis. Journal of Infectious Diseases, 175(5), 1251–1254. https://doi.org/10.1086/593686

Pollock, J. M., & Neill, S. D. (2002). Mycobacterium bovis infection and tuberculosis in cattle. Veterinary Journal, 163(2), 115–127. https://doi.org/10.1053/tvjl.2001.0655

Pollock, J. M., Pollock, D. A., Campbell, D. G., Girvin, R. M., Crockard, A. D., Neill, S. D., & Mackie, D. P. (1996). Dynamic changes in circulating and antigen-responsive T-cell subpopulations post-Mycobacterium bovis infection in cattle. Immunology, 87(2), 236–241. https://doi.org/10.1046/j.1365-2567.1996.457538.x.

Pollock, J. M., Welsh, M. D., & McNair, J. (2005). Immune responses in bovine tuberculosis: Towards new strategies for the diagnosis and control of disease. Veterinary Immunology and Immunopathology, 108(1-2 SPEC. ISS.), 37–43. https://doi.org/10.1016/j.vetimm.2005.08.012

Poole, R. K. (1997). Advances in microbial physiology. Volume 39. Academic Press.

Prideaux, B.,́roniqueDartois, V., Staab, D., Weiner, D. M., Goh, A., Via, L. E., Barry, C. E., & Stoeckli, M. (2011). High-sensitivity MALDI-MRM-MS imaging of moxifloxacin distribution in tuberculosis-infected rabbit lungs and granulomatous lesions. Analytical Chemistry, 83(6), 2112–2118. https://doi.org/10.1021/ac1029049

Prideaux, B., Via, L. E., Zimmerman, M. D., Eum, S., Sarathy, J., O'Brien, P., Chen, C., Kaya, F., Weiner, D. M., Chen, P. Y., Song, T., Lee, M., Shim, T. S., Cho, J. S., Kim, W., Cho, S. N., Olivier, K. N., Barry, C. E., & Dartois, V. (2015). The association between sterilizing activity and drug distribution into tuberculosis lesions. Nature Medicine, 21(10), 1223–1227. https://doi.org/10.1038/nm.3937

Pritchard DG. (1988). A Century of Bovine Tuberculosis 1888-1988: Conquest and Controversy. Journal of Comparative Pathology, 99(4), 357–399. https://doi.org/doi.org/10.1016/0021-9975(88)90058-8

Rački, N., Morisset, D., Gutierrez-Aguirre, I., & Ravnikar, M. (2014). One-step RT-droplet digital PCR: A breakthrough in the quantification of waterborne RNA viruses. Analytical and Bioanalytical Chemistry, 406(3), 661–667. https://doi.org/10.1007/s00216-013-7476-y

Rageade, F., Picot, N., Blanc-Michaud, A., Chatellier, S., Mirande, C., Fortin, E., & Van Belkum, A. (2014). Performance of solid and liquid culture media for the detection of Mycobacterium tuberculosis in clinical materials: Meta-analysis of recent studies. European Journal of Clinical Microbiology and Infectious Diseases, 33(6), 867–870. https://doi.org/10.1007/s10096-014-2105-z

Ramakrishnan, L. (2012). Revisiting the role of the granuloma in tuberculosis. Nature Reviews Immunology, 12(5), 352–366. https://doi.org/10.1038/nri3211

Ramos, D. F., Silva, P. E. A., & Dellagostin, O. A. (2015). Diagnosis of bovine tuberculosis: review of main techniques. Brazilian Journal of Biology = Revista Brasleira de Biologia, 75(4), 830–837. https://doi.org/10.1590/1519-6984.23613

Ranjan, R., Narnaware, S. D., Nath, K., Sawal, R. K., & Patil, N. V. (2018). Rapid diagnosis of tuberculosis in dromedary camel (Camelus dromedarius) using lateral flow assay-based kit. Tropical Animal Health and Production, 50(4), 907–910. https://doi.org/10.1007/s11250-017-1502-6

Rauser, S., Deininger, S. O., Suckau, D., Hfler, H., & Walch, A. (2010). Approaching MALDI molecular imaging for clinical proteomic research: Current state and fields of application. Expert Review of Proteomics, 7(6), 927–941. https://doi.org/10.1586/epr.10.83

Rayner, E. L., Pearson, G. R., Hall, G. A., Basaraba, R. J., Gleeson, F., McIntyre, A., Clark, S., Williams, A., Dennis, M. J., & Sharpe, S. A. (2013). Early lesions following aerosol infection of rhesus macaques (Macaca mulatta) with mycobacterium tuberculosis strain H37RV. Journal of Comparative Pathology, 149(4), 475–485. https://doi.org/10.1016/j.jcpa.2013.05.005

Real Decreto 664/1997. (1997). , de 12 de mayo, sobre la protección de los trabajadores contra los riesgos relacionados con la exposición a agentes biológicos durante el trabajo. Boletín Oficial Del Estado, 124, 1–27.

Real Decreto 1716/2000. (2000). , de 13 de octubre, sobre normas sanitarias para el intercambio intracomunitario de animales de las especies bovina y porcina. Agencia Estatal Boletín Oficial Del Estado, BOE-A-2000-19137, 256, 36737–36753. https://www.boe.es/eli/es/rd/2000/10/13/1716

Real Decreto 2611/1996. (1996). , de 20 de diciembre, por el que se regulan los programas nacionales de erradicación de enfermedades de los animales. Boletín Oficial Del Estado, 307, 1–39. https://www.boe.es/buscar/doc.php?id=BOE-A-1996-28539

Reglamento (CE) no 1226/2002 de la Comisión. (2002). de 8 de julio de 2002, por el que se modifica el anexo B de la Directiva 64/432/CEE del Consejo. 13–18.

Rhodes, S., Gunn-Mooore, D., Boschiroli, M. L., Schiller, I., Esfandiari, J., Greenwald, R., & Lyashchenko, K. P. (2011). Comparative study of IFNγ and antibody tests for feline tuberculosis. Veterinary Immunology and Immunopathology, 144(1–2), 129–134. https://doi.org/10.1016/j.vetimm.2011.07.020

Rhodes, S., Holder, T., Clifford, D., Dexter, I., Brewer, J., Smith, N., Waring, L., Crawshaw, T., Gillgan, S., Lyashchenko, K., Lawrence, J., Clarke, J., De La Rua-Domenech, R., & Vordermeier, M. (2012). Evaluation of gamma interferon and antibody tuberculosis tests in alpacas. Clinical and Vaccine Immunology, 19(10), 1677–1683. https://doi.org/10.1128/CVI.00405-12

Rico Santana, N. (2015). Optimización y estandarización de un protocolo para el estudio de perfiles peptídicos séricos mediante la tecnología Maldi-Tof MS. Aplicación en la búsqueda de nuevos biomarcadores de diagnóstico precoz [Tesis doctoral]. Universitat de Barcelona.

Risalde, M. Á., Thomas, J., Sevilla, I., Serrano, M., Ortíz, J. A., Garrido, J., Domínguez, M., Domínguez, L., Gortázar, C., & Ruíz-Fons, J. F. (2017). Development and evaluation of an interferon gamma assay for the diagnosis of tuberculosis in red deer experimentally infected with Mycobacterium bovis. BMC Veterinary Research, 13(1), 341. https://doi.org/10.1186/s12917-017-1262-6

Risco, D., Fernández-Llario, P., García-Jiménez, W. L., Gonçalves, P., Cuesta, J. M., Martínez, R., Sanz, C., Sequeda, M., Gómez, L., Carranza, J., & de Mendoza, J. H. (2013). Influence of porcine circovirus type 2 infections on bovine tuberculosis in wild boar populations. Transboundary and Emerging Diseases, 60(Suppl 1), 121–127. https://doi.org/10.1111/tbed.12112

Risco, D., Serrano, E., Fernández-Llario, P., Cuesta, J. M., Gonçalves, P., Garcia-Jiménez, W. L., Martinez, R., Cerrato, R., Velarde, R., Gómez, L., Segalés, J., & De Mendoza, J. H. (2014). Severity of bovine tuberculosis is associated with co-infection with

common pathogens in wild boar. PLoS ONE, 9(10), e110123. https://doi.org/10.1371/journal.pone.0110123

Rode, T. M., Berget, I., Langsrud, S., Møretrø, T., & Holck, A. (2009). MALDI-TOF mass spectrometry for quantitative gene expression analysis of acid responses in Staphylococcus aureus. Journal of Microbiological Methods, 78(1), 86–93. https://doi.org/10.1016/j.mimet.2009.05.006

Rodriguez-Campos, S., Smith, N. H., Boniotti, M. B., & Aranaz, A. (2014). Overview and phylogeny of Mycobacterium tuberculosis complex organisms: Implications for diagnostics and legislation of bovine tuberculosis. Research in Veterinary Science, 97(S), S5–S19. https://doi.org/10.1016/j.rvsc.2014.02.009

Romero, B., Bezos, J., de Juan, L., Lozano, F. J., González, S., Perales, A., & Sáez, J. L. (2021). Toma y envío de muestras para diagnóstico mediante PCR directa y cultivo microbiológico en infecciones por miembros del Complejo Mycobacterium tuberculosis. VSAVET y Subdirección General de Sanidad e Higiene Animal y Trazabilidad. MAPA. www.mapa.gob.es/es/ganaderia/temas/sanidad-animal-higiene-ganadera/manualtomademuestrascmt_tcm30-430347.pdf

Römpp, A., Guenther, S., Takats, Z., & Spengler, B. (2011). Mass spectrometry imaging with high resolution in mass and space (HR 2 MSI) for reliable investigation of drug compound distributions on the cellular level. Analytical and Bioanalytical Chemistry, 401(1), 65–73. https://doi.org/10.1007/s00216-011-4990-7

Rook, G. A. W., & Hernandez-Pando, R. (1996). The pathogenesis of tuberculosis. Annual Review of Microbiology, 50, 259–884. https://doi.org/doi.org/10.1146/annurev.micro.50.1.259

Rothschild, B. M., Martin, L. D., Lev, G., Bercovier, H., Kahila Bar-Gal, G., Greenblatt, C., Donoghue, H., Spigelman, M., & Brittain, D. (2001). Mycobacterium tuberculosis complex DNA from an extinct bison dated 17,000 years before the present. Clinical Infectious Diseases, 33(3), 305–316. https://doi.org/10.1086/321886

Rychlik, W., Spencer', W. J., & Rhoads, R. E. (1990). Optimization of the annealing temperature for DNA amplification in vitro. Nucleic Acids Research, 18(21), 6409–6412. https://doi.org/10.1093/nar/18.21.6409

Sakula, A. (1982). Robert Koch: Centenary of the discovery of the tubercle bacillus, 1882. Thorax, 37(4), 246–251. https://doi.org/10.1136/thx.37.4.246

Sakula, A. (1983). Robert Koch (1843–1910) Founder of the science of bacteriology and discoverer of the tubercle bacillus A study of his life and work. The Canadian Veterinary Journal, 24(4), 124–127.

Sallam, R. M. (2015). Proteomics in cancer biomarkers discovery: Challenges and applications. Disease Markers, 2015, 321370. https://doi.org/10.1155/2015/321370

Sánchez-Carvajal, J. M., Galán-Relaño, Á., Ruedas-Torres, I., Jurado-Martos, F., Larenas-Muñoz, F., Vera, E., Gómez-Gascón, L., Cardoso-Toset, F., Rodríguez-Gómez, I. M., Maldonado, A., Carrasco, L., Tarradas, C., Gómez-Laguna, J., & Luque, I. (2021). Real-time PCR validation for Mycobacterium tuberculosis complex detection targeting IS6110 directly from bovine lymph nodes. Frontiers in Veterinary Science, 8, 643111. https://doi.org/10.3389/fvets.2021.643111

Santos, N., Geraldes, M., Afonso, A., Almeida, V., & Correia-Neves, M. (2010). Diagnosis of tuberculosis in the wild boar (sus scrofa): A comparison of methods applicable to hunter-harvested animals. PLoS ONE, 5(9), 1–8. https://doi.org/10.1371/journal.pone.0012663

Sawyer, A. J., Patrick, E., Edwards, J., Wilmott, J. S., Fielder, T., Yang, Q., Barber, D. L., Ernst, J. D., Britton, W. J., Palendira, U., Chen, X., & Feng, C. G. (2023). Spatial mapping reveals granuloma diversity and histopathological superstructure in human tuberculosis. Journal of Experimental Medicine, 220(6), e20221392. https://doi.org/10.1084/jem.20221392

Scanlan, CH. M. (1991). Introducción a la bacteriología veterinaria (CH. M. Scanlan, Ed.). Acribia S.A.

Schiller, I., Oesch, B., Vordermeier, H. M., Palmer, M. V., Harris, B. N., Orloski, K. A., Buddle, B. M., Thacker, T. C., Lyashchenko, K. P., & Waters, W. R. (2010). Bovine tuberculosis: A review of current and emerging diagnostic techniques in view of their relevance for disease control and eradication. Transboundary and Emerging Diseases, 57(4), 205–220. https://doi.org/10.1111/j.1865-1682.2010.01148.x

Schlesinger, L. S. (1993). Macrophage phagocytosis of virulent but not attenuated strains of Mycobacterium tuberculosis is mediated by mannose receptors in addition to complement receptors. Journal of Immunology, 150(7), 2920–2930.

Schober, Y., Guenther, S., Spengler, B., & Römpp, A. (2012). High-resolution matrix-assisted laser desorption/ionization imaging of tryptic peptides from tissue. Rapid Communications in Mass Spectrometry, 26(9), 1141–1146. https://doi.org/10.1002/rcm.6192

Schöne, C., Höfler, H., & Walch, A. (2013). MALDI imaging mass spectrometry in cancer research: Combining proteomic profiling and histological evaluation. Clinical Biochemistry, 46(6), 539–545. https://doi.org/10.1016/j.clinbiochem.2013.01.018

Sevilla, I. A., Molina, E., Elguezabal, N., Pérez, V., Garrido, J. M., & Juste, R. A. (2015). Detection of mycobacteria, Mycobacterium avium subspecies, and Mycobacterium tuberculosis complex by a novel tetraplex real-time PCR assay. Journal of Clinical Microbiology, 53(3), 930–940. https://doi.org/10.1128/JCM.03168-14

Shapouri-Moghaddam, A., Mohammadian, S., Vazini, H., Taghadosi, M., Esmaeili, S. A., Mardani, F., Seifi, B., Mohammadi, A., Afshari, J. T., & Sahebkar, A. (2018). Macrophage plasticity, polarization, and function in health and disease. Journal of Cellular Physiology, 233(9), 6425–6440. https://doi.org/10.1002/jcp.26429

Sharpe, A. E., Brady, C. P., Johnson, A. J., Byrne, W., Kenny, K., & Costello, E. (2010). Concurrent outbreak of tuberculosis and caseous lymphadenitis in a goat herd. Veterinary Record, 166(19), 591–592. https://doi.org/10.1136/vr.b4825

Shrivastava, P., & Bagchi, T. (2016). Difference in mononuclear cell cytokine profile of tuberculosis patients before and after treatment and its influence on in vitro multinucleate giant cell formation. Human Immunology, 77(6), 516–521. https://doi.org/10.1016/j.humimm.2016.04.015

Sica, A., Erreni, M., Allavena, P., & Porta, C. (2015). Macrophage polarization in pathology. Cellular and Molecular Life Sciences, 72(21), 4111–4126. https://doi.org/10.1007/s00018-015-1995-y

Signor, L., Varesio, E., Staack, R. F., Starke, V., Richter, W. F., & Hopfgartner, G. (2007). Analysis of erlotinih and its metabolites in rat tissue sections by MALDI quadrupole time-of-flight mass spectrometry. Journal of Mass Spectrometry, 42(7), 900–909. https://doi.org/10.1002/jms.1225

Smith, N. (1965). Animal pathogenicity of the 'Dassie bacillus'. Tubercle, 46(1), 58–64. https://doi.org/10.1016/s0041-3879(65)80087-3

Smith, N. H., Hewinson, R. G., Kremer, K., Brosch, R., & Gordon, S. V. (2009). Myths and misconceptions: The origin and evolution of Mycobacterium tuberculosis. Nature Reviews Microbiology, 7(7), 537–544. https://doi.org/10.1038/nrmicro2165

Snyder, P. W. (2021). Diseases of immnunity. In J. Zachary (Ed.), James F. Zachary - Pathologic Basis of Veterinary Disease (seventh, pp. 295–339). Elsevier.

Sreevatsan, S., Pan, X. I., Stockbauer, K. E., Connell, N. D., Kreiswirth, B. N., Whittam, T. S., & Musser, J. M. (1997). Restricted structural gene polymorphism in the Mycobacterium tuberculosis complex indicates evolutionarily recent global dissemination. Proceedings of the National Academy of Sciences of the United States of America, 94(18), 9869–9874. https://doi.org/10.1073/pnas.94.18.9869

Stead, W. W. (1997). The origin and erratic global spread of tuberculosis how the past explains the present and is the key to the future. Clinics in Chest Medicine, 18(1), 65–77. https://doi.org/doi.org/10.1016/s0272-5231(05)70356-7

Steinbach, S., Vordermeier, H. M., & Jones, G. J. (2016). CD4+ and πσT Cells are the main producers of IL-22 and IL-17A in lymphocytes from Mycobacterium bovis-infected cattle. Scientific Reports, 6, 29990. https://doi.org/10.1038/srep29990

Stewart, L. D., Tort, N., Meakin, P., Argudo, J. M., Nzuma, R., Reid, N., Delahay, R. J., Ashford, R., Montgomery, W. I., & Grant, I. R. (2017). Development of a novel immunochromatographic lateral flow assay specific for Mycobacterium bovis cells and its application in combination with immunomagnetic separation to test badger faeces. BMC Veterinary Research, 13(1), 131. https://doi.org/10.1186/s12917-017-1048-x

Sukswai, N., & Khoury, J. D. (2019). Immunohistochemistry innovations for diagnosis and tissue-based biomarker detection. Current Hematologic Malignancy Reports, 14(5), 368–375. https://doi.org/10.1007/s11899-019-00533-9

Sun, L., Chen, Y., Yi, P., Yang, L., Yan, Y., Zhang, K., Zeng, Q., & Guo, A. (2021). Serological detection of Mycobacterium tuberculosis complex infection in multiple hosts by one universal ELISA. PLoS ONE, 16(10), e0257920. https://doi.org/10.1371/journal.pone.0257920

Supré, K., Roupie, V., Ribbens, S., Stevens, M., Boyen, F., & Roels, S. (2019). Short communication: Mycolicibacterium smegmatis, basonym Mycobacterium smegmatis, causing pyogranulomatous mastitis and its cross-reactivity in bovine (para)tuberculosis testing. Journal of Dairy Science, 102(9), 8405–8409. https://doi.org/10.3168/jds.2019-16610

Tadmor, A. D., Ottesen, E. A., Leadbetter, J. R., & Phillips, R. (2011). Probing individual environmental bacteria for viruses by using microfluidic digital PCR. Science, 333(6038), 58–62. https://doi.org/10.1126/science.1200758

Taylor, G. M., Worth, D. R., Palmer, S., Jahans, K., & Hewinson, R. G. (2007). Rapid detection of Mycobacterium bovis DNA in cattle lymph nodes with visible lesions using PCR. BMC Veterinary Research, 3(12). https://doi.org/10.1186/1746-6148-3-12

Thacker, T. C., Harris, B., Palmer, M. V., & Waters, W. R. (2011). Improved specificity for detection of Mycobacterium bovis in fresh tissues using IS6110 real-time PCR. BMC Veterinary Research, 7, 50. https://doi.org/10.1186/1746-6148-7-50

Thoen, C., LoBue, P., & De Kantor, I. (2006). The importance of Mycobacterium bovis as a zoonosis. Veterinary Microbiology, 112(2-4 SPEC. ISS.), 339–345. https://doi.org/10.1016/j.vetmic.2005.11.047

Thoen, C. O., & Barletta, R. G. (2006). Pathogenesis of Mycobacterium Bovis. In C. O.; S. J. H.; G. M. J. Thoen (Ed.), Mycobacterium bovis Infection in Animals and Humans (2nd ed., pp. 18–33). Wiley-Blackwell.

Thomas, J., Balseiro, A., Gortázar, C., & Risalde, M. A. (2021). Diagnosis of tuberculosis in wildlife: A systematic review. Veterinary Research, 52(1), 31. https://doi.org/10.1186/s13567-020-00881-y

Thomas, J., Infantes-Lorenzo, J. A., Moreno, I., Cano-Terriza, D., de Juan, L., García-Bocanegra, I., Domínguez, L., Domínguez, M., Gortázar, C., & Risalde, M. A. (2019). Validation of a new serological assay for the identification of Mycobacterium tuberculosis complex-specific antibodies in pigs and wild boar. Preventive Veterinary Medicine, 162, 11–17. https://doi.org/10.1016/j.prevetmed.2018.11.004

Thomas, R., & Chambers, M. (2021). Review of methods used for diagnosing tuberculosis in captive and free-ranging non-bovid species (2012–2020). Pathogens, 10(5), 584. https://doi.org/10.3390/pathogens10050584

Toche, P. (2012). Visión panorámica del sistema inmune. Revista Médica Clínica Las Condes, 23(4), 446–457. https://doi.org/10.1016/S0716-8640(12)70335-8

Tuck, M., Blanc, L., Touti, R., Patterson, N. H., Van Nuffel, S., Villette, S., Taveau, J. C., Römpp, A., Brunelle, A., Lecomte, S., & Desbenoit, N. (2021). Multimodal imaging based on vibrational spectroscopies and mass spectrometry imaging applied to biological tissue: A multiscale and multiomics review. Analytical Chemistry, 93(1), 445–477. https://doi.org/10.1021/acs.analchem.0c04595

Turk, J. L., & Narayanan, R. B. (1982). The origin, morphology, and function of epithelioid cells. Immunobiology, 161(3–4), 274–282. https://doi.org/10.1016/S0171-2985(82)80083-1

Turner, O. C., Basaraba, R. J., & Orme, I. M. (2003). Immunopathogenesis of pulmonary granulomas in the guinea pig after infection with Mycobacterium tuberculosis. Infection and Immunity, 71(2), 864–871. https://doi.org/10.1128/IAI.71.2.864-871.2003

Udhaya, K. S., Saleem, A., Thirumal Kumar, D., Anu Preethi, V., Younes, S., Zayed, H., Tayubi, I. A., & George Priya Doss, C. (2021). A systemic approach to explore the mechanisms of drug resistance and altered signaling cascades in extensively drug-resistant tuberculosis. Advances in Protein Chemistry and Structural Biology, 127, 343–364. https://doi.org/10.1016/bs.apcsb.2021.02.002

Umemura, M., Yahagi, A., Hamada, S., Mst, §, Begum, D., Watanabe, H., Kawakami, K., Suda, T., Sudo, K., Nakae, S., Iwakura, Y., & Matsuzaki, G. (2007). IL-17-Mediated regulation of innate and acquired immune response against pulmonary Mycobacterium bovis bacille Calmette-Guérin infection 1. The Journal of Immunology, 178(6), 3786–3796. https://doi.org/10.4049/jimmunol.178.6.3786

Uusi-Mäkelä, M., & Rämet, M. (2018). Hijacking host angiogenesis to drive mycobacterial growth. Cell Host and Microbe, 24(4), 465–466. https://doi.org/10.1016/j.chom.2018.09.016

Valerga, M., Viola, C., Thwaites, A., Bases, O., Ambroggi, M., Poggi, S., & Marino, R. (2005). Tuberculosis por Mycobacterium bovis en una mujer con SIDA. Revista Argentina de Microbiologia, 37(2), 96–98.

Van Ingen, J., Rahim, Z., Mulder, A., Boeree, M. J., Simeone, R., Brosch, R., & van Soolingen, D. (2012). Characterization of Mycobacterium orygis as M. tuberculosis complex subspecies. Emerging Infectious Diseases, 18(4), 653–655. https://doi.org/10.3201/eid1804.110888

Van Pinxteren, L. A. H., Ravn, P., Agger, E. M., Pollock, J., & Andersen, P. (2000). Diagnosis of Tuberculosis Based on the Two Specific Antigens ESAT-6 and CFP10. Clinical and Diagnostic Laboratory Immunology, 7(2), 155–160. https://doi.org/10.1128/CDLI.7.2.155-160.2000

Van Soolingen, D., Hermans, P. W. M., De Haas,' And, P. E. W., & Van Embden2, J. D. A. (1992). Insertion element IS1081-Associated restriction fragment length polymorphisms in Mycobacterium tuberculosis complex species: A reliable tool for recognizing Mycobacterium bovis BCG. Journal of Clinical Micriobiology, 30(7), 1772–1777. https://doi.org/10.1128/jcm.30.7.1772-1777.1992

Van Soolingen, D., Hoogenboezem, T., De Haas, P. E. W., Marianne, P. W. M., Koedam, A., Teppema, K. S., Brennan, P. J., Besra, G. S., Portaels,', F., Top, J., Schouls, L. M., & Van Embden', J. D. A. (1997). A Novel Pathogenic Taxon of the Mycobacterium tuberculosis Complex, Canetti: Characterization of an Exceptional Isolate from Africa. International journal of systematic bacteriology, 47(4), 1236–1245.

Varello, K., Pezzolato, M., Mascarino, D., Ingravalle, F., Caramelli, M., & Bozzetta, E. (2008). Comparison of histologic techniques for the diagnosis of bovine tuberculosis in the framework of eradication programs. Journal of Veterinary Diagnostic Investigation, 20(2), 164–169. https://doi.org/10.1177/104063870802000204

Vaysse, P. M., Heeren, R. M. A., Porta, T., & Balluff, B. (2017). Mass spectrometry imaging for clinical research-latest developments, applications, and current limitations. Analyst, 142(15), 2690–2712. https://doi.org/10.1039/c7an00565b

Vervenne, R. A. W., Jones, S. L., Van Soolingen, D., Van Der Laan, T., Andersen, P., Heidt, P. J., Thomas, A. W., & Langermans, J. A. M. (2004). TB diagnosis in non-human primates: Comparison of two interferon-γ assays and the skin test for identification of Mycobacterium tuberculosis infection. Veterinary Immunology and Immunopathology, 100(1–2), 61–71. https://doi.org/10.1016/j.vetimm.2004.03.003

Vilaplana, C., Prats, C., Marzo, E., Barril, C., Vegué, M., Diaz, J., Valls, J., López, D., & Cardona, P. J. (2014). To achieve an earlier IFN-γ response is not sufficient to control Mycobacterium tuberculosis infection in mice. PLoS ONE, 9(6), e100830. https://doi.org/10.1371/journal.pone.0100830

Vordermeier, H. M., Whelan, A., Cockle, P. J., Farrant, L., Palmer, N., & Hewinson, R. G. (2001). Use of synthetic peptides derived from the antigens ESAT-6 and CFP-10 for differential diagnosis of bovine tuberculosis in cattle. Clinical and Diagnostic Laboratory Immunology, 8(3), 571–578. https://doi.org/10.1128/CDLI.8.3.571-578.2001

Wagner, J. C., Buchanan, G., Bokkenheuser, V., & Leviseur, S. (1958). An acid-fast bacillus isolated from the lungs of the Cape Hyrax, Procavia capensis (Pallas). Nature, 181(4604), 284–285. https://doi.org/doi.org/10.1038/181284b0

Walch, A., Rauser, S., Deininger, S. O., & Höfler, H. (2008). MALDI imaging mass spectrometry for direct tissue analysis: A new frontier for molecular histology. Histochemistry and Cell Biology, 130(3), 421–434. https://doi.org/10.1007/s00418-008-0469-9

Walther, T. C., & Mann, M. (2010). Mass spectrometry – based proteomics in cell biology. Journal of Cell Biology, 190(4), 491–500. https://doi.org/10.1083/jcb.201004052

Wang, H. Y., Lu, J. J., Chang, C. Y., Chou, W. P., Hsieh, J. C. H., Lin, C. R., & Wu, M. H. (2019). Development of a high sensitivity TaqMan-based PCR assay for the specific detection of Mycobacterium tuberculosis complex in both pulmonary and extrapulmonary specimens. Scientific Reports, 9(1). https://doi.org/10.1038/s41598-018-33804-1

Wang, J., Ramakrishnan, R., Tang, Z., Fan, W., Kluge, A., Dowlati, A., Jones, R. C., & Ma, P. C. (2010). Quantifying EGFR alterations in the lung cancer genome with nanofluidic digital PCR arrays. Clinical Chemistry, 56(4), 623–632. https://doi.org/10.1373/clinchem.2009.134973

Wangoo, A., Johnson, L., Gough, J., Ackbar, R., Inglut, S., Hicks, D., Spencer, Y., Hewinson, G., & Vordermeier, M. (2005). Advanced granulomatous lesions in Mycobacterium bovis-infected cattle are associated with increased expression of type I procollagen, γδ (WC1+) T cells and CD 68+ cells. Journal of Comparative Pathology, 133(4), 223–234. https://doi.org/10.1016/j.jcpa.2005.05.001

Warren, E., Teskey, G., & Venketaraman, V. (2017). Effector mechanisms of neutrophils within the innate immune system in response to Mycobacterium tuberculosis infection. Journal of Clinical Medicine, 6(2), 15. https://doi.org/10.3390/jcm6020015

Waters, W. R., Buddle, B. M., Vordermeier, H. M., Gormley, E., Palmer, M. V., Thacker, T. C., Bannantine, J. P., Stabel, J. R., Linscott, R., Martel, E., Milian, F., Foshaug, W., & Lawrence, J. C. (2011). Development and evaluation of an enzyme-linked immunosorbent assay for use in the detection of bovine tuberculosis in cattle. Clinical and Vaccine Immunology, 18(11), 1882–1888. https://doi.org/10.1128/CVI.05343-11

Waters, W. R., Palmer, M. V., Thacker, T. C., Orloski, K., Nol, P., Harrington, N. P., Olsen, S. C., & Nonnecke, B. J. (2008). Blood culture and stimulation conditions for the diagnosis of tuberculosis in cervids by the Cervigam assay. The Veterinary Record, 162(7), 203–208. https://doi.org/doi.org/10.1136/vr.162.7.203

Waters, W. R., Palmer, M. V., Thacker, T. C., Bannantine, J. P., Vordermeier, H. M., Hewinson, R. G., Greenwald, R., Esfandiari, J., McNair, J., Pollock, J. M., Andersen, P., & Lyashchenko, K. P. (2006). Early antibody responses to experimental Mycobacterium bovis infection of cattle. Clinical and Vaccine Immunology, 13(6), 648–654. https://doi.org/10.1128/CVI.00061-06

Weed, L. A., & Baggenstoss, A. H. (1951). The isolation of pathogens from tissues of embalmed human bodies. American Journal of Clinical Pathology, 21(12), 1114–1120. https://doi.org/doi.org/10.1093/ajcp/21.12.1114

Whale, A. S., Huggett, J. F., Cowen, S., Speirs, V., Shaw, J., Ellison, S., Foy, C. A., & Scott, D. J. (2012). Comparison of microfluidic digital PCR and conventional quantitative PCR for measuring copy number variation. Nucleic Acids Research, 40(11). https://doi.org/10.1093/nar/gks203

White, A. D., Sibley, Laura., Sarfas, Charlotte., Morrison, Alexandra., Gullick, Jennie., Clark, Simon., Gleeson, F., McIntyre, A., Arlehamn, C. L., Sette, A., Salguero, F. J., Rayner, E., Rodriguez, E., Puentes, E., Laddy, D., Williams, A., Dennis, M., Martin, C., & Sharpe, S. (2021). MTBVAC vaccination protects rhesus macaques against aerosol challenge with M. tuberculosis and induces immune signatures analogous to those observed in clinical studies. Npj Vaccines, 6(1), 4. https://doi.org/10.1038/s41541-020-00262-8

Wisztorski, M., Franck, J., Salzet, M., & Fournier, I. (2010). MALDI direct analysis and imaging of frozen versus FFPE tissues: What strategy for which sample? Methods in Molecular Biology, 656, 303–322. https://doi.org/10.1007/978-1-60761-746-4_18

Wolfe, N. D., Dunavan, C. P., & Diamond, J. (2007). Origins of major human infectious diseases. Nature, 447(7142), 279–283. https://doi.org/10.1038/nature05775

Wood, P. R., & Jones, S. L. (2001). BOVIGAMTM: An in vitro cellular diagnostic test for bovine tuberculosis. Tuberculosis, 81(1–2), 147–155. https://doi.org/10.1054/tube.2000.0272

Wu, X., Tan, G., Yang, J., Guo, Y., Huang, C., Sha, W., & Yu, F. (2022). Prediction of Mycobacterium tuberculosis drug resistance by nucleotide MALDI-TOF-MS. International Journal of Infectious Diseases, 121, 47–54. https://doi.org/10.1016/j.ijid.2022.04.061

Xu, B. J., Li, J., Beauchamp, R. D., Shyr, Y., Li, M., Washington, M. K., Yeatman, T. J., Whitehead, R. H., Coffey, R. J., & Caprioli, R. M. (2009). Identification of early intestinal neoplasia protein biomarkers using laser capture microdissection and MALDI

MS. Molecular and Cellular Proteomics, 8(5), 936–945. https://doi.org/10.1074/mcp.M800345-MCP200

Xu, Y., Pooja, & Borah, K. (2022). Mycobacterium tuberculosis carbon and nitrogen metabolic fluxes. Bioscience Reports, 42(2), BSR20211215. https://doi.org/10.1042/BSR20211215

Yang, J., Han, X., Liu, A., Bai, X., Xu, C., Bao, F., Feng, S., Tao, L., Ma, M., & Peng, Y. (2017). Use of digital droplet PCR to detect Mycobacterium tuberculosis DNA in whole blood-derived DNA samples from patients with pulmonary and extrapulmonary tuberculosis. Frontiers in Cellular and Infection Microbiology, 7(AUG). https://doi.org/10.3389/fcimb.2017.00369

Zeineldin, M. M., Lehman, K., Camp, P., Farrell, D., & Thacker, T. C. (2023). Diagnostic evaluation of the IS1081-targeted real-time PCR for detection of Mycobacterium bovis DNA in bovine milk samples. Pathogens, 12(8), 972. https://doi.org/10.3390/pathogens12080972

Zhang, S., Chen, X., Lin, Z., Tan, Y., Liang, B., Pan, Y., Huang, M., Su, B., Hu, X., Xu, Y., & Li, Q. (2023). Quantification of isoniazid-heteroresistant Mycobacterium tuberculosis using droplet digital PCR. Journal of Clinical Microbiology, 61(6), e0188422. https://doi.org/10.1128/jcm.01884-22

Zhang, Y., Li, S., Liu, Q., Long, R., Feng, J., Qin, H., Li, M., Liu, L., & Luo, J. (2020). Mycobacterium tuberculosis heat-shock protein 16.3 induces macrophage M2 polarization through CCRL2/CX3CR1. Inflammation, 43(2), 487–506. https://doi.org/10.1007/s10753-019-01132-9